GESTATIONAL RELATED MORPHOLOGICAL ABNORMALITIES IN PLACENTAL VILLOUS TROPHOBLAST TURNOVER IN COMPROMISED PREGNANCIES

A thesis submitted for the degree of Doctor of Philosophy

by

Kate Louise Widdows

School of Health Sciences and Social Care
Brunel University

August 2009

To

Baby William

18.05.2009

Abstract

Human placental villi are covered by a layer of trophoblast epithelia in direct contact with maternal blood, which exist in a constant steady-state of turnover and renewal ensuring both maternal and fetal health. The process of trophoblast turnover involves proliferation, differentiation and fusion of cytotrophoblast cells to form a terminally differentiated outer syncytiotrophoblast layer which functions as the active transport compartment between mother and fetus. Alterations in the balance between these three processes are thought to diminish both the structural and functional integrity of the syncytiotrophoblast, potentially leading to placental insufficiency associated with severe complications of pregnancy such as pre-eclampsia (PET), intrauterine growth restriction (IUGR) and sudden infant death syndrome (SIDS).

Placentas from early (<32 weeks) and late-onset (>33 weeks) pregnancies complicated by PET, IUGR, SIDS and gestational age-matched controls were systematically uniform randomly sampled to assess the morphological basis of placental villous structure and trophoblast turnover (villi, cytotrophoblast, syncytiotrophoblast, apoptotic syncytial knots) using unbiased stereological techniques (volumes and numbers). Villous cytotrophoblast proliferation was assessed using double immunohistochemistry for Ki67 and cytokeratin 7 (CK-7).

Severe early-onset IUGR placentas (n=5) were smaller displaying significant reductions in the total number of CT cells, within which the density of proliferating CT was further reduced by 50%. Syncytiotrophoblast volume and number was significantly reduced with an increase in apoptotic syncytial knots. Late-onset IUGR placentas (n=4) also displayed significant reductions in the total number of CT and proliferating CT, but were not associated with changes in the density of proliferating CT. SCT numbers were significantly reduced with an increase in apoptotic knots.

Placentas from severe early-onset PET (n=11) were similar to preterm controls, except for a significant increase in apoptotic syncytial knots. However, late-onset PET (n=6) displayed a significant decrease in total CT number, the percentage of which undergoing proliferation was significantly increased for structural villi. There were increased numbers of apoptotic syncytial knots in peripheral villi.

SIDS-NBW (n=12) and SIDS-LBW (n=12) placentas displayed significant increases in the volume density of cytotrophoblast cells, syncytiotrophoblast nuclei and apoptotic syncytial knots when compared to term controls (n=12).

These data suggest that IUGR placentas have a severe impairment in the regenerative capacity of the villous trophoblast population which may contribute to its small placental phenotype, whilst PET is able to maintain overall placental growth with subtle alterations in villous trophoblast turnover. SIDS may represent postnatal sequelae of placental adaptation to an unfavourable intrauterine environment during early gestation.

Acknowledgments

First and foremost, to my amazing supervisor and friend, Dr Tahera Ansari for introducing me to the fascinating world of stereology and for making me think outside the box. For the stimulating discussions regarding all aspects of the study, no matter how far and wide, and for always responding pleasantly to my “can I ask a stupid question”. Without her constant support and believe in me as an undergraduate student this thesis would not have been possible. Thanks “boss”.

John Kingdom for giving me for the opportunity and funding a sabbatical in his lab at Mount Sinai Hospital, Toronto, and to his team (Dora and Sascha) for a welcoming stay and insight into the world of molecular biology. To Shabana and Aleah (the Lye lab) for being great friends during my stay.

Aaron (a.k.a.Azza), for all his technical assistance in putting this thesis together. For keeping my spirits up and entertaining me into the early hours of the morning when writing this thesis. But most of all, for just being a great friend and always being there.

Sascha Drewlo, a friend and colleague, for always keeping me on my toes.

The Scottish Cot Death Trust and the Henry Smith Charity for their sponsorship over the last 3 years.

And last, but by no means least, to my family and friends for their constant support, for making me laugh in stressful times and for always believing in me.

Abbreviations

(m)	all fields analysed
(ref)	reference space
(Y)	area of interest
µm	micron
2D	two-dimensional
3D	three-dimensional
A_f	area of frame
AFI	amniotic fluid index
AGA	appropriate for gestational age
ANOVA	one-way analysis of variance
AREDV	absent reverse end diastolic flow velocity
BrdU	bromodeoxyuridine
CE	coefficient of error
CK-7	cytokeratin 7
CNS	central nervous system
CT	cytotrophoblast
DAB	3, 3'-diaminobenzidine
DM	diabetes mellitus
DVT	deep vein thrombosis
EB	embryoblast
EDF	end diastolic flow
EGF	epidermal growth factor
EVT	extravillous trophoblast
FFPE	formalin fixed paraffin embedded
FGF	fibroblast growth factor
GA	gestational age
GCM1	glial cell missing-1
h	disector height
H_2O_2	hydrogen peroxide
HC/AC	head circumference /abdominal circumference ratio
HELLP	haemolysis elevated liver enzymes low platelet
HIF-1	hypoxia inducible transcription factor-1

ICM	inner cell mass
IGF	insulin-like growth factor
IUD	intrauterine death
IUGR	intrauterine growth restriction
IVS	intervillous space
LBW	low birthweight
M30	antibody to neo-epitope of cleaved cytokeratin 18
MV	mature intermediate villi
NBW	normal birthweight
N_{TOT}	total number
N_v	numerical density
OD	optical density
P	points
PC	post conception
PET	pre-eclampsia
PEDV	positive end diastolic flow velocity
PGF	placental growth factor
pO_2	partial pressure of oxygen
$_P$PROM	preterm premature rupture of the membranes
PS	phosphatidlyserine
PSI	point sampled intercept
Q	disectors
R.T.U.	ready to use
RT	room temperature
Σ	sum
Σ_P	number disector
SCT	syncytiotrophoblast
SEM	standard error of the mean
sFlt1	soluble fms-like tyrosine kinase 1
SGA	small for gestational age
SIDS	sudden infant death syndrome
SpT	spongiotrophoblast
STBM	syncytiotrophoblast microparticles
SUR	systematic uniform random

SV	stem villi
SynT	syncytiotrophoblast (murine)
t	final section thickness
TBS	tris buffered saline
TG	trophoblast giant cell
TS	trophoblast stem cell
TV	terminal villi
UCF	unbiased counting frame
UTAD	uterine artery Doppler
VEGF	vascular endothelial growth factor
N_v	number per unit volume
V_{ref}	reference volume
V_{tot}	total volume
V_v	volume fraction

Declaration

All placental tissues were collected from Mount Sinai Hospital (MSH), Toronto, Canada (Dr. J. Kingdom) and from archived material held at Rotunda Hospital, Ireland, UK (Dr. J. Gillan).

Case selection and collection was undertaken by Dr. J. Kingdom and his team. Clinical data was analyzed by myself and Leslie Proctor (MSH).

Histological and immunohistochemical preparation was carried out by myself with the technical assistance of Carinna Hockham. Molecular analysis in chapter 2 was carried out by myself during a 3 week sabbatical at MSH.

All stereological data collection and analysis was carried out by myself at Dept Surgical Research, Northwick Park Hospital, Harrow, UK.

Kate Widdows

August 2009

Table of Contents

Table of Figures

Table of Tables

Table of Graphs

1 Placental Insufficiency Syndromes

Pre-eclampsia (PET) and intrauterine growth restriction (IUGR) are broadly defined as "placental insufficiency syndromes", implying that placental development is, in some way, inadequate to sustain the health of both mother and infant, but may also have severe postnatal consequences i.e. Sudden Infant Death Syndrome (SIDS). Abnormal placentation in the first trimester is thought to underpin PET and IUGR, which are associated with maldevelopment of the gas-exchanging villi and its accompanying fetal vasculature. It is the under-development of these structures that underpins the placental pathology of IUGR (1; 2), whilst failure to maintain the villous epithelial layer is associated with the maternal symptoms of PET (3). Crucially, these pathological abnormalities are thought to arise at the level of the villous trophoblast. The aim of the present study is to assess the morphological basis of villous trophoblast turnover in placentas from PET, IUGR and SIDS.

1.1 Pre-eclampsia

Pre-eclampsia still remains one of the leading contributors to maternal and perinatal morbidity and mortality and the World Health Organization estimates that over 160,000 women die from PET each year (4). Pre-eclampsia is a multisystem disorder unique to human pregnancy affecting between 5-10% of all births and is diagnosed by the sudden onset of hypertension and proteinuria arising *de novo* after 20 weeks gestation, and is characterized by systemic maternal inflammatory response and diffuse endothelial dysfunction, leading to damage of various organs including kidneys, lungs and heart, and often results in life-long complications (5). Furthermore, approximately 4 million babies are born IUGR due to PET (6).

Although PET is the most extensively studied clinical condition in pregnancy, its cause still largely remains unclear, but it is generally accepted that the placenta is both necessary and sufficient to cause the disorder; pre-eclampsia can occur in the absence of a fetus (hydatidiform mole pregnancy) (7) and uterus (abdominal pregnancy) (8), supported by the prompt resolution of the disorder upon delivery of the placenta, which is the only known cure at present.

1.1.1 Definition and Classification

Pre-eclampsia is a hypertensive disorder of pregnancy defined by the American College of Obstetrics and Gynaecology (ACOG) as "new onset of hypertension on two separate occasions with proteinuria arising *de novo* after the 20th week of pregnancy in a previously normotensive non-proteinuric woman" (9).

The clinical expression of pre-eclampsia is further subdivided according to the severity (mild or severe) indicating the extent of proteinuria and hypertension. Gestational hypertension is defined as an elevation in blood pressure ≥ 140/90 mm Hg or higher after 20 weeks gestation in a woman with previously normal blood pressure. Only in the presence of ≥0.3g of protein in a 24 hour urine specimen, or 1+ proteinuria, classifies the hypertension as mild pre-eclampsia. Pre-eclampsia may also be 'superimposed' in women with pre-existing chronic hypertension i.e. hypertension with or without proteinuria diagnosed prior to, during or after pregnancy (10).

Severe pre-eclampsia is defined as an elevation in blood pressure ≥ 160/110 mm Hg or higher on two occasions at least six hours apart after 20 weeks gestation with at least 5g of protein in a 24 hour urine specimen (3+ proteinuria). Additionally, the presence of any signs of maternal organ failure such as HELLP syndrome (haemolysis, elevated liver enzymes, and low platelet count), edema, headache, epigastric pain, or eclampsia (convulsions), classifies a severely pre-eclamptic woman. Furthermore, the presence of a growth restricted fetus (IUGR) classifies pre-eclampsia as severe (9).

Gestational age (GA) is the most important clinical determinant of maternal and perinatal outcome and pre-eclampsia is associated with different maternal-fetal outcomes depending on its timing-of-onset (early-onset ≤ 34 weeks or late-onset ≥ 35 weeks) (11). Late-onset pre-eclampsia represents about 80% of all pre-eclampsia cases worldwide, and whilst it may present with comparable maternal severity to early-onset, it is usually associated with normal (12) or heavier fetal birthweight (13) and therefore IUGR does not often co-exist; there is a 50% chance of fetal survival if the fetus is delivered > 27 weeks gestation or with a birthweight > 600g (14). In comparison, early-onset disease (representing 5-20% depending on the statistics (15)) involves considerable overlap, whereby pre-eclampsia and IUGR requiring preterm delivery often co-exist (16). Because early-onset pre-eclampsia is associated with a 20-fold

increase in maternal mortality compared to its late-onset phenotype, it has been suggested that early-onset pre-eclampsia represents a different disease to that presenting at term (11).

1.1.2 Etiology and Pathophysiology

The severe pre-eclamptic woman is associated with hypoperfusion and damage of various vital organs including the kidneys, liver, brain and heart, which in the most severe cases, can result in multi-organ failure or 'eclamptic' convulsions (5). These pathological changes are due to systemic vasoconstriction resulting from an increased sensitivity to pressor agents and activation of the intravascular coagulation cascade, secondary to diffuse endothelial dysfunction and a systemic maternal inflammatory response- accountable for the clinical syndrome i.e. hypertension and proteinuria. The underlying etiological factors responsible for the systemic disease are thought to be initiated by the placenta.

In an attempt to describe the pathophysiology of pre-eclampsia, Redman put forward a Two Stage Model (17) (Figure 1-1), forming a widely accepted hypothesis within the placental scientific community. This model proposes that a poorly perfused placenta, secondary to failed spiral artery remodelling in the first trimester of pregnancy, (Stage 1) produces factor(s) which lead to the maternal syndrome of pre-eclampsia in the third trimester (Stage 2) (17; 18).

The link between Stage 1 and Stage 2 remains the 'holy grail' of placental research. Several placentally-derived factors have been suggested which are thought to lead to endothelial dysfunction and systemic inflammatory response leading to vasoconstriction. These include pro-inflammatory cytokines (tumour necrosis factor (TNF-α) (19; 20), endothelin (ET-1), interleukins (IL-6 and IL-8) (21), anti-angiogenic factors (21; 22), syncytiotrophoblast microparticles (STBM) (23), and anti-coagulant factors (thrombodulin and von Willebrand factor) and adhesion molecules (VCAM-1, ICAM-1 and E-selectin) (24), which have been shown to be increased in pre-eclamptic women. Oxidative stress is an attractive component as part of the linkage (20; 25) which would also stimulate release of cytokines, anti-angiogenic factors, microparticles and

other potential linkers, many of whose systemic effects would also be mediated by oxidative stress (23; 26; 27).

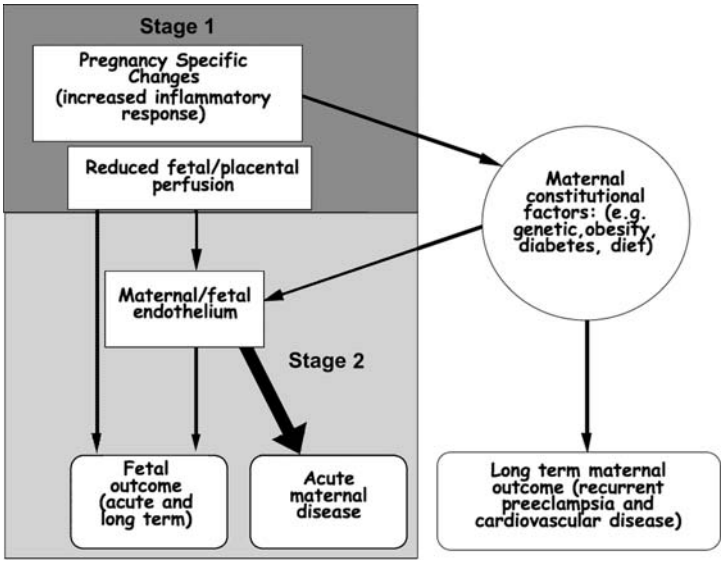

Figure 1-1 Two Stage Model of pre-eclampsia

In the Two Stage Model, reduced placental perfusion in the first trimester (Stage 1) leads to endothelial dysfunction which characterises the maternal syndrome of PET in the late second and third trimester of pregnancy (Stage 2) (adapted from (17)).

Anti-angiogenic growth factors released by the placenta have received much attention as one of the primary causes of endothelial dysfunction in pre-eclampsia providing a direct link between Stage 1 and 2 in the pathophysiology of the disease (18). Several studies have demonstrated increased circulating levels of placental soluble fms-like tyrosine kinase 1 (sFlt1) in serum from pre-eclamptic women (22; 28; 29). SFlt1 is a secreted splice variant of Flt1 that antagonizes the potent angiogenic growth factors, vascular endothelial growth factor (VEGF) and placental growth factor (PGF), from binding and activating endothelial cells of the maternal vascular endothelium. Expression of these growth factors has been shown to be subsequently decreased in pre-eclamptic women (30; 31), suggesting that this imbalance between pro- and anti-angiogenic factors may result in a prolonged 'anti-angiogenic state' in the pre-eclamptic woman leading to endothelial dysfunction. Furthermore, when injected into pregnant rats, sFlt1 is able to induce pre-eclamptic symptoms including hypertension, proteinuria and renal damage, and therefore sFlt1 may play a considerable role in mediating pre-eclampsia (22). Soluble endoglin is also proving to be another potential pathogenic anti-

angiogenic protein and predictive marker since its expression is also elevated in women who subsequently develop pre-eclampsia (32; 33).

The Two Stage Model was recently challenged by Huppertz, suggesting that pre-eclampsia has its origins in the first trimester *prior* to failed transformation of the maternal spiral arteries takes place (15). This is supported by the presence of placentally-derived proteins (i.e. placental protein 13 (PP13)) (34), long pentraxin (PTX3) (35), placenta associated plasma protein A (PAPP-A)) in maternal serum as early as 7-8 weeks gestation in those pregnancies that subsequently developed pre-eclampsia (36). However, failed transformation of the maternal spiral arteries, posited to result in reduced placental perfusion, is also observed in pregnancies resulting in IUGR without clinical signs of pre-eclampsia and in preterm birth (37). Furthermore, abnormal placental protein release is also present in some IUGR pregnancies (i.e. placental protein 13 (PP13) (34), long pentraxin 3 (PTX3) (35)), suggesting that these factors alone are not sufficient for developing pre-eclampsia (38; 39).

This led to the concept that maternal predisposing factors i.e. genetic, behavioural and environmental, modified by the physiological changes of pregnancy were necessary to interact with reduced placental perfusion leading to the maternal abnormalities of pre-eclampsia. Today, the prevailing view is that pathophysiological changes occurring in the placental unit begin well before the clinical symptoms; the onset, severity and progression of which is related to the maternal response to the underlying pathology. Furthermore, many of these factors leading to the maternal syndrome are risk factors for cardiovascular disease in later life (39).

1.2 Intrauterine Growth Restriction

In humans, a newborn may be small for a variety of reasons, and amongst the mammalian species, humans have the largest variation in birthweights compatible with survival. There are certain overt maternal and fetal factors that may lead to, or are strongly associated with poor fetal growth in utero (40; 41). However, there are a group of healthy yet ‘small infants’ delivered after an apparently uncomplicated pregnancy who are karyotypically and phenotypically normal; this is the small for gestational age

infant (SGA) i.e. they are constitutionally small (42). Significantly however, a proportion of these fetuses will be intrauterine growth restricted (IUGR) (40).

IUGR is characterized by failure of a fetus to reach its full growth potential as a result of suboptimal intrauterine growth conditions (43). IUGR complicates 3-10% of pregnancies and 20% of stillbirths are IUGR; perinatal mortality is 5-20 times greater for IUGR infants than those infants who are appropriate for gestational age (44). Examples of neonatal complications include hypoglycemia, hypoxemia leading to polycythemia, hypocalcaemia, pulmonary haemorrhage, hypothermia and toxaemia (40). These fetuses are also at an increased risk of significant life-long complications such as diabetes, hypertension and cardiovascular disease (45; 46).

1.2.1 Defining an IUGR infant

IUGR is an important clinical problem and it is therefore necessary for the clinician to distinguish between fetuses that are small but otherwise healthy (i.e. constitutionally small and not growth restricted) and those that are a consequence of an abnormal condition i.e. placental insufficiency. Accurately defining an IUGR infant from an apparently healthy infant is therefore crucial to lowering the perinatal and adult morbidity and mortality.

At present there is no internationally accepted clinical definition for IUGR (47). The classic definition refers to "an infant with a birthweight equal to or less than the 10th percentile for gestational age" (40), which in other words, refers to an infant weighing less than 90% of the population for gestational age. Population based growth charts should be used (in conjunction with an accurately determined gestational age) that are adjusted for modifiable factors such as gender, previous births, maternal height, weight and ethnicity, all of which are known to influence birthweight (48).

An SGA infant is defined as having a birthweight below a given percentile (usually the 10th) for gestational age (42). Hence, the above definition for IUGR also includes those SGA infants at the extreme lower end of the birthweight spectrum; as many as 70% of infants who weigh below the 10th centile for gestational age are constitutionally small

(49) and are not at high risk of adverse perinatal outcome. Using this definition on the other hand, not all SGA infants will be IUGR.

Birthweight alone should not therefore be used as an indicator of the fetal growth trajectory, since it merely represents the result of the growth process itself, and not the function (i.e. the fetal growth pattern). For example, an SGA infant grows along a consistent albeit lower growth percentile throughout gestation compared to those infants born with a birthweight appropriate for gestational age (AGA). An IUGR infant on the other hand may grow along the same percentile as an AGA *or* SGA fetus, but only when fetal demands outweigh those of placental supply in the third trimester will the infant deviate from its predefined growth trajectory. The severity, duration and nature of the insult will determine the extent of the deviation and hence, perinatal survival.

1.2.2 Classifying an IUGR infant

Birthweight is also generally reflected in longitudinal growth of the fetus, and it has been suggested that alterations in the fetal growth pattern at different developmental stages will lead to different neonatal phenotypes (50; 51). The common classifications are Type I (symmetrical) and Type II (asymmetrical) growth restriction (41).

The asymmetric type of growth restriction develops when oxygen or substrate supply to the fetus is reduced during the last trimester of pregnancy due to a reduced functional capacity of the placenta i.e. placental insufficiency. These infants display a relatively normal head size due to brain sparing in which blood flow is redistributed at the expense of the liver, muscle and fat so as to preserve the vital organs. As a result, these neonates exhibit scrawny limbs due to decreased muscle mass and thinned skin due to decreased body fat (40). This is the most frequent type of growth retardation and is of clinical relevance as it is progressive and from the view of the fetus, of an extrinsic origin; it might induce intrauterine death and stillbirth (41).

In contrast, in symmetrical growth restriction, the reduction in birthweight is usually proportional to reductions in length and head size at birth (51), and is thought to be of intrinsic origin present in early gestation. The fact that the growth of the head, femur and abdomen is equally affected might lead to a wrong assessment when determining

GA by ultrasound. Due to an intrinsic fetal problem, cell division and cell growth is limited and independent of substrate supply (41). However, it is likely that Type I and Type II phenotypes represent a continuum between the two.

1.2.3 Etiology

Unlike pre-eclampsia, there are numerous recognized environmental, maternal and placental causal factors that may result in an IUGR fetus (Table 1-1). However, in at least 40% of all cases of babies born low birthweight, no underlying pathology can be identified; in the case of prematurity, which has significant overlap with IUGR, this percentage increases to 60–70% (41).

Maternal factors for the risk of IUGR cover approximately 40% of the determinants of fetal birthweight. Quantitatively, pregnancy-associated hypertension and/or pre-eclampsia are the most important maternal factors influencing fetal growth; interestingly however a pre-existing hypertensive disorder does not increase the risk of IUGR. The most important environmental factor conferring a risk of IUGR is maternal cigarette smoking during pregnancy, in which 40% of IUGR infants are born to mothers who smoke, and is correlated in a dose-dependent manner. Because fetal causes such as congenital abnormalities are relatively rare, any abnormality occurring in the fetal-placental unit therefore has the capacity to limit fetal growth leading to IUGR (41).

Table 1-1 Etiological factors for IUGR

Maternal/Medical complications	**Environmental factors**
Hypertension, pre-eclampsia Severe chronic infections (inflammatory bowel disease, malaria, etc.) Hypoxia (asthma,, cyanotic heart disease) Other severe diseases (diabetes, glomerulonephritis, collagen disease, Uterus abnormalities *Infections* Viral (TORCH) Bacterial (syphilis) Protozoal (malaria, toxoplasma)	Smoking Alcohol Drugs (antimetabolites, anticoagulants, anticonvulsants) Narcotics High altitude Low socioeconomic status
Other conditions	**Genetic**
Ethnicity Pre-pregnancy weight, maternal height Pregnancy weight gain Prior low-birth-weight infant Low maternal age Reproductive technologies	*Chromosomal abnormalities* Autosomal trisomies, monosomies, deletions Errors of metabolism (inborn) *Malformations* Cardiovascular defects Gastrointestinal defects Genitourinary defects Skeletal dysplasias, etc.
Placental abnormalities	
Chromosomal mosaicism Infarcts, focal lesions Abnormal placentation (placental praevia, placental insufficiency) Reduced placental blood flow	

1.3 Sudden Infant Death Syndrome

Infants born from pre-eclamptic and/or IUGR pregnancies are at an increased risk of succumbing to Sudden Infant Death Syndrome (SIDS) (52-55). SIDS refers to the unexplained death of an infant between 1 month and 1 year of age and despite the recent decline in incidence rates (i.e. the Back to Sleep Campaign (56)), SIDS still remains the leading cause of postnatal infant death in industrialized countries (57-59). Furthermore, women whose first infant died from SIDS are 2 to 3 times more likely to have a preterm delivery or SGA infant in their next pregnancy (52-55).

1.3.1 Definition

SIDS refers to the unexplained death of an infant. SIDS infants are not associated with any overt clinical and/or pathological findings on post-mortem examination. This initially led to the misleading assumption that all SIDS infants were normal; judging by its close association with obstetric complications, it is likely that not all SIDS victims are in fact 'normal'. Diagnosing SIDS is therefore based on the exclusion of other causes of fetal death, such that SIDS is currently defined as " the death of an infant under one year of age which remains unexplained after a thorough investigation, including the performance of a complete autopsy, examination of the death scene, review of the clinical history, and bacteriology and virology" (60).

1.3.2 Epidemiology

There are numerous maternal, fetal and environmental factors which may predispose an infant to succumb to SIDS (61). Prone sleeping position (infants placed on their front to sleep) and cigarette smoking are perhaps the most recognized risk factors for a SIDS event, shown by the rapid decline in SIDS events (from 49% in 1980 to 25% in 1999) following the public campaign in England and Wales to change the infants sleeping position from prone to supine (placing the infant on its back) (62). The majority of SIDS events occur at night and during the early hours of the morning, with a peak incidence of between 4 and 6 months of postnatal life, which indirectly suggests circadian rhythm as a possible contributory pathomechanism for a SIDS event (63). Other risk factors include males, multiple pregnancies (also a risk for pre-eclampsia and IUGR),

prematurity, low birthweight, low socio-economic status, drug abuse during pregnancy and viral/bacterial infections (64; 65).

The first evidence that SIDS may also comprise a genetic component came in 1987 when twin boys simultaneously succumbed to SIDS within 3 to 4 hours after a vaccination against diphtheria-tetanus-pertussis (DTP) (66). More recently, some SIDS infants have been shown to display a polymorphism in the IL-10-592*A allele which is an important anti-inflammatory anti-immune cytokine, hence it was postulated that some SIDS events may result from a genetically determined imbalance in pro- and anti-inflammatory cytokines, supported by the fact that these particular SIDS infants display reduced IL-10 production (67-69).

1.3.3 Pathophysiology

Rather than a specific disease process SIDS represents a heterogeneous entity. In an attempt to explain the pathophysiology of SIDS, Filiano and Kinney (1994) put forward the "Triple Risk Hypothesis". This model proposes that the unexpected death of an infant occurs during a lethal situation, when 1) a *vulnerable* infant is exposed to 2) *external risk factors* during 3) a *critical period* of physiological development (70; 71).

The concept of a vulnerable infant comes from microscopical and biochemical studies into the central nervous system (CNS) (72), cardiovascular system (73) and brain (74-76) showing that some but not all SIDS infants have neurological, cardiovascular and CNS abnormalities. These are postulated to prevent/overwhelm the compromised infant from executing normal arousal mechanisms to environmental external stressors, usually relating to a hypoxic insult (i.e. cigarette smoking, sleeping prone) (64).

External stressors include viral infections/bacterial toxins, inflammation, biochemical disorders and genetic abnormalities, which are thought to be some of the pathomechanisms that could be responsible for a SIDS event (64). Autopsy findings have revealed evidence of fetal hypoxia prior to death (i.e. increased levels of fetal hemoglobulin, immunoglobulins) (166). Several authors believe that SIDS may be a predominantly pathophysiologic reaction to bacterial toxins, viruses and/or cigarette smoke during the early stages of development in utero when the defence mechanisms of

the organs are less effective (63; 64; 77). This is based on the observation that a large proportion of SIDS infants exhibit two or more bacteria or viruses on autopsy (78).

However, because not all SIDS infants display the above abnormalities, such changes may not necessarily result in a SIDS event, and thus there are likely to be other intrinsic/extrinsic factors involved in the context of the triple risk hypothesis. On the other hand, these infants may be more vulnerable compared to other SIDS infants i.e. varying degrees of vulnerability.

Recently, microscopic investigations using stereological analysis revealed that although SIDS infants may appear clinically normal upon pathological analysis, some infants are in fact developmentally compromised and are associated with abnormalities in many of their organs that are critical for survival ex utero including the lung, kidney, diaphragm, phrenic nerve and brain (73; 79; 80). Similar developmental abnormalities are also seen in organs from infants who are growth restricted and as such, SIDS and IUGR are intricately linked; approximately twice the number of infants who die from SIDS have a birth weight below the 10^{th} centile for gestational age (55; 81), hence an IUGR infant is twice as likely to die from SIDS. These developmental abnormalities occurring in utero may therefore place the infant under increased physiological demand postnatally, and when combined with external stressors during a critical developmental period, the vulnerable infant may succumb to sudden and unexpected death.

Similar to pre-eclampsia and IUGR, it can be hypothesised that the origin of these developmental abnormalities is placental insufficiency (82). Given that fetal organogenesis takes place in utero which cannot be compensated for postnatally, any detrimental insult occurring in the transfer capacity of the placenta may potentially lead to delayed or arrested fetal organogenesis in utero placing the compromised infant at risk of SIDS. As such, abnormalities in both placental villous and vasculature are observed in both SIDS-NBW and SIDS-IUGR infants, indicating a possible effect of SIDS independent of birthweight (82).

1.4 Current Placental Hypothesis

Although the clinical manifestations of pre-eclampsia and IUGR are not evident until the second half of pregnancy, early defects in implantation and placentation during the first trimester, resulting in defective uteroplacental blood flow in the second and third trimester, are thought to underpin the pathological processes of these placentally-mediated diseases. Despite this common etiology, the placental villi of pre-eclampsia respond completely differently to the small, maldeveloped villi characteristic of normotensive IUGR. Crucially, this divergence is now thought to result from defects in proper differentiation of the trophoblast cell lineage.

1.4.1 Placental Development in Humans

1.4.2 The Human Placenta

Successful pregnancy is completely dependent upon successful placental development, without the placenta, pregnancy is not viable. Human gestation lasts an average of 40 weeks and during this time the placenta acts as the only organ of exchange between the mother and the fetus, providing nutrition (glucose, amino acids), respiration (oxygen, carbon dioxide) and excretion (waste products) (83). The specialized cells of the placenta, derived from the trophoblast lineage, are responsible for the production and regulation of proteins, peptides and hormones which are necessary for both its own growth, but also that of the fetus. The human placenta thus represents a self-sufficient, self-renewing organ capable of modulating its own growth and function whilst assisting that of the developing fetus.

Placental development is designed to anticipate the exponential growth of the fetus via an adequate supply of oxygen and nutrients from maternal blood throughout gestation. The human placenta therefore functions as a fetomaternal organ with two components, the fetal portion (chorion frondosum) and the maternal portion (decidua basalis) (Figure 1-2). During the first and second trimester of pregnancy, the placental villi proliferate and differentiate to establish both the uteroplacental (anchoring villi), and fetoplacental (floating villi) circulations within the villous trees, which is achieved via cells from the trophoblast lineage. Floating villi comprise an elaborate network of specialized ‘tree-like’ structures that are responsible for all fetoplacental exchange; these are the

chorionic villi which emerge from the fetal chorionic plate (fetal surface) and float in the intervillous space (IVS) filled with maternal blood (84).

Each villus comprises an outer epithelial trophoblast layer (the villous trophoblast) and a central core of fetal vascular endothelium (connected to the fetal circulation by two umbilical arteries and one vein in the umbilical cord), and a population of stromal cells (allantoic mesoderm). In the third trimester, growth of the placenta changes towards the development of the gas-exchanging villi, which comprise a large network of sinusoidally-dilated terminal villi capillaries through which oxygen and nutrients diffuse from the maternal blood into the fetal circulation (85).

The mature placenta comprises approximately 15-20 cotyledons (two or more primary stem chorionic villous branches and corresponding secondary and tertiary branches) that are suspended in the trophoblast-lined IVS. Each cotyledon is supplied with maternal blood from the uterine spiral arteries located in the uterus (85).

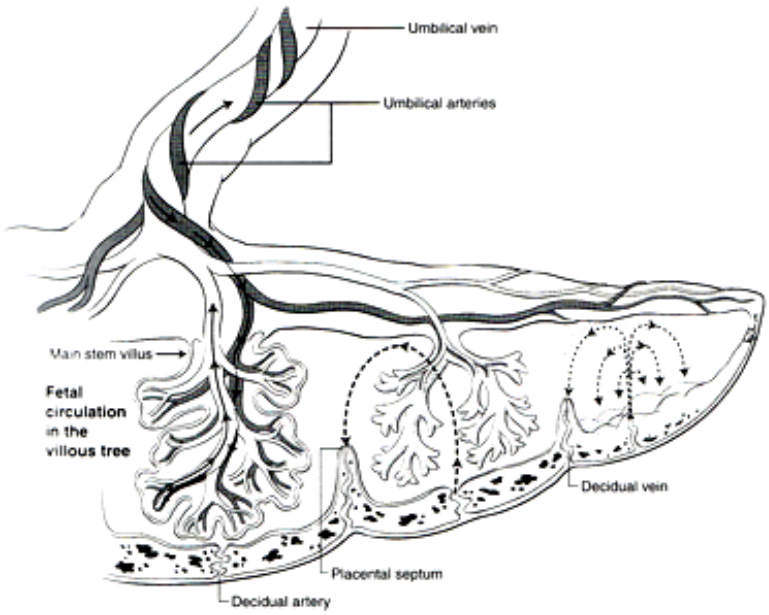

Figure 1-2 Anatomy of the human placenta

Each fetomaternal circulatory unit is composed of one villous tree with a corresponding centrifugally perfused portion of the IVS. This unit is called a placentone. Maternal blood (arrows) enters the IVS near the centre of the villous tree (decidual artery) and leaves near the clefts of neighbouring villous trees (decidual vein). One or only a few villous trees occupy one placental lobule (cotelydon) (adapted from (85)).

1.4.3 Early Events in Placentation: the First Trimester

The human placenta develops from the sperm and the egg that also forms the fetus. After fertilization, the human zygote undergoes a series of symmetrical mitotic divisions forming a mass of totipotent blastomere cells (the morula) which differentiate into embryonic and extra-embryonic tissues. Differentiated cells of the inner cell mass, or embryoblast (EB), go on to form the embryo, umbilical cord, amnion, blood vessels and connective tissue of the chorionic villi, whilst cells of the outer wall, the trophectoderm, surround the blastocyst cavity and go on to form the trophoblast cell lineage and the placental villous trees (85).

Placentation begins with implantation of the blastocyst beneath the maternal uterine epithelium (at around day 7 post conception, PC), which is achieved through invasion of the outer trophoblast cells into the uterine lining (85). Here, trophoblast cells from the embryonic pole of the blastocyst rapidly proliferate forming a trophoblastic cell mass which differentiates into two distinct layers, an outer syncytiotrophoblast layer (SCT), which expands via fusion of underlying proliferating cytotrophoblast cells (CT). The syncytiotrophoblast shell invades and interdigitates the maternal endometrial epithelium forming a series of lacunae which coalesce to become the forerunner of the maternal blood-filled IVS (85).

Proliferating cytotrophoblast cells from the chorionic plate then invade the trophoblastic shell forming trophoblastic protrusions into the lacunae, generating primary villi composed of an outer syncytiotrophoblast layer and an inner cytotrophoblast core, which are then invaded centrally by allantoic mesenchyme (stroma) transforming them into secondary villi (Figure 1-3). Formation of the fetoplacental blood vessels within the stroma, connected proximally to the umbilical arteries, characterizes their transition to tertiary villi which are the forerunners for the development of all floating chorionic villi; the first generations of which are the mesenchymal villi (86). These ‘tri-layered’ villi are therefore composed of 1) an outer syncytiotrophoblast layer in direct contact with maternal blood (hemochorial placentation), 2) an underlying proliferative cytotrophoblast layer, and 3) a stromal core containing the primitive fetal vasculature and stromal cells (Hofbauer cells and fibroblasts) (84).

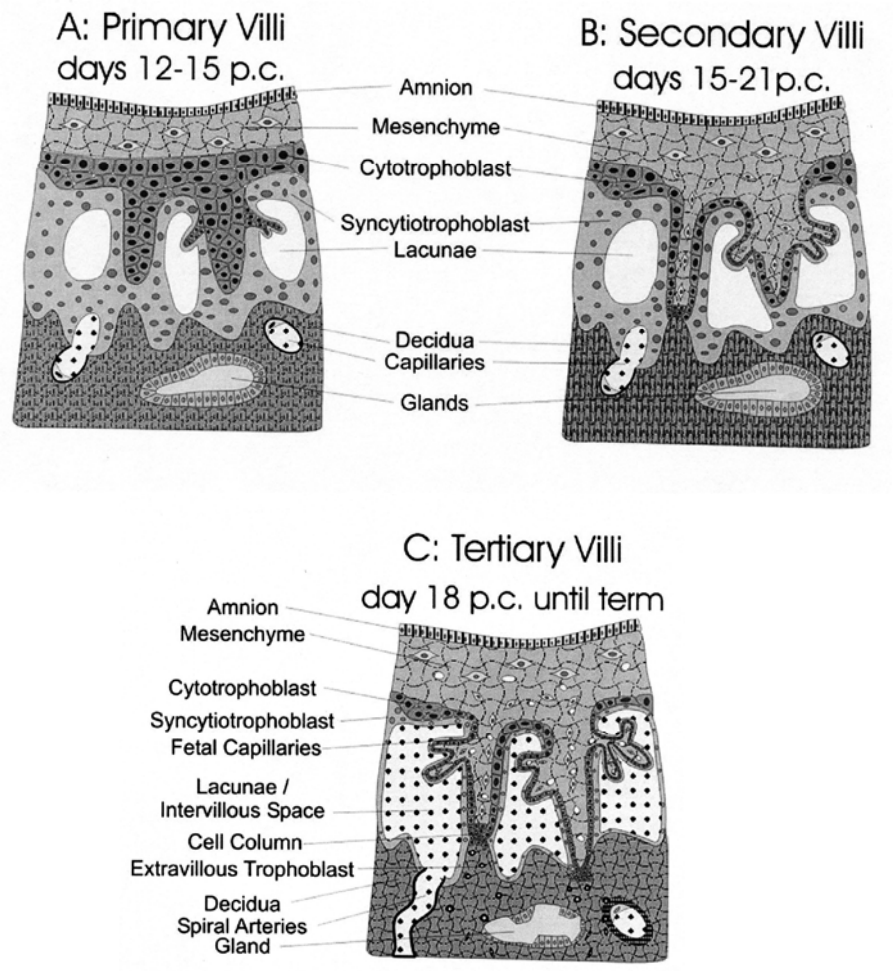

Figure 1-3 Early placental development

(A) At around 12-15 days PC, primary villi are formed as columns of cytotrophoblast cells in the centre covered by an outer layer of syncytiotrophoblast. (B) These columns are then invaded centrally by extra-embryonic mesenchyme (around day 15-21 PC) leading to the formation of secondary villi. (C) The formation of placental blood vessels (vasculogenesis) within the secondary villi transforms them into tertiary villi beginning around day 18 PC (145).

1.4.4 Extravillous Cytotrophoblast Invasion

Those cytotrophoblast cells that penetrate beyond the syncytiotrophoblast shell, having adopted an invasive extravillous cytotrophoblast (EVT) phenotype, move through the syncytium at selected sites forming a cytotrophoblast shell thereby physically attaching those villi to the maternal uterine wall; the so-called cell columns of the anchoring villi (Figure 1-3).

Immediately following their invasion through the syncytiotrophoblast shell, proliferating cytotrophoblast progenitor cells from the proximal portion of the cell columns of the anchoring villi differentiate into two distinct subsets of EVT. These cells display invasive phenotypes that enable invasion, penetration and remodelling of the maternal spiral arteries thereby rerouting maternal blood to the implantation site. This is crucial to successful pregnancy outcome.

There are thought to be two routes of EVT invasion (87). Interstitial EVT invades the decidua stroma (and inner third of myometrium) where they surround the spiral arteries (they do not invade the arteries) and replace the vascular media with matrix-type fibrinoid material converting the spiral arteries into large, dilated vessels of low resistance (88). In contrast, in what is thought to be a separate pathway, endovascular EVT invade the lumen of the spiral arteries where up until the 12th week of gestation, they form an 'endovascular plug' thereby preventing maternal blood from entering the developing IVS, which then migrate in a retrograde fashion (89). The physiological significance of endovascular plugging serves to maintain a 'hypoxic' environment relative to maternal tissues (90), which is essential for fetoplacental angiogenesis of early tertiary villi, the regulation of key cellular events involved in trophoblast differentiation and crucially, fetal organogenesis in utero (90-93). Regression of the endovascular plug at around 10-12 weeks gestation establishes the maternal-fetal circulation (94).

Further differentiation of the EVT occurs and intramural EVT (whether these are derived from endovascular or interstitial EVT remains unclear) infiltrate the walls of the spiral arteries transforming them into uteroplacental vessels, whilst intra-arterial EVT replace the endothelium having adopted a 'vascular' endothelial phenotype. Transformation of these musculoelastic vessels into distended flaccid vessels, plus considerable increase in luminal diameter allows for significantly decreased uteroplacental flow resistance allowing maximal maternal blood flow to the feto-placental unit throughout gestation (95).

Subsequent steps in placentation, and hence fetal viability at the end of the first trimester, is therefore dependent upon the commitment of the trophoblast lineage along two pathways in the 3rd week PC; the EVT which invade the maternal spiral arteries to

promote maternal blood to the intervillous space and the secondly, the villous trophoblast responsible for growth and maintenance of the floating chorionic villi throughout gestation.

1.4.5 Development of the Chorionic Villi

The second trimester of pregnancy marks the beginning of the fetal phase of development in which uteroplacental and fetal circulations commence in preparation for rapid fetal growth. This is accompanied by rapid linear growth and differentiation of the different chorionic villi involving both hyperplastic growth of the villous trophoblast layer and angiogenesis of the underlying fetal vasculature. Coordinated development of the chorionic villi is fundamental to successful pregnancy outcome and subsequently perinatal survival since they are the primary site of all fetoplacental diffusive and active transport between mother and fetus.

Growth and differentiation of the villous trees is geared towards the exponential evolution of the gas-exchanging terminal villi (TV), which are the principal anatomical site of maternal-fetal exchange where growth occurs exponentially throughout the third trimester. At term, their surface area available for exchange reaches $13m^2$ and their capillaries contain 25% of total fetoplacental blood volume (96).

To achieve this, sufficient generations of dichotomous branches, the so-called stem villi (SV), are required to provide the necessary framework leading into these gas-exchanging villi. Stem villi are formed from immature intermediate villi (IV) in a gradual process beginning around the 8^{th} week PC. Here, mesenchymal villi continue to develop from tertiary villi and transform into IV up until the end of the second trimester, predominating between 14 and 20 weeks when the formation of stem villi is most intense. New mesenchymal sprouts form from the tips of IV to continue the cycle of self replication (97). IV are transformed proximally through the formation of muscularised medium into stem villi, characterized by the differentiation of capillaries into arterioles and venules, regression of the capillary network and fibrotic condensation of the loose stroma; participation in maternal-fetal exchange is therefore minimal. No defined function of IV has yet been elucidated except that they act as the ‘growth zone’ of the

developing villous tree, and thus has some involvement in controlling the final size of the villous tree (84; 86).

The third trimester of pregnancy marks the period of rapid fetal growth and maturation in preparation for the transition from intrauterine to extrauterine environments. During weeks 21 to 25 PC, substantial fetal weight gain occurs and as such there is a gradual switch in emphasis from formation of conductance vessels in stem villi to the formation of gas and nutrient exchanging villi, the mature intermediate (MV) and terminal villi (85; 86; 98) (Figure 1-4).

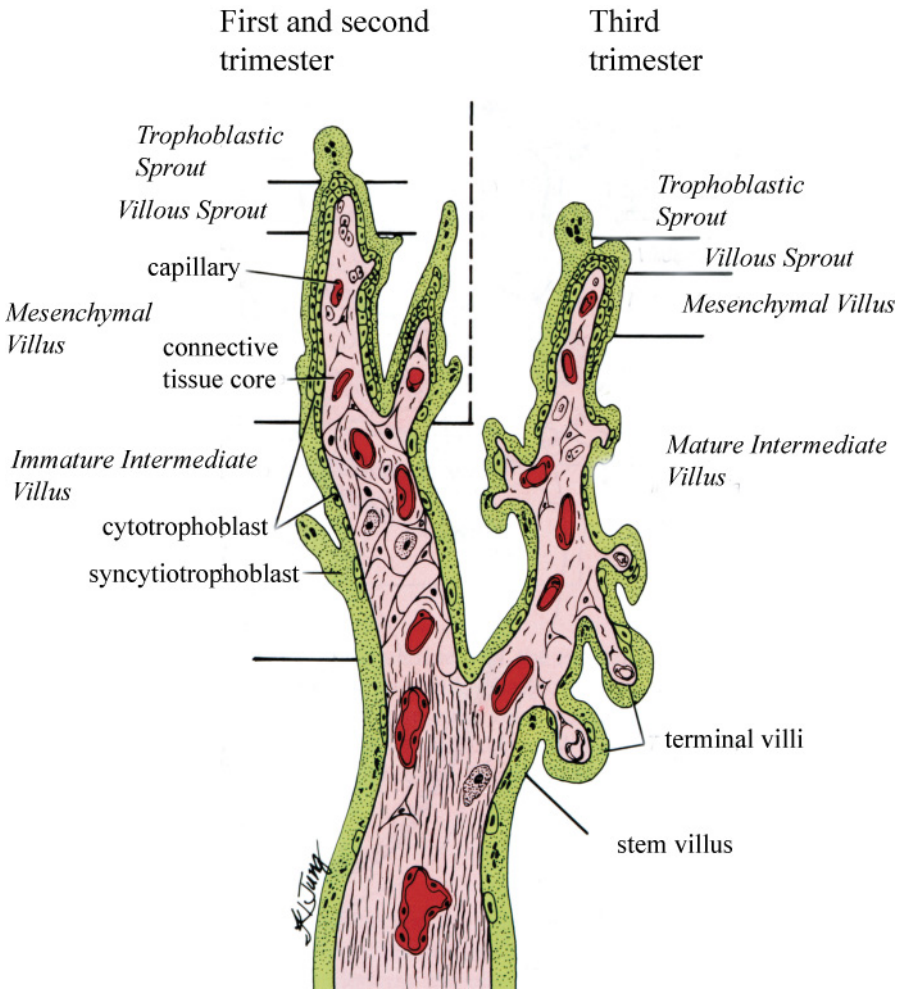

Figure 1-4 Development of the chorionic villi

Starting in the ninth week, tertiary stem villi are transformed (via mesenchymal sprouting) into immature intermediate villi. Near the end of the second trimester, mature intermediate villi develop from the sides of the tertiary stem villi. By week 32, mature intermediate villi produced small nodule like secondary branches called terminal villi (99).

At around 24 weeks gestation, mesenchymal villi switch from forming IV to form MV. Regeneration of the IV thus ceases and those remaining immature intermediate villi continue to differentiate into stem villi until term (85). MV do not self-replicate or go on to form stem villi, instead they elongate and produce terminal villi by 'intussusception" (non-branching angiogenesis) in which longitudinal growth of the fetal capillaries in the MV exceeds longitudinal growth of the villi itself (98). Consequently, the capillary loops 'prolapse' laterally into the overlying trophoblast layer of the MV resulting in thinning of the trophoblastic surface, bringing the fetal circulation close to maternal blood separated only by a thin layer of syncytiotrophoblast, the vasculo-syncytial membrane (100). Formation of these serial sinusoidal dilations which form the terminal villi are of critical importance in achieving low fetoplacental vascular impedance in the third trimester allowing for optimal diffusional exchange. It is the maldevelopment of these structures that underpins the villous pathology of IUGR.

1.4.6 Angiogenesis

Numerous investigations report that villous angiogenesis drives villous development (101), and it is well established that disruptions in villous angiogenesis result in altered villous growth (102; 103). The principle angiogenic regulators of these developmental steps are vascular endothelial growth factor (VEGF) (104), placenta-like growth factor (PGF) (105) and the angiopoietins (Ang-1, Ang-2) (106), all of which are themselves regulated by oxygen availability.

During the first and second trimesters of pregnancy, the fetal vasculature develops predominately by branching angiogenesis. Endothelial tube formation (vasculogenesis (107)) and proliferation is induced by binding of VEGF to its receptors VEGFR-1 (flt-1) and VEGFR-2 (KDR) respectively (108). VEGF is highly expressed in villous cytotrophoblast and stromal macrophages (Hofbauer cells) (109) and is induced under hypoxic conditions by hypoxia-inducible transcription factor 1 (HIF-1) (110); circulating VEGF can be detected in the maternal plasma at 6 weeks of gestation and rises to a peak at the end of the first trimester (111).

During the third trimester of pregnancy, a switch occurs in the expression of the angiogenic growth factors whereby the fetal vasculature develops via non-branching

angiogenesis. Whilst VEGF secretion predominates during the first and second trimesters, PGF is the predominant angiogenic growth factor during the third trimester (112). In contrast to VEGF, oxygen is a potent stimulator of PGF (113) which induces endothelial tube formation through binding to VEGFR-1; synthesis is localized to the villous and extravillous trophoblast (105).

The VEGF/PGF interchange coincides with the switch from predominantly branching to non-branching angiogenesis at around 25 weeks PC (114). VEGF/PGF directed vasculogenesis and angiogenesis may therefore shape villous tree development and its morphology may reflect the underlying angiogenic process (115; 116). For example, branching angiogenesis drives immature intermediate villi growth, which are characteristically large bulbous structures covered by a thick trophoblast layer containing central stem vessels. In contrast, non-branching angiogenesis drives mature intermediate and terminal villi growth which are filiform structures covered by a thin trophoblast layer and tightly coiled capillaries. This suggests that the trophoblast displays some degree of 'plasticity', which may adapt with, or in response to, the underlying angiogenic architecture.

1.5 Defective Placentation in PET and IUGR

1.5.1 Physiological Conversion of Maternal Spiral Arteries

Physiological conversion of the maternal uterine spiral arteries is essential in promoting effective uteroplacental blood supply to the fetal villi at the end of the first trimester, and is achieved by cells from the extravillous cytotrophoblast lineage (85; 87; 95; 117). Maternal blood flow to the human placenta does not begin until 10 to 12 weeks gestation (118), which is prevented from entering the developing IVS by the endovascular plug. Oxygen tension plays a key role in early placental development and EVT invasion, and thus, oxygen is important physiological factor for formation of the maternal-fetal interface and hence, fetal growth (119).

Studies have shown that cytotrophoblasts have the ability to sense oxygen, whereby cytotrophoblasts proliferate under hypoxic conditions. As EVT invade the uterus they encounter increasing levels of oxygen which triggers their exit from the cell cycle and differentiation into the various EVT phenotypes occurs (91; 119) (Figure 1-5). These

cells must continuously invade and physiologically transform the distal myometrial portions of the maternal spiral arteries from the non-pregnant state during the first trimester, into widely dilated flaccid conduits capable of delivering large quantities of maternal blood to the intervillous space in order to meet the exponential demands of the rapidly growing fetus during the second and third trimester. Vascular transformation is thought to involve all 100-150 spiral arteries in the placental bed (120).

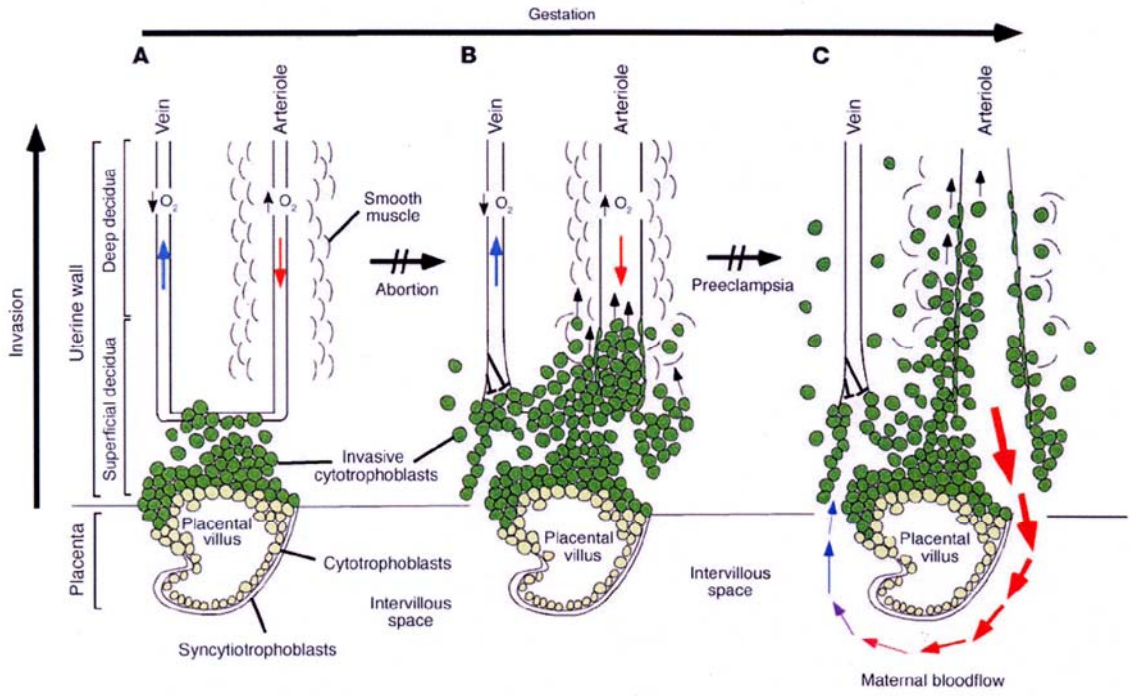

Figure 1-5 Extravillous cytotrophoblast invasion of the maternal spiral arteries

Early placental development occurs in a relatively hypoxic environment (A) that favours CT proliferation rather than differentiation along the invasive pathway. (B) Proliferating CT cells invade the uterine wall and form an endovascular plug (dark green cells). (C) By 10 to 12 weeks, maternal blood flow to the IVS begins and EVT cells continue to migrate along the lumina of the spiral arteries where they replace the endothelial cell lining (adapted from (119)).

In those pregnancies destined to develop pre-eclampsia, placental bed biopsies (although these may not reflect global changes in the placental bed) demonstrate varying degrees (within and between placentas) of defective EVT invasion and failure to physiologically convert the maternal spiral arteries (121-123) (Figure 1-6). Failed physiological conversion has also been demonstrated in some, but not all IUGR pregnancies where IUGR was defined as a birth weight of less than the 10th centile for GA (i.e. SGA). However, SGA infants below the 2.3th centile (high risk of IUGR) exhibit a strong association with failed conversion (123). In both normal and

pathological placentas conversion is maximal in the central bed vessels (124). Failure to transform the arteries in the first trimester is thought to result in defective maternal blood flow to the IVS (125), which in turn, is evidenced *in vitro* to result in hypoxic damage and ischemia-reperfusion injury to the developing chorionic villi (126) and in the most severe cases, chronic fetal hypoxia (127).

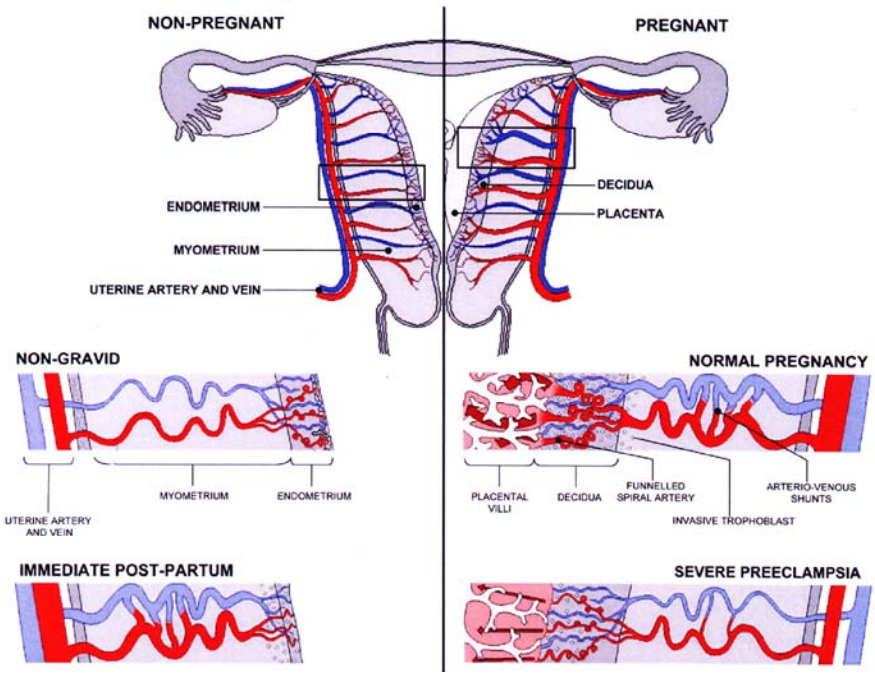

Figure 1-6 Failed spiral artery remodelling in pre-eclampsia

Diagrammatic representation of the uterine vasculature in human pregnancy. Normal pregnancy is characterised by large arterio-venous shunts, which by contrast are minimal in pre-eclampsia with narrower uterine arteries. Depth of trophoblast invasion is also minimal in comparison to normal pregnancy (Adapted from (128)).

Whether defective trophoblast invasion is a primary cause of reduced blood flow *per se,* or whether the placenta is at all hypoxic has recently been debated (128). Nonetheless, the prevailing placental hypothesis still holds that reduced trophoblast invasion and spiral artery transformation, resulting in the clinical entity of 'uteroplacental insufficiency' (129), are key pathological features underpinning pre-eclampsia and IUGR.

1.5.2 Defective EVT Differentiation

Current studies focussed on pre-eclampsia and failed EVT invasion are aimed towards elucidating a link between abnormal EVT invasion and the maternal vascular syndrome. The currently accepted hypothesis is that pre-eclampsia, (particularly severe early-onset disease requiring preterm delivery) is associated with defects in extravillous cytotrophoblast differentiation leading to an altered EVT phenotype with subsequent reduced uterine invasion. Morphologically, placental bed biopsies typically reveal decreased numbers of interstitial EVT around the decidual arteries (130) and rudimentary endovascular EVT invasion of the myometrial spiral arteries (124). The dominant 'pre-eclamptic phenotype' comprises immature, hypoinvasive and pseudo-proliferative extravillous cytotrophoblast cells (88; 95; 117).

1.5.2.1 Altered EVT Phenotypes in PET

Migration and invasion of cytotrophoblasts into the decidua and maternal spiral arteries requires that cytotrophoblasts differentiate thereby adopting an invasive 'vascular-like' phenotype, which is controlled by intrinsic EVT factors (enzymology of adhesion molecules and extracellular matrix degradation (ECM)) and secondly by extrinsic maternal uterine factors (e.g. impaired decidual remodelling, impaired function of uterine natural killer cells (NK)) (89).

Zhou *et al* were the first to describe the failure of cytotrophoblasts to acquire a vascular repertoire of adhesion molecules in pre-eclamptic placentas (131). In pre-eclampsia, cytotrophoblast progenitor cells at the distal cell columns fail to undergo an epithelial (endoderm) to endothelial (mesoderm) transformation. Cytotrophoblasts fail to switch a repertoire of adhesion molecules necessary for invasion of the spiral arteries, such as failure to down regulate expression of E-cadherin (proliferative phenotype) and α6β4 integrin, and therefore persist as a more proliferative population compared to normal pregnancy. In essence, they fail to replace their epithelial-like receptors and turn on receptors that promote invasion through endothelial vascular adhesion molecules characteristic of differentiating/invading cytotrophoblasts, such as α5β4 and α1β1 integrins, VE-cadherin, VCAM-1 and PECAM-1 (88; 132).

The expression of various growth factors involved in regulating the invasive pathway is also impaired in pre-eclampsia including *in vitro* over-expression of TGF-β_3, an inhibitor of migration, and IGFBP-1 *in vivo,* which led to altered trophoblast invasion and differentiation (88). Enzymatic degradation of the ECM necessary for migration is also defective in pre-eclampsia as trophoblasts fail to up regulate MMP-9 (matrix metalloproteinase 9), a proteinase closely associated with the invasive phenotype of trophoblast (88). Furthermore, numbers of invading endovascular (intramural) EVT are reduced in early-onset pre-eclampsia with IUGR due to reduced numbers of interstitial EVT and excessive endovascular EVT apoptosis; increased numbers of activated maternal macrophages expressing pro-apoptotic TNFα and TNF-R1 have been described close to the implantation site (117; 122).

However, can this phenotype be linked to the maternal symptoms of pre-eclampsia? Consistent with the hypothesis that pre-eclampsia is associated with failure to adopt an vascular EVT adhesion phenotype, observations that extravillous cytotrophoblast cells down regulate vascular endothelial growth factor (VEGF) *in vitro* (28; 133), have led to the concept that as well as mediating vasculogenesis and angiogenesis during vessel remodelling, VEGF also plays a pivotal role in EVT migration and spiral artery invasion (94; 133-135).

Invasive cytotrophoblast cells during early gestation express VEGF-A, VEGF-C, and PGF, and their receptors VEGFR-1 (flt-1) and VEGFR-3, and at term VEGF-A, PGF and VEGFR-1 (136). Significantly, invasion and migration of EVT were suppressed when VEGF receptor binding and signal transduction were blocked by receptor fusion proteins. Specifically, in pre-eclampsia, VEGF-A is down-regulated in EVT, whilst secretion of a truncated form of the receptor VEGFR-1, soluble fms-like tyrosine kinase 1 (sFlt-1) *in vitro* is increased (137). In normal pregnancy, circulating sFlt-1 levels increase throughout gestation and binds VEGF and PGF with high affinity, thereby decreasing availability to the trans-membrane receptors VEGFR-1 and VEGFR-2. Presumably, the decrease in EVT VEGF-A expression and increase in the sFlt-1 receptor that sequesters VEGF reduces the bioavailability of VEGF required for EVT migration and invasion of the uterine spiral arteries (138). This provides direct evidence supporting the theory that failed cytotrophoblast invasion and pseudovasculogenesis are linked through abnormal VEGF production to the maternal vascular pathology. Soluble

Flt-1 has therefore become a strong candidate as a pathogenic mediator of the pre-eclamptic syndrome, and a promising predictive marker of pre-eclampsia in high-risk women in the first trimester (139).

1.5.3 Placental Pathology

The placental bed in early-onset pre-eclampsia and IUGR display a range of arterial disease associated with defective maternal blood supply, collectively referred to as decidual vasculopathy, including failed transformation of the uteroplacental arteries, acute atherosis and luminal thrombosis of the maternal vessels (140). Non trophoblast-invaded vessels retain their smooth muscle media and fail to undergo further vasodilation such that uteroplacental vascular resistance remains high (128). As a result, the same volume of maternal blood may enter the IVS but due to the narrowed arteries does so at greater velocity in jet-like streams, potentially disrupting the villous branches and anchoring villi, which is thought to essentially push the placenta up thereby accounting for its "wobbly, jelly-like" appearance (128), which can be seen as early as 14-15 weeks of gestation (141). The resultant changes in intervillous haemodynamics will therefore impair maternal-fetal diffusional exchange and may account for the higher than normal oxygen levels in the uterine vein in severe early-onset IUGR pregnancies (142).

The reduction in uteroplacental blood flow associated with early-onset pre-eclampsia and IUGR can be quantified using colour imaging from pulsed Doppler waveforms as an assessment of the blood flow within the proximal uterine arteries (143; 144). In normal pregnancy, endovascular EVT regression permits maternal blood flow in the uterine arteries by 12 weeks gestation, represented by positive end diastolic flow velocity waveforms (PEDFV), indicating adequate trophoblast invasion and spiral artery remodelling. In the most severe forms of placental insufficiency (i.e. early-onset pre-eclampsia and IUGR delivering <32 weeks), end diastolic flow is persistently absent or even reversed in the uterine arteries (mean pulsatility index >1.45 and/or early diastolic notches) (140), signifying high resistance in the uteroplacental circulation and is therefore an indirect sign of inadequate trophoblast invasion which also correlates well with decidual vasculopathy (145). Since these pathological conditions do not correlate with maternal or fetal thrombophillia disorders, it suggests that the gross pathological

changes to the placental gas-exchanging villi in PET and IUGR are a result of the reduction in uteroplacental circulation (146).

Conversely, abnormal uterine artery Doppler (UTAD) may not necessarily confer malinvasion of the uteroplacental arteries since power Doppler ultrasound and vascular-enhanced uterine artery MRI have recently shown that most of the uterine artery blood flow in the second trimester does not enter the IVS. Instead most of the maternal blood is shunted away from the myometrium (147) and although the involvement in trophoblast invasion is unclear (146), shunting is thought to represent a physiological mechanism to reduce maternal systemic vascular resistance. Hence, in pre-eclampsia and IUGR, changes in UTAD may be the result of arterio-venous fistulas within the uterine myometrium and not due to malinvasion (146). Moreover, this also suggests that EVT promote uterine artery blood flow by additional pathways other than by anatomical erosion of the arterioles, supported by observations that interstitial EVT secrete angiogenic and vasodilatory factors that increase local blood flow to the uterus but also maternal cardiac output, whilst decreasing blood pressure due to systemic vasodilation. Thus, increased blood pressure in the second trimester may result from defects in these pathways.

Uteroplacental insufficiency also confers a high risk of damage to the placental villi, since abnormal UTAD correlates well with thrombotic pathological findings of the placental villous trees (148; 149). Narrow and/or diseased spiral arteries may thrombose, secondary to failed physiological conversion, which as a secondary pathology may lead to poor maternal perfusion of the placenta, leading to focal infarction of placental villi (tissue death due to lack of blood supply) necessary for maternal-fetal gas and nutrient exchange (141). Furthermore, focal accumulations of fibrin around villi (perivillous) and intervillous thrombosis are all typical thrombotic pathological features of the placental villous trees associated with severe placental insufficiency (129). Reduced uteroplacental blood flow is not however a precondition for placental insufficiency as increased fractional oxygen extraction by the chorionic villi, as part of a sustained adaptive response, may preserve placental supply and fetal demand as pregnancy progresses (116; 150). By contrast, these findings are minimal or absent in pre-eclampsia and IUGR at term (140). Furthermore, intermittent spiral artery blood flow resulting in ischemia-reperfusion injury may lead to oxidative stress of the

fetal endothelium and necrotic shedding of trophoblast within the placental villi associated with maternal endothelial dysfunction in pre-eclampsia (126; 151).

1.5.4 Villous Maldevelopment

It is well established that development of the chorionic villous tree and fetal vasculature is abnormal in PET and IUGR (1; 2; 152) compared to normal pregnancy, and more recently in placentas from infants succumbing to SIDS (82). Consistent with the clinical implications, it has become apparent that the severity, timing-of-onset, and umbilical artery Doppler (absent versus positive) are associated with divergent pathways of villous maldevelopment in these pregnancy complications. Given that PET and IUGR are both associated with uteroplacental insufficiency, the placenta responds differently to the expected 'intra-placental hypoxia'. Oxygen is therefore a key regulator of villous development and different pathways of villous maldevelopment have been proposed based on the origin of fetal hypoxia (153).

Following analysis of placental villi in complicated pregnancies, the origin of fetal hypoxia has been classified as pre-placental, uteroplacental, or post-placental (153). In pre-placental hypoxia, the mother, placenta, and fetus are potentially hypoxic due to a reduced oxygen content of the maternal blood, such as in pregnancy at high altitude and maternal anaemia (103). In contrast, in uteroplacental hypoxia, maternal blood flow is normoxic but the placenta and fetus may become hypoxic due to compromised flow into the IVS, i.e. malinvasion of the maternal spiral arteries. In post-placental hypoxia, maternal blood flow is normal in combination with normal or reduced flow into the IVS, but a severe defect in fetoplacental perfusion prevents the fetus from receiving sufficient oxygen, and hence is at serious risk of becoming hypoxic (153).

1.5.4.1 IUGR

In situations of pre-placental hypoxia or uteroplacental hypoxia, the placenta may undergo excessive branching angiogenesis and trophoblast proliferation in order to produce greater amounts of vascularised terminal villi as part of an adaptive response so as to maintain adequate fetoplacental diffusional exchange; maternal supply and fetal demand are therefore carefully balanced by the development of the terminal villi. This type of villous adaptation is associated with late-onset pre-eclampsia (154), and in some

but not all cases of IUGR (150), which have been shown to display increased capillary volume fractions, and degree of branching (for review see (155)). Because such changes are not observed in severe early-onset IUGR, these placentas are thought to represent 'failure to adapt', since they appear to have lost their 'hypoxic' angiogenic drive (153) conferring severe functional consequences to the potentially hypoxic fetus (post-placental hypoxia).

Stereological and morphometric analyses have led to the agreement that the small placentas from IUGR pregnancies are associated with a failure in the development of the gas-exchanging villi, due to malformation of the fetal capillaries in terminal villi secondary to failed branching angiogenesis in the third trimester of pregnancy and the predominance of non-branching angiogenesis. Stereological studies reveal consistent reductions in the elaboration of mature intermediate and terminal villi (102; 152; 156-159) (volumes, surface areas, and lengths) and reduced terminal villous capillarisation (160; 161). 3D scanning electron microscopy and vessel casts confirmed reductions in the numbers of 'malformed' (1), congested, elongated, poorly-branched gas-exchanging villi and underlying fetal vasculature (2). These observations are evident in placentas from both early- (2; 152) and late-onset IUGR (102; 152; 156-159; 161; 162).

The malformed capillaries in severe IUGR placentas confer *high vascular impedance* which is associated with abnormal umbilical artery Doppler (150), representing a severe form of reduced fetoplacental blood flow inferred by absent or reverse end-diastolic flow velocity waveforms (AREDV). Those pregnancies destined to develop severe IUGR are therefore typically associated with severe abnormalities in umbilical artery Doppler, which has become an established test of fetal wellbeing in the second trimester of pregnancy (19-23 weeks) (129).

The compromised fetoplacental circulation is understood to result in reduced extraction of oxygen from maternal blood in the intervillous space leading to poor oxygenation of the severe IUGR fetus (hence the term postplacental fetal hypoxia), evidenced by the inability of the IUGR placenta to maintain adequate transfer of oxygen/nutrients to the fetus (reduced oxygen diffusive conductance, D_p) (159; 163). Consequently, IVS oxygen levels remain similar, but not higher than maternal arterial tensions, such that the oxygen content of maternal blood exiting the uterine veins is close to arterial values

(142). This led to the term placental 'hyperoxia', although this is still debated by some investigators (Figure 1-7).

Given that angiogenesis shapes villous development, the pathway of villous maldevelopment in severe early-onset IUGR is associated with changes in the molecular regulation of the principal angiogenic factors, VEGF and PGF. Whilst in normal pregnancy VEGF predominates in the first trimester and PGF predominates in the third, IUGR placentas demonstrate increased expression of PGF (113) (mRNA and protein) and decreased syncytial expression of VEGF (164). Because PGF mediates non-branching angiogenesis, this imbalance in angiogenic factors is thought to contribute to the poorly branched, elongated gas-exchanging villi that characterize IUGR pregnancies.

1.5.4.2 PET

Although pre-eclampsia is the most extensively studied pregnancy complication at term, its influence/impact on placental morphology is inconsistent and less well understood in early pregnancy. Severe early-onset pre-eclampsia, by definition, often co-exists with IUGR, conferring significant risk for perinatal survival compared to term complications. Distinguishing the contributions of each disease on the pathway(s) of villous maldevelopment is thus hampered by this close association, but is presumed to involve considerable overlap. Consequently, the majority of stereological studies addressing the pathways of placental dysfunction in pre-eclampsia without IUGR focused on term pregnancies which revealed conflicting results.

Initially, stereological studies revealed one distinct pathway of placental dysfunction in pre-eclampsia compared to IUGR. At term, pre-eclamptic placentas displayed normal (102; 156; 161; 165) or 'enhanced' placental villi and vasculature morphology e.g. increases in terminal capillarisation (adaptive branching angiogenesis due to intra-placental hypoxia), placental volume and fetal birth weight in comparison to normal term controls. This led to the prevailing hypothesis that 'pure' pre-eclampsia at term has no overall effect on placental villous and vasculature development in comparison to IUGR. Furthermore, these placentas are typically associated with normal Dopplers represented clinically by preserved end-diastolic blood flow velocity waveforms

(PEDV) conferring minimal vascular impedance (153). IUGR at term is typically, but not exclusively, associated with normal umbilical artery Dopplers indicating normal fetoplacental blood flow associated with favourable perinatal outcome.

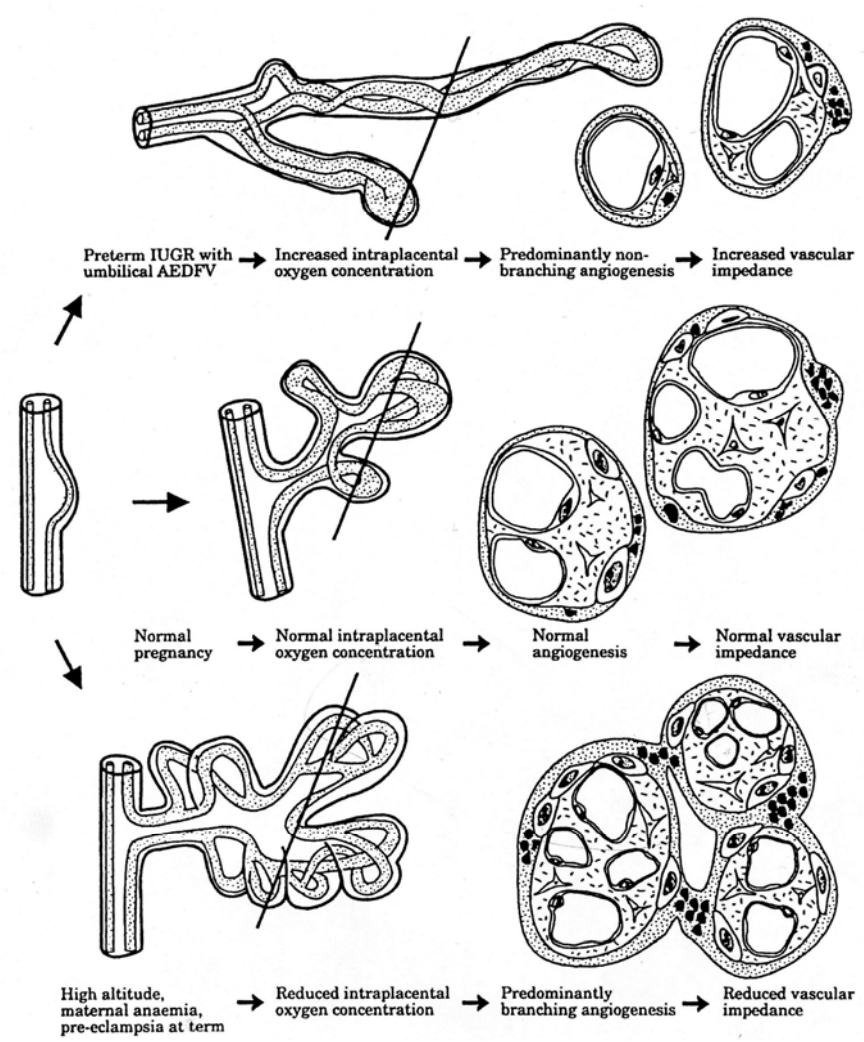

Figure 1-7: Pathways of villous maldevelopment

Pathways of villous angiogenesis according to villous oxygenation. Three different examples of oxygenation, postplacental hypoxia (top), normal pregnancy (middle) and pre-placental as well as uteroplacental hypoxia (bottom) are illustrated by their terminal capillarisation patterns (left) and by typical cross sections of terminal villi (right). The oblique lines refer to the position of the cross sections beneath (153).

Molecular evidence for intra-placental hypoxia in pre-eclampsia at term, (representing a form of uteroplacental hypoxia), came from the observation that expression of the hypoxia inducible transcription factors, HIF-1α and HIF-2α, is significantly increased in these placentas. However, due to the difficulty of measuring serum levels of VEGF (normal or increased) and PGF (normal or decreased), there are inconsistencies in the reported expression of these angiogenic factors in pre-eclampsia at term (155).

This concept was challenged by Egbor *et al* (152) who identified two distinct pathways of villous maldevelopment in pre-eclampsia, illustrating that early-onset pre-eclampsia without IUGR shares similar morphological features to the maldeveloped villi that are typically observed in both early- and late-onset IUGR placentas . This led to idea that the early phenotype of PET may have a different etiology compared to its late-onset phenotype, and that they may represent two different diseases.

1.5.4.3 SIDS

Protracted intrauterine hypoxia occurring during fetal development is also thought to be a primary pathophysiologic factor in SIDS (166). SIDS placentas may represent a form of pre-placental hypoxia due to the high incidence of maternal smoking associated with SIDS. However, previous stereological studies revealed that both SIDS-NBW and SIDS-LBW placentas are associated with altered placental villous (162) and vasculature (82) morphology. Changes observed include reduced volumes and surface areas of placental villi, and reduced surface areas of intermediate and terminal capillaries, which are contrary to the expected intra-placental hypoxia as noted in other forms of pre-placental hypoxia. Because villous development is also driven by the villous trophoblast, it hypothesized that different pathways of villous maldevelopment may reflect divergent villous trophoblast phenotypes.

1.6 Regulation and Maintenance of the Trophoblast Lineage during Pregnancy

Pre-eclampsia is associated with defective differentiation and invasion of EVT cells, whereas by contrast, severe early-onset IUGR is typically characterized by reduced branching of the peripheral villi and the underlying vasculature. On the basis of recent observations using mouse models, it has become apparent that these human placental pathologies may be the result of distinct molecular abnormalities in the differentiation of the trophoblast lineage.

1.6.1 Molecular Basis of Placental Development in Mice

The trophoblast origins of pre-eclampsia and IUGR are difficult to investigate as these diseases represent investigative endpoints, and hence, very early gestational samples are not available. However, the last ten years has seen a substantial increase in our knowledge regarding trophoblast development due primarily to transgenic and knockout studies in the mouse (167). Although they differ in their overall structure (Figure 1-8) their basic developmental plan is the same and as such, they are thought to be quite similar in terms of their molecular regulation (168). Because some genes known to be involved in murine placental development are expressed in an analogous manner in humans, this indicates that key molecular determinants of placental development in mice are also likely to be involved in humans (for full review see (169)). This data, albeit limited, suggests that trophoblast subtype-specific function is conserved between the two species (reviewed in (168)), and have highlighted the importance of the trophoblast and its differentiation into the different lineages in directing the different stages of placental development.

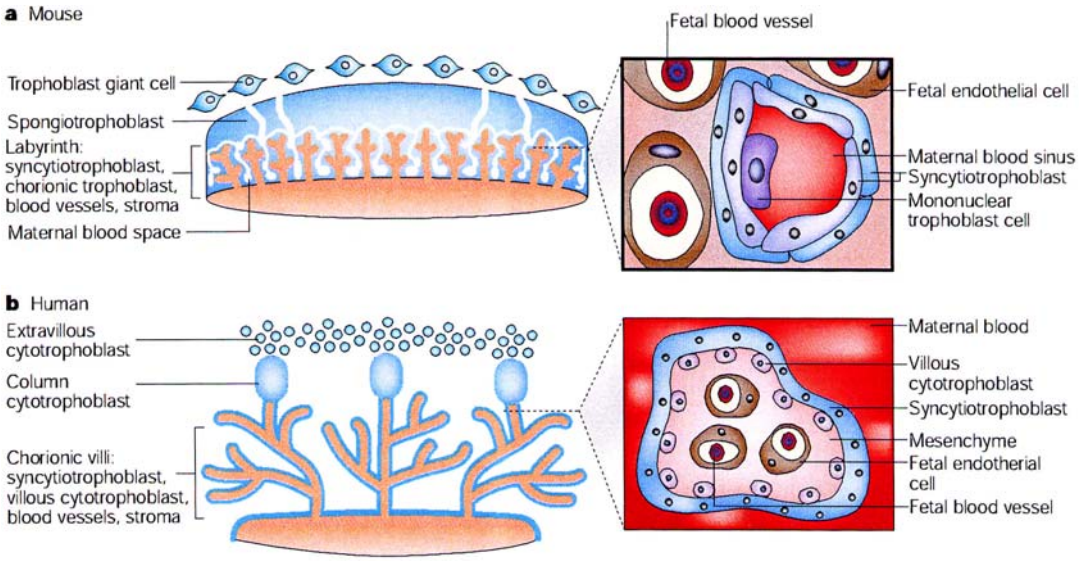

Figure 1-8 Comparative anatomy of the murine and human placenta

(a) Structure of the mouse placenta. The inset details the fetal-maternal interface in the labyrinth (b) Structure of the human placenta. The inset image shows a cross-section through a chorionic villus; trophoblast-derived structures (blue) and mesoderm-derived tissues (orange). The inset images illustrate the number and type of cell layers between maternal and foetal blood (169).

1.6.2 Trophoblast Stem Cell Maintenance and Differentiation

Trophoblast stem cells (TS) arise in the polar trophectoderm (170) and are distributed throughout the extra-embryonic ectoderm (chorion) (171). These cells are characterized by their ability to 1) retain an undifferentiated proliferative phenotype and 2) differentiate into the various trophoblast cell-types in the mouse (i.e. spongiotrophoblast (SpT), trophoblast giant cells (TG), or syncytiotrophoblast (SynT) of the labyrinth). Differentiation into these various cell-types is characterized by arrest of mitosis and the promotion of transcription factor pathways that ultimately determine cell fate decisions (Figure 1-9) (172).

Maintenance of the proliferative TS phenotype is dependent on stimulation by fibroblast growth factor (FGF) signalling through its ligand (FGF4) (173), (expressed in the early embryo, the ICM and the epiblast of the post-implantation embryo (169)) and its receptor, FGFR2 (expressed in the trophectoderm and chorion (174)), and the downstream transcription factors *Cdx2* (175) and *Eomes* (176) (all are promoted by Nodal (170)). Removal of FGF4 from cultured trophoblast stem cells leads to the rapid down-regulation of *Cdx2* and *Eomes* and proliferation ceases owing to their exit from the cell cycle (173) and subsequent differentiation into the various labyrinth trophoblast

cell types via expression of transcription factors (*Hand1, Stra13* (TG), *Gcm1* (SynT)) (172) (For a full review of murine trophoblast genetics, see (169; 170; 177)).

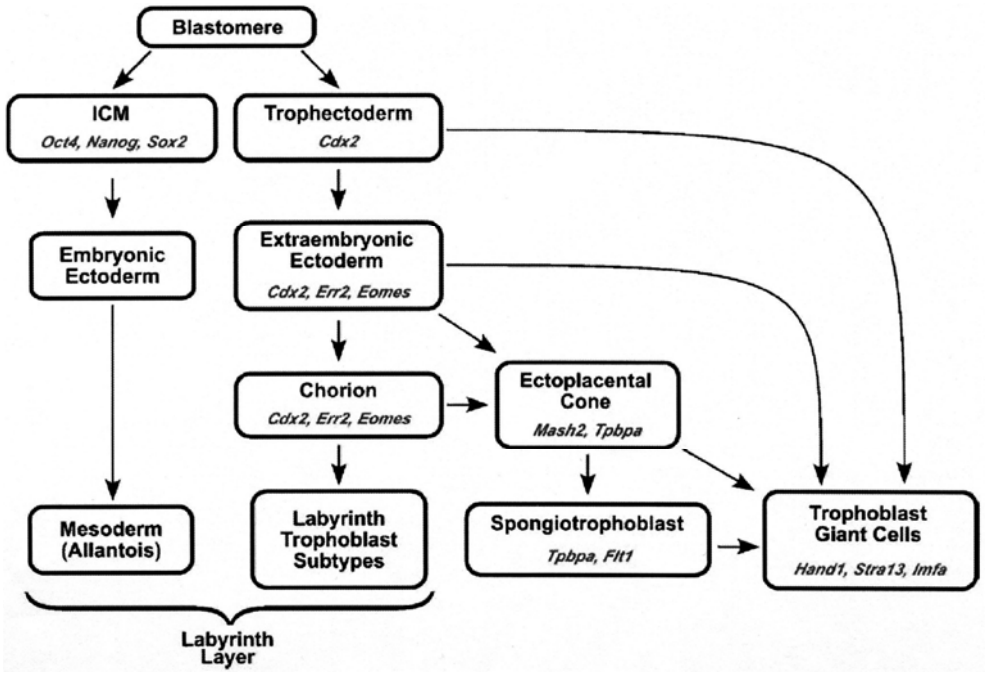

Figure 1-9: Trophoblast stem cell fate in the mouse

Segregation of the murine trophoblast lineage first occurs at the blastocyst stage prior to implantation. Blastomeres on the outside of the conceptus form the trophectoderm destined to become trophoblast, whilst the inner cells become part of the ICM; these cells are prevented from differentiating into trophectoderm by the expression of *Oct4*. Subsequent differentiation of trophoblast stem cells into syncytiotrophoblast, spongiotrophoblast, trophoblast giant cells and glycogen cells is associated with down regulation of *Cdx2* and *Eomes* and upregulation of lineage-specific transcription factors. Differentiation into trophoblast giant cells is induced by up-regulation of two basic helix-loop-helix (BHLH) transcription factors, *Hand 1* and *Stra13,* whilst differentiation into and maintenance of the spongiotrophoblast layer is dependent upon the BHLH *Mash 2,* a subpopulation of which differentiates into trophoblast glycogen cell promoted by the *Igf2* gene (adapted from 170).

Significantly however, the developmental potential of TS cells is lost from the murine placenta coinciding with the development of the labyrinth layer at E8.5, since TS cells can only be derived from the chorion up until E8-8.75 (171; 178). Because the placenta continues to grow almost until term, an as yet uncharacterized population of progenitor cells must therefore persist throughout gestation which account for the formation of the subsequent trophoblast cell types and the labyrinth layer (170). Furthermore, these cells may be lineage-restricted, supported by the observation that *Eomes* and *Ehox* positive

trophoblast cells are detected in the labyrinth layer, and may well represent labyrinth trophoblast progenitors (179; 180). Such progenitor cells are also predicted to exist in the human placenta as these cells act as the germinal layer of the functional syncytial layer of the chorionic villi throughout gestation.

1.6.3 Branching Morphogenesis and Labyrinth Development in Mice

The villous part of the murine placenta, the labyrinth layer- functionally analogous to the chorionic villi in humans, begins to form after embryonic day (E) 8.5 and is dependent upon attachment of the chorioallantois to the allantoic mesoderm (derived from the embryoblast) (181). Here, the mesoderm gives rise to mesenchymal cells and blood vessels within the labyrinth layer, whereas the different trophoblast layers within the chorion give rise to the three layers of differentiated trophoblast in the labyrinth (post-mitotic mononuclear trophoblast cells, and two syncytial layers formed by cell-cell fusion).

Branching morphogenesis and syncytiotrophoblast formation in the labyrinth layer depends upon the trophoblast transcription factor, glial cell missing 1 (*Gcm1*), the expression of which depends upon signalling from the allantois (182). *Gcm1* mutant mice fail to initiate branching morphogenesis and syncytiotrophoblast formation demonstrating the fundamental role of this transcription factor for labyrinth development in the mouse (181). Initially, *Gcm1* is expressed in small clusters in post-mitotic cuboidal trophoblast cells (182) in the flat basal surface of the chorion as early as E7.5 (183) at sites where the chorion begins to fold to form the primary villi; GCM1 positive cells become elongated at the onset of branching morphogenesis (181). Because of its restricted chorion expression to labyrinth-committed cells, it suggests that GCM1 may be critical in maintaining the multi-potent stem cell pool (173) in the early placenta.

Gcm1 expression is subsequently restricted to the tips of the primary branches and differentiated syncytiotrophoblast begin to form (181) where *Gcm1* is localized to the SynT-II cells (182). Syncytiotrophoblast formation requires cell-cycle exit and cell-cell fusion to form a syncytium, although the underlying fusion mechanism(s) or whether this is mediated by *Gcm1* is currently not known in the mouse (170). By E9, primary

villous branches are apparent which undergo further branching and elongation to form the mature labyrinth at around E10.5 (182). However, the cellular processes regulating subsequent growth and expansion of the labyrinth layer are largely unknown, since (in contrast to the human placenta) proliferating trophoblast cells become rare in the labyrinth layer towards the end of gestation after ~E12.5 (182). Instead, mitotically active cells are restricted to the basal part of the labyrinth suggesting that growth may be seeded from the basal layer to the tips, and given that the labyrinth continues to expand in volume towards term (184), growth maybe achieved in part by an increase in cell volume (182).

1.6.4 Trophoblast Stem Cells in the Human Placenta

Despite the knowledge regarding trophoblast stem cell maintenance in murine placentas, the localisation, regulation and fate of human trophoblast stem cells still remains unclear. However, it is generally accepted that in the human placenta, the cytotrophoblast population represents the proliferative stem cell pool. In contrast to the mouse, proliferating cytotrophoblast cells can be found in the base of the anchoring villi and in the chorionic villi as they are needed to regenerate the syncytium throughout gestation.

Studies suggest that cytotrophoblast cells may be a heterogeneous pool, and that these different cell phenotypes arise by lineage specific progenitors. It was originally thought that the villous cytotrophoblast represents a single stem cell pool, in that they produce both syncytiotrophoblast and extravillous trophoblasts during the first trimester. This statement is supported by *in vitro* cell culture studies (185), and the establishment of *in vitro* 3D floating explant models in which villi remain in their native environment. In syncytium-denuded models, cytotrophoblast cells adopt an extravillous phenotype (upon addition of FGF4) at distal portions of cytotrophoblast outgrowths, whilst in the absence of growth factors, cytotrophoblast spontaneously differentiate into syncytiotrophoblast. FGF4 initiates cytotrophoblast proliferation (173), and results in smooth cytotrophoblast outgrowths, the more proximal cells of which adopt an extravillous phenotype (Cx40, α5β1, HLA-G positivity) (132; 186). This is presumably because FGF4 recruits FGFR2-positive cytotrophoblasts to divide rapidly, thereby

physically separating the outer layers of cells from the underlying basal lamina and mesenchymal cells.

Hence what would normally constrain cytotrophoblasts to make syncytiotrophoblast is lost and subsequently cells adopt an extravillous phenotype. Interestingly, cytotrophoblast cells do not enter the extravillous invasive pathway upon addition of FGF4 to syncytium-intact models, suggesting that syncytiotrophoblast may itself be necessary to maintain cells in the villous phenotype and to prevent their differentiation into an extravillous phenotype (for a full review see (185)).

A counter-argument against cytotrophoblast bi-potentiality is presented by James *et al* (187). These authors indicate that villous and extravillous trophoblast populations arise from two separate pools of cytotrophoblast stem cells in the first trimester, in comparison to the generally accepted single pool, and that these cells are lineage-restricted.

The differentiation and/or maintenance of the cytotrophoblast columns, analogous to the spongiotrophoblast layer in mice, is dependent upon an upstream assembly of transcription factors including *Hash2* (188), *Stra13* , *Id2* and *E-factor* (189). As cytotrophoblast cells adopt an invasive phenotype (trophoblast giant cells in mice), *Hash2, Id2* and *E-factor* are down-regulated and *Stra13* is up-regulated *in vitro* (189). These expression patterns are analogous to those seen in the mouse, reinforcing the idea that these are homologous cell types. However, some species disparity may exist as differentiation into invasive extravillous trophoblast in humans is not dependent upon *Hand1* (190), a BHLH transcription factor essential for trophoblast giant cell differentiation in the mouse. Although *Hand1* mRNA is not detectable in both first and third trimester placenta, expression of *Hand1* is detectable in JEG-3 and JAR trophoblast cell lines (190).

As in the mouse, recent studies in humans have found that villous morphogenesis and syncytiotrophoblast formation is completely dependent upon the trophoblast-specific transcription factor, *Gcm1* (181; 183; 191). Originally thought of as a homogenous population of cells, these studies have shown that in fact villous cytotrophoblast represents a *heterogeneous* stem cell population in which a subset of cells display

(likely asymmetrical) expression of GCM1 protein; presumably the post-mitotic daughter cells destined for syncytial fusion, and it is speculated that those negative for GCM1 may retain the stem cell phenotype. The factor(s) behind this asymmetrical expression of GCM1 are at present unknown. Up-regulation of GCM1 in this subset drives the cell to exit the cell cycle and subsequently results in *de novo* formation of syncytiotrophoblast, which is supported by numerous observations that *Gcm1* up-regulates *Syncytin1* (192), a gene involved in trophoblast fusion (193). Furthermore, GCM1 expression is associated with villous sprouts which represent the sites of primary villous formation, suggesting GCM1 initiates villous morphogenesis in the human placenta (191).

1.7 Villous Trophoblast Turnover in Normal Human Pregnancy

In the human placenta, the chorionic villi are covered by the epithelial villous trophoblast compartment. The outer layer, in direct contact with maternal blood, represents a functional post-mitotic multinucleated syncytium (syncytiotrophoblast, SCT) displaying both transcriptional and translational activity (194), and is responsible for the bulk of placental functions including gas, nutrient and waste exchange, immune tolerance and hormone production (85).

Throughout gestation, the syncytium expands in surface area to meet the increasing demands of the growing fetus, which is achieved by the process of trophoblast turnover. This involves the continuous fusion of underlying villous cytotrophoblast cells (CT), a subset of which undergoes asymmetrical proliferation (191) to produce one daughter cell that differentiates and fuses to form the terminally differentiated SCT, whilst the other remains in an undifferentiated progenitor cell phenotype for further rounds of cell division (183). Fusion is not only the basis for growth of the syncytiotrophoblast but is also crucial for keeping it alive; fresh organelles, enzymes and nucleic acids are transferred into the generative-deficient syncytium. Some weeks later, aged syncytial nuclei (syncytial knots) are then removed from the villous membrane by the process of apoptosis and are shed into the intervillous space in the form of membrane-bound apoptotic bodies (195), where they are engulfed and cleared by macrophages in the maternal lungs serving to protect the mother from an imminent inflammatory response

(196). Shed nuclei are then replaced by new fusion events from post-proliferative daughter cytotrophoblast cells (Figure 1-10).

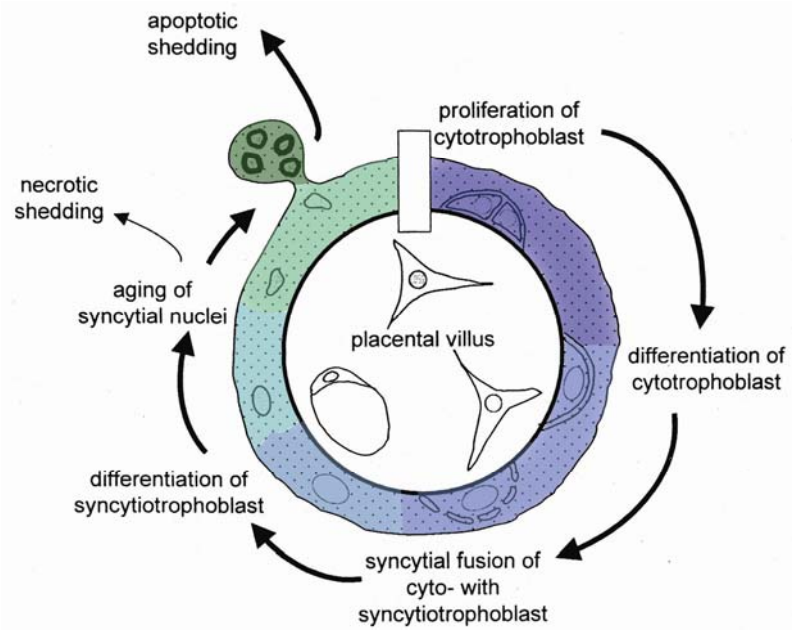

Figure 1-10 Villous trophoblast turnover

The events are arranged in a clock-wise manner around the villous starting at one o'clock. Thickness of arrows indicates the rate of respective process. The cytotrophoblast daughter cells differentiate and fuse to form the syncytiotrophoblast layer. Following differentiation and maturation within the syncytiotrophoblast layer the aging nuclei are shed by apoptosis and to a lesser extent, by necrotic shedding into the IVS. This process is a continuous cycle that is carefully regulated through out gestation (adapted from 228).

Disruptions in the balance of trophoblast turnover suggest alterations in the rates of proliferation, fusion and/or apoptosis. These homeostatic alterations may lead to potential increases or decreases in the amount of material included or extruded from the villous membrane, subsequently affecting membrane function, as seen in pathological conditions such as pre-eclampsia (3; 197) and IUGR (198; 199). Therefore, maintaining a physiological balance between placental villous cytotrophoblast proliferation, apoptosis and shedding is essential for sufficient maternofetal oxygen transfer; dysregulation of this balance may affect the functional integrity of the villous membrane and ultimately result in compromised fetal growth and development.

1.7.1 Proliferation

Growth and integrity of the placental villous trees is completely dependent upon the continuous proliferation and fusion of villous cytotrophoblast progenitor cells throughout gestation (200), as their daughter cells are needed for growth and regeneration of the overlying syncytium; without fresh input of cytotrophoblastic material the syncytium dies necrotically within a few days. Cytotrophoblast proliferation is thus a continuous process from the first trimester to term, albeit to a lesser degree (195; 201-206).

In the placenta, few markers of trophoblast cell cycle initiation and progression leading up to syncytial fusion are known and understanding the molecular regulation of cytotrophoblast proliferation/differentiation into syncytiotrophoblast is still in its infancy. However, is has recently been shown through semi-quantitative immunohistochemical studies to be coordinated with mitotic regulators of the cell cycle which change as a function of both differentiation and gestational age (207). Furthermore, growth factors such as epidermal growth factor (EGF) (208), transforming growth factor alpha (TGFα) (208), and the insulin-like growth factors I and II (IGFI, IGFII) (209) are also involved in the trophoblast life cycle.

Oxygen is a key regulator of cytotrophoblast proliferation *in vitro* such that proliferation is inversely related to oxygen tension (210). These studies showed that under hypoxic conditions, cytotrophoblast proliferation is increased alongside a necrotic syncytiotrophoblast, suggesting that low oxygen levels inhibit syncytial fusion. Conversely, increased oxygen levels lead to decreased cytotrophoblast proliferation which may also lead to necrotic shedding versus apoptotic shedding (Figure 1-11).

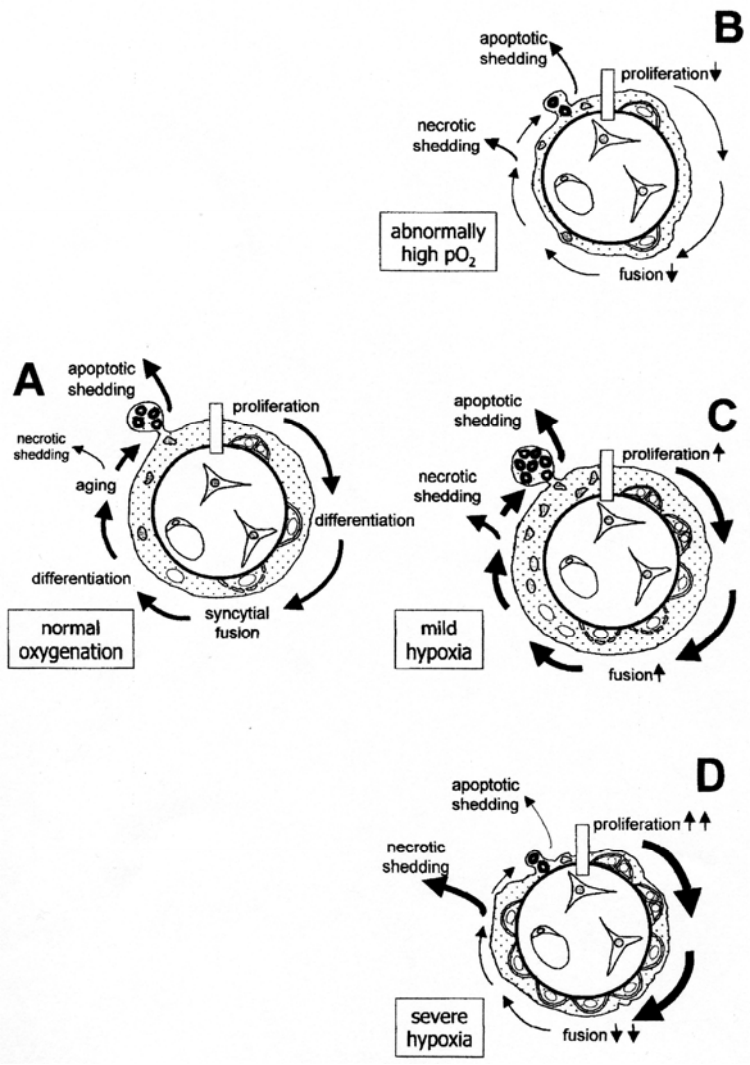

Figure 1-11 The effect of oxygen and cytotrophoblast proliferation

Abnormal oxygenation may alter the balance between apoptotic versus necrotic shedding of trophoblast material into the maternal circulation. Stating with the normal turnover in A, figures B-D describe alterations of the turnover. Thickness of arrows indicates the rate of the respective process (128).

1.7.2 Differentiation and Syncytial Fusion

Recruitment of the cytotrophoblast into the syncytium (syncytial fusion) is coupled to a highly complex and coordinated differentiation process which to a large extent remains unclear, but which is thought to comprise two levels (211). In the first differentiation process fusion of cytotrophoblast cells with syncytiotrophoblast is preceded by the accumulation of RNA, proteins and organelles within the cytotrophoblast (85) together with ongoing changes in nuclear shape, size and contents of heterochromatin and nucleoli as fusion progresses (212). This is followed by a second differentiation process in which the newly incorporated syncytiotrophoblast undergoes functional maturation

thereby adopting a cellular phenotype necessary for a functioning epithelium eventually succeeded by terminal differentiation and sequestration into syncytial knots. Both processes are known to be associated with the apoptosis cascade (213).

Cytotrophoblast differentiation is characterised by arrest of mitosis. The decision of a CT cell to exit the cell cycle, differentiate and fuse with the overlying syncytium is mediated by the asymmetric expression of the trophoblast-specific transcription factor, GCM1 (183; 191). In humans, up-regulation of GCM1 results in reduced cytotrophoblast proliferation and the induction of syncytial fusion subsequently resulting in *de novo* syncytiotrophoblast formation (214)- analogous to its reported function in mice (181). The asymmetric expression of GCM1 therefore serves to maintain the pool of proliferating cytotrophoblast cells, but also which cells are selected for syncytial fusion (191). GCM1 is therefore crucial to syncytiotrophoblast formation.

Syncytin1 is a direct downstream effector of GCM1 (193). Syncytin1, a protein encoded by the envelope gene of an endogenous retrovirus of the HERV-W family (192), is evidenced to play a direct role in mediating syncytial fusion of villous trophoblast (215), although there are inconsistencies within the literature concerning its localization and as to how and why syncytin1 can regulate fusion. Its role in trophoblast fusion has been demonstrated in numerous studies in which addition of cAMP analogues known to stimulate fusion (216), along with forskolin, an agent which increases cAMP intracellular levels (217), leads to the up-regulation of syncytin1 mRNA and subsequent fusion in BeWo cell lines (192), but also in primary cytotrophoblast cultures (218).

The distribution of the protein however is less defined, with separate reports of syncytin1 immunolocalisation to the basal and/or the apical membrane of the syncytiotrophoblast layer, weak staining in cytotrophoblast cells and a subset of EVT cells. The almost exclusive expression of syncytin1 in the syncytiotrophoblast, implying synthesis post-fusion, is a paradoxical finding given the assumption that syncytin1 initiates fusion (219). This implies that the syncytiotrophoblast is too involved in the process of initiating syncytial fusion, in line with studies suggesting that ageing areas of the syncytium are preferably involved in fusion. The involvement of syncytiotrophoblast in initiating fusion is further supported by the localisation of its receptors, ASCT1 and ASCT2 (RDR) to the syncytium (220).

Other key fusogenic proteins recognized in the process of syncytial fusion in the human placenta include ADAM2, ADAM12 (221), CD98 (222), connexin 43 (223), and the adhesion molecules cadherin-11 and E-cadherin (224). Furthermore, proteases involved in the apoptosis cascade also appear to initiate fusion, including caspase 8 (225) and phosphatidlyserine (195) (for full review see (211; 219)).

1.7.3 Apoptosis

Fusion of post-proliferative villous cytotrophoblast cells (GCM1-directed) with the syncytium is balanced by the removal of terminally-differentiated aged syncytial nuclei that have lost their functional importance which subsequently undergo apoptosis (i.e. programmed cell death) and packed into 'syncytial knot' regions. These nuclei are shed from the villous membrane in the form of apoptotic bodies into the maternal circulation so as to avoid a maternal inflammatory response. In normal pregnancy the turnover from syncytial fusion to shedding of syncytial knots takes around 2-3 weeks (195). Typical morphological features of an apoptotic cell include cellular shrinkage, membrane blebbing, nuclear condensation and fragmentation (226).

Differentiation and syncytial fusion of villous cytotrophoblasts with the syncytium is therefore coupled to the initial stages of the apoptosis cascade (Figure 1-12) (227). Studies have shown that the initiator stages of apoptosis are likely activated and confined to a subset of differentiating daughter cytotrophoblast cells, and is involved in initiating and regulating, both temporally and spatially, fusion of daughter cytotrophoblast cells into the syncytium. Once fused, terminal differentiation, functional maturation and extrusion of syncytial nuclei from the syncytium is the result of the execution stages of the apoptosis cascade (195; 225; 228). Apoptosis thus plays a pivotal role in maintaining the balance between the input and output of material within villous membrane.

The initiator stages of the apoptosis cascade are thought to be confined to the GCM1-expressing daughter cytotrophoblast cells that are selected for syncytial fusion (191), thereby maintaining the pool of proliferating cytotrophoblast progenitor cells needed for further syncytial growth and regeneration throughout gestation. Following syncytial

fusion, cytotrophoblasts enter the final stages or 'execution' stages of the cascade in the syncytiotrophoblast.

Although induction of apoptosis is not well understood in the placenta (e.g. death-receptor ligands FasL and TNFα/TNF-R1 (229; 230)), the final pathway leads to the induction of initiator caspases 8, 9 and 10, which are responsible for the first proteolytic events in the apoptotic cascade, such as cleavage of the cytoskeletal proteins vimentin, actin and fodrin, which is partly responsible for membrane blebbing (226). Post-proliferative cytotrophoblast cells destined for fusion begin to express some of these apoptosis-related proteins, some of which have been shown to be a pre-requisite for syncytial fusion itself (195). Huppertz *et al* demonstrated the presence of active caspase 8 in cytotrophoblast cells prior to syncytial fusion, and that blocking caspase 8 activity by either antisense oligonucleotides or peptide inhibition results in considerable reduction in trophoblast fusion in villous explant cultures and the accumulation of cytotrophoblast cells (225). These authors therefore concluded that caspase 8 functions as a pre-requisite for syncytial fusion in the villous cytotrophoblast and blockage of caspase 8 leads to the inhibition of fusion and subsequently progression of the apoptosis cascade in the syncytiotrophoblast. Subsequently, this leads to the 'flip' of phosphatidylserine from the inner to the outer plasma membrane of the trophoblast and acts as a signal for syncytial fusion (217; 231). These events hallmark early apoptosis, and are thus far reversible.

These observations indicate that early apoptosis events are related to the differentiation and syncytial fusion of cytotrophoblast cells with the syncytiotrophoblast. Activation of the initiator caspases thus leads to the fusion of daughter cytotrophoblast cells into the syncytiotrophoblast, and subsequently the transfer of the apoptosis machinery from cytotrophoblast to syncytiotrophoblast.

Once syncytial fusion has occurred, these early yet reversible stages of apoptosis do not immediately advance to the final execution stages of apoptosis, but instead are halted therefore preventing the premature loss of syncytiotrophoblast nuclei. Apoptosis is focally retarded due to the translation of the cytoplasmic anti-apoptosis oncoproteins Bcl-2, Mcl-1, and Mdm2 (expression of these proteins is greater in the syncytiotrophoblast compared to the cytotrophoblast) (228; 232).

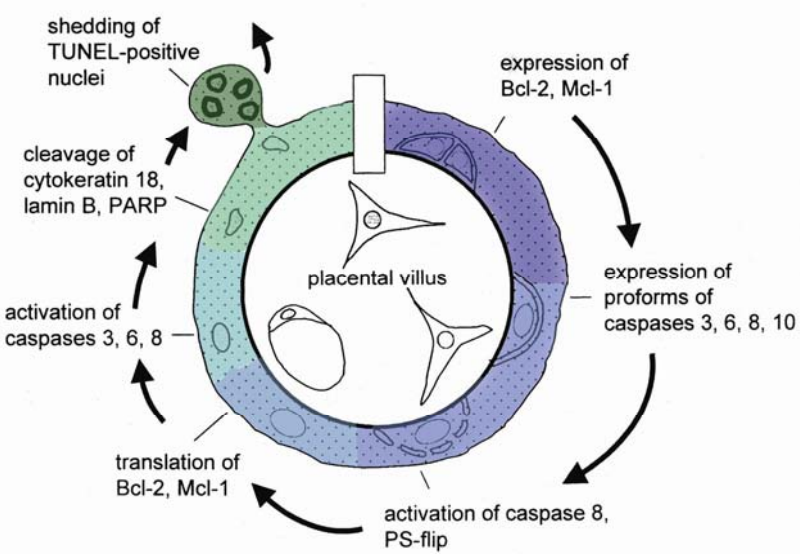

Figure 1-12 Villous trophoblast apoptosis

Molecular markers for certain stages of differentiation/apoptosis of the villous trophoblast. The machinery for the apoptosis cascade is present in the cytotrophoblast; however prior to fusion only the early and still reversible stages of apoptosis takes place. After syncytial fusion, the cascade is halted (e.g. Bcl-2) where it is restarted several weeks later so that the end stages of apoptosis can be found in discrete areas of the syncytiotrophoblast. Finally, late apoptotic nuclei are packed in syncytial knots and extruded into the IVS (adapted from 228).

Progression of the apoptotic cascade may also be regulated at the initiator stage by flice-like inhibitory protein (Flip) expressed in cytotrophoblast cells, which competes with caspase 8 for binding to the activated death-receptors (233). Furthermore, members of the X-linked inhibitor of apoptosis protein family (XIAP) (234) have been shown to be expressed in both cytotrophoblast and syncytiotrophoblast throughout gestation and can inhibit both initiator caspases (caspase 9) (235) and the effector caspases (236).

These focal inhibitions are generally, but not inevitably, followed by activation of the effector caspases 3, 6 and 7 leading to the degradation of cytoskeletal proteins e.g. cytokeratin 18, forming a neo-epitope that can be detected immunohistochemically (M30) (195; 237). Reactivation of the cascade through irreversible activation of the execution caspases several weeks later is characterized by down-regulation of transcription, fragmentation and condensation of DNA, alteration of nuclear and cellular shape and finally formation of syncytial knots (228).

Syncytial knots contain densely-packed, pleiomorphic nuclei of high, mainly-annular, chromatin condensation and are released from the apical syncytiotrophoblast membrane into the IVS in the form of tightly-sealed membrane-bound vesicles serving to protect the mother from an inflammatory response. The mechanisms involved in the formation of these regions are unknown, however, aged nuclei seem to aggregate and move toward the villous tips where they accumulate into syncytial knots, the process of which is hypothesized to be driven by sheer mechanical stress from maternal blood flow; conversely syncytial knots do not form at sites with arrested maternal circulation *in vivo* (228). Furthermore, their mechanism of clearance after release is unclear, although syncytial knot fragments have been detected in the capillary beds of the maternal lungs, indicating that they are phagocytosed in the first capillary system after exit from the placenta i.e. the maternal lungs (212).

1.7.4 Altering the Balance of Villous Trophoblast Turnover

Given the previous analyses, syncytial integrity is therefore dependent upon the rate at which the three processes, proliferation, fusion and apoptotic extrusion occur. Alterations in the rate of only one of these processes will have a direct downstream consequence on the rate of other processes disturbing the placental transfer barrier, potentially leading to impaired placental function and ultimately compromised fetal growth (228).

Proliferation: An increased rate of cytotrophoblast proliferation (provided no change in the rate of syncytial fusion), would lead to thickening of the trophoblast layer, resulting in an increased oxygen diffusion distance, and hence reduced oxygen uptake into the fetal capillaries. Conversely, decreased cytotrophoblast proliferation would result in fewer cytotrophoblast cells incorporated into the syncytium, which may shift trophoblast apoptosis towards necrosis (non-programmed cell death) due to the lack of trophoblast regeneration (210), and limit the growth potential of the chorionic villi.

Fusion: Alterations in the rate of syncytial fusion will have similar effects on the syncytiotrophoblast as for cytotrophoblast proliferation but the effects on the cytotrophoblast will be different. Reduced syncytial fusion will increase the cytotrophoblast layer such that in extreme cases the cytotrophoblast may become

multilayered. The syncytium may become necrotic due to the lack of fusion. Conversely, increased syncytial fusion may deplete the pool of villous cytotrophoblast progenitor cells.

Apoptosis: The effect and the degree to which the subsequent changes in the rate of apoptosis will have on villous membrane function are largely determined by the location of these changes within the apoptotic cascade. Alterations or disturbances in the differentiation-syncytial fusion pathway (i.e. the early stages of the apoptotic cascade) will affect incorporation of the cytotrophoblast into the syncytium. A consequence of this could be failure to incorporate and transfer the molecular machinery required for apoptosis into the syncytiotrophoblast, and so therefore remains in the cytotrophoblast. The lack of mRNA and protein transfer to the syncytiotrophoblast may render the syncytiotrophoblast unable to complete the apoptosis cascade; a direct response to this may be cell-free release of aged syncytial nuclei through non-apoptotic processes such as secondary necrosis (if material is shed but apoptosis has not taken place), or 'aponecrosis' (describes a truncated form of apoptosis with an incomplete execution followed by degeneration by necrosis). On the other hand, because syncytial fusion focally retards the cascade, the rate of syncytial apoptosis may increase. Nonetheless, the final consequence would be that 'late' apoptosis occurs in the cytotrophoblast prior to syncytial fusion (228). Alternatively, if the apoptotic cascade is interrupted during the late stages of apoptosis, then apoptotic nuclei may accumulate within the syncytiotrophoblast leading to areas of apoptotic nuclei aggregates surrounding the villous membrane that will ultimately perturb villous membrane function (3).

Therefore, maintaining a physiological balance between placental villous trophoblast proliferation, apoptosis and shedding is essential for sufficient maternofetal oxygen transfer; dysregulation of this balance may affect the functional integrity of the villous membrane and ultimately result in compromised fetal growth (201).

1.7.5 Villous Trophoblast Turnover in PET and IUGR

Villous trophoblast turnover is evidenced to be altered in pre-eclampsia and IUGR. In pre-eclampsia, several studies have shown an increased rate and number of villous cytotrophoblast cells undergoing proliferation (201; 238; 239), as well as increased syncytiotrophoblast apoptosis and increased syncytial knotting (197; 240; 241). In contrast, studies demonstrate reduced villous cytotrophoblast proliferation, increased syncytiotrophoblast apoptosis and increased syncytial knotting in IUGR pregnancies (198; 240; 242). An altered balance between recruitment and loss of the villous trophoblast (i.e. differentiation) may underpin the villous pathology of these placentally-mediated diseases.

1.7.5.1 Pre-eclampsia

The currently accepted hypothesis is that in pre-eclampsia, the rate of the entire villous trophoblast turnover is accelerated, commencing with increased proliferation of the cytotrophoblast followed by an increased rate of apoptosis in the syncytiotrophoblast (3). This imbalance is hypothesized to lead to the dysregulated shedding of necrotic syncytial nuclei, as opposed to the normal apoptotic release, and the excess release of anti-angiogenic factors (i.e. sFlt-1) which may contribute towards the systemic inflammatory response and endothelial dysfunction that characterizes the maternal syndrome of pre-eclampsia (23). The initiating factor for the alterations in the villous trophoblast is thought to be uteroplacental insufficiency (153). In a recent set of experiments, Huppertz correlated the pO_2 of the uterine vein with the rates of villous cytotrophoblast proliferation and apoptosis and found that at any given rate, cytotrophoblasts from pre-eclamptic placentas displayed a higher rate of proliferation and apoptosis when compared to controls (3).

What remains to be determined from these studies is the link between the increased rate of apoptosis and the pathophysiology of the condition. The process of apoptosis removes unwanted or old material in a temporally and spatially controlled manner (via apoptotic bodies) as to prevent the organism from eliciting an inflammatory response, which is the result of otherwise non-programmed cell death such as necrosis. Because of this, it seems unlikely that the apoptotic release of material in one case has no effect

(IUGR), whereas it should have a detrimental effect in the other case (PET) which is characterized by a maternal inflammatory response (213).

Huppertz proposed that the increased rate of villous cytotrophoblast proliferation in pre-eclampsia may lead to a higher rate of syncytial fusion, since a multilayered cytotrophoblast layer is not a feature of these placentas. This in turn, may lead to a greater amount of trophoblast material being introduced into the syncytiotrophoblast in comparison to the normal situation. Subsequently, syncytiotrophoblast apoptosis may be increased to counterbalance the increased cytotrophoblast input so as to maintain syncytial integrity. However, the syncytiotrophoblast may be unable to equal the increased incorporation rate of material into the syncytium with the rate of exclusion by increasing the rate of apoptosis. As a direct result, material is shed into the maternal circulation by 'aponecrosis'; cells enter the apoptotic cascade but undergo incomplete execution and are therefore removed and degenerated by necrosis (213); hence the term '*aponecrosis*'. Necrotic release of apoptotic subcellular fragments into the maternal circulation in pre-eclampsia may, in part, be responsible for the clinical manifestations of the syndrome such as the maternal inflammatory response (243), endothelial dysfunction (27) (Figure 1-13).

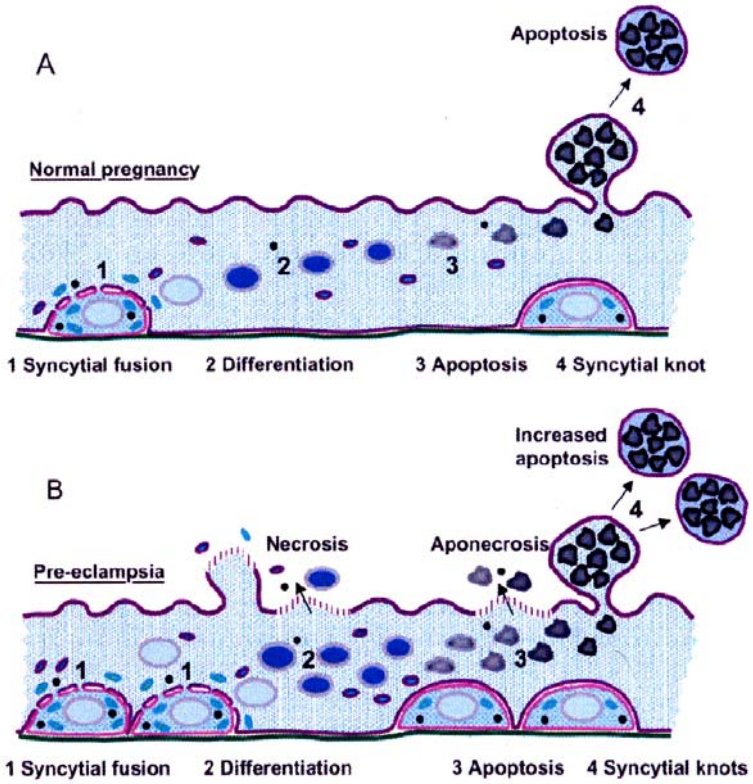

Figure 1-13: Schematic representation of trophoblast turnover.

Normal pregnancy (A): (1) final events in cytotrophoblast differentiation (2) syncytiotrophoblast differentiation and finally (3) apoptosis takes place where material is extruded via syncytial knots (4). Pre-eclampsia (B): enhanced proliferation and syncytial fusion (1) may overwhelm the capacity of the syncytiotrophoblast in terms of differentiation (2) and apoptotic release (3) resulting in necrotic release (4) (adapted from (3)).

1.7.5.2 IUGR

Ultrastructural and 3D studies have demonstrated that the malformed terminal villi from IUGR pregnancies with abnormal umbilical artery Doppler display decreased numbers and mitotic activity of villous cytotrophoblast cells, accompanied by an ageing syncytium displaying increased numbers of apoptotic syncytial knots (1; 195; 212). These authors concluded that villous trophoblast turnover may be arrested in severe early-onset IUGR, and that reduced villous cytotrophoblast proliferation may account for reduced growth and elaboration of the gas-exchanging villi in combination with failed branching angiogenesis (100).

These same authors suggested that arrested trophoblast turnover may be a consequence of rising intra-placental oxygen levels due to the inability if the malformed terminal villi capillaries to extract it, which in turn may further compromise cytotrophoblast proliferation and syncytial fusion. Because syncytial fusion transfers the necessary mRNA, proteins and organelles needed for a functioning syncytium, the net result of these change may lead to a functional deficit in the active transport capacity of the syncytiotrophoblast, which in turn, may lead to fetal growth restriction independent of the impaired surface area for diffusional exchange (100).

Other authors have subsequently confirmed reduced villous cytotrophoblast proliferation (244; 245) and increased trophoblast apoptosis (198; 240; 242) in IUGR pregnancies. Importantly, the increased rate of villous trophoblast apoptosis in IUGR is not accompanied by an increase in proliferation and so shedding of aged syncytial nuclei occurs via apoptosis, and hence IUGR is not associated with the same clinical manifestations as pre-eclampsia.

1.7.5.3 SIDS

The present investigation comprises a pilot study analyzing villous trophoblast turnover in placentas from infants succumbing to SIDS. Although not statistically significant, previous in-house studies revealed a trend towards a thicker villous membrane (82) in both the SIDS normal birthweight (NBW) and SIDS low birthweight (LBW) placentas which have the potential to limit physiological exchange of oxygen and nutrients from the maternal blood to the fetal capillaries.

The present study is aimed at further investigating these changes, more specifically, potential morphological alterations in placental villous trophoblast; the cytotrophoblast and syncytiotrophoblast respectively. Because these placentas represent a form of pre-placental hypoxia (52; 246; 247), proliferation and apoptosis may be increased in comparison to normal pregnancies at term. Such changes may lead to placental insufficiency resulting in compromised fetal growth and development through delayed or arrested fetal organogenesis in utero, contributing to the sudden and unexpected death of an infant *ex utero.*

1.8 Stereology and the Trophoblast

Much of our current knowledge and understanding of human placental development stems from studies employing 3D quantitative stereological techniques. In the context of the placenta, stereology has identified and quantified the relevant developmental processes, including villous growth and maturation, villous trophoblast turnover, fetoplacental angiogenesis and passive diffusion, in both normal and complicated pregnancies (248; 249). The ability to count nuclei and obtain absolute numbers is however perhaps the most biologically valuable and informative property of stereology. These studies that showed that villous trophoblast is a continuously-renewing epithelium involving cytotrophoblast proliferation and recruitment, and syncytiotrophoblast differentiation and extrusion (212).

However, despite this wealth of information, there remains a complete lack of stereological studies investigating trophoblast kinetics (i.e. proliferation, fusion and apoptosis) in normal and pathological pregnancies. A major limitation of such studies at present is the inability to accurately identify and phenotype subsets of villous cytotrophoblasts that either proliferate or are destined to fuse into the overlying syncytiotrophoblast. The implication of altered cytotrophoblast proliferation in pre-eclampsia and IUGR is therefore based on 2D counting methods leads to inaccurate and irreproducible results in 2D. The integration of stereological techniques and immunohistochemistry in the present study therefore permits the accurate and reproducible quantification of proliferating cytotrophoblast cells and syncytiotrophoblast structure including evidence of apoptotic shedding via syncytial knots.

1.9 Hypothesis

The overall hypothesis is that placentas from severe early-onset pre-eclampsia, IUGR and SIDS display divergent phenotypes of villous cytotrophoblast turnover and that these also differ from their late-onset phenotypes.

The specific hypotheses are that:

1. The small placentas from severe early-onset IUGR pregnancies display a reduced number of proliferating villous cytotrophoblast cells (similar to that of the mouse) with a reduced regenerative capacity for sustained villous growth leading to villous maldevelopment. This is hypothesized to reflect a reduction in the pool of villous cytotrophoblast progenitor cells.

2. In pre-eclampsia, an increase in proliferating cytotrophoblast cells makes sufficient numbers of syncytiotrophoblast, but results in dysregulated syncytial shedding (necrotic and apoptotic) into the IVS contributing towards the maternal syndrome.

3. In SIDS, cytotrophoblast proliferation and syncytiotrophoblast apoptosis are increased due to pre-placental hypoxia, leading to placental insufficiency resulting in compromised fetal growth and development through delayed or arrested fetal organogenesis in utero, contributing to the sudden and unexpected death of an infant.

1.10 Aim

Using stereological techniques, the first aim is identify the villous morphology in these diseases. Secondly, by integrating immunohistochemistry with stereological techniques, the subsequent aim is to estimate the volumes and numbers of proliferating villous cytotrophoblast cells, syncytiotrophoblast nuclei and syncytial knots in both early and late-onset PET, IUGR and SIDS.

2 Clinical Methodology

Gestational age is the most important clinical variable in predicting maternal and perinatal outcomes. Severe early-onset pre-eclampsia and IUGR (<32 weeks) are associated with significant risk of maternal and fetal morbidity and mortality, whereas late-onset (32> weeks) disease is generally associated with favourable maternal and fetal outcome (16).

Late-onset pre-eclampsia and IUGR are typically associated with different maternal and fetal phenotypes. Late-onset pre-eclampsia may present with comparable maternal severity to early-onset, but is usually associated with normal (12) or heavier fetal birth weight (13) and therefore IUGR does not often co-exist. Similarly, IUGR at term is usually evident as fetal distress in utero with favourable neonatal outcome. In comparison, early-onset disease involves considerable overlap, such that pre-eclampsia and IUGR requiring preterm delivery often co-exist (combined disease) (250; 251), and are associated with the most severe maternal and fetal phenotypes. Because these two diseases often co-exist in early gestation, clinical delineation between pre-eclampsia and IUGR is therefore difficult.

There is, however, evidence demonstrating major differences in the placental phenotype between early-onset (252) and late-onset pre-eclampsia (152; 253) and IUGR (152), which may reflect different disease etiologies and trophoblast phenotypes.

Therefore, the clinical aim was to:
1. Determine pure disease from combined disease
2. Distinguish trophoblast phenotypes in early- and late-onset placental disease

2.1 Cases

Placentas were collected at delivery following local ethics approval from two hospitals:

1. Mount Sinai Hospital (MSH), Toronto, Canada

For high-risk pregnancies complicated by:

Early (n=11) versus late-onset (n=6) PET

Early (n=5) versus late-onset (n=4) IUGR

Early (n=19) versus late-onset (n=6) PET-IUGR

Gestational age-matched preterm (n=12) and term controls (n=13)

2. Rotunda Hospital, Dublin, Ireland

Placentas were retrieved from archived material from infant deaths as a result of SIDS:

SIDS-NBW (n=12) versus term control (n=12)

SIDS-LBW (n=12) versus term control

2.1.1 Clinical criteria

Early-onset was defined as infants delivered ≤ 32+6 weeks gestation.

Late-onset was defined as infants delivered ≥ 33 weeks gestation.

1. Pre-eclampsia

Hypertensive disorders were defined according to criteria set by the American College of Obstetrics and Gynaecology (9).

Pre-eclampsia was defined as:

- blood pressure of 140/90 mm Hg or higher occurring ≥ 20 weeks gestation in a previously normotensive woman
- proteinuria of 0.3g (+1) or higher in a 24 hr urine sample occurring ≥ 20 weeks gestation in a previously normotensive woman

Severe pre-eclampsia was defined as:

- blood pressure ≥160/110 mm Hg or higher occurring ≥ 20 weeks gestation in a previously normotensive woman
- proteinuria (3+) or higher in a 24 hr urine sample occurring ≥ 20 weeks gestation in a previously normotensive woman
- HELLP syndrome occurring *de-novo* after 20 weeks gestation
- co-existent IUGR

Pre-eclampsia without IUGR was defined using the following fetal criteria:

- normal fetal health tests including: amniotic fluid index (AFI), umbilical artery Doppler (PEDV), non-stress test
- birthweights above the 10^{th} centile for Canadian sex and gestation-specific birthweight centiles (254).

No patients developed eclampsia.

2. IUGR

Small for gestational age (SGA) was defined as a birth weight $\leq 10^{th}$ centile using Canadian sex and gestation-specific birthweight centiles (254).

IUGR was defined as a subset of SGA based on (140):

- serial ultrasound assessment showing falling growth centiles
  - estimated fetal weight $<10^{th}$ centile accompanied by fetal asymmetry
  - (elevated HC/AC ratio)
- low AFI (<10 cm)
- abnormal umbilical artery Doppler (AREDV) ultrasound assessment prior to delivery

Hypertensive disorders were excluded. Stillbirths and intrauterine deaths were included in all pathological groups representing the most severe disease phenotype.

3. SIDS

SIDS cases were defined using the definition following the "Back to Sleep" campaign (255): "The sudden death of an infant between 1 month and 1 year of age which remains unexplained after a thorough investigation, including the performance of a complete

autopsy (Dr John Gillan, Ireland) examination of the death scene and a review of the clinical history, virology and bacteriology"

SIDS placentas were subdivided into two categories

- SIDS-NBW: birth weight above the 10th centile for gestational age
- SIDS-LBW: birthweight below the 10th centile for gestational age

4. Controls

Controls cases were defined as fetuses that had

- birthweight above the 10th centile for Canadian sex and gestation-specific birthweight centiles
- normal umbilical Doppler velocimetry
- no evidence of hypertension, proteinuria, and/or HELLP syndrome or IUGR

Preterm controls were selected from pregnancies resulting from preterm premature rupture of the amniotic membranes (pPROM), spontaneous vaginal delivery, or cervical incompetence.

2.2 Stereology

Stereology is a morphometric tool. It combines strict sampling rules and simple estimation tools that allow the *unbiased* and *efficient* estimation of 3D quantities such as volumes, surface areas, lengths and numbers of cells/tissues/organs from 2D histological sections. It provides global quantities as well as information concerning the local characteristics of the organ/object of interest, both of which are crucial to our understanding of how biological systems function at the whole organ level (256; 257).

To obtain such information, the object/organ of interest must be sliced/sectioned generating thin two dimensional (2D) sections allowing the visualisation of otherwise unidentifiable objects. Sectioning however causes loss of dimensionality of geometrical information and the 2D profile will undoubtedly deviate from the natural situation in 3D. By systematically randomising sampling, and the orientation and direction of slices through them, the 'sectioning effect' is overcome (258). For these reasons, stereology generates more reliable and accurate 3D quantities compared to *ad hoc* 2D quantification techniques (259).

2.2.1 The Stereological Design

The stereological design begins with sampling. The objective of sampling is to obtain samples that mimic the biological reality of the tissue/organ of interest; they must be representative of the whole tissue/organ. If the final sample of fields is to be representative, the selection of items at every stage (individuals, blocks, sections, fields of view, and measurements) of a multistage design must be randomised (260).

The human placenta represents a heterogeneous organ which varies in structure both spatially and temporally. Due to this inherent variation, the final stereological estimate is completely dependent and biased towards *how* and *where* samples are obtained from the placenta. Restricting sampling to the periphery and maternal aspect will bias estimates towards terminal villi. In contrast, restricting sampling beneath the umbilical cord and fetal aspect will bias estimates toward stem and immature intermediate villi. Since it is the combination of all villous types which ultimately determines placental function, an unbiased sample should represent all villous types. Such samples are obtained stereologically using *systematic uniform random sampling* (SUR) (261),

ensuring every part of the placenta has the same chance (probability) of being included into the final estimation thereby generating *unbiased* and *efficient* estimates.

2.2.2 Unbiasedness and Efficiency

Stereological estimates are unbiased and efficient. Unbiasedness (accuracy) and efficiency (precision) represent two statistical attributes used to describe the quality of a sample or outcome measure (Figure 2-1). In the context of stereology, accuracy refers to 'without systematic deviation from the true value' (which is unknown) and precision refers to 'with low variability after spending a moderate amount of time' (262). Both depend upon systematic uniform random sampling.

Precision

A precise estimate is one which is efficient, repeatable and reliable (263). These attributes are associated with variation around the 'true' value. Variation is introduced into a stereological estimate in two ways, (i) biological variation reflecting inter-individual variance, and (ii) sampling errors involving sampling, measurement precision and analytical technique. A stereological design should generate reliable estimates regarding the magnitude and variation (the mean and standard deviation) of the structural parameters of interest, and do so efficiently (264).

The stereological aim is to ensure that biological variation exceeds sampling error since biological variation is so diverse it can rarely be eliminated. Sampling error is reduced, and precision increased, by increasing sample sizes and thus reducing the standard error of the mean for a group of individuals (264).

Accuracy

An accurate (unbiased) estimate is one which represents the 'true value'- which is inherently unknown. Deviation from the 'true' value is introduced by systematic error (bias) leading to over- and under-estimations.

Systematic error or bias consists of an unknown but consistent amount of deviation (inaccuracy) in an unknown but consistent direction. If systematic error is introduced due to assumptions and models, the bias can never be removed, and it is embedded in

the theory of the methodology. Increased sampling leads to more precise estimates, but does not result in more accurate estimates. In fact, increased sampling with a biased method leads to a greater deviation from the true value. Thus, once bias (e.g. methodology) is present, it can never be removed by increasing sampling at any level of the stereological investigation. Accuracy is therefore not synonymous with precision (257; 264; 265).

The degree of bias is thus determined by the degree of deviation. Stereology calculates this deviation, known as the coefficient of error (see section 2.5.4) allowing the investigator to assess how accurately the estimate represents the true value.

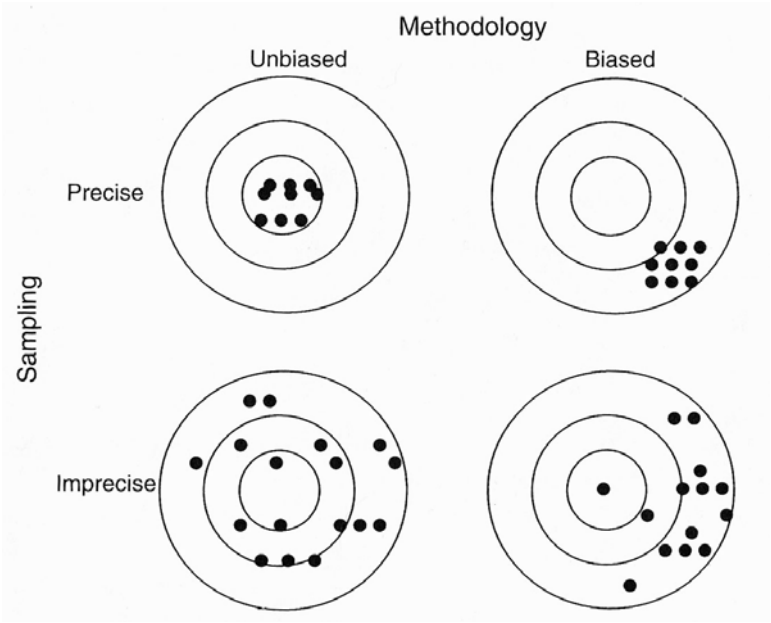

Unbiased and precise	accurate answer reached with relatively few measurements
Biased but precise	inaccurate answer reached with relatively few measurements
Biased and imprecise	accurate answer never reached even with vast measurements
Unbiased and imprecise	accurate answer reached but required a large number of measurements

Figure 2-1 Unbiasedness and efficiency in stereological analysis

A graphical illustration of the difference between accuracy and precision in an experiment. The top row of targets show high precision, that is the hits are closely clustered together, whereas the bottom row of targets show low precision, illustrated by the marked scatter of hits. In the left hand column, the average

of the cluster of hits tends towards the bull's-eye, which means they are accurate. The right hand column shows the converse case, these hits are inaccurate or 'biased'. In a given experiment we want to be in the left hand column, which can be achieved by using the correct sampling design and measurement tool. Whether the estimate is precise or imprecise depends on the object of interest, and in many cases can be controlled by working harder (adapted from 265).

2.2.3 Systematic Uniform Random (SUR) Sampling

Randomness

By definition, sampling with equal probability equals random sampling. A deviation from randomisation introduces bias (inaccuracy) by increasing the probability that a particular outcome will be favoured above others. The fundamental requirement of stereological analysis is that all objects within the organ/object of interest have an equal probability of being sampled i.e. randomness of position and orientation (266).

In random sampling, the position of every item in the sample is an independent choice, and this can lead to a particular area of the specimen being over-sampled, thus decreasing the efficiency of the estimate (260). Such clustering would generate imprecise estimates which take numerous trials before converging on the true value. Random sampling is therefore unbiased but inefficient.

A more efficient way to sample is through systematic uniform random sampling which arrives at the theoretically unbiased estimate with less sampling, time, effort and cost.

SUR Sampling

Systematic uniform random sampling captures most of the biological variation by efficiently sampling a small but representative percentage of the total population with minimum sampling noise- "do more less well" (261).

In SUR, the position of the first point on the specimen to be sampled is selected at random, after which each point has a predefined pattern at equal distances. This pattern must be kept uniform to eliminate bias and ensures that all parts of the specimen have the same chance of being included in the sample (261).

Two examples of uniform random sampling are illustrated in (Figure 2-2). In A, the specimen is systematically sampled by uniformly slicing at predefined distances throughout the whole of the specimen (x). Randomness of location is achieved by allowing the first slice to occur with uniform probability in the interval 0-d (A). Such a sample is said to be uniform random in position. It is not acceptable to always locate the first slice image at some predetermined distance from zero (e.g. 1cm) as this will not give all parts of the specimen the same chance of being sampled, resulting in a biased estimate (263). In B, randomness of sample position (0-d) is achieved by randomly 'throwing' a uniform grid of holes of fixed distance apart onto the surface of the specimen thereby allowing each part of the specimen the same chance of being sampled (263). All placentas in the present study were sampled using SUR sampling in Figure 2-2 B.

SUR is also applied to 2D histological sections (Figure 2-3). Just as it is not acceptable to choose where you select your specimen samples, one cannot simply choose where to take your profile measurements. Each part of the section must have the same chance of being sampled.

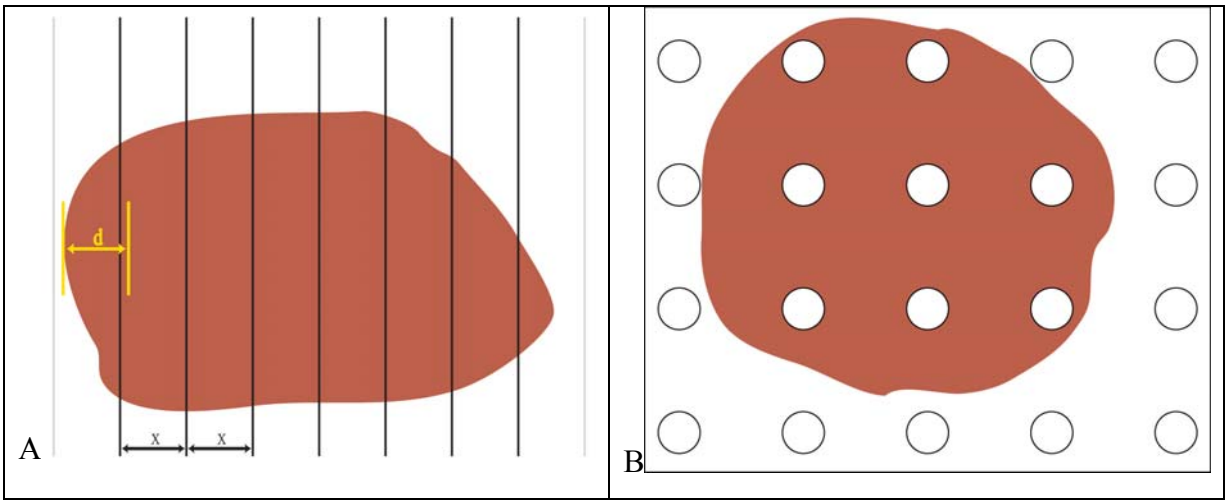

Figure 2-2: Systematic uniform random sampling

(A) The object is uniformly sliced at predefined distances with a random start in the interval (0-*d*). (B) A uniform grid of holes of fixed distance apart is thrown onto the object surface. Both methods generate systematic uniform random samples.

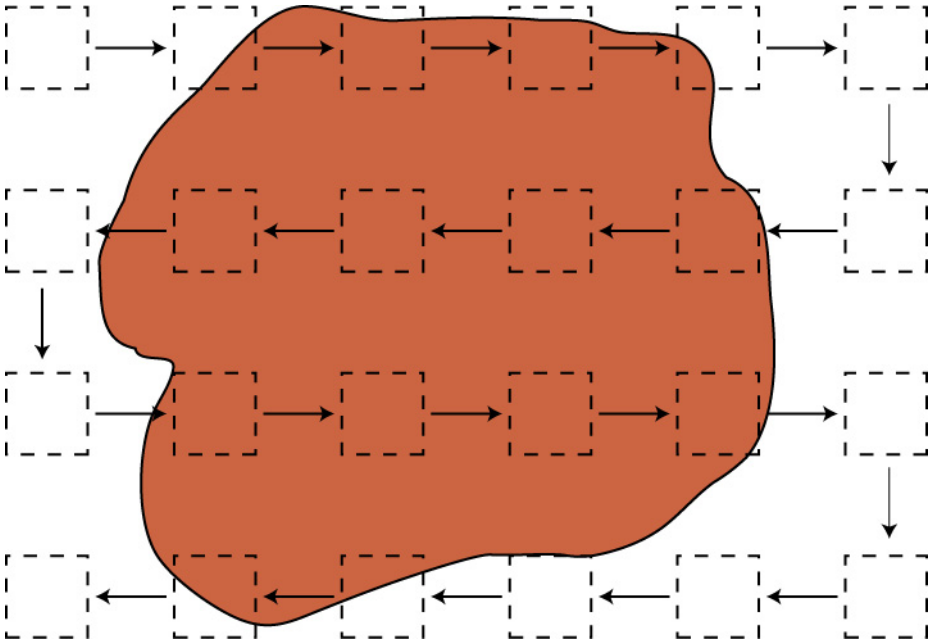

Figure 2-3: Uniform random sampling within 2D histological sections

Fields of view (dashed boxes) are sampled SUR using the X and Y axes. The first point on the section is chosen at random, and from then on the distance between each point (dashed boxes) along the X-axis is kept uniform. The distance between points (dashed boxes) on the Y-axis is also kept uniform, but may differ from the distances employed for the X-axis. The values chosen must be kept consistent throughout each specimen (individual) to eliminate bias.

2.2.4 Estimating Quantities in 3D

2.2.4.1 Volume

Estimation of the reference volume is crucial in stereology in order obtain absolute (global or total) quantities (267), which provide information regarding the whole organ i.e. the total number of cells in the human placenta. The reference volume represents the 'space' within which the particular stereological measure is to be estimated, it can be anything, (e.g. individual, plant, organ, tissue). Failure to estimate the reference volume dictates that structure can no longer be related to function; hence this step is fundamental to a biological study.

Volumetry can be performed in various ways, for example, the volume of a large object can be obtained from its weight or by fluid displacement (e.g. the placenta). The most

commonly used method for estimating the reference volume is the Cavalieri Principle (261; 268).

Cavalieri demonstrated that the volume of an arbitrary shaped object could be determined in a serially sectioned structure by the product of the slice areas and the slice thickness. A series of uniform parallel sections is cut through the object of fixed distance apart, producing slices of known equal thickness. The area of only one face of each section (e.g. anterior) is estimated by randomly superimposing a systematic array of test points on each face in turn, and counting the number of points overlying each face. Volume can then be estimated by multiplying the total number of points for all slices (disregarding the end section) by the area associated with each point and by the mean section thickness (268).

2.2.4.2 Volume Density

The Cavalieri Principle however, cannot provide direct estimates of component volume. Instead this is obtained by estimating volume density, or relative volume (V_v), which is the mean volume of a particular phase/feature of interest within the reference volume. Simply put, the volume fraction of 'phase Y' (e.g. trophoblast) within a reference volume (e.g. placenta) is the proportion of each unit volume of the reference space taken up by Y (269; 270).

Volume density is estimated by the technique of point counting (271), such that volume density (fraction) is equal to the number of points falling within the phase of interest divided by the total number of points within the reference space. If the number of points falling within the reference space varies (heterogeneous morphology), then the estimator of volume fraction becomes a 'ratio estimator' (272). In this type of estimator, the phase of interest and the reference space vary from field to field, and it is not correct to simply average the individual estimates of volume fractions over all fields. Instead, the sum of all points hitting the phase of interest over all fields analyzed (m) is divided by the sum of all points hitting the reference space over all fields analyzed:

$$V_v = \frac{\sum_{i=1}^{m} P(Y)_i}{\sum_{i=1} P(ref)_i}$$

Total volume (V_{tot}) is estimated by multiplying volume density (V_v) by the reference volume (V_{ref}) of the organ/object of interest:

$$V_{tot} = V_v \times V_{ref}$$

2.2.4.3 Point Sampled Intercept

In addition to estimating the total volume of an organ/tissue (e.g. the placenta) and the volume occupied by trophoblast (volume density), point sampled intercept (PSI) is a method for estimating the mean volume of an object (e.g. mean volume of a syncytial knot) thereby generating a measure of object/particle size within an organ/tissue (265).

The point sampled intercept (PSI) is a direct method for measuring the mean volume-weighted particle volume (ν_v) (273). Objects are selected for analysis based on their volume rather than by number, whereby larger objects have more chance of being selected than smaller objects i.e. an object will be hit with a probability determined by its volume rather than by its mere presence. This is distinct from number-weighted mean volume (ν_N) where selection is based purely on the number of objects within the area of interest.

Volume-weighted particle selection is achieved by randomly 'throwing' points into 3D space (systematic array of test points) and only measuring a particle if it is hit (i.e. sampled) by a point. Where a point hits a particle profile (e.g. syncytial knot), a line which crosses the profile is drawn through this point at a randomly selected angle to the outer edges of the profile, which is repeated for all points hitting particle profiles.

The volume of each of the sampled particles is then estimated by measuring the length of the line passing from each of the sampled points. The part of the line intercepting the particle constitutes an isotropic point sampled intercept, l_0, and its length provides the

basis for estimating mean volume-weighted particle volume. The third power of these intercept lengths averaged over all intercepts multiplied by π/3 is an unbiased estimator of (ν_v): where $\bar{l}_0^3$ is the mean cubed length of all intercepts.

$$\hat{\overline{V_v}} = \frac{\pi}{3} \cdot \bar{l}_0^3$$

2.2.4.4 Numerical Density

The assumptions associated with counting objects in 2D are overcome stereologically by counting particles within volumes (3D) rather than areas (2D) (267). The disector principle (274) can be applied as a physical or optical technique for the estimation of total object number.

2.2.4.4.1 The Disector

The disector principle of counting objects requires the estimation of object number within a known volume. This volume can be generated using physical sections or alternatively optical sections. The volume is determined by the disector height (*h*) and the area of an unbiased counting frame (UCF) (258). The disector height is determined by the size (height) of the cell to be counted in relation to section thickness i.e. a cell of 15μm cannot be counted in a 10μm thick section. In the physical disector, the disector height is generated by a known (fixed) distance between pairs of perfectly registered parallel sections (e.g. sections cut 10 μm apart). Particles are counted in 3D based on the presence of object transects within the 'reference' section and corresponding absence in the 'lookup' section (274).

In contrast to the physical disector, the optical disector does not require the comparison of a pair of registered sections. Instead, two sections are created optically. This is possible if the sections are thin enough, which can only be achieved if using a microscope with a lens that has a thin focal plane thus creating the 'optical section'. When the in-focus plane is thin, the in-focus image acts like a section. The observer focuses down through the slice. When a particle comes into focus the observer stops.

Since the particle has not been into focus up to this point it means that the particle did not exist in the look-up section. Particles are counted based on the counting frame rules (see section 2.2.4.4.2).

2.2.4.4.2 The Optical Brick

A more efficient way of generating direct counts of objects in 3D space is to count objects in one thick section of a defined volume, using an unbiased counting brick (265). Cells are counted within each optical disector using an unbiased optical 'brick' i.e. the volume of space generated by sweeping a 2D unbiased counting frame down through 3D space (Figure 2-4). It consists of three acceptance planes and five forbidden planes. Particles are counted only if they are totally inside the brick and do not intersect any of the forbidden planes. This removes bias introduced by counting cells with assumptions concerning size, shape and orientation. For a full review of unbiased counting rules see (258).

In practice, counts are made using a microscope fitted with a microcator, which is used to measure depth (μm) in the *z* direction (the disector height). Objects are counted on the basis of the unbiased counting brick (258). An object close to the upper surface of the section is brought into sharp focus (e.g. a cytotrophoblast cell), the microcator zeroed, and the section is scanned downwards at a defined distance, for example 15 μm; this is the optical disector height (*h*). As each cell comes into sharp focus, two considerations need to be made. The first is whether the cell is sampled correctly within the unbiased counting brick, and secondly whether the optical section containing the particle is within the height of the optical disector. All particles of interest coming into sharp focus within these considerations are counted and recorded as 'new events'.

This is repeated for each uniform randomly selected field of view for the entire sample/subject generating a numerical density (N_V); number per unit volume (V_f). This volume is generated by multiplying the area of the UCF (A_f) by the disector height (*h*):

$$V_f = A_f \times h$$

Numerical density (N_v) is then estimated by dividing the number of objects counted (Q) by the volume of the tissue sampled multiplied by the number of disectors counted $\sum P$:

$$N_v = \frac{\sum Q}{\sum P \cdot (A_f \cdot h)}$$

Total number of objects (N_{tot}) is estimated by multiplying the numerical density (N_v) by total volume of the organ/object of interest, i.e. the reference volume (V_{ref}):

$$N_{tot} = N_v \times V_{ref}$$

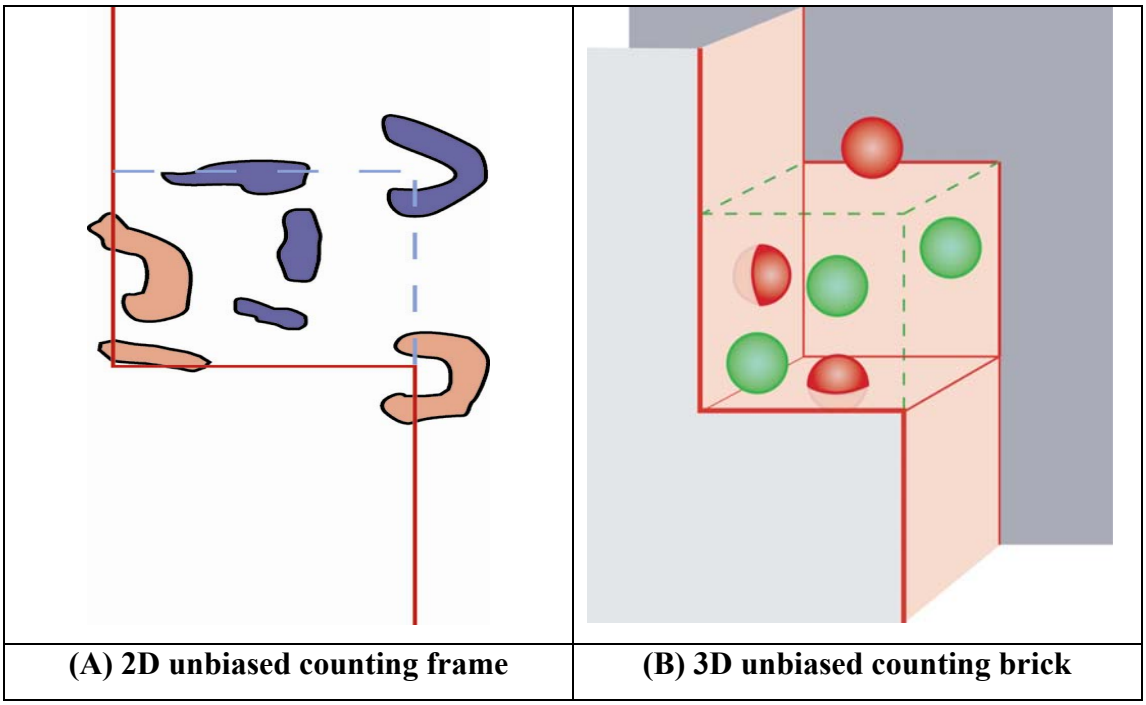

(A) 2D unbiased counting frame	(B) 3D unbiased counting brick

Figure 2-4: Unbiased counting frame applied to thin (A) and thick histological sections (B).
(A) The 2D counting frame consists of one acceptance line (dashed blue line) and one forbidden line (red line). Objects that intercept the acceptance line or are completely within the counting frame and not touching either of the forbidden lines are counted (i.e. purple objects n=5). Those objects that intercept the forbidden line are not counted (i.e. orange objects, n=3). (B) The unbiased brick consists of a central volume, bounded by three acceptance planes and three forbidden planes, which at the edges of the diagram extend to infinity. Any object that is wholly within the brick or cuts the acceptance planes without anywhere cutting any forbidden surface is counted (adapted from 265).

2.2.4.5 Tissue Deformation of Thick Sections

Estimating number using the optical disector in thick paraffin sections requires the estimation of tissue deformation in the z-axis. Deformation, usually in the form of shrinkage, can be introduced from tissue fixation and processing, histological preparation and/or immunohistochemical procedures (275). Broadly speaking, regardless of the spatial distribution (homogenous or differential), uniformity (uniform or non-uniform), or local deformation, the number of particles (the cardinality) is preserved. Specific requirements for optical designs dictate that no particles should be lost from the disector sample (e.g. the use of guard volumes), the final section thickness, *t*, should be known, and no differential deformation in the z-axis may occur (275).

If, after estimation of V_{ref}, there is homogenous, uniform deformation of sections in the z-axis, then local section thickness will differ from the original section thickness, meaning number is estimated using:

$$N_V := \frac{\bar{t}}{BA} \bullet \frac{\sum Q^-}{h \bullet \left(\frac{a}{p}\right) \bullet \sum P}$$

Where $\bar{t}$ is the mean final section thickness, *BA* is the block advance; *h* is the dissector height, *a* is the area of the counting frame, *p* is the number of reference points per counting frame, $\sum P$ is the total number of counting frame points hitting the reference volume and $\sum Q^-$ is the total number of particles sampled.

Under these same circumstances, if homogenous, non-uniform deformation is present, then local section thickness should be estimated for each field of view, and number becomes dependent on number-weighted mean section thickness:

$$N_V := \frac{\bar{t}_{Q^-}}{BA} \bullet \frac{\sum Q^-}{h \bullet \left(\frac{a}{p}\right) \bullet \sum P}$$

Where $\bar{t}_{Q^-}$ is the particle weighted mean section thickness.

The most likely scenario however, is the presence of all three kinds of deformation-deformation of the blocks, deformation of the sections in the plane of the section, and homogenous non-uniform deformation in the direction of the z-axis, in which case number is estimated using:

$$N_V := VD \bullet AD \bullet \frac{\bar{t}_{Q^-}}{BA} \bullet \frac{\sum Q^-}{h \bullet \left(\frac{a}{p}\right) \bullet \sum P}$$

Where VD is the volume deformation before sectioning and AD is the volume deformation after sectioning.

2.3 Systematic sampling of fresh placental tissues

All placentas were sampled using strict criteria that fulfil stereological requirements (263). Prior to sampling, placental weight and volume (fluid displacement) were determined from trimmed placentas (fetal membranes and umbilical cord removed).

A perspex grid of systematic-uniformly arranged holes was randomly overlain onto the fetal aspect of each placenta (Figure 2-5). Approximately 4-6 full-depth pieces of tissue (fetal through to maternal) were obtained using a steel borer from *every* overlaying hole. Each sample was immediately washed in phosphate buffered saline (PBS) and cut in half along the longitudinal axis. One half was retained for molecular analysis and the other fixed in 10% neutral buffered formalin (NBF) and subsequently paraffin wax-embedded (FFPE) for stereological analysis. Placental samples were randomly orientated during embedding as a defined orientation is not a requirement of volume or number estimation.

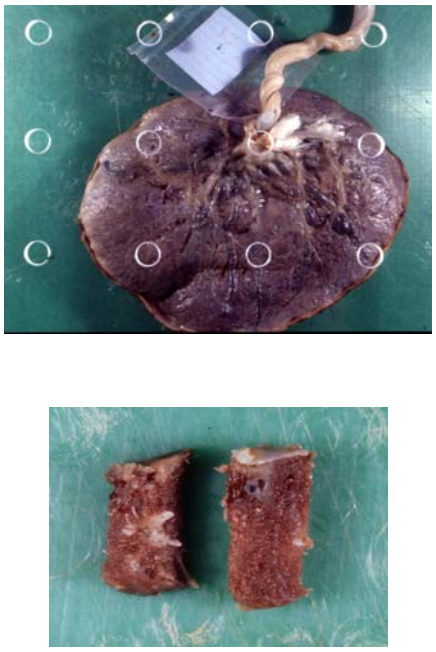

Figure 2-5 SUR sampling of the human placenta

2.4 Immunohistochemistry

2.4.1 Immunolabelling of Cytokeratin 7

A monoclonal antibody to cytokeratin 7 (CK-7) was used to immunolocalise cytotrophoblast cells in 5µm sections, thereby distinguishing them from syncytiotrophoblast nuclei and stromal cells. This was required for volume estimation of 1.) cytotrophoblast cells and 2.) syncytiotrophoblast nuclei

5µm sections were:

1. Deparaffinised in Xylene 1: 5 min
   Xylene 2: 5 min
2. Rehydrated in 100 % IMS: 2 min
   95 % IMS: 2 min
   75 % IMS: 2 min
3. Running tap water for 2 min
4. Incubated with 10 % hydrogen peroxide (H_20_2) in methanol (MeOH) for 20 min
5. Washed 3 x 3 min TBS (100mM Trisma Base, 150mM NaCL, pH 7.6) (Sigma)
6. Incubated with Vector ready-to-use (R.T.U) 2.5 % normal horse serum for 30 min
7. Incubated with CK-7 mAb (Mouse Monoclonal Anti-Human, clone OV-TL 12/30, Dako) diluted [1:150] in TBS for 1hr at room temperature (RT)
8. Washed 3 x 3 min TBS
9. Incubated with Vector ImmPress Peroxidase Anti-mouse Ig for 30 min at RT
10. Washed 3 x 3 min TBS
11. Incubated with Vector ImmPact DAB (using manufacturer's instructions) for 10 min
12. Immersed in distilled water for 5 min
13. Counterstained: Harris Haematoxylin 10 sec, Eosin 2 mins
14. Rinsed in 1 % Acid-alcohol for 3 x 3 sec
15. Dehydrated in 75 % IMS for 30 sec
    95 % IMS for 30 sec
    100 % IMS for 2 min
16. Cleared in xylene for 2 x 2 min and mounted

2.4.2 Double Immunolabelling of CK-7 and Ki-67

Antibodies to CK-7 and Ki-67 were used in a sequential double-labelling protocol to immunolocalise cytotrophoblast cells and proliferating cytotrophoblast cells in 25µm thick paraffin sections, respectively. This protocol allowed the simultaneous estimation (in one thick section) of the number of 1.) cytotrophoblast cells 2.) proliferating cytotrophoblast cells, and 3.) syncytiotrophoblast nuclei (see Appendix 6).

First antigen: CK-7

25µm sections were:

1. Deparaffinised in Xylene 1: 10 min
   Xylene 2: 5 min
2. Rehydrated in 100 % IMS: 2 min
   95 % IMS: 2 min
   75 % IMS: 2 min
   Running tap water for 2 min
3. Incubated with 10 % H_20_2 in MeOH for 30 min
4. Washed 3 x 3 min TBS-T (100mM Tris-HCl, 300mM NaCl, 0.05 % Tween, pH 7.6)
5. Incubated with Dako Protein block for 30 min
6. Incubated with CK-7 mAb (Mouse Monoclonal Anti-Human, clone OV-TL 12/30, Dako) diluted [1:300] in TBS for 20 min at RT
7. Washed 3 x 3 min TBS-T
8. Incubated with Vector ImmPress Peroxidase Anti-mouse Ig for 20 min at RT.
9. Washed 3 x 5 min TBS-T
10. Incubated with Vector ImmPact DAB (using manufacturer's instructions) for 1 min
11. Immersed sections in distilled water for 5 min

Second antigen: Ki-67

12. Slides were incubated in a coplin jar filled with Citrate Buffer antigen retrieval solution (20 mM Citrate Trisodium Anhydrous, 2mM EDTA, pH 6.2, 0.05 % Tween) heated to 90^{o}C for 15 min and then cooled for 20 min at RT
13. Washed 3 x 3 min TBS-T
14. Incubated with Dako protein block for 30 min

15. Incubated with Ki-67 mAb (Mouse Monoclonal Anti-Human, clone MIB-1, Dako) diluted [1:50] in TBS for 2 hr at RT
16. Washed 3 x 3 min TBS-T
17. Incubated with Vector ImmPress Peroxidase Anti-mouse Ig for 30 min at RT
18. Washed 3 x 5 min TBS-T
19. Incubated with Vector VIP chromagen (manufacturer's instructions) for 2 min
20. Immersed sections in distilled water for 10 min
21. Counterstained with Methyl Green (Vector) for 2 min at RT
22. Immersed slides in distilled water to remove excess stain for 10 seconds
23. Dehydrated immediately in 95% ethanol for 2 min, followed by 100% ethanol 2 for 2 min
24. Differentiated in 0.05% acetic acid/acetone for 10 seconds
25. Cleared in xylene for 2 x 2 min and mounted using permanent non-aqueous media

2.5 3D Analysis of the Villous Trophoblast

The morphological basis of villous trophoblast turnover was quantified stereologically by estimating the relative and absolute volume and number of (i) villous cytotrophoblast cells, (ii) cytotrophoblast cells positive for Ki-67, (iii) syncytiotrophoblast nuclei, and (iv) the relative volume and size (mean individual volume) of syncytial knots (SK). All analyses were carried out at the light microscope level aided by Visiopharm Integrator System for volume estimation (x40 magnification) and Kinetic Digital Stereology 5.0 software for number estimation (x100 magnification, NA 1.25), with the aid of a BH2 Olympus light microscope and a Heidenhain microcator (ND 281A) attached to the z-axis of the microscope stage. Approximately 50 fields of view were analysed for each parameter per placenta.

2.5.1 Volume Estimations

Volume densities of placental components (the different classes of villi, villous cytotrophoblast cells, syncytiotrophoblast nuclei, and syncytial knots) were estimated using the technique of point counting (260) employing a quadratic array of coarse and fine test points (Figure 2-6, Figure 2-7).

The number of coarse points overlying the different classes of villi were counted for each uniformly-random selected field of view (villi were identified using previously defined histological criteria (115)). Using the same lattice, the numbers of fine points falling within the different classes of villi were used to estimate the proportion occupied by cytotrophoblast (CK-7 positivity), syncytiotrophoblast (densely stained H&E nuclei at the maternal-fetal interface and corresponding absence of CK-7) and syncytial knots (H&E).

Due to sectioning artefacts (276), true syncytial knots, (signifying syncytial degeneration in the final stages of normal villous trophoblast turnover) were defined as those SCT knot regions containing apoptotic nuclei displaying morphological features characteristic of the final stages of apoptosis (small densely stained nuclei, distinct annular chromatin). Knots displaying morphologically normal syncytial nuclei were subsequently quantified as non-apoptotic knots and were interpreted to contain a mixture of villous sprouts, bridges and flat sectioning. Necrotic nuclei were not

distinguished from apoptotic nuclei. The sum of all points hitting each of the different placental components divided by the sum of all points hitting the area of interest over all fields analyzed generated a volume density (V_v), which when multiplied by total placental volume, yielded absolute volume (V_{TOT}). Stem and immature intermediate villi were grouped as 'structural villi' (SV) and mature and terminal villi were grouped as 'peripheral villi' (PV). For SIDS cases, immature and mature intermediate villi were grouped as intermediate villi (INT).

Mean individual volume of syncytial knots (i.e. an indicator of size) was estimated using the point sampled intercept, PSI, (a direct measure of mean volume-weighted particle volume) (see references (273; 277) for full explanation). Briefly, twelve randomly orientated test lines, each containing twenty points per line, were randomly superimposed onto each field of view. Syncytial knots were selected based on the presence of a test point (from a line) overlying its surface and the length of each intercept line within each syncytial knot was measured. The third power of these intercept lengths averaged over all intercepts multiplied by π/3 generated PSI.

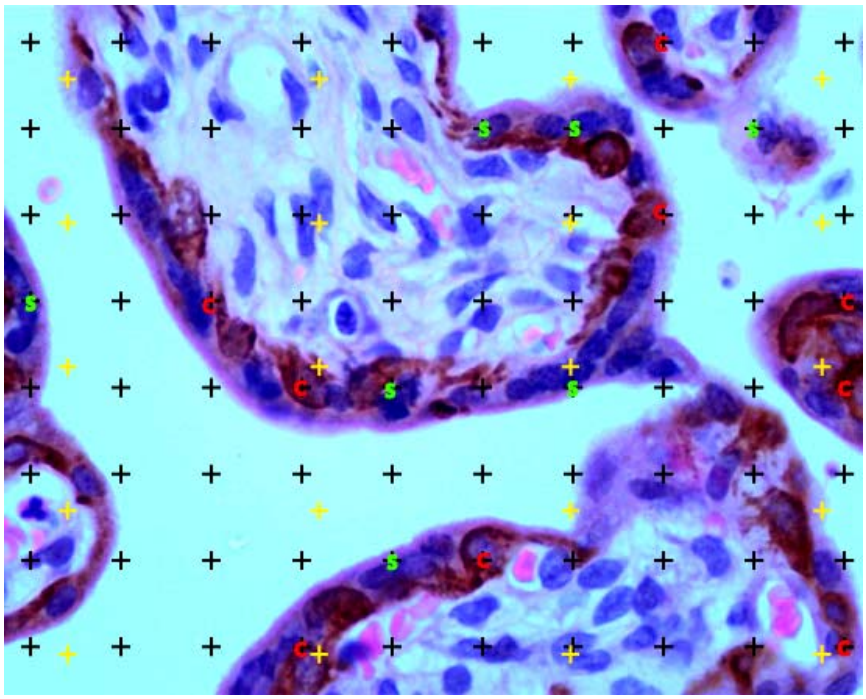

Figure 2-6 Volume density estimation of the villous trophoblast.

The number of points overlying the different villi types were counted (yellow points, 14) for each field of view. Points landing in the intervillous space were not counted. The number of points overlying

cytotrophoblast cells, C (9 points) and syncytiotrophoblast nuclei, S (7 points) were counted for the different villi types within each field of view.

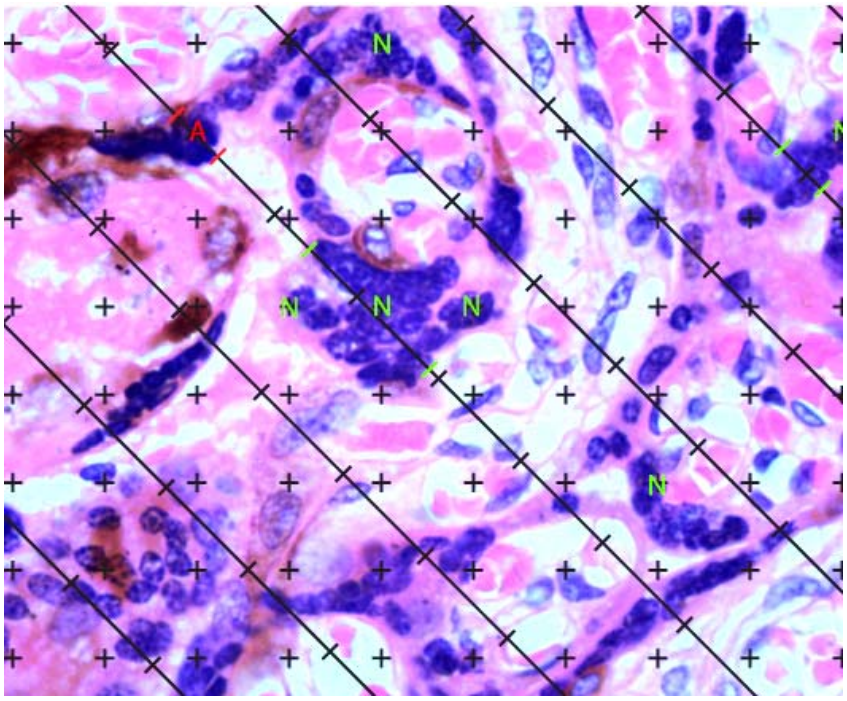

Figure 2-7 Volume density estimation of syncytial knots

For volume density estimation, a uniform random grid of 256 points was randomly overlain onto each field of view. The number of points overlying non-apoptotic syncytial knots (N) and apoptotic syncytial knots (A) was counted. Densities were estimated for the different villous types and converted to total volumes by multiplying by total placental volume. For PSI estimation, twelve randomly orientated test lines, each containing twenty points per line (not to scale in image), were randomly superimposed onto each field of view. Syncytial knots were selected based on the presence of a test point (from a line) overlying its surface and the length of each intercept line within each syncytial knot was measured.

2.5.2 Numerical Density Estimations

The double-labelled sections were used to estimate the numerical density of (i) CK-7 and Ki-67 positive villous cytotrophoblast cells, and (ii) syncytiotrophoblast nuclei, for the different classes of placental villi using the optical brick technique as previously described (278).

An unbiased counting frame (UCF) (red and green lines) is randomly superimposed onto each uniform-randomly sampled field-of view (Figure 2-8). Each field of view was focused through in the z-axis as a continuous motion; cells in the first (0-5µm) and last (20-25µm) 5µm of the 25µm sections were not counted to avoid the lost cap effect (279), generating a disector height of 15µm within which cells/nuclei were counted. As the section was scanned through the z-axis within the disector height (i.e. 15µm), each labelled cytotrophoblast cell (brown chromagen) that came into sharp focus and did not intercept the red forbidden line of the UCF was counted as a *'new event'*. The number of proliferating villous cytotrophoblast cells co-localised with Ki-67 (purple *and* brown chromagen) were also counted, as were the number of syncytiotrophoblast nuclei (green).

The sum of the counts (per placenta) was then multiplied by the disector volume (i.e. 15µm x area of the UCF) generating a number per unit volume of placenta, or, numerical density. This is then multiplied by total placental volume (estimated using the fluid displacement method) generating the total number of cytotrophoblast cells/Ki-67 positive cytotrophoblast cells for the entire placenta.

Section thickness at each field of view was recorded (µm) for subsequent estimation of tissue deformation, measured by focussing through the entire section.

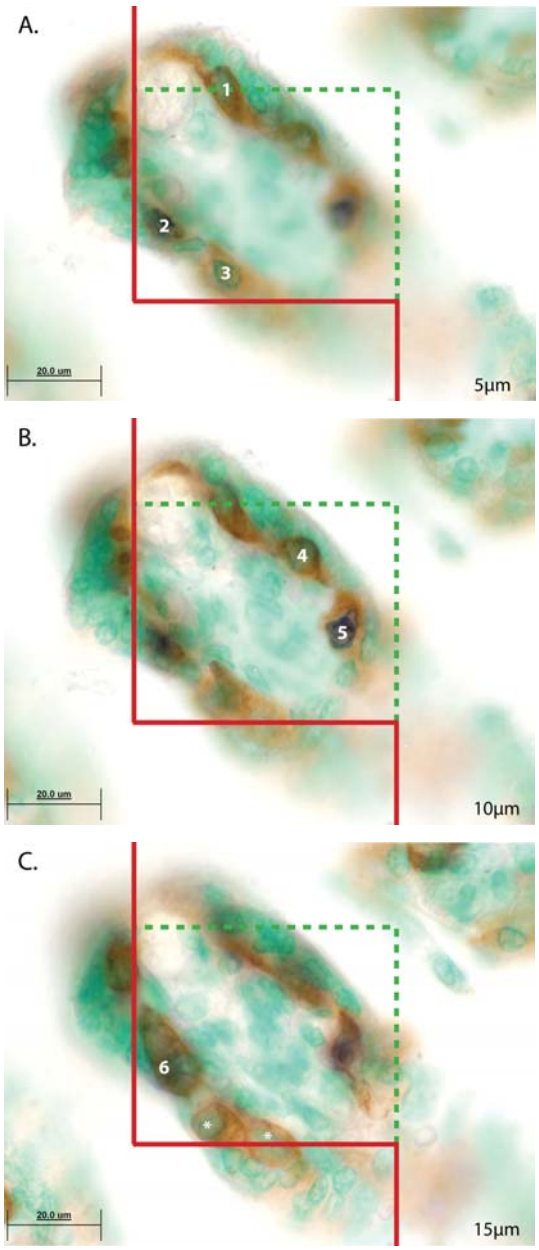

Figure 2-8 Numerical density estimation of proliferating cytotrophoblasts

Counting the number of proliferating cytotrophoblast cells in 25µm sections double immuno-labelled with CK 7 and Ki-67 using the optical brick technique (A-C, x1000). An unbiased counting frame (UCF) (red and green lines) is randomly superimposed onto each uniform-randomly sampled field-of view. As the section is scanned through the z-axis within the disector height (i.e. 15µm), each labelled cytotrophoblast cell (brown chromagen) that comes into sharp focus and does not intercept the red forbidden line of the UCF (cells marked with an asterisk) is counted as a *'new event'* (A, no.1, 2, and 3) (B, no. 4 and 5) (C, no.6). The number of cytotrophoblast cells co-localised with Ki-67 (purple *and* brown chromagen) is also counted (A, no. 2, C no. 5). Hence, for this field of view, 6 cytotrophoblast cells are counted, 2 of which are positive for Ki-67. The sum of the counts (per placenta) is then multiplied by the disector height (i.e. 15µm x area of the UCF) generating a numerical density.

2.5.3 Statistical Analysis

2.5.3.1 Co-efficient of Error

The amount of sampling error produced by a stereological estimate (the difference between an estimate and a true value) is unknown. By estimating to co-efficient of error (CE), one can determine how accurate the stereological estimate represents the true value; the CE is essentially therefore a measure of 'how good' the stereological estimate is. A CE of less than 5 % is desired i.e. only a 5 % chance the estimate is inaccurate and does not represent the true value.

Volume Density

$$CE = \left[\frac{k}{k-1} \left\{ \frac{\sum u^2}{\sum u \sum u} + \frac{\sum v^2}{\sum v \sum v} - 2\frac{\sum uv}{\sum u \sum v} \right\} \right]^{\frac{1}{2}}$$

where k is the number of fields analysed, u is the number of points hitting the intervillous space and v is the number of points hitting the placenta (trophoblast).

Point Sampled Intercept

$$CE\left(\overline{l_0^3}\right) = \sqrt{\frac{\sum_{i=1}^{n}\left(\overline{l_0^3}\right)^2}{\left(\sum_{i=1}^{n}\overline{l_0^3}\right)^2} - \frac{1}{n}}$$

where n is the total number of intercepts counted per placenta, and l is the intercept length estimated for each syncytial knot.

Numerical Density

$$CE = \sqrt{\frac{n}{n-1} x \left[\frac{\sum (Q)^2}{\sum Q \times \sum Q} + \frac{\sum (f)^2}{\sum f \times \sum f} - \frac{\sum (Q \times f)}{\sum Q \times \sum f} \right]}$$

where Q is the number of trophoblast, and f is the total number of disectors falling within the placenta.

2.5.3.2 Group Comparisons

All data in this study was expressed as mean and standard error of the mean (SEM). A one-way analysis of variance (ANOVA) was used for:

Pure disease:

- Early-onset PET versus preterm controls
- Early-onset IUGR versus preterm controls
- Early-onset PET-IUGR versus preterm controls

- Late-onset PET versus term controls
- Late-onset IUGR versus term controls
- Late-onset PET-IUGR versus term controls

Combined disease:

- Early-onset PET-IUGR versus early-onset PET = change due to IUGR
- Early-onset PET-IUGR versus early-onset IUGR = change due to PET

- Late-onset PET-IUGR versus late-onset PET = change due to IUGR
- Late-onset PET-IUGR versus late-onset IUGR = change due to PET

- SIDS-NBW versus term control
- SIDS-LBW versus term control

P-values below p=0.05 were considered statistically significant. Statistical analysis was carried out using Sigma Stat (2.0) aided by Microsoft Excel 2000.

2.6 Western Blotting for Cleaved-Cytokeratin 18 (CK 18)

Protein expression of apoptosis-specific cleaved CK18 (recognised by the monoclonal antibody M30), was semi-quantified by western blotting. Analysis of full-length CK8/18 protein was carried out to validate M30 detection of cleaved CK18. This was repeated 3 times and the average data was reported.

1. Samples

Systematic uniform-random samples were used from the following cases:

Preterm control	Early-onset PET	Early-onset PET-IUGR
(n=3)	(n=4)	(n=6)

2. Western blotting

Total protein extraction

1. Placental tissues were washed twice in ice-cold PBS and homogenised in RIPA lysis buffer (50mM Tris, 150mM NaCL, 1% Triton X 100, 1% Sodium Deoxycholate, 0.1% sodium dodecyl sulphate (SDS), pH 7.5) supplemented with complete protease inhibitor cocktail (Roche)
2. Samples were left for 30 min to 1hr on ice and centrifuged at 4^{o}C 10,000 rpm for 15 min.
3. Supernatants containing total protein were transferred to eppendorfs and protein concentration was determined according to the Bradford assay (280).
4. Equal amounts of extracted protein (85µg) were resuspended in 4x SDS reducing loading buffer and denatured by boiling for 5min.
5. 15µl of total protein was loaded and separated on 10% SDS-PAGE gel (15 well, 1.5mm) by electrophoresis for 2hrs at 50V and transferred (2hrs) to Polyvinylidene Fluoride (PVDF) membrane.

Immuno-detection for M30 and CK 8/18

1. Membranes were blocked with 5% skimmed milk in 0.1% TBS-T for 1hr at RT
2. Anti-M30 [1:500] (Peviva, clone M30) or anti-CK8/18 [1:1000] were diluted with 5% skimmed milk in TBS-T and incubated at 4^{o}C overnight
3. Membranes were then washed with TBS-T for 3x10 min

4. Incubation with either anti-mouse HRP conjugated Ig [1:1000] or anti-guinea pig HRP conjugated Ig [1:3000] respectively, diluted with 5% skimmed milk in TBS-T for 1hr at RT
5. Antibody reactions were visualised using ECL detection kit (Pierce) and visualised using X-ray film.
6. Membranes were then stripped and re-probed with goat polyclonal anti-beta actin [1:3000] (Santa Cruz) diluted with 5% skimmed milk in TBS-T and incubated at 4^{o}C overnight, allowing for standardisation of data.

Quantification

Bands were semi-quantified by densitometry (Image J). The optical density (OD) of the analysed samples was normalised to an internal control sample run on each blot allowing for inter-blot comparisons. This was followed by overall standardisation to beta actin OD.

3 Placental Pathology

3.1 Introduction

Severe early-onset IUGR due to placental insufficiency is characterised by significant reductions in uteroplacental and fetoplacental blood flow, represented by abnormal uterine and umbilical artery Dopplers respectively (140). Failure to physiologically increase uteroplacental blood flow in the early second trimester due to failed trophoblast invasion of the maternal spiral arteries leads to a reduced blood supply relative to the growth demands of the fetus. Approximately one third of such pregnancies will develop abnormal umbilical artery Doppler (140). The underlying causes of abnormal umbilical artery Doppler are complex and include both damage to areas of placental tissue due to infarction, and increased vascular impedance from poorly developed capillaries in terminal villi secondary to a defective angiogenic drive in the late second trimester of pregnancy. The inability of the poorly developed capillaries to extract oxygen ultimately creates an arterialized or 'hyperoxic' intervillous space relative to maternal tissues, further limiting placental angiogenesis and trophoblast proliferation (100). These changes contribute to the stepwise deterioration in placental function and umbilical artery Doppler flow patterns that characterize severe IUGR pregnancies, which often co-exist with pre-eclampsia in early gestation.

The pathological changes are associated with are numerous stereological and morphometric studies demonstrating reduced elaboration of the peripheral villous tree in severe early-onset IUGR (1; 2; 102; 152; 156; 161). Less understood is the impact of pre-eclampsia without IUGR on villous development in early gestation, mainly due to the lack of clinical delineation between the two. The aim of this chapter is to determine stereologically the villous phenotype of these diseases.

3.1.1 Hypothesis

The specific hypotheses are that:

1. Severe early-onset IUGR is associated with reduced volumes of peripheral villi compared with gestational age-matched controls.

2. Severe early-onset pre-eclampsia without IUGR is associated with normal or increased volumes of villi compared with gestational age-matched controls.

3. The villous phenotype in each early-onset disease differs from that observed in the late-onset variants of these pathologies.

4. The villous phenotype of the SIDS placenta is similar to that of the late-onset pre-eclampsia or IUGR placenta.

3.1.2 Experimental Aim

Determine the density and total volume of placental villi in placentas from early- and late-onset pre-eclampsia, IUGR, and SIDS using the stereological technique of point counting.

3.2 Results

Patient profiles of all 76 women involved in the Toronto cohort are presented in Appendix 1. (It should be noted that clinical data sets are incomplete and data is presented where available).

Placentas were delivered from non-smoking, chromosomally-normal, singleton pregnancies. All preterm and term controls showed no clinical or pathological signs of pre-eclampsia, IUGR, or any significant maternal co-morbidity.

3.2.1 Early-onset pathologies

3.2.1.1 Clinical data

Clinical and placental characteristics for severe early-onset pathologies are summarised in Table 3-1. A total of 35 women required delivery before or at 32 weeks of gestation (70% caesarean delivery) due to severe pre-eclampsia and/or IUGR. Twenty of these women were nulliparous with median maternal age of 30 years (range 17-43 years) and gestational age of 29 weeks (range 24-32 weeks). Birthweights were significantly reduced (median 840g; range 420-1550g) for both IUGR and pre-eclampsia with co-existing IUGR (50% $<3^{rd}$ centile and 79% 3-10^{th} centile respectively), as were placental weights (43% and 45% respectively).

All infants delivered as a result of maternal pre-eclampsia weighed between the 10-50^{th} birthweight centile for gestational age with placental weights comparable to preterm controls. Since 58% of preterm controls had a birthweight between the 50-90^{th} centile (weighing significantly more than expected), this may account for the significant reduction in birthweight in infants delivered as a result of severe early-onset pre-eclampsia ($P=0.013$). There were no significant differences in placenta: fetus weight ratio for either early-onset pathology.

All women delivering due to PPROM or cervical incompetence (preterm controls) or IUGR were normotensive throughout gestation and peripartum. The majority of pre-eclamptic women presented with severe hypertension (91%> 160/90 mm Hg) and ≥3+ proteinuria (82%). Two out of these 11 women had pre-existing chronic hypertension

with superimposed pre-eclampsia. This prevalence increased to 32% (6 out of 19 women) when pre-eclampsia co-existed with IUGR, 78% of whom presented with severe hypertension (>160/90 mm Hg) with ≥3+ proteinuria (63%). Thirty-six percent of pre-eclamptic women subsequently developed HELLP syndrome, the incidence of which fell to 21% when pre-eclampsia co-existed with IUGR.

Complex obstetric and medical histories, including previous pre-eclampsia requiring preterm delivery (3 out of 35 women) and well controlled diabetes mellitus (DM) (2 insulin dependent, 2 diet controlled and 1 gestational diet controlled DM) were observed for both pre-eclampsia with and without IUGR. Of the 2 women with diet controlled DM, 1 woman with pre-eclampsia with IUGR had a longstanding history of retinopathy and nephropathy. Idiopathic thrombocytopenia was observed in 1 woman from the preterm control study group. No previous obstetric or medical complications were noted for IUGR.

Infant mortality was low (11%), with perinatal deaths arising as a result of stillbirth (3 out of 5 mortalities) or intrauterine fetal death (IUD) from pregnancies complicated by IUGR with and without pre-eclampsia.

All preterm controls had normal Doppler assessment of umbilical artery blood flow. Abnormal uterine artery Doppler (UTAD) was observed in 11 of the 35 severe preterm pathologies. Nine of these were documented for women presenting with pre-eclampsia with co-existing IUGR; 8 bilateral and 1 unilateral diastolic notching. Only 1 of the 11 women with pre-eclampsia had abnormal UTAD (unilateral diastolic notching). UTAD was mostly normal for IUGR pregnancies with 1 documented case of bilateral diastolic notching in the uterine arteries.

Nearly all women (90%) with pre-eclampsia with co-existing IUGR had abnormal umbilical artery Doppler. Of the 17 documented abnormal findings, 11 women had absent EDF in the umbilical arteries whilst 6 had reversed EDF in the umbilical arteries. Three out of the 5 IUGR cases (60%) had documented AREDV in the umbilical arteries. The majority of pre-eclamptic women (82%) had positive end diastolic flow in the umbilical artery Dopplers (3 cases of ‘acute’ AREDV at delivery).

Table 3-1 Clinical and placental characteristics for severe early-onset pathologies

Characteristic	Control (*n*=12)	PET (*n*=11)	IUGR (*n*=5)	PET-IUGR (*n*=19)
Gestational age† (weeks)	30 (26-32)	29 (26-32)	29 (26-31)	28 (24-32)
Birthweight‡ (g)	1555 (970-1810)	1210* (710-1550)	700* (475-1260)	770** (420-1370)
Placental weight† (g)	343 (220-500)	330 (150-410)	198* (150-260)	204• (100-290)
Placenta:fetus wt ratio	0.241 (0.015)	0.291 (0.026)	0.285 (0.034)	0.263 (0.016)
BW centile				
> 50th (n)	7	0	0	0
10-50th (n)	5	11	0	0
< 10 (n)	0	0	5	19
Caesarean delivery (n)	5 (42%)	9 (82%)	4 (80%)	14 (74%)
Male‡ (n)	8/12 (67%)	5/9 (56%)	2/5 (40%)	10/18 (56%)
Female‡ (n)	4/12 (33%)	4/9 (44%)	3/5 (60%)	8/18 (44%)
Maternal age† (y)	28 (17-38)	30 (17-43)	28 (24-33)	32 (19-41)
Nulliparous‡ (n)	6/11 (55%)	7/8 (88%)	3/3 (100%)	10/17 (59%)
Blood pressure (mm Hg)				
systolic†	-	166 (140-180)	131 (127-140)	169 (144-200)
diastolic†	-	109 (90-123)	89 (74-98)	104 (96-110)
Proteinuria	0	≥3+ (73%)	0	≥3+ (67%)
HELLP (n)	0	4 (36%)	0	4 (21%)
Obstetric/Medical History				
Pre-eclampsia (n)	0	1	0	2
Chronic hypertension (n)	0	2	0	6
Diabetes Mellitus (n)	1	2	0	2
Abnormal Uterine artery Doppler (n)		1 (9%)	1 (20%)	9 (47%)
Unilateral diastolic notching (n)	-	1	0	1
Bilateral diastolic notching (n)	-	0	1	8
Abnormal Umbilical artery Doppler (n)		3 (27%)	3 (60%)	17 (90%)
Absent end-diastolic blood flow (n)	-	2	1	11∞
Reversed end-diastolic blood flow (n)	-	1	2	6
Abnormal AFI (<10) (n)	4	3	2	5
Perinatal mortality (n)	0	0	1	4

† data presented as the mean and range

‡ data presented as the median and range

‡ (n) presented as a ratio of available data

* significant difference compared to control

** significant difference compared to PET

• significant difference compared to IUGR

∞ includes 6 cases with absent/ intermittent reverse flow

3.2.2 Total Volumes of Placental Villi

All volumetric data is presented in Appendix 2.

Table 3-2 Volumetric estimates of placental villi for early-onset pathologies

Parameter	Control (n=12)	PET (n=11)	IUGR (n=5)	PET-IUGR (n=19)
Total Placental volume	323 ± 23	322 ± 27	158 ± 21*	169 ± 14**
Total Villous volume (cm^3)	147 ± 11	153 ± 18	72 ± 12*	82 ± 7**
V_{TOT} Structural villi (cm^3)	82 ± 12	90 ± 17	49 ± 11	51 ± 5**
V_{TOT} Peripheral villi (cm^3)	64 ± 8	63 ± 7	23 ± 3*	31 ± 4**
% peripheral villi: total villi	45 ± 6	45 ± 4	36 ± 7	38 ± 3
Total Villous Density	0.46 ± 0.02	0.47 ± 0.02	0.45 ± 0.03	0.48 ± 0.01
V_v Structural villi	0.25 ± 0.03	0.27 ± 0.03	0.30 ± 0.05	0.31 ± 0.02
V_v Peripheral villi	0.21 ± 0.03	0.20 ± 0.02	0.15 ± 0.02	0.18 ± 0.01

Data are presented as mean and SEM

*significant difference compared to controls

**significant difference compared to pre-eclampsia

Early-onset PET had no significant effect on total placental or villous volumes (totals or densities) compared to preterm controls.

Early-onset IUGR was associated with a significant reduction in total placental ($P<0.001$), total villous ($P=0.001$), and total volume of peripheral villi ($P=0.005$). No significant differences were observed for volume density estimates.

Early-onset PET-IUGR was associated with significant reductions in the total placental ($P<0.001$), structural ($P=0.013$) and peripheral villous volume ($P<0.001$). No significant differences were observed for villous densities.

3.2.3 Late-onset Cases

3.2.3.1 Clinical Data

Table 3-3 summarises the clinical and placental characteristics for late-onset pathologies.

A total of 16 women presented with either pre-eclampsia and/or IUGR in the second half of pregnancy requiring delivery (55% caesarean) at a median gestational age of 37 weeks (range 33-41 weeks) and with a median birthweight of 2640g (range 570-4690g). Birthweights were significantly reduced in IUGR with (100% $<3^{rd}$ centile, $P<0.001$) and without pre-eclampsia (75% $<3^{rd}$ centile, $P=0.003$), as were placental weights ($P=0.004$, $P<0.001$ respectively). All infants born as a result of maternal pre-eclampsia weighed between the $10\text{-}50^{th}$ centile for gestational age with placental weights comparable to controls; 46% of infants were between the $50\text{-}90^{th}$ centile for gestational age. Mean placenta: fetus weight ratio increased in late-onset pre-eclampsia with co-existing IUGR in comparison to controls, pre-eclampsia and IUGR, but failed to reach significance ($P=0.065$).

The majority of infants were male (65%) and born predominantly to second-time mothers (75% biparous) at a median maternal age of 33 years (range 26-43). Approximately 50% of pre-eclamptic women with and without IUGR presented with severe hypertension (>160/90 mm Hg) (50% and 33%) and ≥3+ proteinuria (33% and 50%). One of these women had pre-existing hypertension and one woman subsequently developed HELLP syndrome. All women from control and IUGR pregnancies were normotensive before and throughout gestation.

No complex obstetric or medical problems or perinatal mortalities were recorded for any of the term pathologies; however a history of DVT was noted in 1 woman in the control group.

UTAD was normal for term controls. Abnormal findings were noted for pre-eclampsia with (1 case of unilateral diastolic notching) and without IUGR (1 case of documented uteroplacental insufficiency). Abnormal umbilical artery Doppler was noted for IUGR at term; absent EDF in the umbilical arteries was documented in IUGR with (60%) and

without pre-eclampsia (67%). PEDV in the umbilical arteries was associated with all pre-eclamptic and control cases.

Table 3-3 Clinical and placental characteristics for late-onset pathologies

Characteristic	Control (n=13)	PET (n=6)	IUGR (n=4)	PET-IUGR (n=6)
Gestational age† (weeks)	38 (33-41)	36 (33-40)	36 (33-37)	36 (34-38)
Birthweight‡ (g)	3090 (2020-4690)	3000 (1970-4020)	1672* (1160-2400)	1600** (570-2325)
Placental weight† (g)	547 (360-700)	496 (352-603)	273* (180-338)	385** (256-500)
Placenta:fetus wt ratio	0.172	0.172	0.163	0.296
BW centile				
> 50th (n)	6	0	0	0
10-50th (n)	7	6	0	0
< 10 (n)	0	0	4	6
Caesarean delivery (n)	9 (69%)	2 (33%)	3 (75%)	3 (50%)
Male‡ (n)	9/13 (69%)	3/3 (100%)	3/4 (75%)	3/4 (75%)
Female‡ (n)	4/13 (31%)	0	1/4 (25%)	1/4 (25%)
Maternal age† (y)	33 (26-42)	30 (28-38)	32 (27-38)	34 (28-42)
Nulliparous‡ (n)	6/13 (46%)	2/3 (67%)	1/4 (25%)	2/4 (50%)
Blood pressure (mm Hg)				
systolic†	-	157 (150-164)	115	151 (140-160)
diastolic†	-	99 (91-107)	67	98 (80-110)
Proteinuria	0	≥3+ (33%)	1 (1+)	≥3+ (50%)
HELLP (n)	0	1 (17%)	0	0
Abnormal Uterine artery Doppler (n)		1 (16%)	0	1 (16%)
Unilateral diastolic notching (n)	-	1 utero.insufficiency	0	1
Bilateral diastolic notching (n)	-	0	0	0
Abnormal Umbilical artery Doppler (n)		0	2 (50%)	3 (50%)
Absent end-diastolic blood flow (n)	-	0	2	3
Reversed end-diastolic blood flow (n)	-	0	0	0
Abnormal AFI (<10) (n)	0	1	1	1
Perinatal mortality (n)	0	0	0	0

† data presented as the mean and range

‡ data presented as the median and range

‡ (n) presented as a ratio of available data

*significant difference compared to control

**significant difference compared to PET

HELLP= hemolysis, elevated liver enzymes, low platelet syndrome

3.2.3.2 Total Volume of Placental Villi

Table 3-4 Volumetric estimates of placental villi for late-onset pathologies

Parameter	Control (n=13)	PET (n=6)	IUGR (n=4)	PET-IUGR (n=6)
Total Placental volume (cm^3)	555 ± 33	487 ± 49	275 ± 42*	369 ± 40**
Total Villous volume (cm^3)	248 ± 14	247 ± 37	147 ± 26*	167 ± 14**
V_{TOT} Structural villi (cm^3)	129 ± 14	89 ± 8	80 ± 14	87 ± 15
V_{TOT} Peripheral villi (cm^3)	119 ± 13	157 ± 36	67 ± 18	80 ± 15
% peripheral villi: total villi	48 ± 4	60 ± 6	44 ± 6	48 ± 9
Total Villous density	0.45 ± 0.02	0.50 ± 0.04	0.53 ± 0.03*	0.46 ± 0.03
V_v Structural villi	0.24 ± 0.02	0.19 ± 0.02	0.29 ± 0.03	0.25 ± 0.05
V_v Peripheral villi	0.22 ± 0.02	0.31 ± 0.05	0.23 ± 0.04	0.21 ± 0.03

Data are presented as mean and SEM

*significant difference compared to controls

**significant difference compared to pre-eclampsia

Late-onset PET had no significant effect on total placental volume or total villous volume. However, there was a trend towards an increase in the volume density and percentage of peripheral villi compared to term controls (P=0.066).

Late-onset IUGR was associated with significant reductions in total placental (P<0.001) and total villous volume (P=0.017). There was no significant difference in the total volume of structural or peripheral villi. Total villous density was significantly increased (P=0.038) due to a slight increase in stem villous density.

Late-onset PET with IUGR displayed significant reductions in total placental (P=0.004), and total villous volume (P=0.003). No significant difference was observed in the total volume or density of structural villi or peripheral villi.

3.2.4 SIDS Cases

3.2.4.1 Clinical Data

Table 3-5 summarises the clinical data from the SIDS cohort. Patient profiles of all 24 women are presented in Appendix 1. Eight term controls were used from the Toronto cohort for comparison.

SIDS infants were born either spontaneously (58%) or by elective caesarean section (33%) to predominantly biparous women at a mean gestational age of 40 weeks (range 38-41 weeks). Postnatal age at death was not documented. SIDS-LBW infants had birthweights below the 10^{th} centile for gestational age which were significantly reduced ($P<0.001$) compared to term controls. SIDS-NBW cases were comparable to term controls for birthweight. Placental weights were significantly reduced in SIDS-LBW ($P=0.003$) but not in SIDS-NBW. Placenta: fetus weight ratios for SIDS-NBW and SIDS-LBW were comparable to controls.

SIDS-NBW infants were born to significantly younger mothers ($P<0.009$) with a mean maternal age of 24 years (range 15-39 years) compared to term controls (mean 32; range 26-37 years). SIDS-LBW infants had a high incidence of maternal smoking during pregnancy (82%); this fell to 58% in SIDS-NBW. All women were normotensive. No prevalence of male births was observed for all SIDS cases.

A high prevalence of previous perinatal deaths (cause unknown) were observed for both SIDS-LBW (42%) and SIDS-NBW infants (33%).

Uterine and/or umbilical artery Doppler was not documented for SIDS cases due to the retrospective study design. No pathological lesions (Dr.J.Gillan, personal communication) characteristic of placental insufficiency were noted for all SIDS and control cases.

Table 3-5 Clinical and placental characteristics for SIDS placentas

Characteristic	Control (n=12)	SIDS-LBW (n=12)	SIDS-NBW (n=12)
Gestational age† (weeks)	40 (38-41)	39 (37-41)	40 (39-41)
Birthweight† (g)	3507 (2640-4690)	2609* (1740-3420)	3425 (3110-3910)
Placental weight† (g)	549 (398-700)	391* (176-676)	511 (280-700)
Placenta:fetus wt ratio	0.16 (0.010)	0.15 (0.010)	0.15 (0.009)
BW centile			
> 10th centile (n)	12	0	12
< 10th centile (n)	0	12	0
Caesarean delivery (n)	5/12 (42%)	4 (33%)	4 (33%)
Male (n)	10/12 (83%)	6/12 (50%)	5/12 (42%)
Female (n)	2/12 (17%)	6/12 (50%)	7/12 (58%)
Maternal age† (y)	32 (26-37)	29 (19-46)	24* (15-39)
Nulliparous‡ (n)	6/12 (50%)	3/12 (25%)	1/12 (8%)
Smoker (n)	2 (17%)	10 (83%)	7 (58%)
BMI			
>24 (n)	2	2	1
<19 (n)	0	1	2
History of perinatal mortality (n)	3	5	4

† data presented as the mean and range

‡ (n) presented as a ratio of available data

*significant difference compared to control

3.2.4.2 Total Volume of Placental Villi

Table 3-6 Volumetric estimates of placental villi for SIDS cases

	Control (n=12)	SIDS-LBW (n=12)	SIDS-NBW (n=12)
Total Placental volume (cm^3)	513 ± 29	381 ± 34*	493 ± 23
Total Villous volume (cm^3)	264 ± 16	262 ± 22	347 ± 19*
V_{TOT} Stem villi (cm^3)	57 ± 6	55 ± 7	66 ± 15
V_{TOT} Intermediate villi (cm^3)	134 ± 14	84 ± 8*	109 ± 10
V_{TOT} Terminal villi (cm^3)	71 ± 19	122 ± 19	174 ± 13*
% terminal villi: total villi	24 ± 6	43 ± 5*	52 ± 3*

Data are presented as mean and SEM

*significant difference compared to controls

SIDS-NBW placentas were comparable to controls in terms of total placental volume. However, there was a significant increase in total villous volume (P=0.003). This was due to a significant increase in the total volume of terminal villi (P<0.001) and percentage occupied by terminal villi (P<0.001).

SIDS-LBW placentas were associated with significant reductions in total placental volume (P=0.008) and total volume of intermediate villi (P=0.008). The percentage occupied by terminal villi was significantly increased compared to term controls (P=0.025).

3.3 Discussion

3.3.1 Volumes

Volume is a crude measure of growth based on mass and physical composition in 3D. Stereological estimates of the volume of the placenta and its villi provide a measure of the overall growth and development of these structures, providing an index of placental function.

Total placental volume is a global quantity providing an estimate of net functional capacity since this organ must attain a certain size to meet the increasing demands of the growing fetus as gestation advances. This in turn is dependent upon an exponential increase in the total volume of its functional units, the chorionic villi, or more specifically the gas-exchanging villi during the third trimester of pregnancy when fetal maturation takes place. Both of these estimates are relevant to the pathology of pre-eclampsia, IUGR and SIDS.

Unbiased estimates of villous volume were obtained using the technique of point counting (269), to produce a volume density (ratio of placental villi to total placental volume). Changes in volume density may arise from changes in one or both of the associated variables; a reference trap appears when these changes are presumed to be due to changes in volume without considering the reference space i.e. total placental volume (281). Villous densities therefore give no indication of function and total placental volume must be taken in account to obtain absolute volumes relating to the entire organ.

Global changes in the total volume of villi result from an alteration in the number and/or size of placental villi and its subcomponents. Volumes of the underlying vasculature, the stromal core and the cytotrophoblastic tissues therefore determine the total volume of placental villi. Local changes in the volume density of placental villi (ratio of placental villi per unit volume of placenta) may not necessarily result in changes at the global level i.e. total placental volumes. For example, human adaptations to pregnancies associated with hypobaric hypoxia (282) and maternal anaemia (283) demonstrate total placental volumes comparable to normal pregnancy, however, they display increased volume densities of peripheral villi.

There is some degree of bias when estimating villous volumes inherent to placental collection. Blood loss and vasculature collapse as a result of spontaneous vaginal delivery may alter vasculature volume density (284) but should have minimal effect on villous density and trophoblast volumes. Nonetheless, every effort was made to ensure the umbilical cord was clamped immediately following delivery in order to preserve villous architecture. Although they may not be an exact representation of the *in vivo* state, estimates in this study are comparable to previous investigators.

Numerous investigations report that villous angiogenesis drives villous development (101), and it is well established that disruptions in villous angiogenesis results in altered villous growth (102; 103). In this study, volumes of fetal vasculature were not estimated which may limit accuracy when assessing villous pathology in severe early-onset pre-eclampsia, IUGR, and SIDS, since the former are largely determined by the oxygenation state of the intervillous space and subsequently the fetal vasculature (153). As such, the significance of this limitation stems from the fact that changes in total villous volume may not necessarily result from identical changes in the volume of the fetal vasculature. For example, whilst there may be a decrease in the total volume of villi, capillary volume density may be increased as part of an adaptive response; pre-eclampsia with IUGR at term is typically associated with reduced total volumes of terminal villi and an associated increase in capillary volume density (161).

3.3.2 Early-onset PET and IUGR: Divergent Villous Phenotypes?

The overall aim of this chapter was to determine the villous phenotype in severe early-onset pre-eclampsia and IUGR on which the trophoblast hypotheses were based. Because severe early-onset pre-eclampsia and IUGR often co-exist, few studies have 'clinically' separated the two pathologies. By carefully selecting pre-eclamptic cases with normal umbilical artery Doppler, the principal finding from this chapter is that severe early-onset pre-eclampsia and IUGR differ in their impact on placental villous volume. Whilst pre-eclampsia had no significant effect on villous volume, severe early-onset IUGR had a major impact on placental morphology. This suggests different patterns of villous development, indicative of divergent trophoblast phenotypes, in severe early-onset pre-eclampsia and IUGR.

There is general agreement between investigators using both molecular (113) and morphometric analyses (2; 152) that IUGR is associated with major defects in the development of the gas-exchanging villi, due to defective angiogenesis represented by AREDV in the umbilical artery (150). The pattern of villous maldevelopment is referred to as 'failed branching angiogenesis' associated with intraplacental 'hyperoxia', in which the oxygen content of maternal blood in the IVS increases (relative to maternal tissues) due to the inability of the malformed terminal villi capillaries to extract it (153). In the present study, placentas from severe early-onset IUGR with AREDV in the umbilical arteries displayed significant reductions in placental weight, total placental volume, the total volume of villi and the total volume of peripheral villi. This confirms the villous phenotype on which the trophoblast hypotheses are based, and is consistent with morphometric data describing villous maldevelopment in severe early-onset IUGR (1; 2; 102; 152; 156; 161). Significant reductions in the above parameters were also observed in severe early-onset PET-IUGR, plus an additional reduction in the total volume of structural villi.

Interestingly, there was a trend towards an increase in the volume density of both stem and immature intermediate villi in severe early-onset IUGR placentas (with and without pre-eclampsia), which may account for the fact there where no changes in total volume. The increase in density may result from an increase in either the number or size of these villi and/or accompanying vessels. From a developmental perspective, the decisive factors for placental growth and maturation depend upon when and to what extent

mature intermediate villi develop out of immature ones. Increased numbers indicates failure of immature villi to form mature intermediate villi, such that these vessels continue to branch into mainly immature villi resulting in less mature intermediate villi and terminal villi; hence, placental immaturity (285).

Equally likely is an increase in size of the vessels. One study reported tertiary-stem villi vessel wall hypertrophy with a reduction in luminal circumference in IUGR (between 28-38 weeks gestation), hypothesised to be due to the release of vasoactive substances that cause chronic vasoconstriction and vascular wall hypertrophy (286). Increased stem vessel density in this study is inconsistent with numerous investigations (using mainly 2D histological quantification) demonstrating significant reductions in stem artery density, postulated to be due to 'obliteration' of pre-formed arterioles, as previously reported (287). However, no significant differences in stem villi vascularisation were identified using systematic sampling and stereological tools (288).

Villous immaturity is an attractive concept in the placental pathology for severe early-onset IUGR, but is a rare finding at term (289). It is not clear whether in the severe IUGR placenta, the delay in villous maturation is defective from the outset of pregnancy or whether there is an "arrest" of development of a previously normal maturing villous tree. However, the trend towards an increase in the density of immature intermediate and stem villi in the present study support the latter theory, giving even more credence to the notion of an 'early origin' of 'early-onset' IUGR via dysregulated cytotrophoblast biology.

A more widely supported villous phenotype has been suggested based on the scarcity of the villous pathology as mentioned above, and secondly, on the observed failure in VEGF-directed branching angiogenesis and predominance towards PGF mediated non-branching angiogenesis leading to slender, longer capillaries with fewer loops, suggesting premature maturation of fetal vessels in terminal villi (155).

Stereological analyses report an increased severity of the alterations associated with IUGR in the presence of co-existing pre-eclampsia; clinically the most severe phenotype (161). The data in this study is in disagreement with these observations. Severe early-onset IUGR displayed the most severe placental phenotype (in terms of

volumetric data) in comparison to early-onset IUGR with pre-eclampsia. Villous volumes resembled that of isolated IUGR, but the severities of the alterations were lessened by the presence of severe early-onset pre-eclampsia. This suggests a potential interaction effect of severe early-onset pre-eclampsia with severe early-onset IUGR. Is it therefore possible that pre-eclampsia has a 'dampening' effect on IUGR since on its own, severe early-onset pre-eclampsia has no overall effect on the volumes of villi in this study?

Significantly, placentas from severe early-onset pre-eclampsia without any clinical signs of IUGR (normal umbilical artery Dopplers) were comparable to preterm controls in terms of placental weight, total placental volume, the total volume and density of villi, and the total volume and density of structural and peripheral villi. Umbilical artery Doppler is considered an indicator of placental vasculature resistance (290). Severe early-onset IUGR is typically associated with abnormal umbilical artery Doppler representing increased vascular resistance, associated with malformed terminal villi capillaries secondary to defective angiogenesis (290). A clinical criterion of this study for separating severe early-onset pre-eclampsia from IUGR was (in comparison to IUGR with AREDV) the selection of pre-eclamptic cases with PEDV in the umbilical artery, thereby signifying normal fetal growth i.e. birthweights were between the 10-50th centile for gestational age indicating adequate oxygen and nutrient exchange and hence normal fetal growth.

The finding that severe early-onset pre-eclampsia with normal umbilical artery Doppler has no effect on villous volumes in the present study is unique, and is in disagreement with the only other published stereological assessment of villous morphology in early-onset pre-eclampsia without IUGR (152).

The previous study showed that early-onset pre-eclampsia with normal umbilical artery Doppler is associated with abnormally developed terminal villi compared to preterm controls; similar abnormalities to those observed in severe early-onset IUGR placentas with documented AREDV. Significant reductions were noted in the total volume, surface area and capillary volume of terminal villi. The discrepancy may be due to the fact that the previous study used a smaller, less strictly defined group of pre-eclamptic cases with significantly reduced birthweights and placental volumes compared to

preterm controls *and* IUGR. However, the present study used a more homogeneous group of strictly defined severe pre-eclamptic cases without any signs of IUGR based on normal Dopplers and birthweights above the 10th centile for gestational age. Significantly, the fact that the same pathway of villous maldevelopment was documented for both early-onset pre-eclampsia and IUGR, but that abnormal umbilical artery blood flow was only documented in some IUGR cases and not pre-eclampsia, seems confounding. It is therefore possible that some infants in early-onset pre-eclampsia maybe subject to some degree of growth restriction in utero.

One non-stereological morphometric assessment of villous development in pre-eclampsia between 29-37 weeks gestation noted a high incidence of placental hypermaturity (285). Immature intermediate villi are transformed into mature ones too quickly producing vast numbers of terminal branches which is abnormal at every stage of gestation. Histologically there are many clusters of terminal villi with excessive capillarisation (153; 154) as a result of increased branching angiogenesis secondary to uteroplacental hypoxia. This pattern of villous development has been observed in both pre-eclampsia and IUGR (150) at term with PEDV in the umbilical arteries (153), which disagrees with the data in the present study. This could be due to the fact that a mixture of both mild and severe pre-eclamptic cases were used across a wider gestational age, and that analyses were based on one full-thickness section obtained from directly beneath the umbilical cord. Significantly, there were no cases of terminal villi deficiency as was seen in severe early-onset IUGR (stereological studies assessing fetal vasculature are reviewed in (155)).

In the present study, fetal birthweights from severe early-onset pre-eclamptic pregnancies were between the 10-50th centile for gestational age. A birthweight above the 10th centile for gestational age is an indicator of adequate oxygen extraction by the 'appropriately-grown' fetus, such that supply and demand between the placenta and fetus has been achieved.

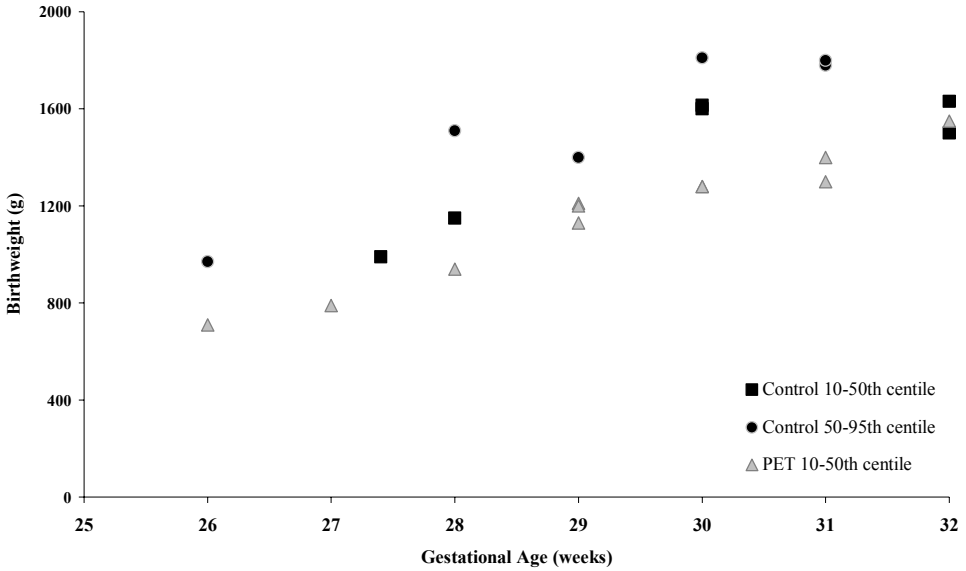

Graph 3-1 Birthweight centiles in preterm control and severe early-onset PET

Significantly, mean fetal birthweight was reduced in severe early-onset pre-eclampsia in comparison to controls. Importantly, the preterm control population used in this study displayed fetal birthweights that were considerably heavier than expected for gestational age; over half of the infants born prematurely had fetal birthweights above the 50th centile for gestational age. This is likely to account for the significant reduction observed in pre-eclamptic (mean) birthweight in this study. Crucially however, comparison of birthweights between the 10-50th centile for gestational age from preterm control pregnancies with pre-eclamptic birthweights revealed no significant difference (Graph 3-1), signifying normal fetal growth.

The reduction in mean fetal birthweight (although not statistically significant when accounting for birthweight centiles) in severe early-onset pre-eclampsia lead to an increase in placental to fetal weight ratio in comparison to preterm controls (approaching statistical significance, P=0.077), which was similar to the increase observed for severe early-onset IUGR with fetal birthweights below the 10th centile for gestational age. An increase in the placental weight to birthweight ratio has been previously observed in pre-eclamptic placentas (between 31-39 weeks of gestation) (161); all infants had significantly reduced birthweights.

3.3.2.1 Summary

- Severe early-onset pre-eclampsia was not associated with alterations in the volume if placental villi
- Severe early-onset IUGR displayed significant reductions in the total volume of villi and the total volume of peripheral villi

3.3.3 Late-onset PET, IUGR and SIDS: Similar Villous Phenotypes?

Pre-eclampsia and IUGR in late pregnancy are typically associated with normal umbilical artery Doppler indicating normal fetoplacental vascular impedence. Adaptive angiogenesis in peripheral villi is thought to reduce capillary resistance leading to normal umbilical Doppler velocimetry in late gestation, thereby 'prolonging' pregnancy. In the present study, placentas from late-onset IUGR and SIDS infants demonstrate increased villous volumes indicating possible villous adaptation (161). Pre-eclampsia had no significant effect on villous volumes in late gestation.

Placentas from late-onset IUGR displayed significant reductions in total placental and total villous volume, similar to their severe early-onset IUGR phenotype. However, in contrast, the volume density of placental villi was significantly increased in comparison to term controls. This increase was more attributable to a trend towards an increase in the volume density of stem and immature intermediate villi, rather than peripheral villi, a feature also observed for severe early-onset IUGR with AREDV. This is inconsistent with previous investigations reporting adaptive angiogenesis in peripheral villi (increased capillary volume fraction) from IUGR placentas at term with positive end-diastolic flow in the umbilical artery (155). Interestingly, 2 of the 4 cases in the late-onset IUGR group had absent end diastolic flow in the umbilical artery at 33 and 34 weeks of gestation. From a physiological point of view, failure to detect such changes may be logical considering the growth restricted neonates required delivery before reaching full term, implying that the peripheral villous tree failed to initiate adaptive changes as previously documented. However, it is not possible with the current number of cases (n=4) to determine with any degree of accuracy whether this is a true morphological characteristic of this pathology at term.

Late-onset pre-eclamptic placentas were comparable to late gestation controls (33-41 weeks of gestation) in terms of total placental volume and total villous volume. Although not statistically significant, there was an apparent shift towards an increase in the total volume and density of peripheral villi (increase from 119 cm^3 in controls to 157 cm^3 in late-onset pre-eclampsia) and decrease in structural villi (from 129 cm^3 in controls to 89 cm^3 in late-onset pre-eclampsia). However, these estimates displayed large variation and coupled with the low number of cases in this group, statistical significance was not reached.

Interestingly, the above changes were not evidenced in the combined disease. Reductions in total placental and total villous volumes were due to the effects of IUGR, and similar to severe early-onset cases PET-IUGR, was not the most severe phenotype in terms of villous maldevelopment.

SIDS-NBW placentas were comparable to term controls with respect to total placental volume, whilst placentas from SIDS-LBW infants were significantly smaller. A novel finding from this study is that SIDS placentas display a significant increase in the total volume of terminal villi compared to term controls independent of fetal birthweight. Both SIDS-LBW and SIDS-NBW were associated with a 42% and 59% increase in the volume of terminal villi, respectively. Histologically terminal villi appeared congested with dilated capillaries. These observations suggest that the placenta has increased its surface area for diffusional exchange which may be a compensatory mechanism for 'potential insults' that may have occurred early in gestation. Secondly, that these compensatory mechanisms have been initiated by factors relating to SIDS and not to LBW.

The observed increase in the total volume of terminal villi in SIDS is a feature typically associated severe maternal anaemia (283), pregnancies at high altitude (282), and in some (291) but not all (292; 293) cases of maternal smoking during pregnancy. Placentas from these pregnancies are associated with 'pre-placental' hypoxia (153) and adaptive villous angiogenesis resulting in increased capillary volume density have been reported using both stereological (103) and corrosion casting methods (291).

There is a strong correlation between fetal hypoxia and an increased risk of SIDS. The origin of fetal hypoxia is proposed to be associated with the high incidence of maternal smoking in SIDS events (166). In this study, the majority of SIDS infants were born to mothers who smoked throughout gestation; 10 out of 12 SIDS-LBW infants and 7 out of 12 SIDS-NBW infants were born to mothers who smoked. This data implies that smoking is more associated with LBW than to SIDS, and recent studies report an average 377g decrease in fetal birthweight as a result of maternal smoking during pregnancy (294).

Based on the considerations of placental adaptation to the maternal environment above, it may be presumed that the increase in terminal villi volume observed in SIDS placentas is due to the effects of maternal smoking, such that adaptive angiogenesis is initiated during early pregnancy secondary to 'pre-placental' hypoxia, thereby ensuring adequate diffusional exchange throughout gestation. However, by separating smoking- from non-smoking mothers in SIDS-NBW, there remains a significant increase in terminal villi volume in non-smoking SIDS-NBW mothers compared to non-smoking term controls (P=0.007). This suggests that the increase in terminal villi volume is independent of maternal smoking and LBW due to factors relating specifically to SIDS. As maternal smoking during pregnancy has been demonstrated to lead to fetoplacental insufficiency, and hence fetal hypoxia, it may be concluded that hypoxia is a prerequisite for the occurrence of SIDS. It is unsurprising then that hypoxic perinatal risk factors for SIDS include both pre-eclampsia (53) and intrauterine growth restriction.

The increase in terminal villi volume in both SIDS-LBW and SIDS-NBW is more severe than that observed for late-onset pre-eclampsia and IUGR. Two interpretations are possible based on the assumption of increased terminal villi volume as an adaptive response to fetal hypoxia. First, that the origin of the presumed fetal hypoxia is uteroplacental insufficiency as documented for pre-eclampsia and IUGR. Second, that the SIDS placenta is able to compensate fully for the presumed pre-placental hypoxia, and thus remove the potential to develop pre-eclampsia and/or IUGR.

These results suggest that SIDS-NBW placentas have sufficient compensatory reserve to maintain fetal growth in utero until term e.g. normal birthweights, which SIDS-LBW placentas lack. However, since these infants are still victims of SIDS, it suggests that these in utero mechanisms are insufficient to compensate for developmental abnormalities in organs critical for survival *ex utero*. Other causally associated mechanisms must therefore be present that do not necessarily result in altered placental morphology. Hence, while it is assumed that the placental abnormalities are causative for SIDS fetal deficiencies, it is also equally likely that these factors are first present in the fetus and are causative for placental abnormalities (82). As such, it is possible a fetally derived abnormality of the trophoblast may be sequelae of abnormalities in villous development.

3.3.3.1 Summary

- Late-onset PET was not associated with any significant changes in villous volumes
- Late-onset IUGR placentas displayed a significant increase in villous density
- SIDS placentas displayed a significant increase in the total volumes of terminal villi independent of fetal birthweight

4 Cytotrophoblast Biology

4.1 Introduction

Fetal growth and survival are dependent upon successful villous development. Villous growth is proliferative, which is dependent upon the ability of a pool of villous cytotrophoblast progenitor cells to continually proliferate, such that the products of cell division can differentiate and fuse with the overlying syncytium throughout gestation. Studies in mice (181; 187; 191) and human villous explant models (185; 191) show that syncytial fusion is required for syncytial integrity and that the asymmetric roles for cytotrophoblasts is created by the asymmetric expression of the transcription factor GCM1. These studies suggest that the developmental potential of the villous cytotrophoblast lineage and its regenerative capacity are dependent upon the relative proportions of proliferating and differentiating cytotrophoblasts, and that this balance maybe the key player in determining the elaboration and final size (i.e. the physical parameters) of the placental villous tree, and subsequently its functional capacity. Reduced numbers of villous cytotrophoblast progenitor cells may therefore contribute to the small placental phenotype and reduced elaboration of the peripheral villous tree in severe early-onset IUGR.

Studies also suggest that maternal health is dependent upon the balance between proliferating and differentiating villous cytotrophoblast cells (3). An accelerated regenerative capacity of villous cytotrophoblast cells (i.e. preference of villous progenitor cells over differentiating cytotrophoblast cells displaying an increased rate of proliferation and syncytialisation) is hypothesised to result in abnormal shedding of syncytiotrophoblast (e.g. aponecrosis) (210; 214), resulting in the excessive release of anti-angiogenic proteins (e.g. soluble Flt-1) (28) which contributes towards the systemic endothelial syndrome of pre-eclampsia.

4.1.1 Hypothesis

The overall hypothesis is that severe early-onset PET and IUGR display an altered balance between villous cytotrophoblast proliferation and differentiation.

The specific hypotheses are that:

1. Severe early-onset IUGR placentas display reduced total numbers and density of proliferating villous cytotrophoblast cells in comparison to preterm controls

2. Severe early-onset pre-eclamptic placentas display normal or increased numbers and density of proliferating villous cytotrophoblast cells in comparison to preterm controls

3. Villous cytotrophoblast proliferation is normal or increased in late-onset pre-eclampsia late-onset IUGR in comparison to term controls

4. The villous cytotrophoblast phenotype in SIDS is similar to that observed for late-onset pre-eclampsia or IUGR placentas

4.1.2 Experimental Aim

Using stereological analysis, the following parameters will be estimated:

1. The volume of villous cytotrophoblast cells immuno-localised for cytokeratin 7

2. The number of non-proliferating and proliferating villous cytotrophoblast cells by simultaneously estimating (i) the density of villous cytotrophoblast cells immuno-localised with cytokeratin 7 and (ii) the density of villous cytotrophoblast cells co-localised with the nuclear proliferation marker, Ki-67, in 25μm paraffin sections.

4.2 Results

All volumetric and numerical data for the villous cytotrophoblast is presented in Appendix 3.

4.2.1 Early-onset pathologies

4.2.1.1 Total Volume of Villous Cytotrophoblast

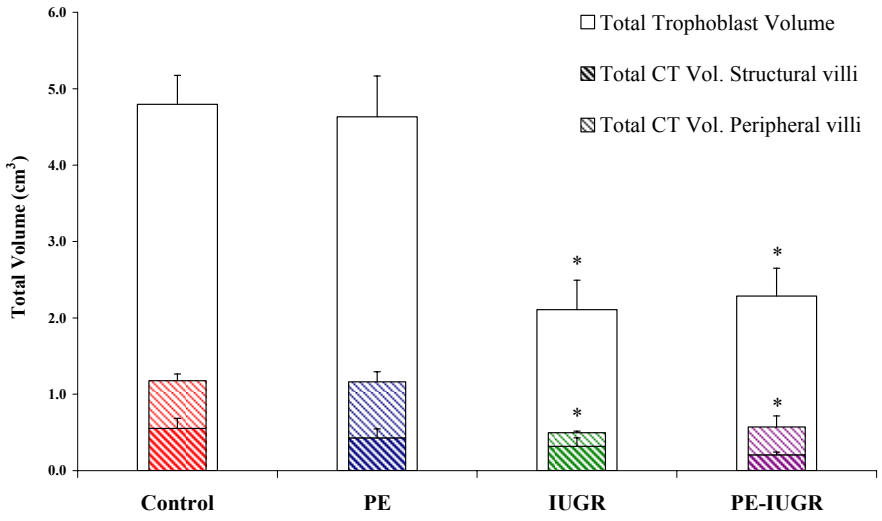

Graph 4-1 Total CT volume in early-onset pathologies

There were significant reductions in:

IUGR total trophoblast volume (P<0.001)
total volume of CT (P=0.004)
total volume of CT for peripheral villi (p=0.018)

PET-IUGR total trophoblast volume (P<0.001)
total volume of CT (P<0.001)
total volume CT for structural villi (p=0.005)
total volume of CT for peripheral villi (p=0.009)

Table 4-1 Volume density of CT in early-onset pathologies

	Control (n=12)	PET (n=11)	IUGR (n=5)	PET-IUGR (n=19)
Volume density	0.016 ± 0.001	0.016 ± 0.002	0.014 ± 0.001	0.013 ± 0.002
Structural villi	0.006 ± 0.001	0.004 ± 0.001*	0.006 ± 0.001	0.004 ± 0.0004*
Peripheral villi	0.010 ± 0.001	0.011 ± 0.001	0.008 ± 0.001	0.010 ± 0.001

Data presented as mean and ± SEM

* significant difference compared to controls

There were significant reductions in:

PET volume density of CT for structural villi (p=0.027)

PET-IUGR volume density of CT for structural villi (P=0.013)

4.2.1.2 Total Number of Villous Cytotrophoblast cells

Graph 4-2 Total CT number in early-onset pathologies

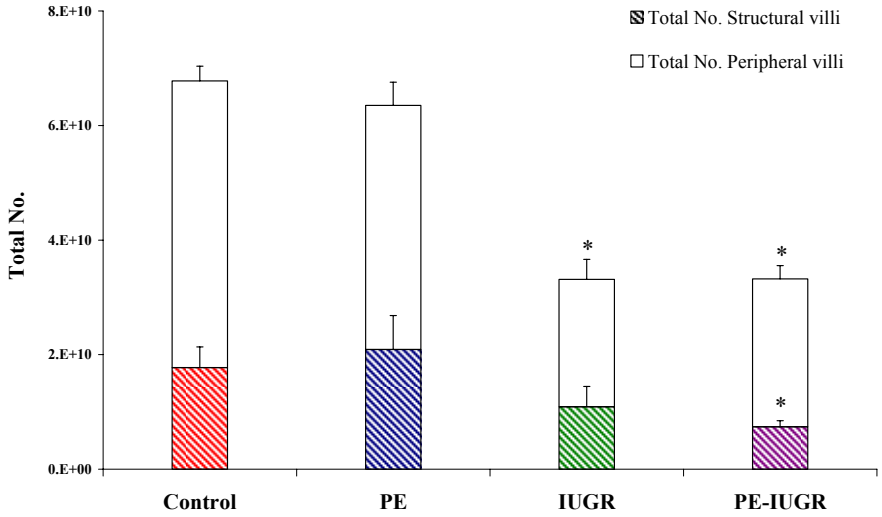

Total numbers of cytotrophoblast were significantly decreased in

IUGR peripheral villi ($P<0.001$)

PET-IUGR structural ($P=0.045$) and peripheral villi ($P=0.019$)

Table 4-2 Numerical density of CT in early-onset pathologies

	Control (n=12)	**PET (n=11)**	**IUGR (n=5)**	**PET-IUGR (n=19)**
Total Density (μm^{-3})	$2.1x10^{-4} \pm 1.2x10^{-5}$	$1.9x10^{-4} \pm 1.1x10^{-5}$	$2.1x10^{-4} \pm 1.6x10^{-5}$	$2.0x10^{-4} \pm 6.7x10^{-6}$
N_v Structural villi	$5.4x10^{-5} \pm 1.0x10^{-5}$	$5.8x10^{-5} \pm 1.4x10^{-5}$	$6.2x10^{-5} \pm 1.3x10^{-5}$	$4.4x10^{-5} \pm 1.3x10^{-5}$
N_v Peripheral villi	$1.6x10^{-4} \pm 1.0x10^{-5}$	$1.3x10^{-4} \pm 8.1x10^{-6}$	$1.4x10^{-4} \pm 1.2x10^{-5}$	$1.5x10^{-4} \pm 5.5x10^{-5}$

There were no significant differences in the numerical density of cytotrophoblast cells. There was however a trend for CT density to decrease in PET ($P=0.071$) (peripheral villi).

4.2.1.3 Total Number of Ki-67 positive Villous Cytotrophoblast cells

Graph 4-3 Total number of Ki-67 positive CT in early-onset pathologies

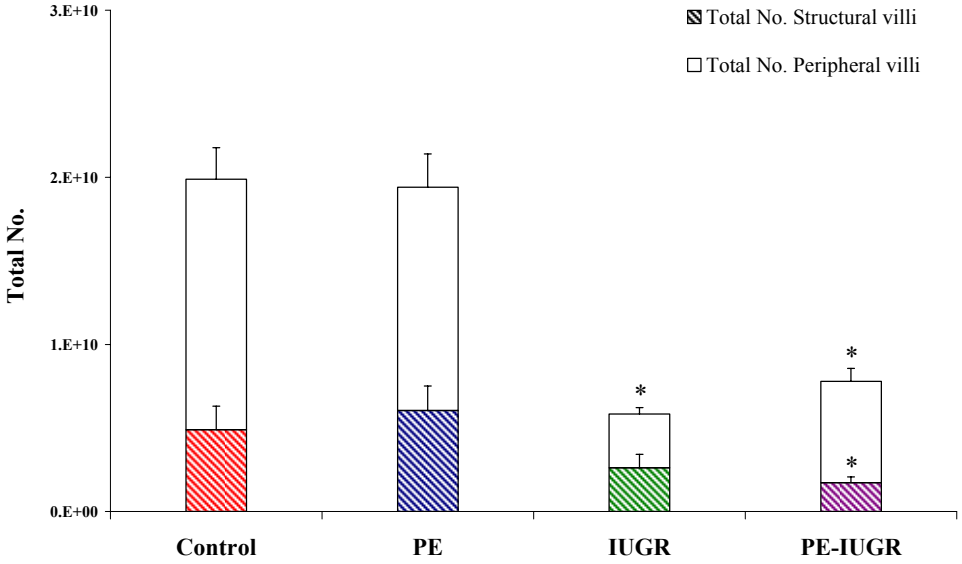

Table 4-3 Numerical density of Ki-67 positive CT in early-onset pathologies

	Control (n=12)	PET (n=11)	IUGR (n=5)	PET-IUGR (n=19)
Numerical density (um^{-3})	$6.2x10^{-5}$ (± 7.6)	$6.1x10^{-5}$ (± 5.6)	$3.6x10^{-5}$ (± 3.8)*	$4.5x10-^{5}$ (± 2.8)**
N_v Structural villi	$1.5x10^{-5}$ (± 3.8)	$1.7x10^{-5}$ (± 3.5)	$1.5x10^{-5}$ (± 3.9)	$1.0x10^{-5}$ (± 1.8)
N_v Peripheral villi	$4.7x10^{-5}$ (± 5.5)	$4.4x10^{-5}$ (± 6.4)	$2.1x10^{-5}$ (± 3.0)*	$3.5x10^{-5}$ (± 2.6)**

Data presented as the mean and ± SEM ($x10^{-6}$)

* significant difference compared to controls

** significant difference compared to pre-eclampsia

Significant reductions for

IUGR total number (p=0.006) and total density of Ki-67 +ve CT (p=0.044) density of Ki-67 +ve CT for peripheral villi (p=0.009)

PET-IUGR total number (p<0.001) and total density of Ki-67 +ve CT (p=0.046) total number and density of CT for peripheral villi (p=0.009, p=0.007)

Graph 4-4 Percentage (%) of Ki-67 positive CT in early-onset pathologies

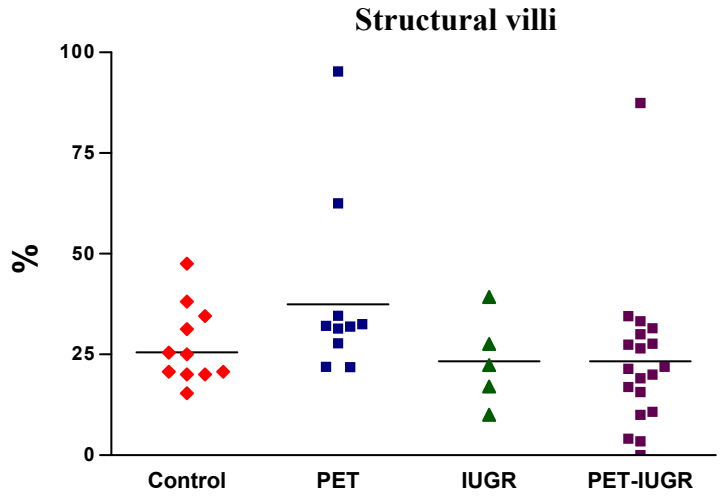

Ratio Ki-67:CT	1:5	1:3	1:5	1:7
	p value	0. 097	0. 833	0. 743

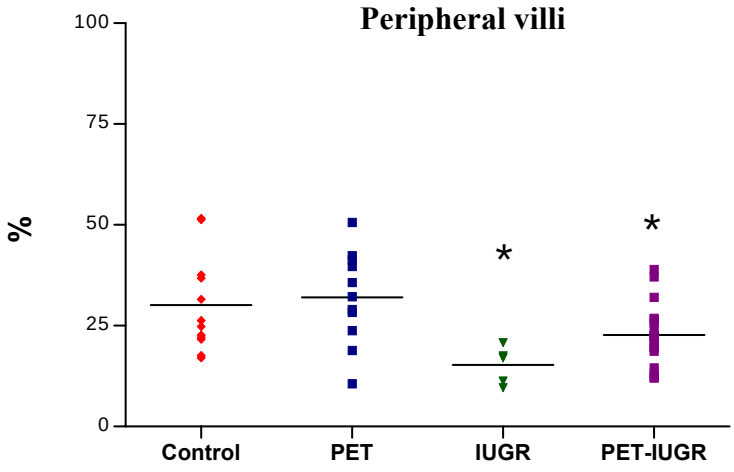

Ratio Ki-67: CT	1:4	1:3	1:7	1:5
	p value	0. 069	0. 002	0. 025

There were no significant differences in the % or ratio of Ki-67 positive CT in structural villi compared to controls

The percentage and ratio of Ki-67 positive CT cells was significantly reduced in peripheral villi in:

- **IUGR** 50% reduction compared to preterm controls (P=0.018)
- **PET-IUGR** 25% reduction compared to preterm controls (P=0.041)

4.2.1.4 Summary

Severe early-onset PET

- significant decrease in the volume density of cytotrophoblast in structural villi (Table 4-1)

Severe early-onset IUGR and PET-IUGR

Significant reductions in

- the total volume of cytotrophoblast cells (Graph 4-1)
- the total number of cytotrophoblast cells (Graph 4-2)
- the total number and density of Ki-67 positive cytotrophoblast cells (Graph 4-3, Table 4-3)
- the percentage of cytotrophoblast cells positive for Ki-67 (
-
-
- Graph 4-4)

4.2.2 Late-onset pathologies

4.2.2.1 Total Volume of Villous Cytotrophoblast cells

Graph 4-5 Total volume of CT in late-onset pathologies

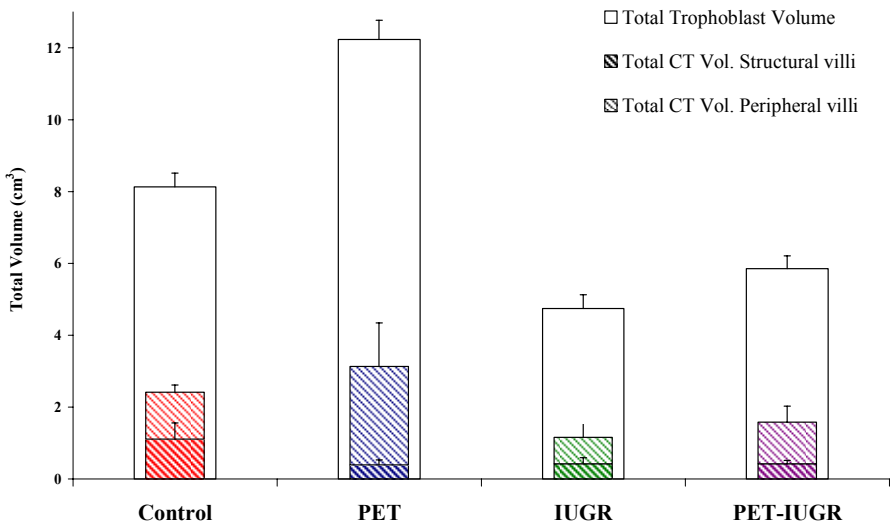

There was no statistically significant difference in total trophoblast volume or total CT volume compared to controls

Table 4-4 Volume density of CT in late-onset pathologies

	Control (n=13)	PET (n=6)	IUGR (n=4)	PET-IUGR (n=6)
Volume density	0.018 ± 0.003	0.018 ± 0.004	0.013 ± 0.005	0.017 ± 0.003
V_v Structural villi	0.007 ± 0.002	0.004 ± 0.001	0.005 ± 0.002	0.005 ± 0.001
V_v Peripheral villi	0.011 ± 0.001	0.014 ± 0.004	0.009 ± 0.003	0.012 ± 0.003

Data presented as mean and ± SEM

There were no statistically significant differences in CT volume density when compared to controls.

4.2.2.2 Total Number of Villous Cytotrophoblast cells

Graph 4-6 Total number of CT in late-onset pathologies

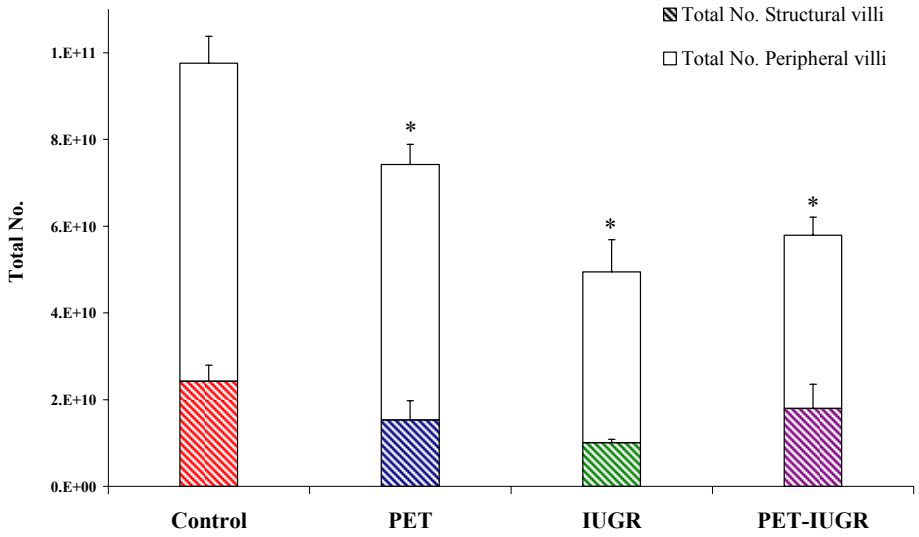

There was a significant decrease in the total number of CT in comparison to controls for:

PET total CT volume (P=0.048)

IUGR total CT volume (p=0.003), total CT volume for peripheral villi (P=0.013)

PET-IUGR total CT volume (p=0.004), total CT volume for peripheral villi (P=0.004)

Table 4-5 Numerical density of CT in late-onset pathologies

	Control (n=13)	**PET (n=6)**	**IUGR (n=4)**	**PET-IUGR (n=6)**
Numerical Density (μm^{-3})	$1.8x10^{-4} \pm 8.6x10^{-6}$	$1.6x10^{-4} \pm 1.6x10^{-5}$	$1.8x10^{-4} \pm 1.3x10^{-5}$	$1.6x10^{-4} \pm 1.2x10^{-5}$
N_v Structural villi	$4.5x10^{-5} \pm 6.5x10^{-6}$	$3.0x10^{-5} \pm 7.1x10^{-6}$	$4.0x10^{-5} \pm 8.4x10^{-6}$	$4.5x10^{-5} \pm 1.1x10^{-5}$
N_v Peripheral villi	$1.3x10^{-4} \pm 8.3x10^{-6}$	$1.3x10^{-4} \pm 1.5x10^{-5}$	$1.4x10^{-4} \pm 9.8x10^{-6}$	$1.1x10^{-4} \pm 6.3x10^{-6}$

Data presented as mean and ± SEM

There were no significant differences in the numerical density of CT cells for late-onset pathologies in comparison to controls.

4.2.2.3 Total Number of Ki-67 positive Villous Cytotrophoblast cells

Graph 4-7 Total number of Ki-67 positive CT in late-onset pathologies

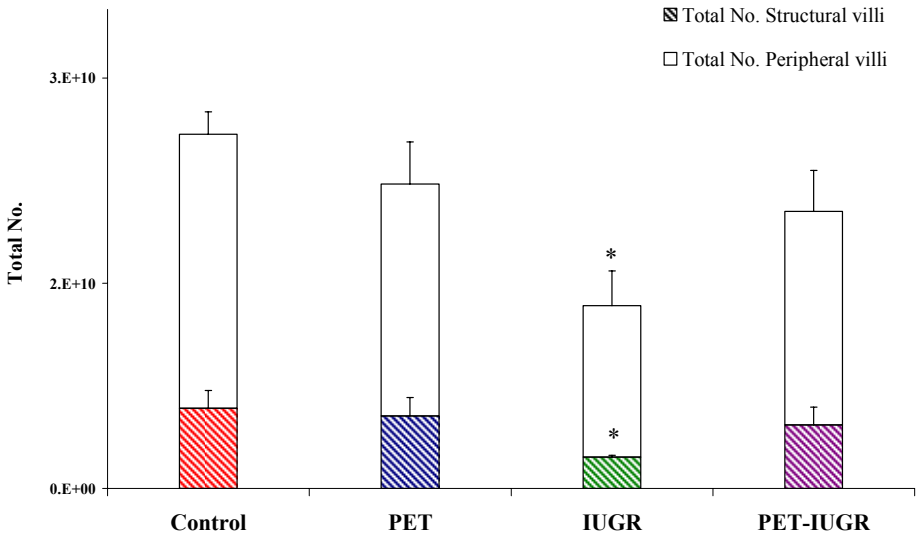

IUGR displayed significant reductions in the total number of Ki-67 positive CT cells (P=0.009). This was specific for both structural (P=0.020) and peripheral villi (P=0.015).

Table 4-6 Numerical density of Ki-67 positive CT in late-onset pathologies

	Control (n=13)	PET (n=6)	IUGR (n=4)	PET-IUGR (n=6)
Numerical Density (μm^{-3})	$4.7x10^{-5}$ (± 3.3)	$4.6x10^{-5}$ (± 6.7)	$4.8x10^{-5}$ (± 2.6)	$5.4x10^{-5}$ (± 7.8)
N_v Structural villi	$1.1\ x10^{-5}$ (± 2.0)	$1.1x10^{-5}$ (± 2.6)	$9.3x10^{-6}$ (± 2.2)	$1.2x10^{-5}$ (± 2.4)
N_v Peripheral villi	$3.6x10^{-5}$ (± 2.4)	$3.5x10^{-5}$ (± 5.6)	$3.9x10^{-5}$ (± 4.1)	$4.3x10^{-5}$ (± 6.3)

Data presented as mean and ± SEM ($x10^{-5}$)

There were no significant differences in the numerical density of Ki-67 positive CT when compared to controls.

Graph 4-8 Percentage of Ki-67 positive CT in late-onset pathologies

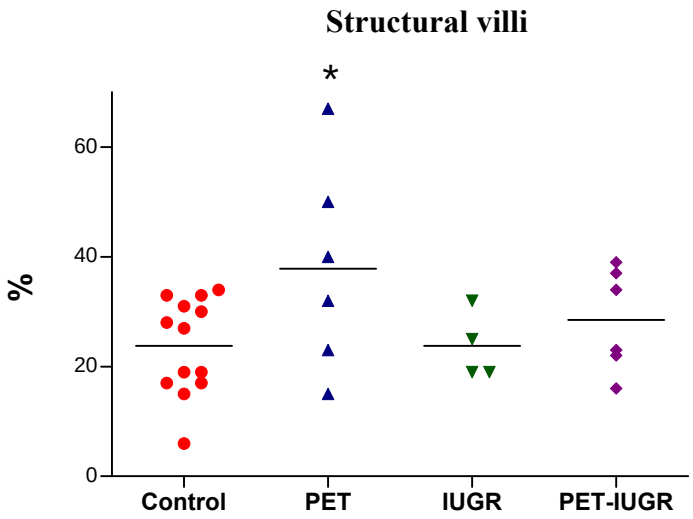

Ratio	1:5	1:3	1:5	1:4
Ki-67:CT	p value	0. 114	0. 665	0. 394

There was a significant increase in the percentage of Ki-67 positive CT for structural villi in **PET** (P=0.037).

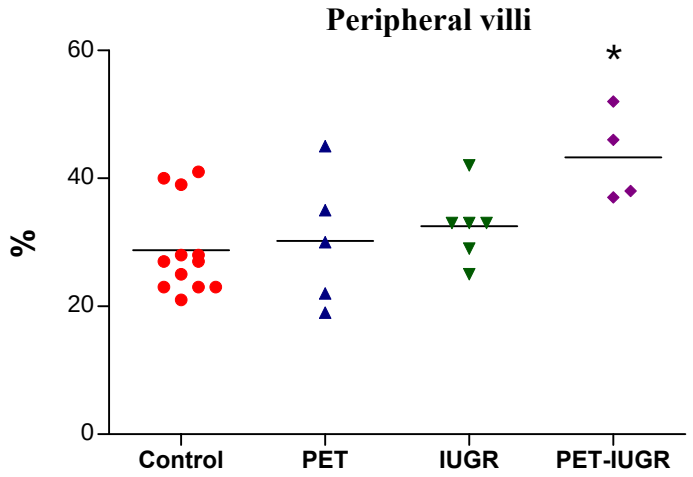

Ratio	1:5	1:5	1:4	1:5
Ki-67:CT	p value	0. 625	0. 945	0. 340

There was a significant increase in the percentage of Ki-67 positive cytotrophoblast cells in **PET-IUGR** (P=0.051)

4.2.2.4 Summary

Late-onset PET

- significant decrease in the total number of cytotrophoblast cells (Graph 4-6)
- significant increase in the percentage of Ki-67 positive cytotrophoblast cells for structural villi (Graph 4-8)

Late-onset IUGR

Significant reductions in

- the total volume of trophoblast (Graph 4-5)
- the total number of cytotrophoblast cells (Graph 4-6)
- the total number of Ki-67 positive cytotrophoblast cells (Graph 4-7)

Late-onset PET-IUGR

- significant reduction in the total number of cytotrophoblast cells (Graph 4-6)
- significant increase in the percentage of cytotrophoblast cells positive for Ki-67 specifically for peripheral villi (Graph 4-8)

4.2.3 SIDS

4.2.3.1 Total Volume of Villous Cytotrophoblast cells in SIDS

Graph 4-9 Volume density of CT cells in SIDS placentas

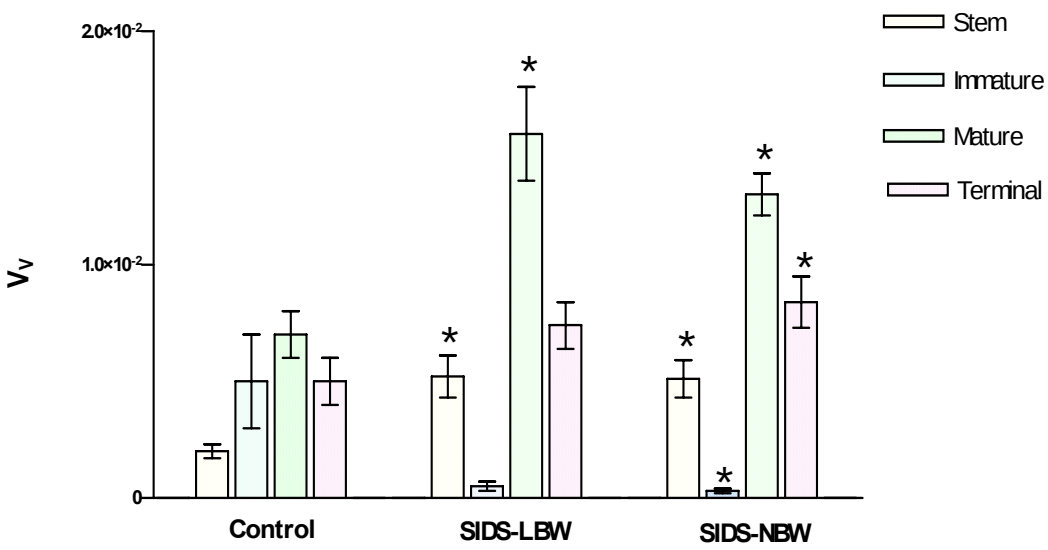

Table 4-7 Total volume of CT in SIDS

Total Volume (cm^3)	Control (n=12)	SIDS-LBW (n=12)	SIDS-NBW (n=12)
V_{TOT} Stem villi	0.60 ± 0.08	1.30 ± 0.26*	1.79 ± 0.32*
V_{TOT} Intermediate villi	3.32 ± 0.90	4.09 ± 0.59	4.59 ± 0.35
V_{TOT} Terminal villi	1.37 ± 0.32	2.03 ± 0.29	2.99 ± 0.50*

Data presented as mean and ±SEM

Immature and mature intermediate villi are grouped as intermediate villi

* significant difference compared to control

SIDS-NBW displayed a significant increase in CT volume density (stem p=0.006, mature p<0.001, and terminal villi, p=0.042), and total CT volume (stem p=0.002, terminal p=0.012).

SIDS-LBW displayed a significant increase in CT volume density (stem p=0.008 and mature villi p=0.002) and total CT volume (stem villi p=0.017).

4.2.3.2 Summary

SIDS-NBW

- significant increase in the total volume and volume density of cytotrophoblast (stem, mature intermediate terminal villi) (Table 4-7,Graph 4-9)
- significant decrease in cytotrophoblast volume density for immature intermediate villi (Graph 4-9)

SIDS-LBW

- significant increase in the total volume of cytotrophoblast cells for stem villi (Table 4-7)
- significant increase in the volume density of stem and mature intermediate villi (Graph 4-9)

4.3 Discussion

4.3.1 Methodology

Estimating the number of proliferating villous cytotrophoblast cells using stereological analysis

Although stereologically-derived numbers, volumes and surface areas of the villous cytotrophoblast compartment have long established the structural parameters of syncytial and villous growth (i.e. hyperplastic vs. hypertrophic growth) (200; 295; 296), the actual growth fraction of this population (i.e. the number of proliferating cytotrophoblast cells) has not, until now, been determined stereologically in either normal or pathological pregnancies. The implication of increased villous cytotrophoblast proliferation in pre-eclampsia and decreased cytotrophoblast proliferation in IUGR is therefore based purely on 2D counting methods (typically using the proliferation marker Ki-67) and non-randomised sampling regimes, which are generally limited to mild disease presenting in the third trimester (Table 4-8). Furthermore, accuracy of these studies is in itself conflicted by comparable 2D studies describing no change in cytotrophoblast proliferation in both pathologies (199; 239; 297). This inconsistency is due to the lack of sampling methodology and *ad hoc* cell counting methods which lead to inaccurate and irreproducible results in 2D.

2D vs. 3D estimation of villous cytotrophoblast proliferation

Why count in 3D?

The estimation of the number of cells/nuclei in a histological section generating a 'number per unit area' is to a certain degree valid, but *only* to the area in which they were analysed; the fact that this area does not represent the entire organ is a major avenue for misinterpretation of reality, which is inherently 3D. The advantage of using stereological analysis is that it estimates the *total number* of cells in the entire placenta (i.e. in 3D), thereby relating structural changes to potential functional changes at the whole organ level (256).

Table 4-8 Studies of CT proliferation using Ki-67 and 2D counting methods

Proliferation marker	Pathology	GA	Results	Reference
Ki-67	IUGR + AREDV	24-41 wks	↓ CT proliferation	(244)
	IUGR + AREDV	28-36 wks	↓ CT proliferation	(1)
Ki-67	IUGR	Term	No difference	(199; 239; 297)
	IUGR + PET	26-39 wks	↓ CT proliferation	(245)
Ki-67	PET	37-42 wks	↑ MIB-1/BrdU ratio	(201)
	PET		↑ CT proliferation	(238)
	PET	Term	No difference	(239)
Ki-67	PET + HELLP	Term	↑ CT proliferation	(239)

The numerous 2D cross sections of villi that appear in a histological section vary from field-to-field, in the number of villous cytotrophoblast cells and in the number of those undergoing proliferation, which are both spatially (immature intermediate villi display the highest proliferation index (201)) and temporally regulated (the density of proliferating cytotrophoblast cells declines with increasing gestational age (212)). Since it is the combination of all villi which determines the functionality of the 3D placenta, an unbiased representation of all villi should be obtained, which is achieved stereologically by uniform-random sampling at the placental and histological levels, thus giving all villi and cytotrophoblast cells the same probability of being selected for estimation. Restricting estimations to 'one or two areas' within a histological section from a single 'chosen' sample in 2D studies (e.g. many 2D studies use a single sample obtained directly beneath the umbilical cord) will lead to extremely inaccurate and erroneous conclusions of little biological worth.

2D studies rely on 'assumption-based' counting methods

A further inaccuracy of 2D studies is that cells/nuclei are counted based on their frequency within a histological section, which is governed by their size, shape and orientation (i.e. assumption-based counting). The number of 2D profiles (a 'transect' through a 3D cell) appearing in a histological section will therefore rarely mimic the number of 3D cells in reality. In practice, the angle and thickness at which the histological section is 'physically' taken (e.g. microtome sectioning) will ultimately determine the number of 2D profiles in a histological section biased to a cells size,

shape and orientation. This is likely to result in over/underestimation of particle number as:

S*ize*: large cells have more chance of being cut by a microtome blade than small cells possibly resulting in overestimation of cell number. Conversely, smaller cells have a higher improbability of being included into any given section thickness resulting in underestimation.

S*hape*: irregular particles (e.g. ganglion) will be cut in several places by the blade in the same plane resulting in multiple profiles appearing in one histological section, making it difficult to distinguish whether the multiple profiles belong to the same cell or not, leading to overestimation of particle number.

Orientation: fusiform cells (e.g. smooth muscle cells) will be cut more times using transverse sections than by longitudinal sections, therefore cell morphology also needs to be taken into account.

Given the dangers highlighted above and the fact that 2D rarely mimics reality, if you *ass-u-me*, you make *ass* out of *u* and *me* (259). To overcome these assumptions, stereological counts are made within a defined volume of tissue, using either one thick section (optical brick technique (279)) or a pair of thin, perfectly-registered serial sections a known distance apart (physical disector technique (274)). Cells are counted within an unbiased counting frame (258) ensuring cells are counted only *once*, generating the number of cytotrophoblast cells per unit volume of placenta, or numerical density.

Interpreting total numbers in stereological analysis

The total number of proliferating cytotrophoblasts cells in the human placenta is estimated by multiplying numerical density by total placental volume. From a stereological perspective, the total number of cytotrophoblast cells in the placenta therefore depends upon placental volume and the numerical density of cytotrophoblast cells. For there to be no change in the total number of proliferating cells, the reference volume and numerical density must remain unchanged compared to a population parameter. Alternatively, total numbers would remain unchanged if the reference volume increased whereas the numerical density decreased, and vice versa.

An increase in numerical density therefore does not dictate a global increase in the total number of cells, since the reference space in which the cells are contained may be significantly smaller (i.e. reduced placental volume), resulting in no change or a significant increase in the total number of cells. Conversely, a decrease in numerical density does not automatically result in a global decrease in the total number of cells since the reference space in which they are contained may be larger (i.e. increased placental volume), resulting in no change or a significant decrease in the total number of cells.

A 'true' change occurs when the nature of change in both parameters follows suite, i.e. a reduction in numerical density is matched by a reduction in the reference space and ultimately, the total number of cells, and vice versa. In this scenario, changes in the local characteristics of the tissue have resulted in global changes at the whole organ level. A more difficult situation to interpret arises when there are no changes in local characteristics (i.e. numerical density), yet there is a significant change at the global level. For example, if there is no change in numerical density, a reduction in the total number of cells can only result from a significantly reduced reference volume. In this situation, the reduction in the total number of cells may be loosely regarded as a 'false-positive' because it is the local characteristics of the tissue in question which ultimately determine the global characteristics and hence function of the tissue at the whole organ level. The question then arises of how and why local characteristics do not imitate global changes. Information regarding the physiological/biochemical characteristics of the tissue is therefore required.

4.3.1.1 Double-immunolabelling of proliferating CT cells in thick sections

Stereological assessment of the cytotrophoblast population involves the estimation of volume and number. The estimation of the total number of cytotrophoblast cells in the human placenta has, until now, been estimated using the physical disector technique (274) based on morphology and topography using 5μm tinctorially-stained sections. Morphological estimation of cytotrophoblast number may introduce bias (albeit minimal) into the final estimation by failure to resolve cytotrophoblast nuclei from syncytiotrophoblast nuclei and stromal cells. The most efficient way to estimate cell number is achieved by applying the disector principle to one thick section (≥25 μm) in which cells are counted within a known volume using an optical brick (279). There is, however, limited application of the optical brick technique in placental research since the use of thick sections reduces the ability to unambiguously identify different cell populations (discussed in the following section).

Stereological analysis of cytotrophoblast proliferation is based on the supposition that an increase in cell number is synonymous with an increase in the number of proliferating cells (200). Whilst these interpretations are valid since an increase in cell number can only occur by cell division, these methods do not quantify or distinguish the population currently undergoing proliferation, the growth fraction, from non-proliferating cells. In this study, a novel double-immunolabelling protocol was developed in 25μm thick paraffin sections using monoclonal antibodies to cytokeratin 7, a cytoplasmic marker of cytotrophoblast cells, and Ki-67, a nuclear marker of proliferation, thereby allowing the unbiased estimation of the total number of proliferating cytotrophoblast cells using the optical brick technique.

The application of this double-labelling technique for stereological analysis is advantageous since 1) the estimation of number using the optical brick technique is more efficient than using the physical disector 2) the use of cytokeratin 7 to distinguish cytotrophoblast cells from syncytium and stromal cells removes the experimental bias introduced when assigning trophoblast nuclei to different compartments based purely on morphology, and 3) the use of Ki-67 precludes the assumptions concerning trophoblast proliferation based on an increase in cell number.

Although immunohistochemistry has previously been achieved in thick paraffin sections in the mouse placenta (184), and similarly antibodies to cytokeratin 7 and Ki-67 have been employed to identify trophoblast and proliferating cell in double-labelling on single sections (239) or individually on parallel sections (204), the superiority of the double-stain arises from the adaptation of these two markers into one combined stain in thick paraffin section therefore allowing quantification of cell number using the optical brick technique.

4.3.1.2 Cytokeratin 7 as an immuno-histochemical marker for quantifying CT

Present methods to study villous cytotrophoblast cells using light microscopy include the use of tinctorial stains (e.g. haematoxylin & eosin) or the immuno-histochemical localisation of phenotypic subsets of these cells i.e. progenitor (185), proliferating or differentiating cytotrophoblast cells (189; 214). A current limitation in quantifying the total complement of cytotrophoblast cells is the lack of a generic immunohistochemical marker which identifies all phenotypes of the cytotrophoblast population, thus permitting the unambiguous delineation of *all* cytotrophoblast cells from syncytiotrophoblast nuclei and stromal cells. This is a crucial requirement of stereological analysis, as failure to accurately distinguish (and count) different cell populations increases the risk of stereological bias at the level of the observer, which may ultimately lead to under or overestimation of cell number.

In thin tinctorially-stained paraffin sections, cytotrophoblast cells can be readily delineated from syncytiotrophoblast nuclei morphologically and topographically. Undifferentiated cytotrophoblast cells residing on the basal lamina exhibit a large ovoid nucleus with ample chromatin, resulting in weak nuclear staining which is easily distinguished from the dense staining pattern of syncytiotrophoblast nuclei (85). Conversely, differentiating cytotrophoblast cells which have lost contact with the basal lamina, exhibit similar staining patterns to syncytiotrophoblast nuclei, making this phenotype more difficult to distinguish histologically without the use of antibodies (85). These limitations are greatly amplified when using thick paraffin sections (i.e. 25µm) that are required for number estimation using the optical disector technique. Antibody criteria for the estimation of cytotrophoblast cell number therefore included 1) the constitutional expression of the antigen within the cytoplasm of all cytotrophoblast cells

throughout gestation 2) no cross-reactivity with syncytiotrophoblast nuclei or stromal cells and 3) the ability to penetrate 25μm thick paraffin sections.

A review of the literature revealed three commercially available markers specifically for cytotrophoblast cells. These included antibodies to E-cadherin [6], a cell-cell adhesion protein expressed in the cytoplasm of cytotrophoblast cells, hepatocyte growth factor activator inhibitor-1 (HAI-1) (298-300), a membrane protein expressed in cytotrophoblast cells, and cytokeratin 7, an intermediate filament protein expressed in the cytoplasm of epithelial cells (301). HAI-1 localised to a subset of villous cytotrophoblast cells displaying inconsistent staining ranging from apical, to basal, to whole cytoplasmic localisation and was thus excluded. A recent study showing failure of *HAI-1* deficient mice to undergo branching morphogenesis (300) suggests a similar expression pattern (e.g. asymmetric expression in a subset of villous cytotrophoblast cells) and role to GCM1 (191) in directing human villous cytotrophoblast differentiation (214).

Cytokeratin 7 is a member of the intermediate filament family of proteins expressed in epithelial cells which interact with the basement membrane (via integrins) linking the cytoskeleton to the extracellular matrix (302). In the human placenta, different populations of cytotrophoblast cells express cytokeratins in a developmental, differentiative (301) and functional manner (303). In first trimester placentas, cytokeratin 7 is expressed in extravillous (cell islands and columns) and villous cytotrophoblast cells, but also in the basal plasma membrane of the syncytiotrophoblast layer (301). During the second and third trimester, cytokeratin 7 expression increases throughout the whole of the syncytium (301). Because cytokeratin 7 is expressed in cytotrophoblast *and* syncytiotrophoblast, immunolocalisation of cytokeratin 7 specifically to cytotrophoblast cells (in both second and third trimester placentas) was achieved though the omission of antigen retrieval. Staining was localised to the cytoplasm of cytotrophoblast cells and no cross-reactivity was observed for the syncytiotrophoblast nuclei or stromal cells. A pilot study estimating cytotrophoblast cell number at term using the optical brick technique demonstrated a significant increase in the number of cytotrophoblast cells counted when using the mAb cytokeratin 7 (presented at the European Histopathology Meeting, Northampton, UK 2007) in comparison to counts made on tinctorially stained sections (H&E).

4.3.1.3 Ki-67 as an immunohistochemical marker of proliferating CT

Ki-67 is an established marker of cell proliferation (304), as the antigen is present in the of all active phases of the mammalian cell cycle, G_1, S, G_2, and M phase, and absent in quiescent cells (G_0) or non-cycling cells (305). In the human placenta, only a subset of villous cytotrophoblast nuclei express Ki-67. Its expression has been semi-quantified in numerous 2D analyses in both normal and pathological pregnancies (Table 4-8) but cell numbers have not, until now, been accurately quantified stereologically (restricted to villous cytotrophoblast cells). There are however recognised caveats when using Ki-67 as a proliferation marker:

Proliferation is an indicator of growth by means of an increase in cell number; hence, an ideal proliferation marker must therefore identify cells which are *going to divide*. Ki-67 however is a phase-labelling index, and Ki-67 expression does not declare that a cell is unquestionably going to divide as the cell may still decide to exit the cell cycle and enter a quiescent or terminally differentiated state (306). Ki-67 positivity should therefore be used to indicate the *potential* of a cell to divide, and not to predict the actual division of the cell (306).

Furthermore, Ki-67 positivity gives no indication of the rate of proliferation. The rate of cytotrophoblast proliferation is determined by the duration of interphase (G_1, S, and G_2 phases), and to a lesser extent, by the time it takes for the cell to divide in mitosis. For any given population, cytotrophoblast cells may differ in inter-mitotic times such that they exhibit different proliferative activity (G_1, S, and G_2 phases) but a constant S phase, or differ in the duration of S phase but have a constant proliferative phase. Thus, Ki-67 only labels those cells actively involved in the cell cycle and provides no indication of the rate of proliferation. Further analysis of the different phases of the cell cycle (BrdU for S phase and mitotic counts for M phase) would allow identification of the growth fraction of cells that is actively dividing (306).

In the human placenta, Ki-67 will be expressed in both villous cytotrophoblast progenitor cells and in a population of their daughter cells undergoing transit cell divisions prior to syncytial fusion. Its expression therefore is not a direct determinant of the progenitor cell pool. In fact, quiescent (G_0) villous cytotrophoblast cells (Ki-67

negative) may be regarded as 'true progenitor' cells *per se* as they remain in an undifferentiated state destined for future mitotic cycles throughout gestation, whilst their daughter cells undergo syncytial fusion or further transit cell divisions prior to syncytial fusion (Ki-67 positive). Relevant murine immunohistochemical markers to Cdx2 and FGF-R2 (170) should be employed in future studies in an attempt to identify true progenitor cells representing the villous trophoblast stem cell lineage.

4.4 Results

4.4.1 Villous Cytotrophoblast Proliferation in Normal Pregnancy

Between the first and third trimester of pregnancy, the human placenta undergoes a significant increase in the total volume and surface area of the chorionic villous trees. During the first trimester, linear growth of stem and immature intermediate villi occurs via a steady state of proliferating cytotrophoblast, endothelial and stromal cells (200). During the second and third trimester of pregnancy, growth of mature intermediate and terminal villi is vascular-mediated (115), such that endothelial proliferation prevails over cytotrophoblast proliferation resulting in capillary coiling and morphogenesis of terminal villi from the surfaces of mature intermediate villi. The functional consequence of these changes serve to thin the trophoblast layer thereby decreasing the diffusional distance of oxygen and nutrients between maternal and fetal circulations needed to maintain adequate fetal growth in the second half of pregnancy. In this context, it may be concluded that proliferation is more important during the first half of pregnancy, whereas cytotrophoblast differentiation is more relevant in later gestation thus regenerating the villous trees.

In the present study, volumetric growth of the cytotrophoblast increased significantly from an average 1.18 cm^3 to 2.42 cm^3 between 26 and 41 weeks of gestation. This reflects the increase in total placental and villous volume with increasing gestational age, consistent with previous reports (200); however total cytotrophoblast volume estimates were considerably lower (307). This is because total villous volume as opposed to total placental volume was used as the reference volume, allowing potential changes to be related to specific villous types, which are an indicator of gestational changes and hence functionality.

Gestational changes in villous cytotrophoblast proliferation in the normal human placenta between 26 and 41 weeks of gestation are illustrated in Graph 4-10. In proportion to the increase in total cytotrophoblast volume, the total number of cytotrophoblast cells increased significantly with increasing gestational age (Graph 4-10, B), consistent with previous stereological data. In contrast, when looking at relative numbers, the density (N_v) of cytotrophoblast cells decreased significantly with increasing gestational age, which was paralleled by a significant decline in the density of proliferating cytotrophoblast cells (Graph 4-10, A). The decrease in numerical density is accountable to the fact that villous surface area expands with increasing gestational age, thereby dispersing cytotrophoblast cells across the villous surface resulting in a reduced number of cytotrophoblast cells per unit volume of placenta. This indicates a genuine decline in the density of proliferating cytotrophoblast cells in the normal human placenta between 26 and 41 weeks of gestation.

There is however a mismatch between the total number of cytotrophoblast cells and the total number of proliferating cytotrophoblast cells (Graph 4-10, B). Whilst the total number of cytotrophoblast cells significantly increased between 26 and 41 weeks of gestation, the total number of proliferating cytotrophoblast cells remained constant, equivalent to approximately 30% of the total complement of cytotrophoblast cells. Together, these results confirm that the *relative pool* of proliferating villous cytotrophoblast cells decreases significantly between 26 and 41 weeks of gestation in the normal human placenta, but the proportion of proliferating cytotrophoblast cells remains constant throughout gestation (Graph 4-10, C). This suggests that a definite number of proliferating cytotrophoblast cells is required to maintain the epithelial steady state in the second half of pregnancy, which is estimated to be approximately 30%, or that 1 in 4 villous cytotrophoblast cells are actively cycling in the human placenta between 26 and 41 weeks of gestation.

Given the basic considerations of villous physiology in the third trimester of pregnancy (i.e. vascular-mediated villous growth), there are likely functional consequences of altering the pool/definite number of proliferating cytotrophoblast cells in the second half of pregnancy. An increase in the number of proliferating cytotrophoblast cells would result in an increased number of cytotrophoblast cells and subsequently villous membrane thickness, (providing no change in extrusion), thus impeding diffusional

exchange of oxygen and nutrients to the fetus. Alternatively, the reverse holds true in that insufficient numbers of proliferating cytotrophoblast cells in the third trimester may lead to depletion in cytotrophoblast number and subsequent growth and regeneration of the syncytium, thereby limiting active transport and endocrine function needed to maintain fetal growth (via the villous tree) in the third trimester of pregnancy.

A single proliferative unit can be expressed as a ratio of the number of cytotrophoblast cells to the number of syncytiotrophoblast nuclei. Previous stereological analyses estimated a single proliferative unit to be composed of one cytotrophoblast cell associated with between 9 and 13 syncytiotrophoblast nuclei. In the present study, these estimates in both early and late gestation were considerably higher at 1:5 (range 1:4 to 1:7). The preterm placenta (between 26 and 32 weeks of gestation) in the present study was estimated to contain approximately $6.8x10^{10}$ cytotrophoblast cells. However, between 27 and 31 weeks of gestation Mayhew estimated there to be $0.36x10^{10}$ cytotrophoblast cells in the human placenta, whilst Simpson estimated these placentas to contain 0.34 $x10^{10}$ cytotrophoblast cells. The disparity is likely due to the fact that the previous investigators used the physical disector technique to count cytotrophoblast nuclei morphologically, whereas in this study cytokeratin 7 was used to immunolocalise cytotrophoblast cells which is likely to increase the number of cells identified.

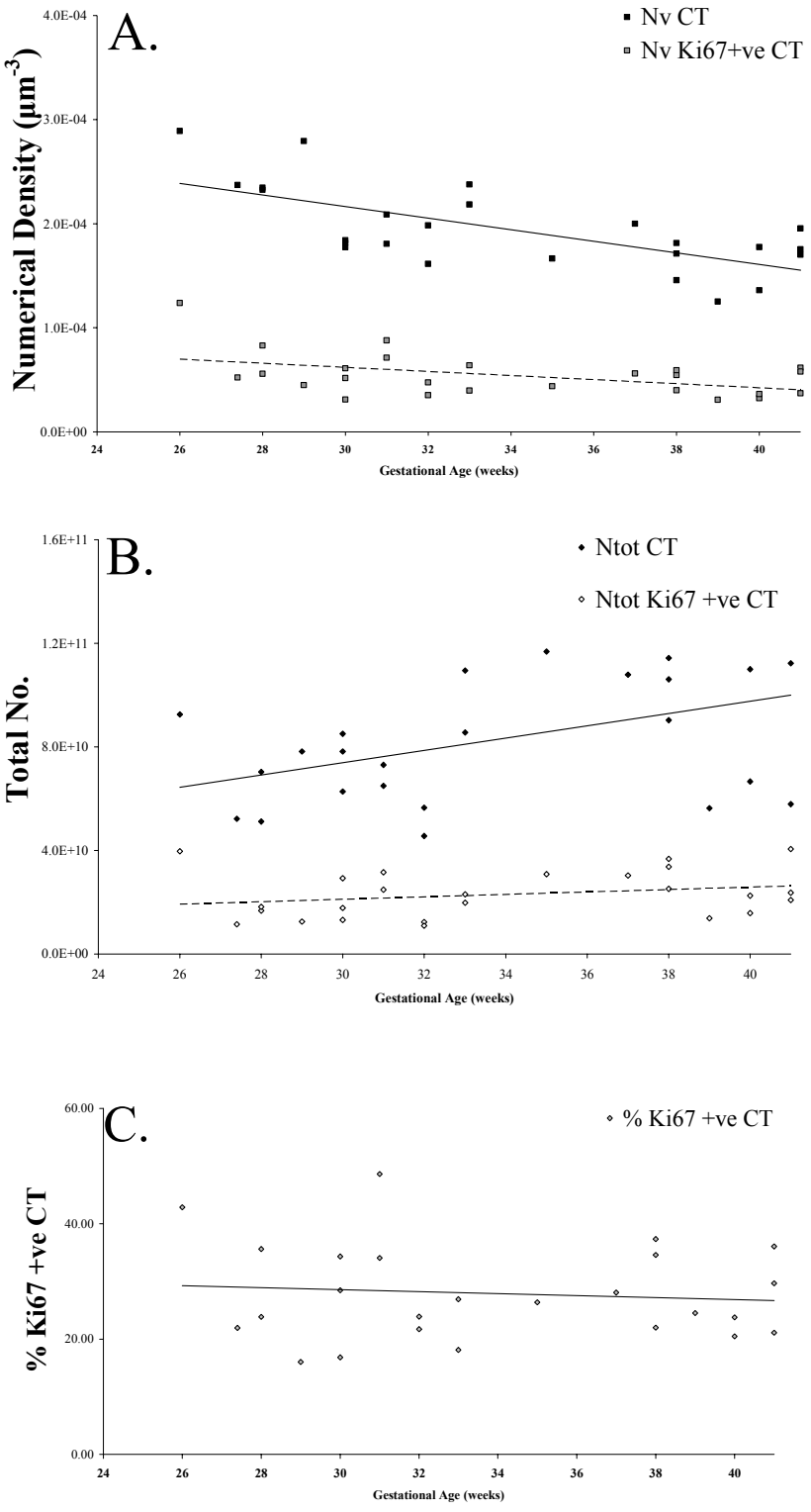

Graph 4-10 Gestational changes in the number of proliferating CT cells in control placentas between 26 and 41 weeks

(A) The numerical density of cytotrophoblast cells and Ki-67 +ve CT significantly declines with gestational age ($P<0.001$, $P=0.021$) (B) Total numbers of CT cells significantly increase with gestational age ($P=0.019$) whereas Ki-67 +ve CT cells do not (C) Percentage of proliferating cytotrophoblast cells remains constant across gestation.

4.4.2 Villous Cytotrophoblast Proliferation in Early-onset PET and IUGR

The present findings confirm the hypothesis that severe early-onset IUGR placentas with documented AREDV in the umbilical arteries have reduced numbers of proliferating villous cytotrophoblast cells. Conversely, data does not support the hypothesis that severe early-onset pre-eclampsia with PEDV in the umbilical arteries is associated with increased numbers of proliferating villous cytotrophoblast cells. This may indicate divergent villous trophoblast phenotypes in severe early-onset pre-eclampsia and IUGR.

4.4.2.1 Decreased Villous CT proliferation in Severe Early-onset IUGR

By 26 weeks of gestation, severe early-onset IUGR placentas show a significant reduction in the total number of cytotrophoblast cells in peripheral villi, and that within this reduced complement of cells, the percentage undergoing proliferation (i.e. Ki-67 positive) is also significantly reduced (50%) in comparison to age-matched controls. This may indicate a severe impairment in the regenerative capacity of villous cytotrophoblast cells, which may reflect premature loss of villous progenitor cells that can proliferate, differentiate and fuse with the overlying syncytium throughout gestation, thereby contributing to the small placental phenotype of IUGR.

The reduction in cytotrophoblast proliferation in severe early-onset IUGR was spatially and temporally regulated. Peripheral villi did not display any significant changes in cytotrophoblast density in comparison to control placentas, however 50% fewer cells were undergoing proliferation; equivalent to 1 in 7 cytotrophoblast cells undergoing proliferation compared to 1 in 4 in controls. Conversely, structural villi were not associated with alterations in cytotrophoblast volume, number or those undergoing proliferation. This suggests arrest of mitosis immediately prior to or at the onset of development of the gas-exchanging villi.

Cytotrophoblast proliferation is upregulated by intra-placental hypoxia and down-regulated by increasing intra-placental oxygen levels *in vitro* (100). The observed reduction in the number of proliferating cells in this study is therefore consistent with the notion of intra-placental ‘hyperoxia’ in severe early-onset IUGR. Increased oxygen levels (relative to maternal blood) in placentas from IUGR with AREDV are thought to

result from the inability of the poorly developed terminal villi to extract it (153). Since these placentas had reduced volumes of peripheral villi, placental 'hyperoxia' is a plausible, but not an exclusive explanation for reduced cytotrophoblast proliferation in severe early-onset IUGR.

Villous cytotrophoblast cells represent a heterogeneous population of cells displaying distinct cellular phenotypes, including 1) progenitor cells (185) 2) mitotic or cycling cells 3) differentiating/fusing cells (189) and more recently 4) apoptotic/necrotic cytotrophoblast cells (308). Based on a simple model of cell division, a decrease in cytotrophoblast proliferation should result in a decrease in the number of daughter cells. Significantly, this was not observed in severe early-onset IUGR and the reduced density of proliferating cytotrophoblast cells was not paralleled by a reduced density of cytotrophoblast cells (Ki-67 negative cells).

Cytotrophoblast differentiation is characterised by arrest of mitosis. The decision of a cytotrophoblast cell to exit the cell cycle and fuse with the overlying syncytium (differentiation) has recently been described in the human placenta to be regulated by the trophoblast specific GCM1 transcription factor (214)- analogous to its reported function in mice (181). Forskolin-induced up-regulation of GCM1 in BeWo cells and first trimester floating villous explants results in reduced cytotrophoblast proliferation and the induction of cell-cell fusion (GCM1 induces the fusion protein syncytin1 (193)) producing a thick syncytiotrophoblast layer (214). GCM1 therefore promotes cell cycle arrest, and hence GCM1 positive cells are post-mitotic (Ki-67 negative). The asymmetric expression of GCM1 (191) therefore serves to maintain the pool of proliferating cytotrophoblast cells but also which cells are selected for fusion.

Based on these observations, it may be hypothesised that reduced cytotrophoblast proliferation in severe IUGR results from an increase in the number of villous cytotrophoblast cells expressing GCM1, resulting in a reduced density (per unit area) of villous cytotrophoblast cells secondary to increased syncytial fusion as demonstrated *in vivo* (214). In the present study, severe early-onset IUGR placentas are associated with reduced GCM1 mRNA yet increased GCM1 protein expression (30%) in comparison to preterm controls (personal communication, Sascha Drewlo, Toronto). It can be speculated that reduced GCM1 mRNA (presumably in villous cytotrophoblast) is

associated with reduced syncytial fusion through failure to upregulate syncytin1, resulting in surplus numbers of 'undifferentiated' villous cytotrophoblast cells relative to proliferating villous cytotrophoblast cells, as shown in the present study. This is supported by the recent observation of reduced syncytin1 expression in PET-IUGR (309).

The cellular origin of increased GCM1 protein expression in severe IUGR is more difficult to explain without further immunolocalisation studies. The mismatch between increased GCM1 protein expression, reduced GCM1 mRNA and 'normal' cytotrophoblast density does suggest however that increased GCM1 protein in severe IUGR may not be causally associated but rather an effect of 1) the surplus number of undifferentiated cytotrophoblast cells relative to proliferating cytotrophoblast cells in comparison to preterm controls (i.e. Ki-67 negative) 2) the presence of the GCM1 protein within the syncytium (310) and to a lesser extent in stromal and chorionic cells, and 3) the continued translation of GCM1 protein within pathological syncytial knots.

4.4.2.2 Normal Villous CT Proliferation in Severe Early-onset Pre-eclampsia

Severe early-onset pre-eclampsia with PEDV in the umbilical arteries displayed no significant difference in the total volume, density and number of cytotrophoblast cells and those undergoing proliferation compared to preterm controls. However, despite there being no significant difference in numbers, there was a trend towards an increase in the percentage of proliferating cytotrophoblast cells. Whilst the global increase was negligible (29% in preterm controls versus 32% in severe early-onset pre-eclampsia) there was a 32% increase in the number of proliferating cytotrophoblast cells in stem and immature intermediate villi. This however did not reach significance due to large variation.

Current hypotheses hold that pre-eclampsia is associated with an increase in the rate of villous trophoblast turnover (3). Increased cytotrophoblast proliferation is associated with an increase in the rate of syncytial fusion, since a multi-layered cytotrophoblast has not been described for pre-eclamptic placentas. Consequently, increased apoptotic and necrotic shedding of syncytiotrophoblast nuclei is proposed to counterbalance the accelerated input of cytotrophoblastic material as part of an adaptive response.

The increase in cytotrophoblast proliferation in pre-eclampsia is thought to result from intra-placental hypoxia (153) secondary to reduced placental perfusion as a consequence of malinvasion of the maternal spiral arteries by extravillous cytotrophoblast cells (124). Increased numbers of villous cytotrophoblast cells (inferring increased proliferation) have been documented for several pathological conditions related to placental hypoxia, including maternal anaemia (204), pre-eclampsia (311), and pregnancies at high altitude (312-314). Stereological data from the present study does not support the association between intra-placental hypoxia and increased numbers of proliferating cytotrophoblast cells.

Intra-placental hypoxia is heterogeneous, and the oxygen content of the intervillous space has been shown to be spatially restricted. The inherent variation in intraplacental hypoxia may result in areas of increased as well as decreased proliferation and hence syncytial fusion, likely resulting in local, rather than global changes in cytotrophoblast proliferation. This may account for the failure of the increase in the number of proliferating cytotrophoblast cells in stem and immature intermediate villi to reach statistical significance.

In addition to focal restrictions, the oxygenation status of the intervillous space is also temporally regulated. During normal villous development, hypoxia drives villous cytotrophoblast proliferation during early pregnancy which declines with the onset of the maternal blood supply in the early second trimester, thereby increasing intra-placental oxygenation. Severe early-onset pre-eclampsia displayed temporal alterations in the number of cytotrophoblast cells undergoing proliferation. Whereas stem and immature intermediate villi were associated with a trend towards an increase in cytotrophoblast proliferation, mature intermediate and terminal villi displayed normal cytotrophoblast proliferation, indicating normalisation of oxygenation in the second trimester around the development of the peripheral villous tree. This suggests that placental entry and fetal extraction of oxygen is matched by the late second trimester in severe early-onset pre-eclampsia.

Despite the above inconsistencies, normal cytotrophoblast numbers and proliferation is consistent with the normal villous volumes observed for severe early-onset pre-eclampsia in this study. Physiologically this makes sense, since a significant increase in

cytotrophoblast proliferation, assuming no change in the rate of syncytial fusion, would result in increased numbers of cytotrophoblast cells. As a consequence, villous membrane thickness would increase serving to limit diffusional exchange, likely resulting in a growth-restricted neonate. However, fetal birthweights in severe early-onset pre-eclampsia were between the 10-50th centile for gestational age indicating adequate oxygen extraction by the fetus and hence growth.

The pre-eclamptic placentas in this study are associated with decreased GCM1 protein expression (personal communication, Sascha Drewlo, Toronto), consistent with previous observations (310). Given that up-regulation of GCM1 is associated with reduced cytotrophoblast proliferation *in vitro*, a decrease in the number of cytotrophoblast cells expressing GCM1 *in vivo* may be inferred to result in an increase in the number of cytotrophoblast cells with the potential to proliferate. Of particular interest is the observed trend towards a decrease in the density of villous cytotrophoblast cells in mature and terminal villi in severe early-onset pre-eclampsia. Whilst there was no change in the density of proliferating cytotrophoblast cells, the decrease in the density of cytotrophoblast cells suggests increased cytotrophoblast fusion consistent with the current trophoblast hypothesis of pre-eclampsia. Thus, decreased GCM1 protein expression may be due to a reduction in the number of villous cytotrophoblast cells.

4.4.3 Villous Cytotrophoblast Proliferation in Late-onset PET, IUGR, and SIDS

Present findings confirm the hypothesis that pre-eclampsia and IUGR in late gestation display different CT morphologies when compared to its early-onset phenotype.

IUGR presenting in late gestation had no significant effect on the percentage of proliferating villous cytotrophoblast cells, but were associated with a 50% reduction in the total number and volume of villous cytotrophoblast cells and those undergoing proliferation; densities remain similar to age-matched controls. However, the combination of the low number of cases (n=4) and the large intra-group variation (two 33 week cases with abnormal umbilical artery Doppler, and two cases at 37 weeks with normal Dopplers) in the late-onset IUGR group means that conclusions regarding cytotrophoblast turnover cannot be determined with any degree of accuracy.

Late-onset pre-eclampsia was not associated with any significant changes in the volume or numerical density of villous cytotrophoblast cells or those undergoing proliferation. Interestingly, the total number of cytotrophoblast cells significantly decreased in comparison to controls leading to a significant increase in the percentage of proliferating cytotrophoblast cells specifically for structural villi. This may indicate that a higher proportion of cytotrophoblast cells retain a proliferative phenotype compared to controls, supported by the significant reduction in the number of Ki-67 negative cells (28%) (non-proliferating cytotrophoblast cells).

The same holds true for late-onset pre-eclampsia with co-existing IUGR. These placentas displayed a trend towards a decrease in the numerical density of cytotrophoblast cells for peripheral villi, the total number of which significantly decreased (40%). In conjunction with the subtle increase in the density of proliferating cytotrophoblast cells (14%), the percentage of proliferating cytotrophoblast thus significantly increased (26%) in comparison to age-matched controls, indicating that a higher proportion of cytotrophoblast cells retain a proliferative/progenitor cell phenotype compared to controls.

In contrast to the normal placental phenotype of late-onset pre-eclampsia without IUGR, the presence of IUGR is associated with reduced total placental and villous volumes. This begs the question as to why these placentas are smaller if they (presumably) retain more proliferative/progenitor cells. One hypothesis is that the cytotrophoblast progenitor pool may be depleted due to the effects of IUGR therefore impeding villous growth potential, but the remaining cytotrophoblast cells adopt a proliferative phenotype undergoing ‘faster’ transient cell divisions in comparison to controls, which may contribute to the development of pre-eclampsia.

Both SIDS-NBW and SIDS-LBW placentas displayed significant increases in the volume density of cytotrophoblast cells for stem (44%, 55%), mature intermediate villi (43%, 53%) and terminal villi (39%, 31%) in comparison to term controls, representing a SIDS effect independent of infant birthweight (two-way ANOVA). The total volume cytotrophoblast cells subsequently increased in SIDS-NBW due to the increase in total villous volume, which was not observed for SIDS-LBW displaying no change in villous volumes.

An increase in the relative volume of cytotrophoblast may arise due to hypertrophy or hyperplasia. Although numerical density estimates and proliferation indices are needed to clarify this situation, both growth mechanisms are equally plausible. Histologically, cytotrophoblast cells appear extremely large (Figure 4-1, A) in terms of nuclear size, which could indicate proliferation, or alternatively endoreduplication (315), providing no change in nuclear number (although no polyploid nuclei were observed). Cytotrophoblast hyperplasia (multi-layering) (Figure 4-1, B, C) was also noted in distinct areas of villi displaying intravillous fibrinoid deposition and syncytial denudation, indicating a lack of syncytial fusion. This primarily indicates diminished syncytiotrophoblast differentiation, but the possibility also exists that these cells have adopted an extravillous cytotrophoblast phenotype (185), associated with up-regulation of integrin α5β1, a receptor for fibronectin, (a matrix-type fibrinoid) related to intracytotrophoblastic deposition (316). This is not an unreasonable explanation as in the absence of an intact syncytium, a subset of villous cytotrophoblast cells exposed to exogenous FGF4 (which maintains the proliferative state of murine trophoblast stem cells (173)), differentiate down the extravillous pathway as shown by positivity for integrins α5β1 and α1β1 antibodies, HLA-G and connexin-40 (185).

Implications and possible consequences of these changes for both early and late-onset pathologies will be discussed in Chapter 5 in light of results describing syncytial integrity.

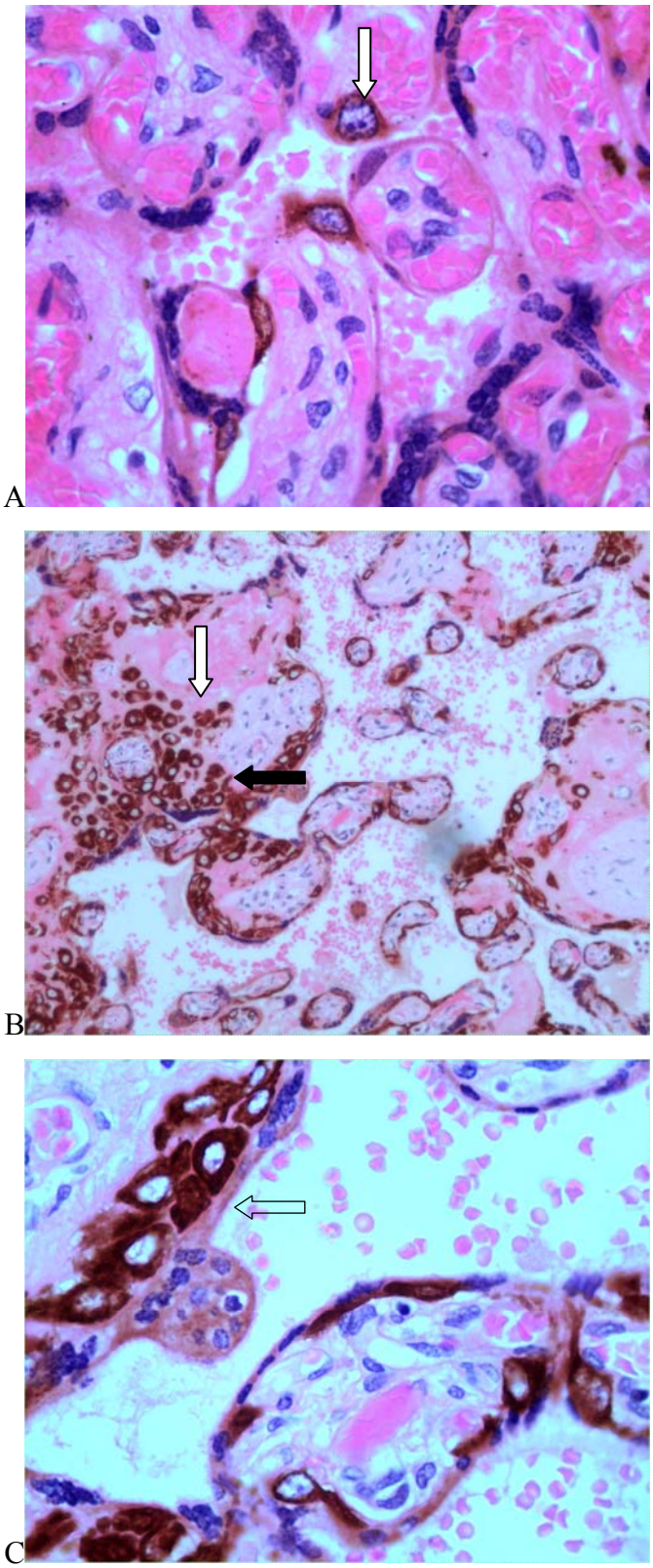

Figure 4-1 Cytotrophoblast morphology in SIDS-NBW placentas immunolocalised for mAb CK-7 counterstained with H&E

(A) Cytotrophoblast nuclei appear larger in size with a small cytoplasm, with visible mitotic figures (white arrow) (x400) (B) Intravillous fibrinoid (white arrow) and cytotrophoblast deposition (black arrow) with syncytial denudation , x200 (C) Multi-layered cytotrophoblast (clear arrow) underlying a syncytial knot displaying nuclei with morphological characteristics of necrosis x400.

5 Syncytial integrity

5.1 Introduction

Fetal growth in utero is primarily determined by nutrient availability (317), which is dependent upon the functional and morphological transport capacity of the syncytium (SCT), responsible for the bulk of placental function including gas, nutrient and waste exchange, immune tolerance, and hormone production (85). Throughout gestation, the multinucleate syncytium grows and regenerates via continual syncytial fusion of post-proliferative villous cytotrophoblast cells, which is coupled to a tightly regulated differentiation process involving the initiator stages of the apoptosis cascade (225). Initially, fusing "differentiating" villous cytotrophoblast cells, (directed by the transcription factor, GCM1) (214), express 'anti-apoptosis' proteins (e.g. Bcl-2 and Mcl-1) which serve to focally retard syncytial death thereby allowing maturation of a cellular phenotype necessary for a functioning epithelium (195). This is eventually succeeded by terminal differentiation associated with the execution stages of apoptosis, followed by sequestration and extrusion of syncytial knots into the maternal circulation.

Alterations in the balance between villous cytotrophoblast proliferation, differentiation and syncytial fusion will therefore exert direct effects on syncytiotrophoblast integrity and morphology, and are thought to be primary pathogenic events of pre-eclampsia and placental IUGR (85). Under normal conditions, syncytial fusion is counterbalanced by extrusion of syncytial nuclei, in the form of syncytial knots. Reductions in the number of syncytial nuclei may therefore result from either decreased input via reduced syncytial fusion and/or proliferation, or alternatively accelerated shedding/extrusion. Conversely, an increase in syncytial nuclei may result from increased syncytial fusion, accompanied by increased proliferation, but normal or reduced shedding.

5.1.1 Hypotheses

1. In severe early-onset IUGR, a reduced number of proliferating villous cytotrophoblast cells and syncytial fusion events leads to reduced numbers and volume of syncytiotrophoblast nuclei and increased syncytial apoptosis in comparison to preterm controls

2. In severe early-onset pre-eclampsia, numbers of syncytial nuclei remain similar to preterm controls due to sufficient cytotrophoblast input, balanced by accelerated terminal differentiation and syncytial extrusion in comparison to preterm controls

3. The late-onset variants of each disease display normal syncytiotrophoblast morphology

4. The syncytium in SIDS placentas resembles that of placentas from late-onset pre-eclampsia or IUGR

5.1.2 Experimental Aims

The above hypotheses will be tested by estimating the following parameters:

1. The volume and number of SCT nuclei and individual syncytial knot volume (i.e. PSI) and morphology (apoptotic vs. non-apoptotic) of syncytial knots

2. The expression of the apoptosis-related protein, cleaved cytokeratin 18, will be semi-quantified by western blotting in the severe early-onset pathologies

5.2 Early-onset pathologies

Raw data for SCT volume and number are presented in Appendices 4 and 5

5.2.1 Total Volume of Syncytiotrophoblast

Graph 5-1 Total volume of SCT in early-onset pathologies

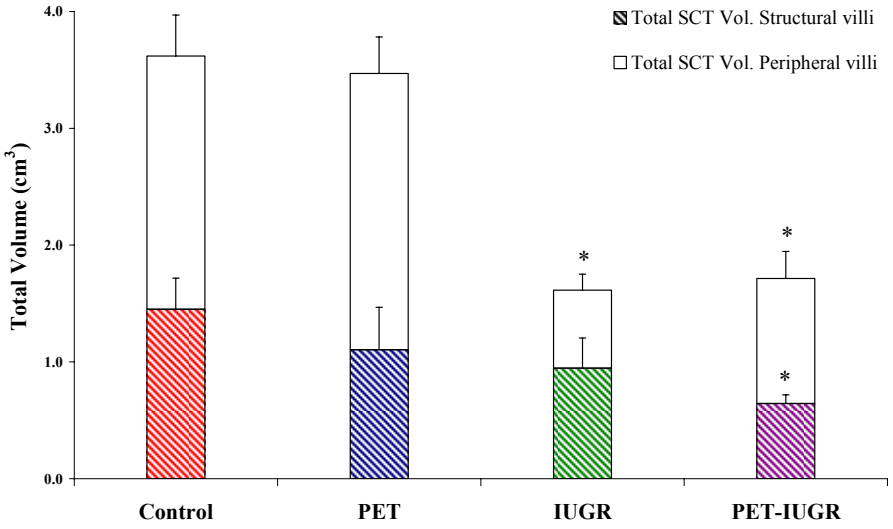

Total volume of SCT was significantly reduced in comparison to controls for

IUGR peripheral villi (P=0.018)

PET-IUGR structural and peripheral villi (P=0.019)

Table 5-1 Volume density of SCT in early-onset pathologies

	Control (n=12)	PET (n=11)	IUGR (n=5)	PET-IUGR (n=19)
Volume density SCT	0.048 ± 0.002	0.048 ± 0.002	0.048 ± 0.005	0.045 ± 0.002
Structural villi	0.016 ± 0.001	0.011± 0.001*	0.020 ± 0.004	0.013± 0.001*
Peripheral villi	0.031 ± 0.003	0.037 ± 0.002	0.028 ± 0.003	0.033 ± 0.002

Data presented as mean and ± SEM

* significant difference compared to controls

Volume density of SCT was significantly reduced in comparison to controls for:

PET structural villi (P=0.013)

PET-IUGR structural villi (P=0.052)

5.2.2 Total Number of Syncytiotrophoblast Nuclei

Graph 5-2 Total number of SCT nuclei in early-onset pathologies

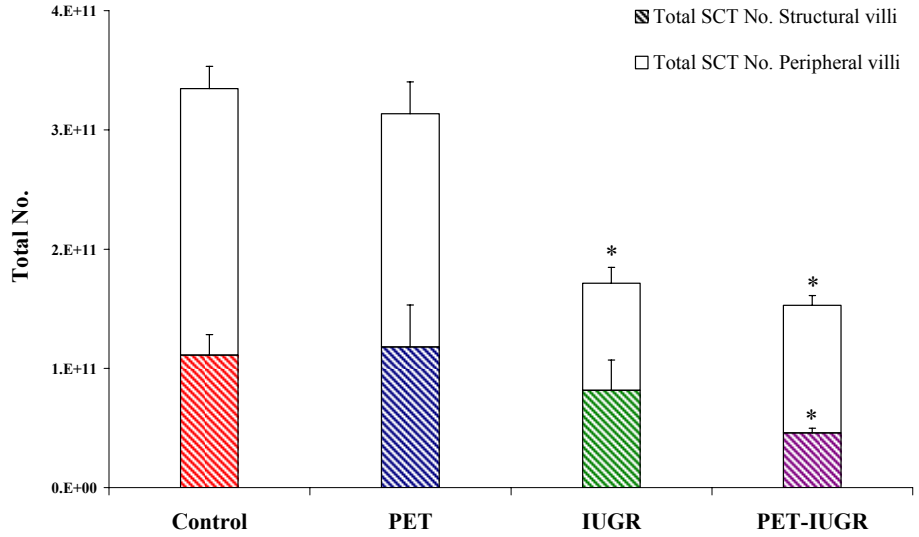

Total numbers of syncytiotrophoblast were significantly decreased in

IUGR peripheral villi ($P<0.001$)

PET-IUGR structural and peripheral villi ($P<0.001$)

Table 5-2 Numerical density of SCT nuclei in early-onset pathologies

	Control (n=12)	PET (n=11)	IUGR (n=5)	PET-IUGR (n=19)
Total Density (μm^{-3})	$1.1x10^{-3} \pm 5.2x10^{-5}$	$9.6x10^{-4} \pm 9.4x10^{-5}$	$1.0x10^{-3} \pm 1.2x10^{-4}$	$9.3x10^{-4} \pm 4.1x10^{-5*}$
N_v Structural villi	$3.4x10^{-4} \pm 4.5x10^{-5}$	$3.3x10^{-4} \pm 7.9x10^{-5}$	$4.8x10^{-4} \pm 1.1x10^{-4}$	$2.9x10^{-4} \pm 2.4x10^{-5}$
N_v Peripheral villi	$7.1x10^{-4} \pm 5.3x10^{-5}$	$6.3x10^{-4} \pm 7.6x10^{-5}$	$5.6x10^{-4} \pm 2.4x10^{-5}$	$6.4x10^{-4} \pm 3.5x10^{-5}$

Data presented as mean and ± SEM

* significant difference compared to controls

PET-IUGR displayed a significant decrease in the numerical density of syncytiotrophoblast nuclei ($P=0.053$).

IUGR displayed a trend towards a decrease in syncytial nuclei ($P=0.097$).

5.2.3 Total Volume of Syncytial Knots (SK)

Graph 5-3 Volume density of syncytial knots in early-onset pathologies

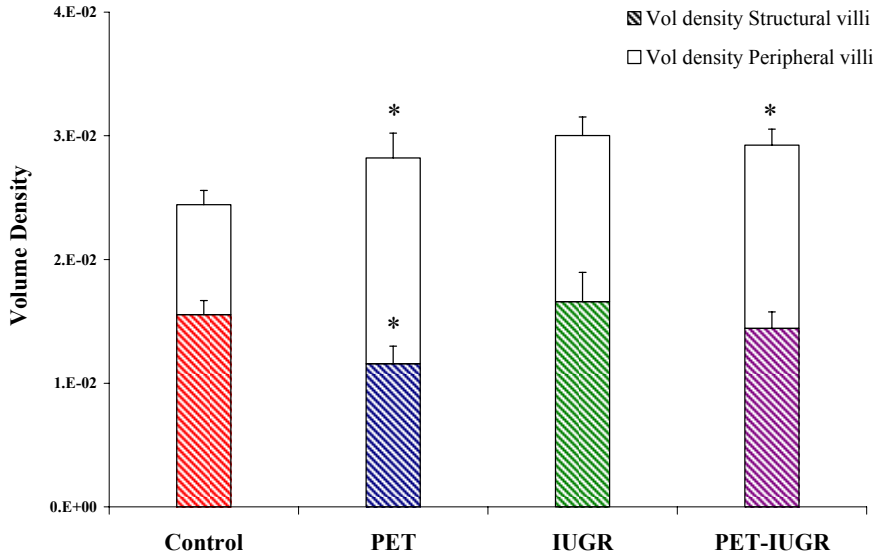

Significant differences in the volume density of SK were observed in comparison to controls:

PET ↑ peripheral villi (P<0.001), ↓ structural villi (P=0.036)

PET-IUGR ↑ total density (P=0.015), ↑ peripheral villi (P=0.007)

Table 5-3 Total volume of syncytial knots in early-onset pathologies

	Control (n=12)	PET (n=11)	IUGR (n=5)	PET-IUGR (n=19)
Total volume (cm^3)	7.98 ± 0.81	9.22 ± 1.13	4.66 ± 0.68*	4.87 ± 0.37**
Structural villi	5.00 ± 0.49	3.81 ± 0.68	2.61 ± 0.47*	2.38 ± 0.27
Peripheral villi	2.99 ± 0.47	5.37 ± 0.68*	2.07 ± 0.28	2.51 ± 0.30**

Data presented as the mean and ± SEM * significant difference compared to controls

** significant difference compared to pre-eclampsia

Significant differences in the total volume of SK were observed in comparison to controls for:

IUGR ↓ total volume (P=0.026), ↓ structural villi (P=0.011)

PET-IUGR ↓ total volume (P<0.001), ↓ peripheral villi (P<0.001)

5.2.4 Mean Individual Syncytial Knot Volume (PSI)

Graph 5-4 Individual syncytial knot volume in early-onset pathologies

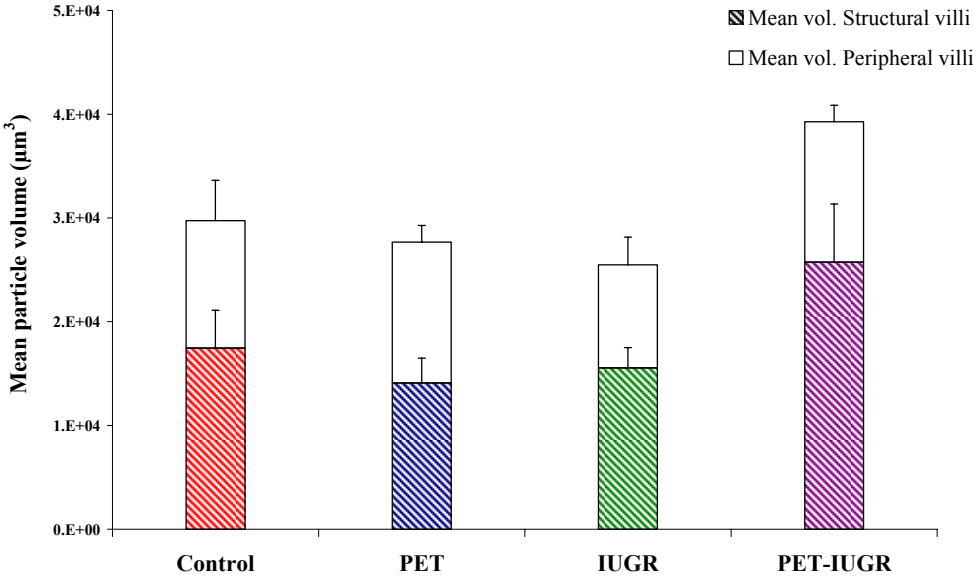

There were no significant differences in the mean volume of syncytial knots in either pathology when compared to controls.

However, there was a trend towards an increase in mean syncytial knot volume for PET-IUGR, but failed to reach statistical significance (P=0.078).

5.2.5 Volume of Apoptotic Syncytial Knots

Graph 5-5 Volume density of apoptotic syncytial knots in early-onset pathologies

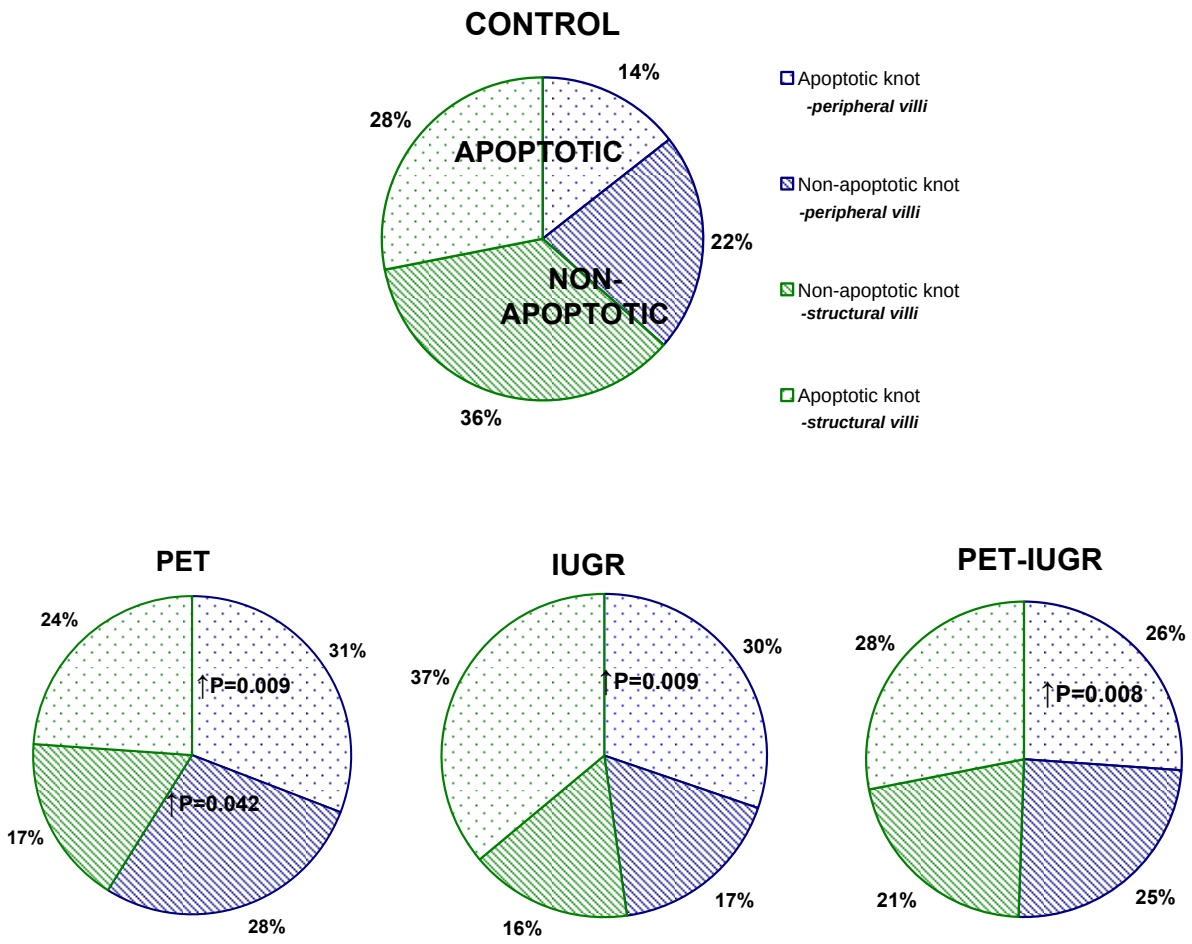

PET, **IUGR** and **PET-IUGR** were associated with a significant increase in the volume density of apoptotic knots for peripheral villi when compared to controls

PET also displayed a significant increase in the volume density of non-apoptotic knots for peripheral villi when compared to controls

5.2.6 Mean Individual Apoptotic Syncytial Knot Volume (PSI)

Graph 5-6 Mean individual apoptotic knot volume in early-onset pathologies

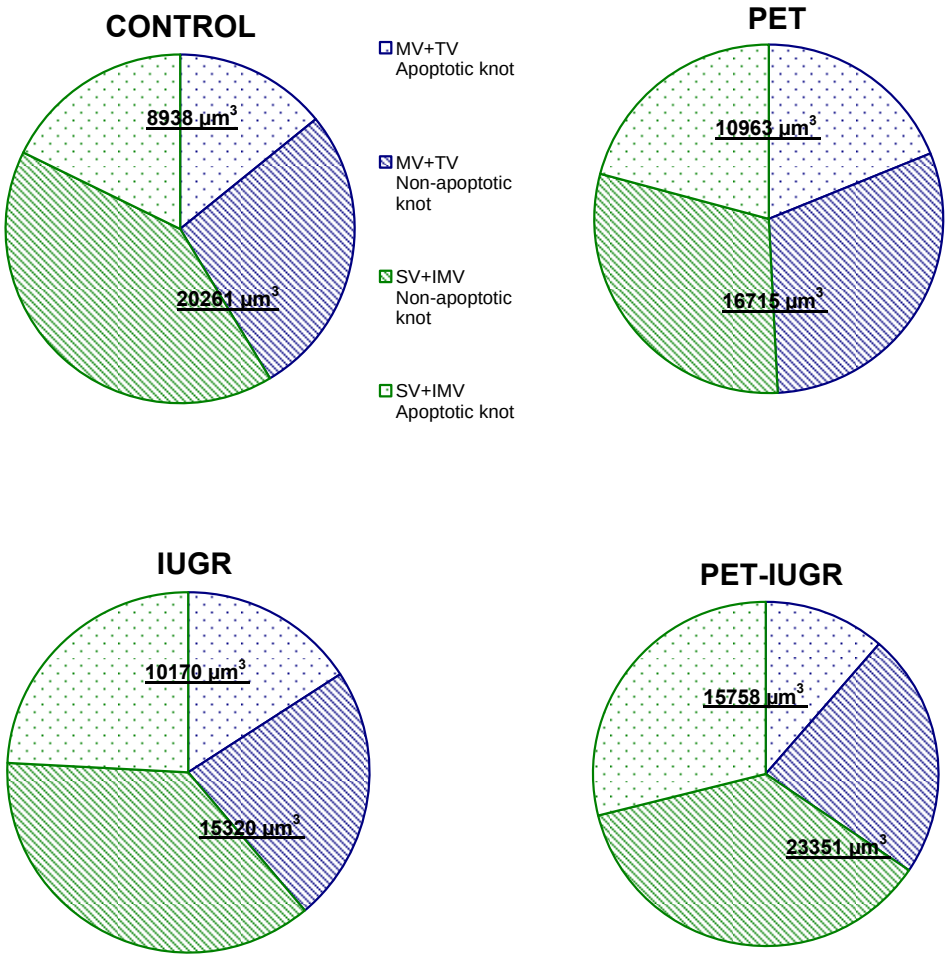

There were no statistically significant differences in mean apoptotic syncytial knot volume for either pathology when compared to controls

5.2.7 Western Blotting for Cleaved Cytokeratin-18

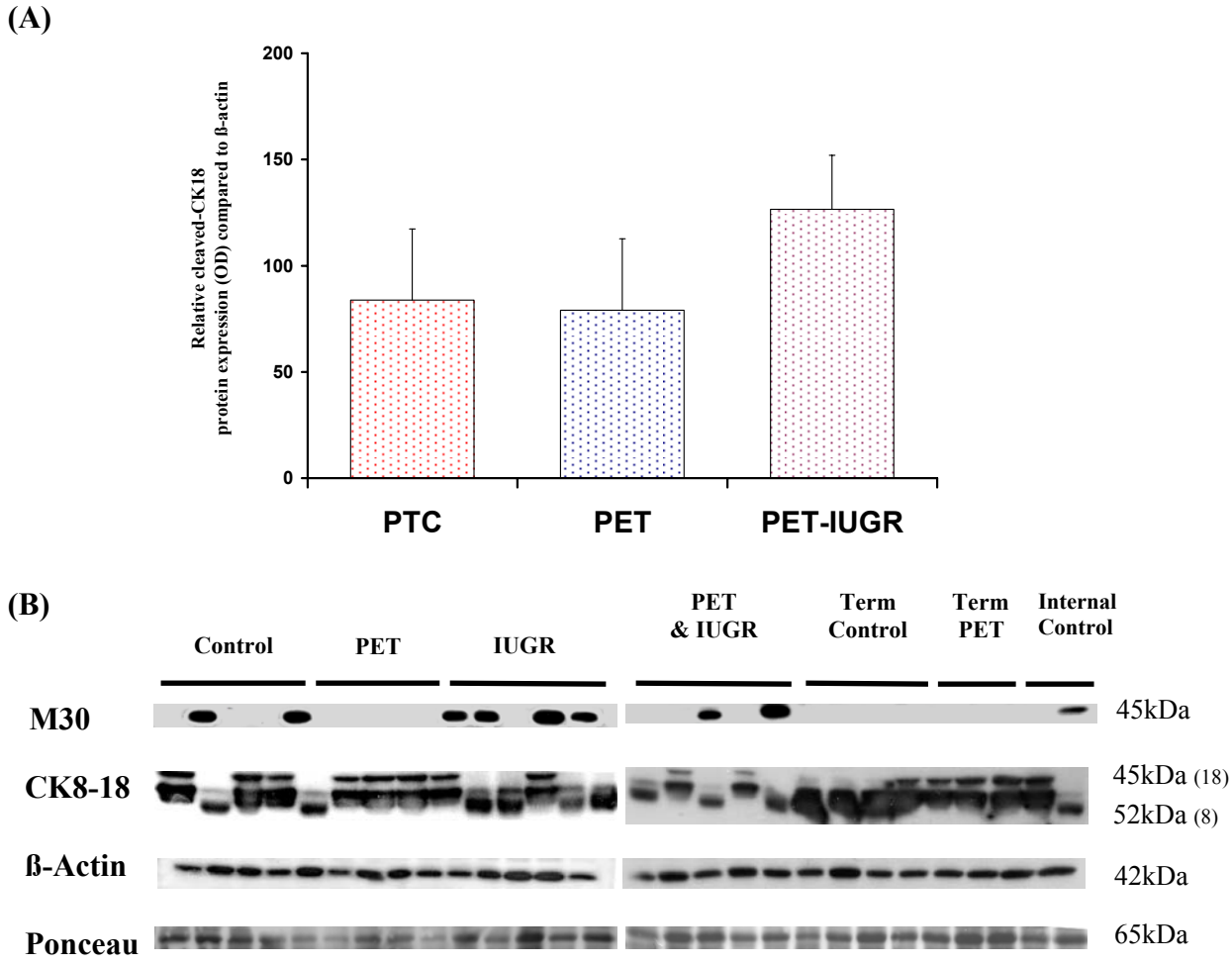

Graph 5-7 Relative expression (OD) and representative western blot of cleaved cytokeratin-18 in pathological pregnancies. (A) Relative optical density (OD) of cleaved CK8-18 protein (M30) in preterm control (PTC), PET and PET-IUGR placentas in comparison to ß-actin OD. (B) Representative western blot of M30 protein expression and cleaved CK8-18 expression in preterm control, PET, IUGR and PET-IUGR placentas, and in control and PET placentas at term. M30 was expressed in preterm control and PET-IUGR placentas. M30 expression was associated with the corresponding cleavage of CK8-18, demonstrating the specificity of the M30 antibody at detecting CK8-18 cleavage. M30 was not expressed in control or PET placentas at term. Following an unforeseen clinical re-audit, IUGR placentas were reclassified as PET-IUGR placentas and are thus absent in the graphical representation above.

M30 protein expression was assessed using western blot analysis on placental samples (repeated 3 times). Relative M30 expression (OD, Image J software) was estimated by normalization to beta actin OD (CK8-18 was not semi-quantified) representing the house keeping control. M30 was expressed in preterm control, preterm IUGR, and pre-term PET-IUGR placentas. There were no significant differences in the expression of

M30 in pre-eclampsia with or without IUGR in comparison to preterm controls. M30 was not expressed in preterm PET or in control or PET placentas at term.

5.2.8 Summary

Severe early-onset pre-eclampsia

- significant decrease in the volume density of syncytiotrophoblast in structural villi (Table 5-1)
- significant increase in the volume density and total volume of syncytial knots (Graph 5-3, Table 5-3)
- significant increase in the volume density of apoptotic syncytial knots (Graph 5-5)

Severe early-onset IUGR

- significant decrease in the total volume of syncytiotrophoblast (Graph 5-1)
- significant decrease in the total number of syncytiotrophoblast nuclei (Graph 5-2)
- significant increase in the volume density of apoptotic syncytial knots (Graph 5-5)

Severe early-onset PET-IUGR

- significant decrease in the total volume of syncytiotrophoblast (Graph 5-1)
- significant decrease in the total number of syncytiotrophoblast nuclei (Graph 5-2)
- significant increase in the volume density of syncytial knots (Graph 5-3)
- significant increase in the volume density of apoptotic syncytial knots (Graph 5-5)

5.3 Late-onset pathologies

5.3.1 Total Volume of Syncytiotrophoblast

Graph 5-8 Total volume of SCT in late-onset pathologies

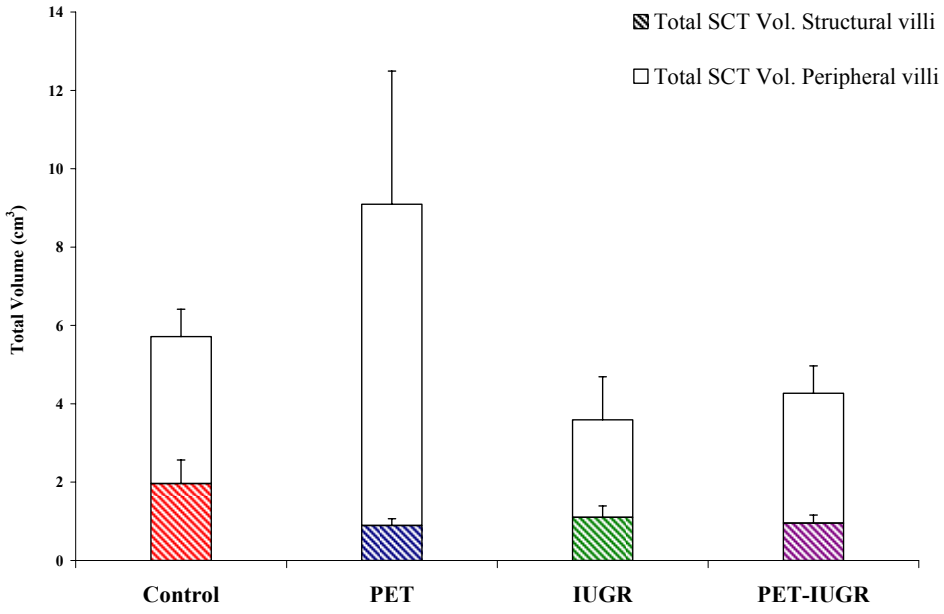

There were no significant differences in the total volume of syncytiotrophoblast for either pathology when compared to controls

Table 5-4 Volume density of SCT in late-onset pathologies

	Control (n=13)	PET (n=6)	IUGR (n=4)	PET-IUGR (n=6)
Volume density SCT	0.042 ± 0.004	0.052 ± 0.010	0.046 ± 0.002	0.051 ± 0.004
Structural villi	0.013 ± 0.003	0.010 ± 0.001	0.009 ± 0.001	0.011 ± 0.001
Peripheral villi	0.029 ± 0.003	0.042 ± 0.010	0.033 ± 0.003	0.041 ± 0.004

Data presented as mean and ± SEM

There were no statistically significant differences in the volume density of syncytiotrophoblast for either pathology when compared to controls. The trend towards an increase in the volume density of syncytiotrophoblast for peripheral villi in PET-IUGR, which just failed to reach statistical significance (P=0.068).

5.3.2 Total Number of Syncytiotrophoblast Nuclei

Graph 5-9 Total number of SCT in late-onset pathologies

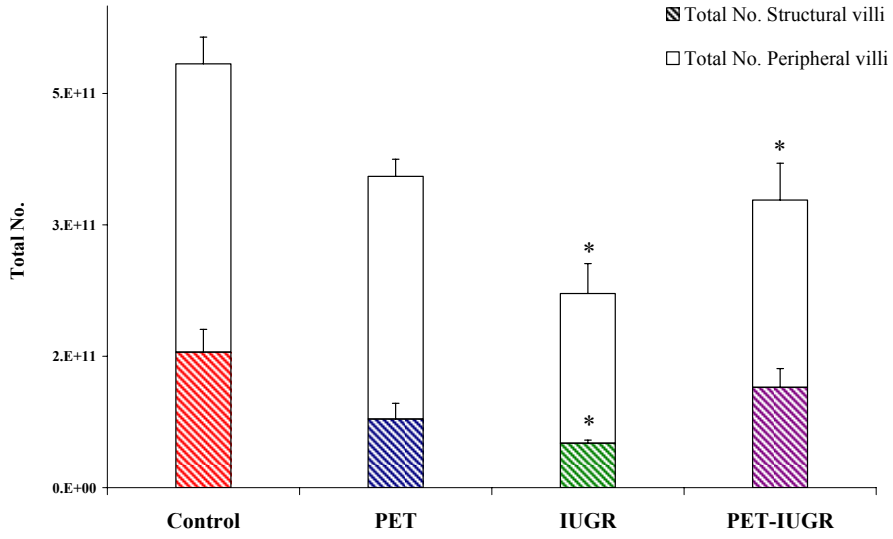

There was a significant decrease in the total number of syncytiotrophoblast nuclei in comparison to controls for:

IUGR structural villi (P=0.042) peripheral villi (P=0.013)

PET-IUGR peripheral villi (P=0.045)

Table 5-5 Numerical density of syncytiotrophoblast nuclei in late-onset pathologies

	Control (n=13)	**PET (n=6)**	**IUGR (n=4)**	**PET-IUGR (n=6)**
Total Density (μm^{-3})	$8.7x10^{-4}$ (± 6.2)	$7.5x10^{-4}$ (± 5.2)	$8.2x10^{-4}$ (± 6.1)	$8.9x10^{-4}$ (± 9.6)
N_v Structural villi	$2.8x10^{-4}$ (± 4.1)	$1.6x10^{-4}$ (± 3.5)	$2.1x10^{-4}$ (± 6.3)	$3.1x10^{-4}$ (± 6.9)
N_v Peripheral villi	$5.9x10^{-4}$ (± 3.5)	$5.9x10^{-4}$ (± 5.0)	$6.1x10^{-4}$ (± 4.6)	$5.7x10^{-4}$ (± 7.2)

Data presented as mean and ± SEM ($x10^{-5}$)

There were no significant differences in the numerical density of syncytiotrophoblast nuclei for either pathology when compared to controls.

5.3.3 Volume of Syncytial Knots

Graph 5-10 Volume density of syncytial knots in late-onset pathologies

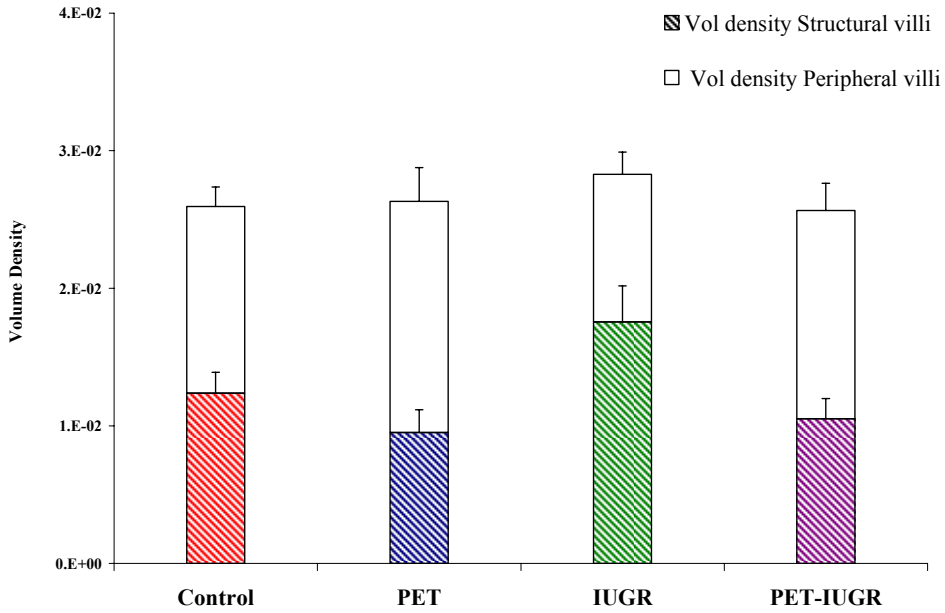

There were no significant differences in the volume density of syncytial knots for either pathology when compared to controls

Table 5-6 Total volume of syncytial knots in late-onset pathologies

	Control (n=13)	PET (n=6)	IUGR (n=4)	PET-IUGR (n=6)
Total volume (cm^3)	14.52 ± 1.39	13.23 ± 4.73	7.55 ± 0.99*	9.33 ± 0.98**
Structural villi	7.08 ± 1.13	4.73 ± 0.95	4.52 ± 0.40	4.02 ± 0.89
Peripheral villi	7.37 ± 0.75	8.52 ± 1.78	3.03 ± 0.73*	5.27 ± 0.90

Data presented as the mean and ± SEM

* significant difference compared to controls

** significant difference compared to pre-eclampsia

Total volume of syncytial knots was significantly reduced compared to controls for:

IUGR total volume (P=0.018), peripheral villi (P=0.008)

PET-IUGR total volume (P=0.029)

5.3.4 Mean Individual Syncytial Knot Volume (PSI)

Graph 5-11 Mean syncytial knot volume in late-onset pathologies

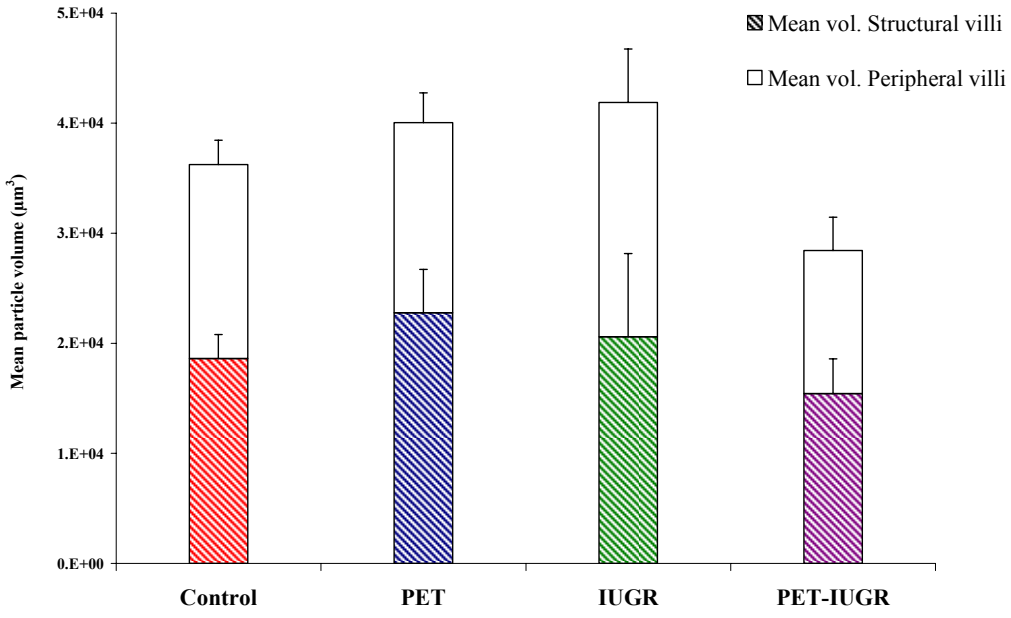

There were no significant differences in the mean volume of syncytial knots in either pathology when compared to controls.

5.3.5 Volume of Apoptotic Syncytial Knots

Graph 5-12 Volume density of apoptotic syncytial knots in late-onset pathologies

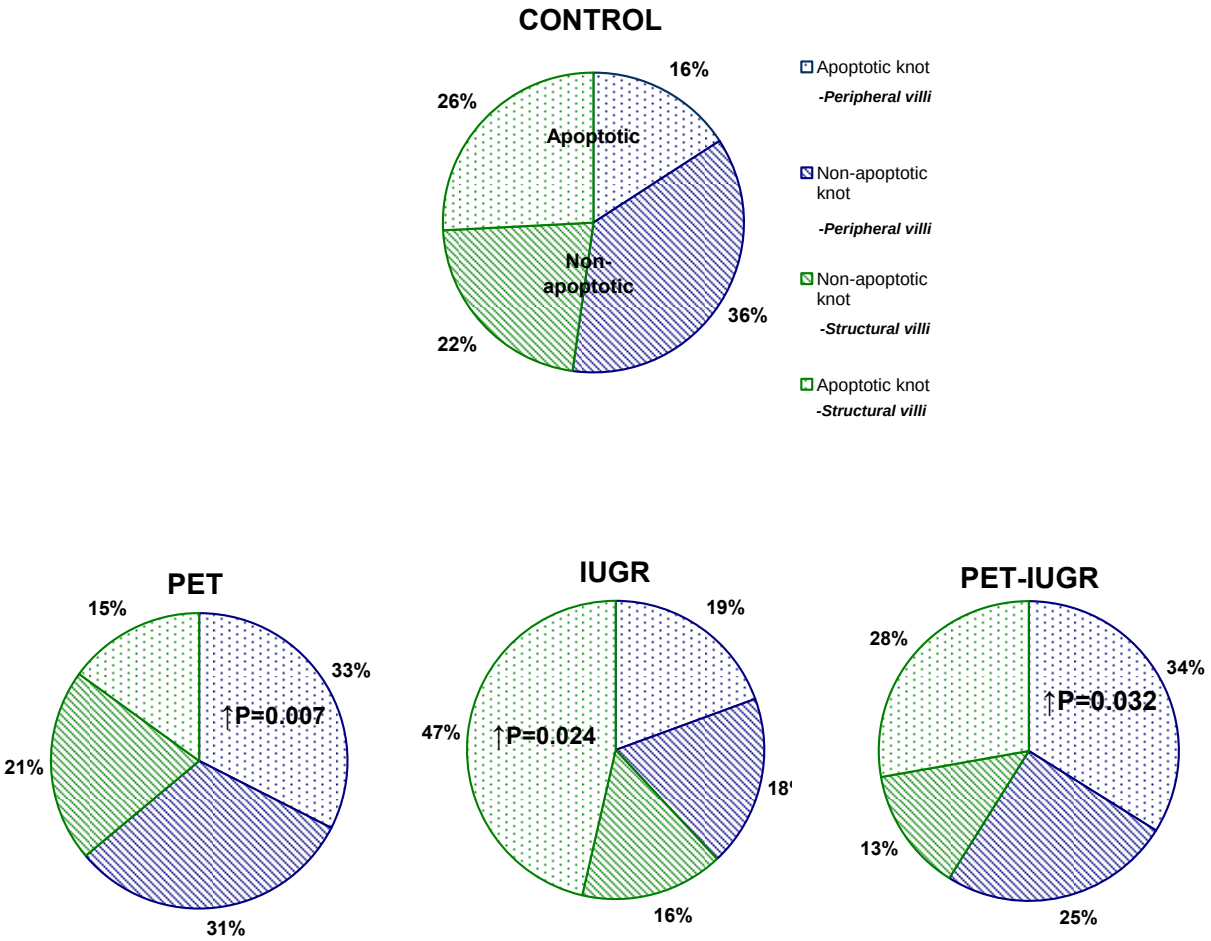

PET, **IUGR** and **PET-IUGR** displayed a significant increase in the volume density of syncytial knots which were apoptotic.

5.3.6 Mean Individual Apoptotic Syncytial Knot Volume

Graph 5-13 Mean apoptotic knot volume for late-onset pathologies

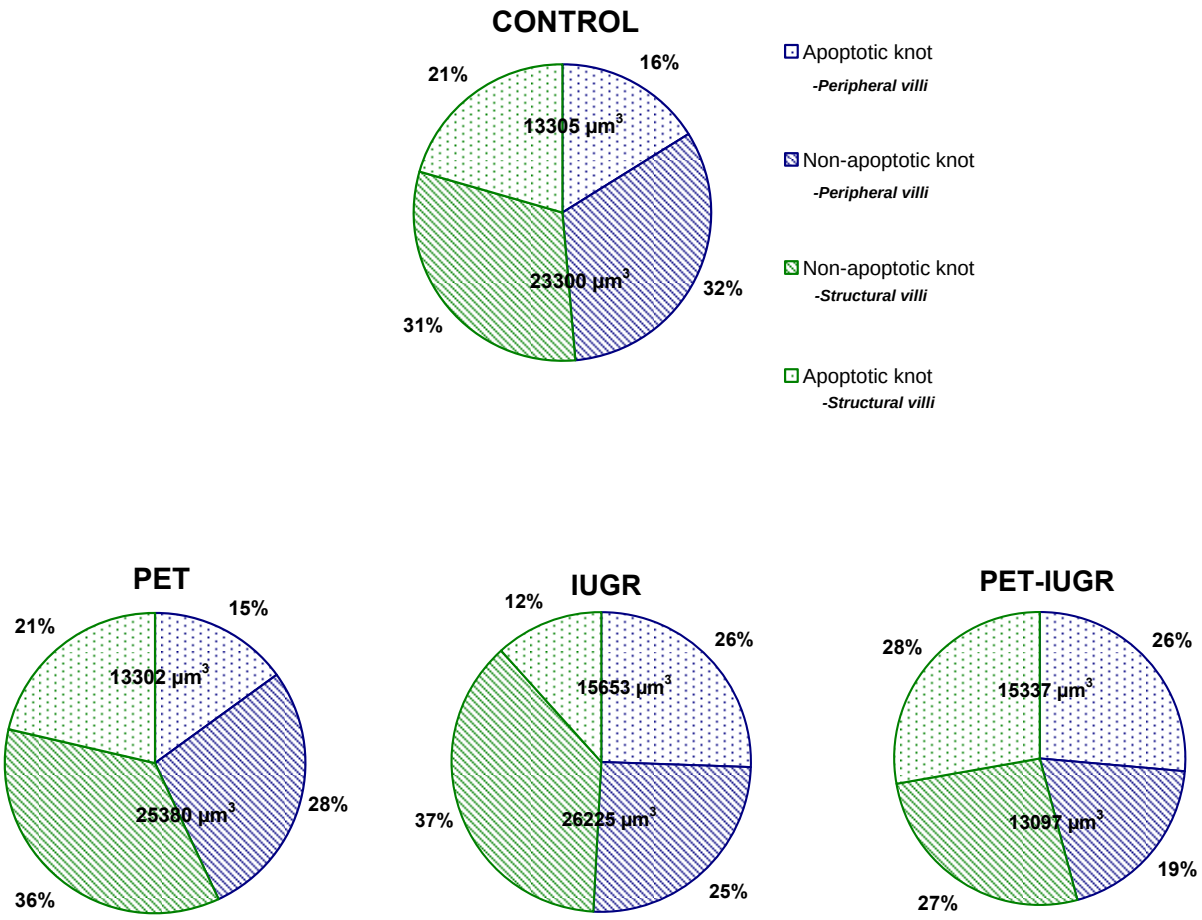

There were no significant differences in mean apoptotic volume for either pathology when compared to controls

There was a significant decrease in mean non-apoptotic volume for PET-IUGR (P=0.023)

5.3.7 Summary

Late-onset pre-eclampsia

- significant increase in the volume density of apoptotic knots (Graph 5-12)

Late-onset IUGR and PET-IUGR

- significant decrease in the total number of syncytiotrophoblast nuclei (Graph 5-9)
- significant decrease in total volume of syncytial knots (Table 5-6)
- significant increase in the density of apoptotic syncytial knots (Graph 5-12)

5.4 SIDS

5.4.1 Total Volume of Syncytiotrophoblast

Graph 5-14 Total volume of syncytiotrophoblast in SIDS

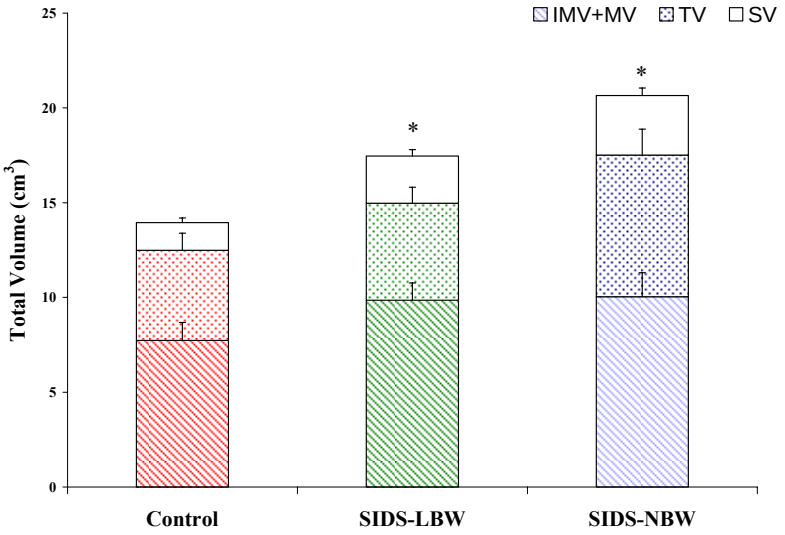

There was a significant increase in the total volume of syncytiotrophoblast in comparison to controls for

SIDS-LBW stem villi (P=0.023)

SIDS-NBW total volume (P=0.029), stem villi (P=0.002)

Table 5-7 Volume density of syncytiotrophoblast in SIDS

Volume Density	Control (n=12)	SIDS-LBW (n=12)	SIDS-NBW (n=12)
V_v Stem villi	0.006 ± 0.001	0.009 ± 0.001*	0.009 ± 0.001*
V_v Intermediate villi	0.020 ± 0.003	0.038 ± 0.002*	0.029 ± 0.003*
V_v Terminal villi	0.018 ± 0.003	0.018 ± 0.002	0.020 ± 0.002

Data presented as mean and ±SEM. Immature and mature intermediate villi are grouped as intermediate villi, * significant difference compared to control

There was a significant increase in the volume density of syncytiotrophoblast in comparison to controls for

SIDS-LBW stem villi (P=0.009), intermediate villi (P=0.017)

SIDS-NBW stem villi (P=0.017)

5.4.2 Total Volume of Syncytial Knots

Graph 5-15 Total volume of syncytial knots in SIDS

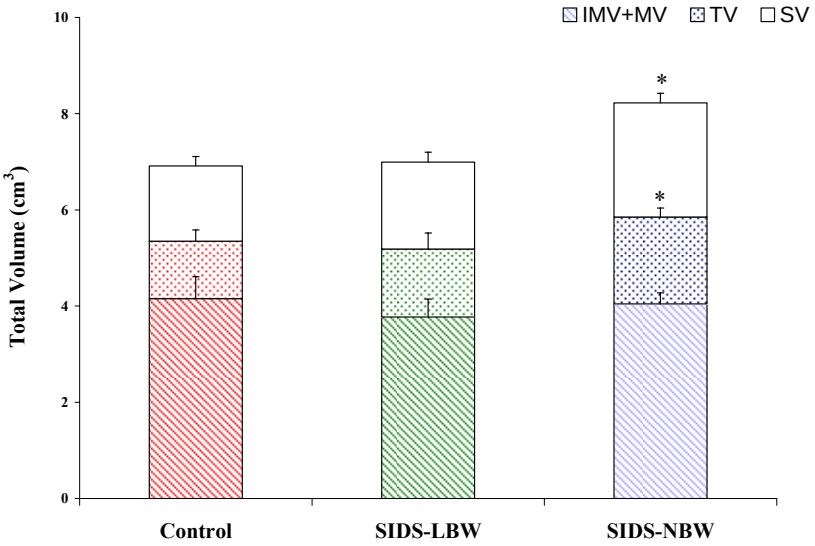

There was a significant increase in the total volume of syncytial knots in comparison to controls for

SIDS-NBW stem villi (P=0.002), terminal villi (P=0.051)

Table 5-8 Volume density of syncytial knots in SIDS placentas

Total Volume (cm^3)	Control (n=12)	SIDS-LBW (n=12)	SIDS-NBW (n=12)
V_{TOT} Stem villi	0.006 ± 0.001	0.007 ± 0.001	0.007 ± 0.0003
V_{TOT} Intermediate villi	0.016 ± 0.002	0.016 ± 0.002	0.012± 0.001*
V_{TOT} Terminal villi	0.004 ± 0.001	0.005 ± 0.001	0.005 ± 0.001

Data presented as mean and ±SEM.

Immature and mature intermediate villi are grouped as intermediate villi

* significant difference compared to control

There was a significant decrease in the volume density of syncytial knots in comparison to controls for

SIDS-NBW intermediate villi (P=0.046)

5.4.3 Total Volume of Apoptotic Syncytial Knots

Graph 5-16 Total volume of apoptotic syncytial knots (SK) in SIDS placentas

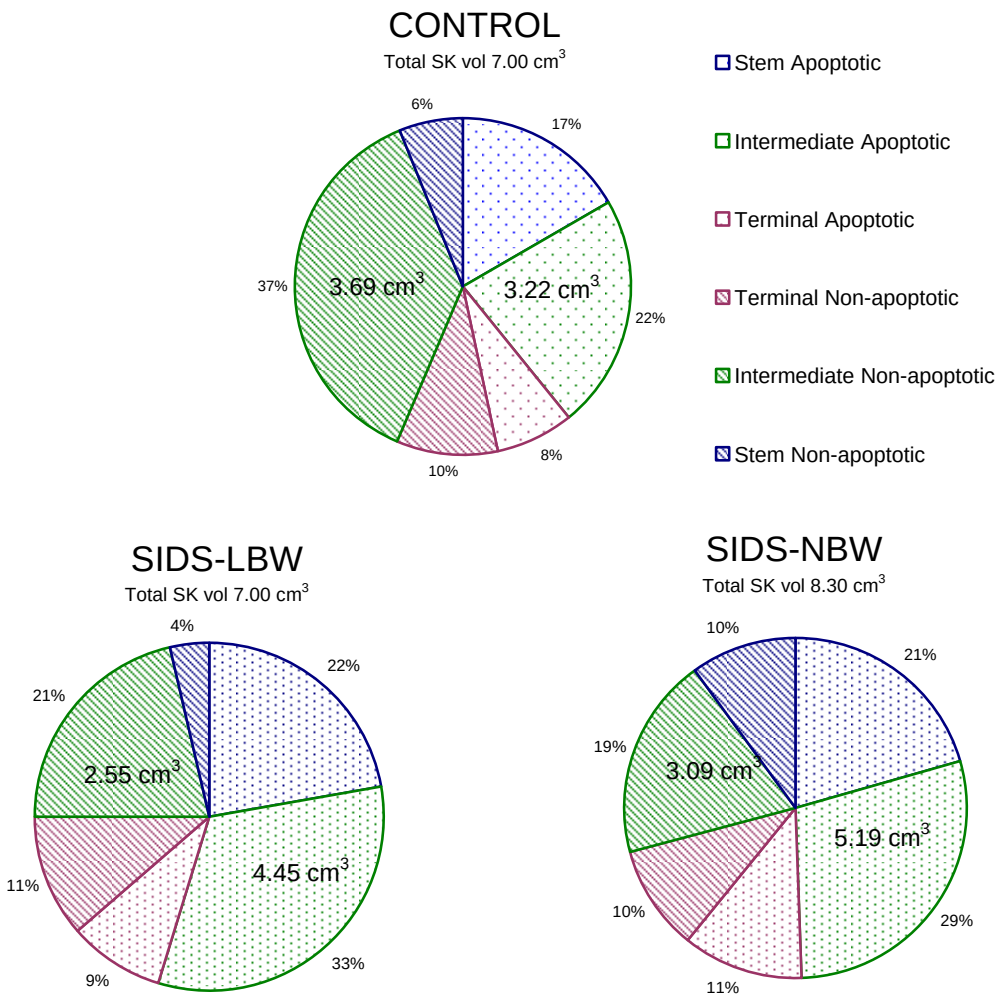

There was a significant increase in the total volume of apoptotic syncytial knots in:

SIDS-LBW total volume (P=0.031), intermediate villi (P=0.045)

SIDS-NBW total volume (P=0.003), intermediate villi (P=0.011)**,** terminal villi (P=0.029)

5.4.4 Mean Individual Volume (PSI) and Number of Syncytial Knots

Graph 5-17 Mean syncytial knot volume in SIDS placentas

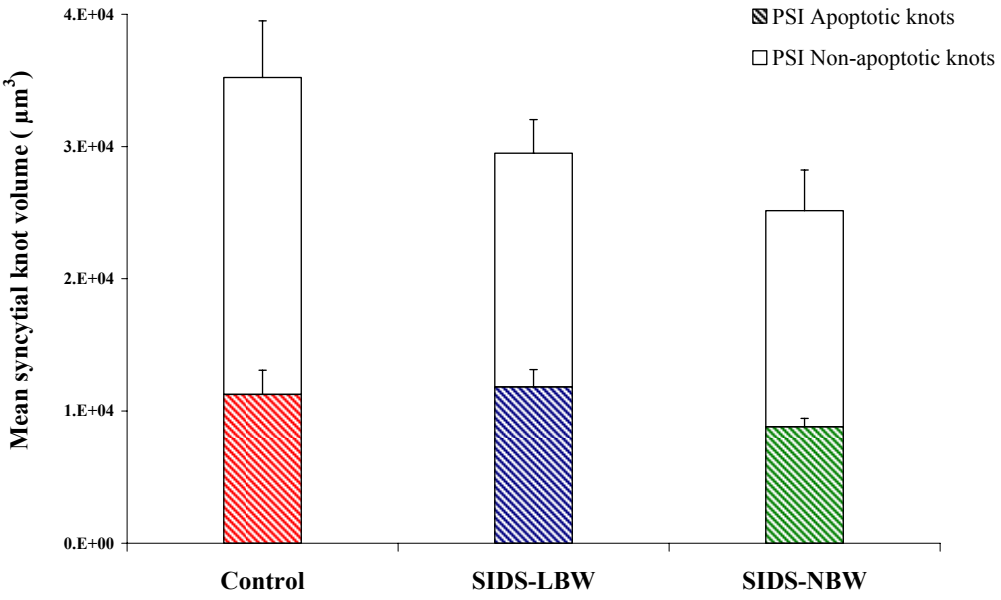

There were no significant differences in mean syncytial knot volume for SIDS placentas.

SIDS-LBW displayed a trend towards an increase in mean apoptotic syncytial knot volume for mature intermediate villi (P=0.075)

Graph 5-18 Total number of syncytial knots in SIDS placentas

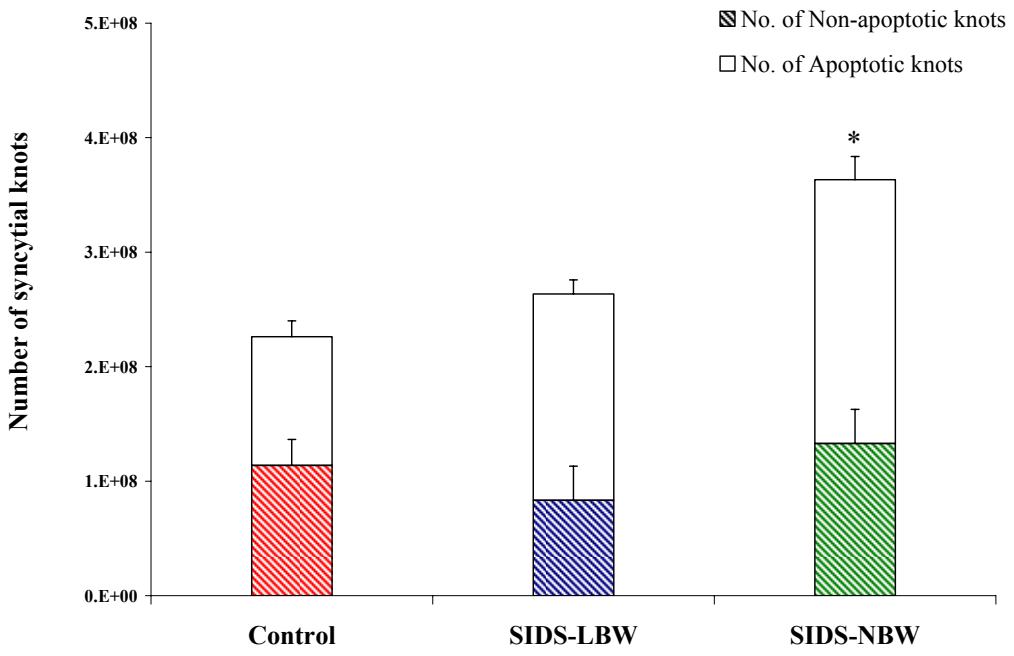

SIDS-NBW displayed a significant increase in the total number of syncytial knots (P=0.011) due to an increase in the total number of both apoptotic (P=0.021) and non-apoptotic syncytial knots (P=0.012).

5.4.5 Summary

SIDS-LBW

- significant increase in the volume density and total volume of syncytiotrophoblast (Graph 5-14, Table 5-7)
- significant increase in the total volume of apoptotic knots (Graph 5-16)

SIDS-NBW

- significant increase in the volume density and total volume of syncytiotrophoblast (Graph 5-15, Table 5-7)
- significant increase in the total volume of syncytial knots (Graph 5-15)
- significant increase in the total volume of apoptotic knots (Graph 5-16)
- significant increase in the total number of syncytial knots (Graph 5-18)

5.5 Discussion

Quantitative data regarding syncytialisation (relative numbers) provides a direct measure of the epithelial steady state in human villous trophoblast turnover. Terminally differentiated syncytiotrophoblast represent the end stage of this process, the extrusion of which (in the form of syncytial knots) balances the input from villous cytotrophoblast progenitor cells. A change in the number of syncytiotrophoblast nuclei therefore represents either defective input (e.g. cytotrophoblast depletion, failure or down-regulation of proliferation), or accelerated output of trophoblast material (e.g. altered differentiation pathway, extrinsic insults), both of which may perturb syncytial integrity and villous growth.

5.5.1 Volume and Number of SCT in Normal Human Pregnancy

Data from this study supports previous findings (200; 307) showing that the total volume and number of syncytiotrophoblast nuclei increases significantly between 26 and 41 weeks of gestation. This is due to the increase in the total volume of gas-exchanging villi in the third trimester of pregnancy. Conversely, the numerical density of syncytiotrophoblast nuclei decreased significantly between 26 and 41 weeks of gestation (supporting previous estimations (318)), due to the expansion of villous surface area and subsequent thinning of the trophoblast layer (Figure 5-1). This however was not paralleled by a decrease in the volume density of syncytiotrophoblast nuclei, which remained constant over gestation (previously reported at term (319)). This is because, whilst total trophoblast mass increases with gestational age reflecting villous growth, the spatial distribution of syncytiotrophoblast nuclei within this mass also changes due to the formation of vasculo-syncytial membranes (thus accounting for the decrease in numerical density) and denudation (local injury or mechanical shedding), leaving a non-uniform syncytiotrophoblast layer spread over a larger surface area. Thus, the proportion occupying villi does not significantly decline; volume density does not change.

Although values were higher than previously estimated (318), the ratio of cytotrophoblast cells to syncytiotrophoblast nuclei remained constant at approximately 1 to 5 between 26 and 41 weeks gestation. This indicates a steady balance between

recruitment and loss of trophoblast throughout the second and third trimester of normal pregnancy.

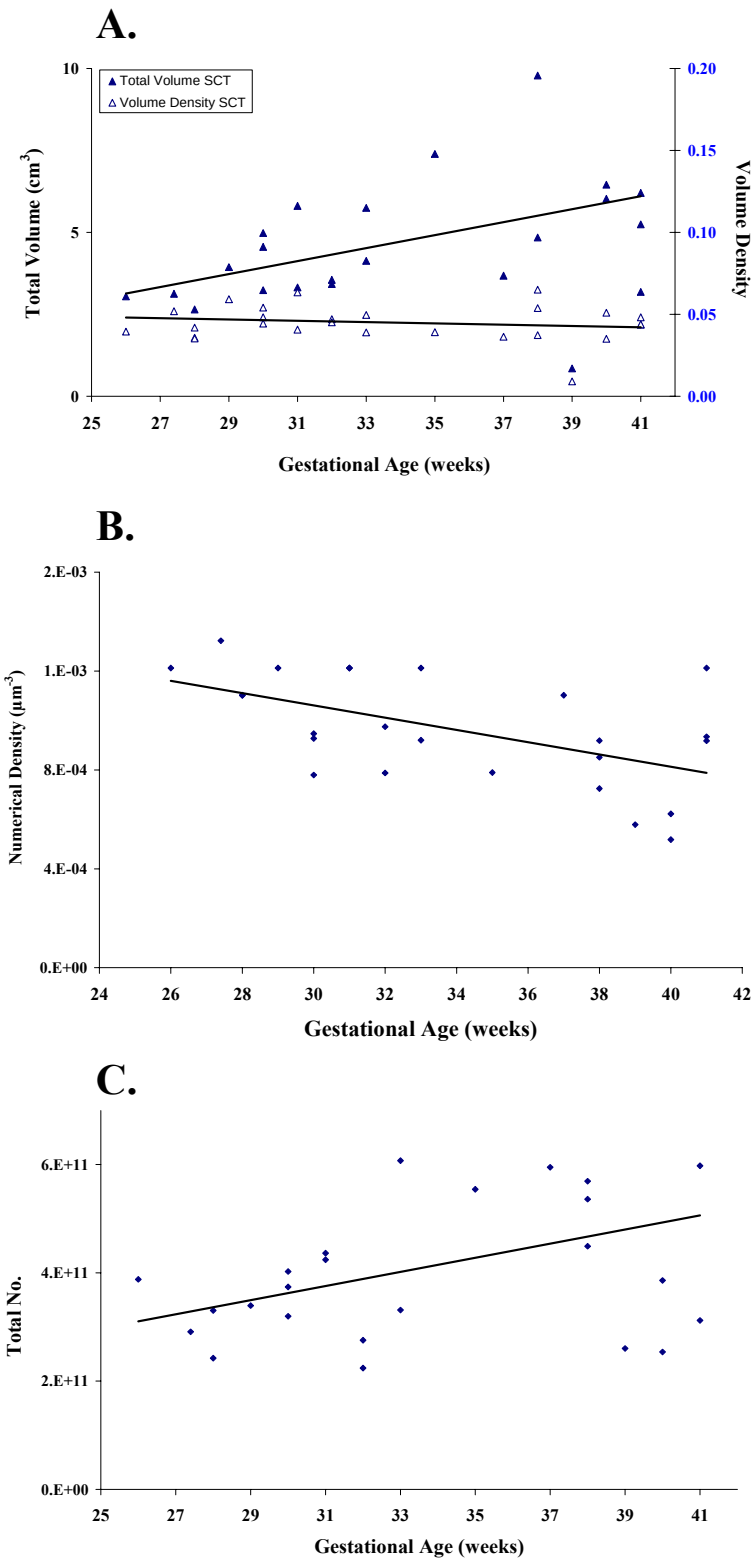

Figure 5-1 Volume and number of SCT in control placentas between 26 and 41 weeks of gestation.

The total volume and number of SCT significantly increased with GA (A, P=0.031; C, P=0.031). The volume density of SCT did not change over gestation (A). Numerical density of SCT significantly declined with increasing gestational age (B, P=0.004).

5.5.2 Quantifying Syncytial Knots and Apoptosis

'Syncytial knotting' (SK) (or Tenney-Parker changes (320)) is a broad histopathological term used to describe the histological appearance of a focal aggregation, or clumping, of syncytiotrophoblast nuclei on the outer surface of placental villi (276; 321). It encompasses those knots arising as part of a normal physiological event i.e. 'true syncytial knots' (i.e. villous trophoblast turnover, villous sprouting), but mostly those arising as a consequence of tangential sectioning of irregularly shaped and branched villous trees i.e. 'flat sectioning' (276).

Previous non-stereological studies describing increased syncytial knotting and apoptotic shedding in pre-eclampsia and IUGR (85; 320; 322) are confounded by (i) the assumption that all syncytial knots represent the final stages of villous trophoblast turnover, (i.e. syncytial degeneration), when in fact they will contain a mixture of knots, and (ii) the inherent bias associated with counting the 'number of syncytial knots per unit area' in 2D. Thus, there is always a degree of error and inaccuracy attached to morphological assessment of syncytial knots- the advantage of quantifying syncytial knots stereologically is that it permits the estimation of this error which can therefore be kept to a minimum.

Due to sectioning artefacts, true syncytial knots, (signifying syncytial degeneration in the final stages of normal villous trophoblast turnover) were defined as those SK regions containing apoptotic nuclei displaying morphological features characteristic of the final stages of apoptosis (small densely stained nuclei with distinct annular chromatin). Knots displaying normal syncytial nuclei were subsequently quantified as non-apoptotic knots and were interpreted to contain a mixture of villous sprouts, bridges and flat sectioning.

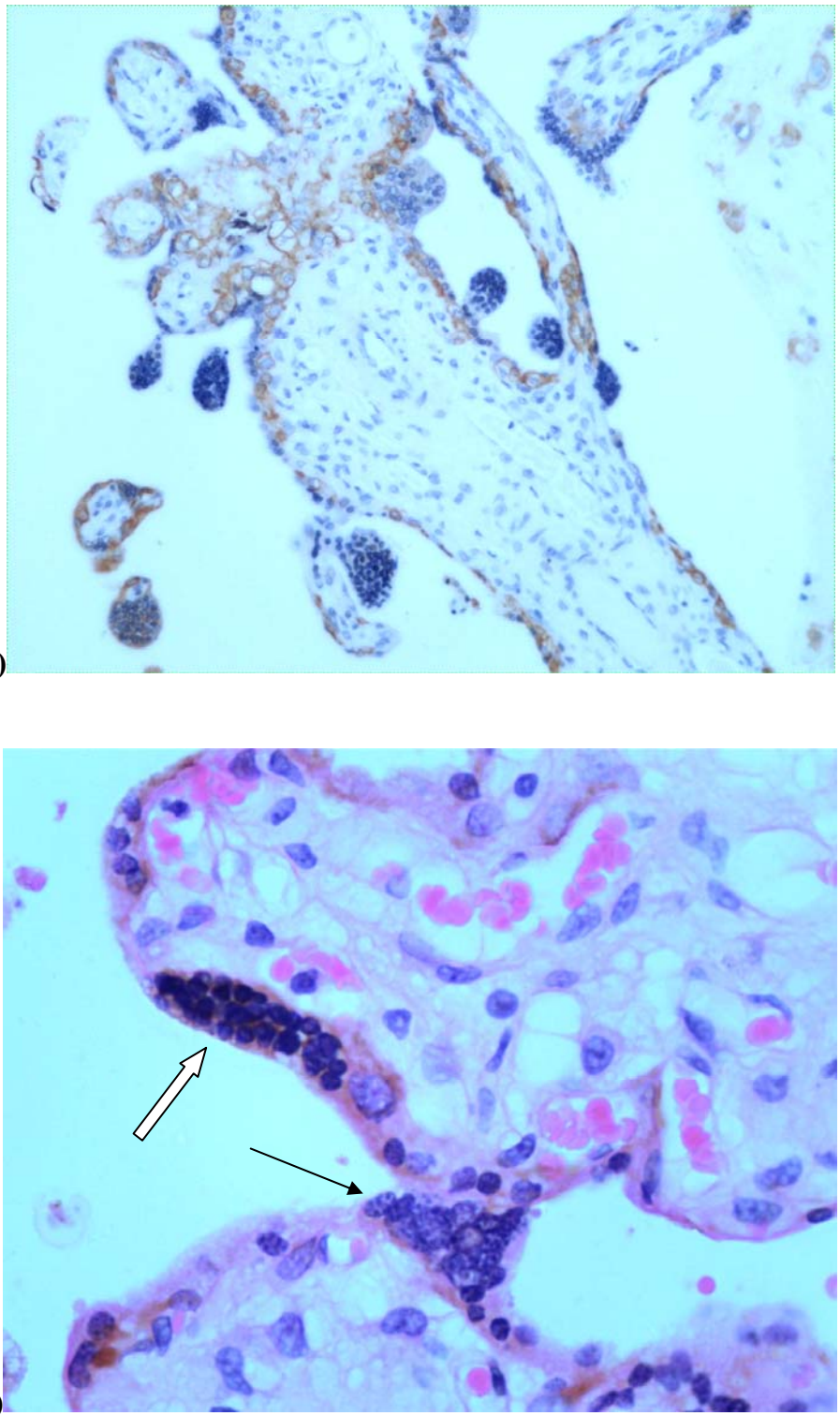

Figure 5-2: Syncytial Knot Morphology

Distinguishing between apoptotic and non-apoptotic syncytial knots. (A). At a low magnification it is impossible to determine the morphology of syncytial knots, and whether or not some of these contain apoptotic nuclei i.e. true syncytial knots (x100). (B). In contrast, apoptotic syncytial knot (white arrow) and non-apoptotic knot (black arrow) can be determined at a higher magnification (x400). The latter was used to identify apoptotic syncytial knots for this thesis.

5.5.3 Morphology of Syncytial Knots is Spatially and Temporally Regulated

The volume, mean individual volume and morphology of syncytial knots between 26 and 41 weeks gestation is described in the following section with the use of Figure 5-3.

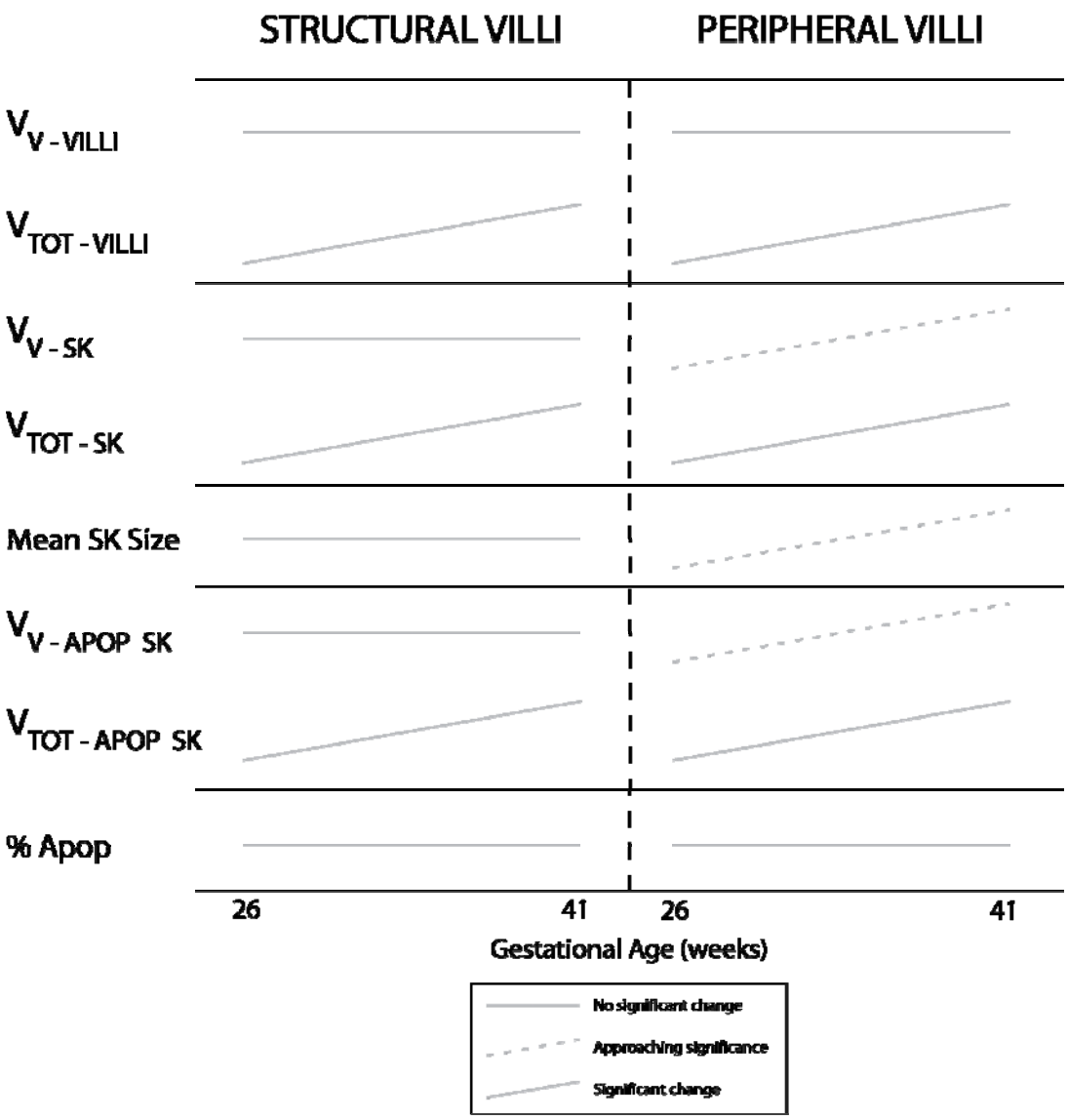

Figure 5-3 Syncytial knot (SK) volume, size and morphology between 26 and 41 weeks of gestation in control placentas.

The volume of villi, syncytial knots and apoptotic syncytial knots (volume and size) increase between 26 and 41 weeks of gestation. (V_v = Volume Density, V_{TOT} = Total Volume, Apop = Apoptotic SK. Structural villi = stem and immature intermediate villi, Peripheral villi = mature intermediate and terminal villi).

5.5.4 Volume of Syncytial Knots

Total volume of syncytial knots

Both structural and peripheral villi were associated with a significant increase in the total volume of syncytial knots ($P=0.025$, $P<0.001$) between 26 and 41 weeks of gestation. Whilst the volume density of SK on structural villi did not change over gestation, peripheral villi displayed a trend towards an increase, which just failed to reach statistical significance, ($P=0.055$). The former is an expected observation, as stem villi are continuously transforming into mature intermediate villi from around 22 weeks of gestation, thus the relative volume of SK on stem and immature intermediate villi will remain linear between 26 and 41 weeks of gestation.

Mean individual volume of syncytial knots

Although there were no significant changes in mean individual SK volume for structural villi between 26 and 41 weeks of gestation, preterm controls (26-32 weeks) were associated with a significant increase in mean SK size in comparison to peripheral villi ($P=0.021$). This likely contributes to the increased volume density of SK in comparison to peripheral villi, indicating that structural villi are associated with "fewer larger knots"; although "more knots of equal or greater volume" is equally likely. In contrast, peripheral villi displayed a trend towards an increase in mean SK size between 26 and 41 weeks, which just failed to reach statistical significance ($P=0.066$). This is indirect evidence for accelerated extrusion of syncytial nuclei in the third trimester of pregnancy, consistent with the redistribution of syncytial mass thinning the villous membrane via the formation of vasculo-syncytial membranes (212); a high incidence of SK regions are associated with a low incidence of vasculo-syncytial membranes (323).

Morphology of syncytial knots

Approximately half the total volume of syncytial knots were comprised of "true syncytial knots" i.e. those containing apoptotic syncytial nuclei, showing that apoptosis is a normal component of villous trophoblast turnover. The overall volume density of apoptotic SK nuclei on structural villi was significantly increased compared to peripheral villi. In the mature placenta, knots formed on villi during early gestation (i.e. structural villi) will likely show increased numbers of ageing nuclei (i.e. apoptosis), whereas in comparison those formed in later gestation (i.e. peripheral villi) will contain relatively little apoptotic nuclei (321). Hence, even though peripheral villi outweigh

structural villi in terms of total volume in late gestation, they actually contain less apoptotic nuclei *per se*.

Over gestation, the total volume of apoptotic nuclei increased in both structural and peripheral villi reflecting the increase in villous volume. The volume density of apoptotic nuclei displayed a trend towards an increase (P=0.055) with gestational age in peripheral villi.

5.6 Syncytial Integrity in Early-onset Pathologies

5.6.1 Volume and Number of SCT in Severe Early-onset PET and IUGR

Severe early-onset IUGR displayed a 50% reduction in the total volume and number of syncytiotrophoblast nuclei, specifically for peripheral villi, in comparison to age-matched controls. Whilst the volume density of syncytiotrophoblast was unaffected, the numerical density of syncytiotrophoblast displayed a trend towards a decrease (20% less nuclei per unit volume of placenta). The discordance between volume and number densities is indirect evidence for an increase in the average 'size' of syncytiotrophoblast nuclei in severe early-onset IUGR. In contrast, severe early-onset pre-eclampsia was not associated with any changes in the total volume or number of syncytiotrophoblast nuclei when compared to age-matched controls. Volume density of syncytiotrophoblast was however significantly reduced in structural villi.

Severe early-onset pre-eclampsia with IUGR (combined group) displayed significant reductions in the total volume and number of syncytiotrophoblast nuclei. There was a decrease in the numerical density of syncytiotrophoblast nuclei which just failed to reach statistical significance (P=0.053). Since these changes were not observed in severe early-onset PET, reductions in the total volume and number of syncytiotrophoblast nuclei in the combined group were due to the effects of IUGR. In contrast, the reduction in volume density of syncytiotrophoblast in structural villi for the combined group was due to the effects of pre-eclampsia.

Clinically, severe early-onset pre-eclampsia with IUGR is the most severe phenotype. The combination of PET with IUGR is therefore predicted to represent the most severe phenotype in terms of abnormal trophoblast biology. Accordingly, the reductions in the

total number and density of syncytiotrophoblast were more severe in the combined group (compared to pure IUGR or PET) demonstrating a potential synergistic interaction of PET and IUGR on numbers of syncytiotrophoblast nuclei. This is in direct contrast to villous cytotrophoblast, whereby pre-eclampsia reduced the severity of alterations in the combined group; consequently pure IUGR displayed the most severe villous cytotrophoblast phenotype.

The functional consequence of reduced syncytiotrophoblast nuclei is predicted to severely impair the transport (i.e. of amino acids) and endocrine activity of the syncytium upon which fetal growth and viability depend in the second half of pregnancy. Diminished growth of the IUGR fetus thus occurs not only by reduced volumes and surface area of gas-exchanging villi responsible for diffusional exchange of oxygen and nutrients, but is exacerbated by reduced numbers of syncytiotrophoblast nuclei available for active transport of amino acids and protein production necessary for fetal *and* subsequent placental growth. Based on these considerations, it is logical that 'pure' severe early-onset pre-eclampsia with normal fetal birth weights and normal umbilical artery Dopplers display similar volumes of placental villi and numbers of syncytiotrophoblast nuclei to age-matched controls.

5.6.2 Increased Volumes of Apoptotic Syncytial Knots in Early-onset PET and IUGR

Results from this study confirm stereologically that severe early-onset pre-eclampsia and IUGR are associated with increased numbers of apoptotic syncytial knots. Furthermore, the average size of these knots increases when pre-eclampsia co-exists with IUGR.

Severe early-onset pre-eclampsia displayed a significant increase (45%) in the total volume and density of apoptotic *and* non-apoptotic syncytial knots specifically for peripheral villi. Conversely, volume density was significantly decreased for structural villi. Although severe early-onset IUGR displayed the largest volume density of syncytial knots compared to all study groups, statistical significance was not reached likely due to the small number of cases. Nonetheless, a significant proportion of these knots contained apoptotic nuclei in comparison to controls, shown by a 36% increase in the volume density of apoptotic knots in peripheral villi. When combined with pre-

eclampsia, severe early-onset IUGR displayed a significant increase in the volume density of syncytial knots (apoptotic only) for peripheral villi. These were 57% larger than apoptotic knots in control placentas, but did not reach significant due to the large variation between placentas.

Volume density is a measure of the percentage of the reference volume Y, i.e. the placenta, taken up by X, i.e. syncytial knots. An increase in volume density of syncytial knots can therefore result from an increase in the number or size of syncytial knots, or both. In severe early-onset pre-eclampsia and IUGR, volume density was significantly increased but there was no change in individual SK volume (PSI), indicating a genuine increase in the number of syncytial knots in these placentas. Conversely, in pre-eclampsia co-existing with IUGR, both the PSI (trend) and volume density of knots increased. This situation may result from the presence of fewer larger knots, or alternatively, more knots of equal or larger size.

5.6.3 Impaired Syncytialisation in Severe Early-onset IUGR with and without PET

Growth, regeneration and functional integrity of the syncytiotrophoblast layer is completely dependent upon the continuous fusion of post-proliferative villous daughter cytotrophoblast cells throughout gestation; a lack of cytotrophoblast input via syncytial fusion leads to necrotic shedding and rarefaction of syncytiotrophoblast nuclei *in vivo* (214). Reduced numbers of villous cytotrophoblast cells therefore reflects proliferation below what is normally required to maintain growth, maintenance and integrity of the syncytiotrophoblast layer. The reduction in syncytiotrophoblast volume and number in severe early-onset IUGR was thus hypothesised to result from a reduced number of syncytial fusion *events*, secondary to reduced numbers and density of villous cytotrophoblast cells (due to premature depletion of progenitor cells), and reduced numbers of proliferating cytotrophoblast cells responsible for regenerating the syncytiotrophoblast layer.

The reduction in syncytiotrophoblast density is indirect evidence for absence of cytotrophoblast fusion in severe early-onset IUGR with and without co-existing pre-eclampsia. Globally, severe early-onset IUGR placentas are associated with a 50% reduction in the total volume and number of villous cytotrophoblast cells, 30% reduction in in those undergoing proliferation, subsequently resulting in 50% fewer syncytiotrophoblast nuclei in comparison to age-matched controls, confirming the hypothesis. However, given that the number of syncytiotrophoblast nuclei is positively correlated with the number of cytotrophoblast fusion events, the fact that the reduction in syncytiotrophoblast density was not paralleled by a similar reduction in the density of villous cytotrophoblast cells implies impaired syncytial fusion (Figure 5-4).

This suggests that ‘impaired recruitment’ of villous cytotrophoblast cells into the syncytium, in preference to ‘depletion of cytotrophoblast progenitor cells’ cells *per se,* is causative for reduced syncytiotrophoblast density in severe early-onset IUGR.

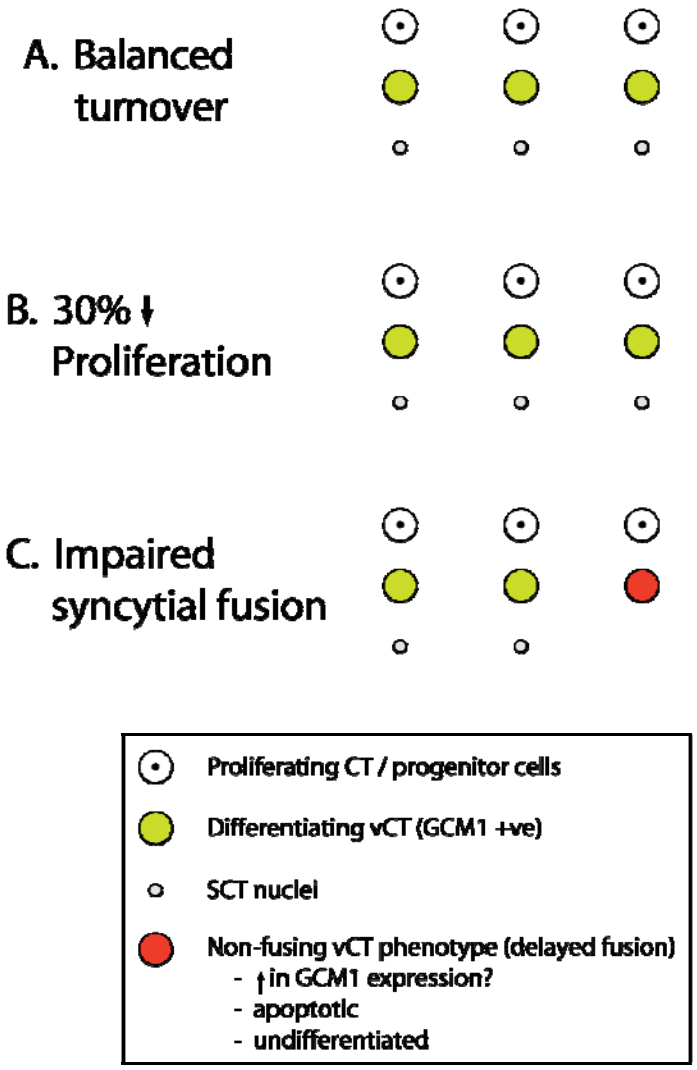

Figure 5-4 Impaired syncytialisation in severe early-onset IUGR

In normal placentas (A), four proliferating villous cytotrophoblast cells exit the cell cycle (GCM-1 directed), giving rise to four syncytial nuclei indicating proper syncytial fusion. In comparison, in severe early-onset IUGR, in addition to the 30% global reduction in the total number of proliferating villous cytotrophoblast cells (B), the density of syncytial nuclei is further reduced by 50% in comparison to preterm controls (C), which in conjunction with the 'normal' density of villous cytotrophoblast cells, indicates impaired syncytialisation of villous cytotrophoblast cells.

Syncytial fusion is coupled to cytotrophoblast differentiation and the 'initiator' stages of apoptosis (213; 225). Impaired syncytial fusion and reduced syncytiotrophoblast density in severe early-onset IUGR therefore indicates defective villous cytotrophoblast differentiation; a similar observation to that reported *in vitro* for Trisomy 21 affected placentas in Down's syndrome (324).

The decision of a cytotrophoblast cell to exit the cell cycle, differentiate and fuse with the overlying syncytium is shown to be mediated by the trophoblast-specific transcription factor, GCM1 (182; 214). GCM1 induces the expression of the gene *syncytin* (193), specifically expressed in the syncytiotrophoblast (192; 215), which transcribes a fusogenic membrane protein, syncytin1 (192), that mediates fusion of cytotrophoblast cells into the syncytiotrophoblast (193; 218; 219); both syncytin1 and GCM1 expression increase from the first trimester to 37 weeks gestation (310; 325). The cellular action of syncytin1 is however unidentified. The reduced syncytiotrophoblast density and 'normal' cytotrophoblast density in severe early-onset IUGR (Figure 5-4) may therefore be associated with dysregulated syncytin1 expression. Accordingly, a recent study using primary cytotrophoblast cultures and tissues showed that syncytin mRNA and protein expression is significantly reduced in IUGR with co-existing pre-eclampsia at mean gestational age of 32 weeks, resulting in reduced numbers of SCT nuclei (per unit area) inferring impaired syncytial fusion (309).

Given that GCM1 is a trans-activator of *syncytin*, reduced syncytin1 protein expression in IUGR with PET is inconsistent with the increased GCM1 protein expression observed for severe early-onset IUGR in this study (personal communication, Sascha Drewlo, Toronto); increased GCM1 protein expression would be expected to increase syncytin1 expression *in vivo*. This inverse relationship suggests that initiation of syncytial fusion by syncytin1 is expression level-dependent. Huppertz *et al* demonstrated reduced numbers of cytotrophoblast cells upon antisense oligonucleotide inhibition of syncytin1, contrary to the expected increase, suggesting that decreased, rather than increased syncytin1 expression may stimulate syncytial fusion (211). It may be reasoned that increased syncytin1 expression (via upregulation of GCM1 and subsequently reduced Ki-67 expression) therefore leads to delayed/impaired syncytial fusion, further diminishing cytotrophoblast cell differentiation.(214). Furthermore, the presence of an intact syncytium is a precondition for cytotrophoblast fusion and syncytialisation (185; 214). First trimester floating villi denuded of syncytiotrophoblast *in vivo* fail to undergo *de novo* syncytiotrophoblast formation following forskolin treatment or up-regulation of GCM1. An alternative viewpoint is that decreased syncytiotrophoblast density in severe early-onset IUGR perpetuates the already delayed/impaired syncytial fusion secondary to defective cytotrophoblast differentiation.

Premature death of villous cytotrophoblast cells in severe early-onset IUGR?

Whilst villous cytotrophoblast progenitor cells feed growth and regeneration of the syncytiotrophoblast, the daughter cells are responsible for executing its programmed cell death. As cytotrophoblast cells fuse with the overlying syncytium, they transfer the necessary apoptotic machinery confining the "execution stages" to syncytiotrophoblast nuclei, which are extruded in the form of syncytial knots some 3-4 weeks later (195). In normal placental villi, apoptotic cell death is thus almost exclusively (308) confined to discrete areas of the syncytiotrophoblast, predominantly aggregated within syncytial knot regions (321). Semi-quantitative immuno-histochemical studies have shown an increased expression of pro-apoptotic proteins and correspondingly reduced expression of anti-apoptotic proteins in the syncytiotrophoblast layer, in both term (198; 240; 242; 326) and preterm IUGR placentas (327) (reviewed in detail in (328)). More recently, increased apoptosis (assessed using terminal dUTP end-labelling, Annexin V binding potential, and the measurement of ADP: ATP levels) has been demonstrated in isolated villous cytotrophoblasts from pre-eclampsia and IUGR at term (329). Similarly results from the present study suggest that (albeit indirectly) in severe early-onset IUGR, villous cytotrophoblast cells may well undergo the execution stages of apoptosis prior to entering the syncytiotrophoblast, consequently reducing syncytiotrophoblast density.

Although the stimulus is unknown, ultra-structural studies in normal human pregnancy between 6 and 15 weeks gestation confirmed that a small percentage of villous cytotrophoblast cells do in fact undergo the execution stages of apoptosis, and to an even lesser extent, primary necrosis (308). Given that the process of syncytial fusion transfers the necessary apoptotic machinery to execute the final stages of apoptosis in syncytiotrophoblast (195; 225), it may be postulated that the 'fusion-disabled' villous cytotrophoblast cells thus undergo the execution stages of apoptosis prior to entering the syncytiotrophoblast. Interestingly, over-expression of syncytin1 in choriocarcinoma cells (CHO) transfected with the apoptosis inducer staurosporine, significantly reduced the rate of apoptotic cell death (reduced caspase-3 activation and increased Bcl-2 expression), demonstrating the anti-apoptotic effects of syncytin1 in *fusing* CHO cells (330). By inference, reduced syncytin1 expression in IUGR (309) may therefore exert pro-apoptotic cellular effects in *non-fusing* cytotrophoblast cells. Moreover, because the process of syncytial fusion transfers anti-apoptotic proteins (e.g.Bcl-2 expression is reduced in severe IUGR (240)) which focally retard the apoptosis cascade (195), the

lack of syncytial fusion in severe early-onset IUGR may also result in accelerated syncytiotrophoblast apoptosis, supported by the significant increase in number of apoptotic syncytial knots.

Although numbers of apoptotic nuclei (cytotrophoblast or syncytiotrophoblast) were not quantified in the present study, expression of the apoptosis-induced cleaved cytokeratin-18 was semi-quantified by western blotting. During the 'irreversible' stages of caspase-mediated apoptosis, caspases -3 and -7 proteolytically cleave the intermediate filament protein, cytokeratin-18 (CK-18) producing a neo-epitope (42kDa protein) which is recognised specifically in epithelial cells by the apoptosis-specific monoclonal antibody, M30 (237); M30 does not detect necrosis (303). In normal placentas undergoing apoptosis, cleaved CK-18 is predominantly immuno-localised to the syncytiotrophoblast cytoplasm, syncytial knots, and to a lesser extent in villous cytotrophoblast cells, which under experimentally-induced hypoxia, reverses this expression pattern (210).

In the present study, cleavage of CK-18 (M30 mAb) was detected in equal amounts in preterm controls and severe early-onset pre-eclampsia, and was elevated in severe early-onset IUGR with co-existing pre-eclampsia (35% increase). This however was not statistically significant due to large inter-placental variation and small study groups. The corresponding absence of the full-length CK-18 protein verified CK-18 cleavage and M30 specificity. Neither M30 nor full-length CK-18 expression were quantified in severe early-onset IUGR without pre-eclampsia due to unforeseen circumstances.

Despite these limitations, the results still provide reasonable evidence that villous cytotrophoblast cells may undergo premature death in severe early-onset IUGR. This can be explained for the following reasons. Firstly, since both severe early-onset pre-eclampsia and IUGR display increased numbers of apoptotic syncytial knots, the fact that cleaved CK-18 was not increased in pre-eclampsia but increased in IUGR with PET indicates that syncytial knots are not responsible for elevated cleaved CK-18 expression. Secondly, syncytiotrophoblast density was significantly reduced in IUGR with PET and not pre-eclampsia, which given the above considerations, should reduce the expression of cleaved CK-18. Thirdly, severe early-onset IUGR with pre-eclampsia is associated with increased numbers of non-dividing cytotrophoblast cells relative to pre-eclampsia. For these reasons, increased cleaved CK-18 expression in IUGR with pre-eclampsia can

be inferred to result from an increased number of villous cytotrophoblast cells undergoing the execution stages of the apoptosis cascade in comparison to preterm controls. Furthermore, given that the morphological and molecular pathology of IUGR with pre-eclampsia typically resembles that of isolated IUGR, increased cleaved CK-18 expression, and hence villous cytotrophoblast apoptosis, may be a presumed feature of severe early-onset IUGR placentas.

Increased numbers of apoptotic syncytial knots in severe early-onset IUGR

In line with the above observations, the decrease in syncytiotrophoblast density and increase in the number of apoptotic syncytial knots in severe early-onset IUGR and PET-IUGR placentas may reflect accelerated formation of syncytial knots. During the second and third trimester of normal pregnancy, fetal maturation is accompanied by redistribution of syncytial mass into knot regions corresponding to the formation of thin vasculo-syncytial membranes, which serve to decrease the diffusional distance of oxygen and nutrients between maternal and fetal circulations. As such, a high incidence of syncytial knots has been shown to be associated with a low incidence of vasculo-syncytial membranes. Thus, from a physiological perspective, the reduction in syncytiotrophoblast nuclei and increase in syncytial knots may serve to thin villous membrane thickness thus compensating for impaired cytotrophoblast fusion.

Apoptotic syncytial knots are undoubtedly physiological, and are thought to represent the end stage in the turnover of villous trophoblast. Although the exact mechanism of extrusion is unknown, sheer mechanical stress from ‘fast-flowing’ maternal blood in the intervillous space is postulated to remove such knots. Increased numbers of apoptotic syncytial knots are unlikely to be directly involved in the pathophysiology of severe early-onset IUGR, as increased numbers are also observed in pre-eclampsia displaying normal fetal birth weights, indicating that syncytial knots do not impede diffusional exchange. An alternative explanation is that in IUGR pregnancies with reduced uterine artery Dopplers, sluggish and/or intermittent uteroplacental blood flow results in less mechanical shedding leading to large accumulations of syncytial nuclei. As a consequence, such knots may become apoptotic post-formation. Concordantly, experimentally-induced hyperoxia (20% oxygen) (presumed to represent intervillous oxygen content in severe early-onset IUGR), increased the number of apoptotic syncytial knots per mm^2 of terminal villi (322).

5.6.4 Accelerated Terminal Differentiation in Severe Early-onset Pre-eclampsia?

There is general agreement that hypoxia/re-oxygenation injury promotes (331) the increased release of placental factors (e.g. cytokines (19), eicosanoids (332), peroxides (333), soluble Flt-1 (22), soluble endoglin (334), and trophoblast debris such as syncytiotrophoblast microparticles (STBM) (335) and necrotic and/or apoptotic syncytial material (210)), from a 'dysfunctional' syncytium which are both necessary and sufficient (23) to reproduce the maternal syndrome of pre-eclampsia, i.e. maternal endothelial dysfunction, clinically evident as maternal hypertension and proteinuria. Despite the pathogenic evidence (24), the stimuli(s) for their release is currently undefined, but is generally ascribed to dysregulated cytotrophoblast biology (3). Findings from the present study indicate that the *rate* of the entire turnover of villous trophoblast is increased in severe early-onset pre-eclampsia, likely contributing to abnormal syncytial shedding.

The hypothesis under investigation was that in pre-eclampsia, an increased rate of cytotrophoblast proliferation and syncytial fusion makes sufficient numbers of syncytiotrophoblast, but results in dysregulated shedding of syncytial nuclei (necrotic and apoptotic) into the intervillous space constituting the maternal syndrome. The fact that severe early-onset pre-eclampsia was not associated with any significant changes in the number or volume of syncytial nuclei when compared to age-matched controls, partly confirms this hypothesis.

Sufficient numbers of syncytial nuclei signifies 'matched', or even 'accelerated' cytotrophoblastic input providing this is matched by accelerated extrusion; failure to extrude would increase syncytial thickness which is not a feature of pre-eclampsia. Although there was no significant increase in the number of proliferating cytotrophoblast cells, peripheral villi displayed a trend towards a decrease in cytotrophoblast density ($P=0.071$) whereas syncytiotrophoblast density was unchanged. Given that the number of syncytiotrophoblast nuclei is directly correlated with the number of cytotrophoblast fusion events, this mismatch between cytotrophoblast and syncytiotrophoblast density indirectly indicates increased syncytial fusion and accelerated terminal differentiation of villous cytotrophoblast cells in severe early-onset pre-eclampsia. This concept is explained in (Figure 5-5).

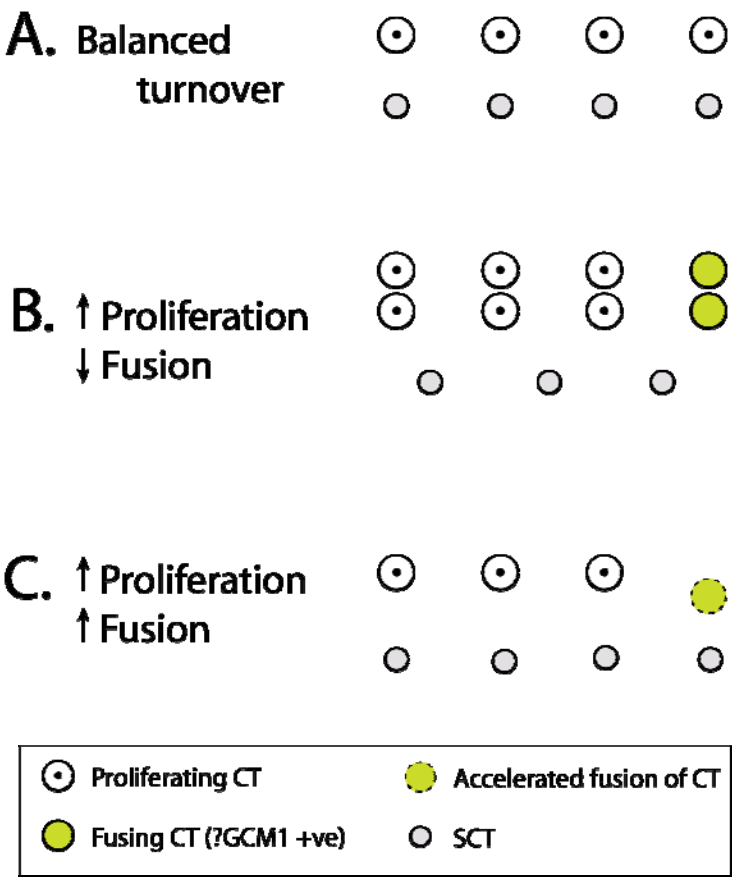

Figure 5-5 Rudimentary model of accelerated trophoblast turnover in peripheral villi in severe early-onset pre-eclampsia

In control placenta (A), trophoblast turnover is balanced such that the number of syncytiotrophoblast nuclei is paralleled by an equal number of proliferating and fusing cytotrophoblast cells i.e. four post-mitotic cytotrophoblast cells (GCM1-positive) differentiate and fuse producing four terminally-differentiated syncytial nuclei. In (B), an increase in cytotrophoblast proliferation with reduced cytotrophoblast fusion leads to a multilayered cytotrophoblast layer and rarefaction of syncytiotrophoblast nuclei. This scenario is described for severe early-onset pre-eclampsia *in vivo* via inhibition of GCM1 (214). In contrast (C), whilst there are an equal number of proliferating cytotrophoblast cells and syncytial nuclei to controls, there are less cytotrophoblast cells. The reduction in cytotrophoblast density is therefore indirect evidence for an increase in the *rate* of cytotrophoblast fusion. The imbalance between proliferation and fusion (leading to an increase, although not statistically significant, in the percentage of proliferating cytotrophoblast cells) indicates accelerated villous cytotrophoblast differentiation, demonstrating a shorter transition time between cytotrophoblast and syncytiotrophoblast phenotypes.

Crucially, for there to be an increase in the *rate* of cytotrophoblast fusion, the *rate* of cytotrophoblast proliferation must also increase or else the pool of syncytially-fusing cytotrophoblast cells would be exhausted, leading to rarefaction of syncytiotrophoblast

nuclei. The accelerated turnover of cytotrophoblast proliferation and fusion may therefore preclude detection of the hypothesised increase in the *number* of proliferating villous cytotrophoblast cells.

Morphological data in this study is consistent with the molecular pathology of severe early-onset pre-eclampsia (*in vitro* and *in vivo*). Placentas in the present study are associated with decreased protein and mRNA expression of GCM1 (Personal communication, Sascha Drewlo, Toronto), as previously described (310). GCM1 is differentially expressed in post-mitotic daughter villous cytotrophoblast cells destined for syncytial fusion (183; 191). Inhibition of GCM1 in non-denuded first trimester villous explants prevents *de novo* syncytiotrophoblast formation leading to a multilayered cytotrophoblast layer and rarefaction of a necrotic syncytium (214), signifying the vital role of GCM1 in regulating human villous cytotrophoblast differentiation. Concordantly, expression of the fusogenic protein syncytin1, a direct downstream effector of GCM1, is significantly reduced in severe early-onset pre-eclampsia (336-338). Thus, the alterations in GCM1 and syncytin1 are presumed to contribute to reduced cytotrophoblast differentiation and fusion, subsequently impairing syncytiotrophoblast formation. However, the morphological consequences of GCM1 inhibition *in vivo* (representing decreased GCM1 expression in pre-eclampsia) oppose the stereological data indicating accelerated cytotrophoblast differentiation and fusion, alongside normal syncytiotrophoblast formation.

This may be explained by the fact that the reduction in cytotrophoblast density (via presumed accelerated fusion) diminishes the number of GCM1-positive syncytially-fusing cytotrophoblast cells. Given that up-regulation of GCM1 induces arrest of mitosis (counter-expression to Ki-67), the above explanation is justified by an observed 20% reduction (trend) in the number of Ki-67-negative (i.e. differentiating) cytotrophoblast cells (P=0.088). Although this does create a circular argument since *in vivo*, reduced GCM1 expression retards syncytial fusion. Nonetheless, together this data indicates ‘under-differentiation’ of villous cytotrophoblast cells which as a consequence have to increase the rate of syncytial fusion to maintain syncytial morphology at the expense of functional integrity i.e. abnormal shedding.

Severe experimental hypoxia (1% O_2), presumed to represent an acute model of placental ischemia in severe early-onset pre-eclampsia, also reduces GCM1 and syncytin1 transcripts and fusion of primary term human trophoblasts (339). A practical explanation is that these and the above 'acute models' fail to mimic the local changes in oxygen tension and intervillous haemodynamics, which change both spatially and temporally. Hence, stereological analysis of pre-eclamptic placentas might identify more subtle changes in trophoblast morphology, which may well originate from a less severe, yet comparable defect/insult initiated during early placental development.

Is accelerated villous trophoblast turnover sufficient to cause dysregulated syncytial shedding?

Circulating syncytiotrophoblast microparticles (i.e. loss of brush border membranes, cytoplasmic protrusions, microvillous blebs (340)) arise as part of the normal turnover of syncytiotrophoblast, evidenced by their detection in maternal plasma of normal pregnancy, and are present in significantly increased amounts in pre-eclampsia (335). Such particles are the hallmark of apoptosis (341), which is proposed to coordinate the extrusion of aged syncytial nuclei into the IVS, allowing for continuous renewal of the syncytial surface (195).

It has recently been shown that diminished villous cytotrophoblast differentiation (GCM1-silenced) *in vitro* and *in vivo* leads to the increased release and expression of the anti-angiogenic factor, soluble sFlt-1 (22), in culture media and syncytiotrophoblast respectively, establishing a link between abnormal villous cytotrophoblast differentiation and the release of pathogenic placental factors (342).

5.7 Late-onset Pathologies

5.7.1 Volume and Number of SCT in Late-onset Pathologies

Although there was no significant decrease in the total volume of syncytiotrophoblast in late-onset IUGR, the total number of syncytial nuclei significantly decreased by 50% (both structural and peripheral villi) in comparison to age-matched controls. This however reflects the small placental phenotype, as volume and number densities of syncytiotrophoblast nuclei remained similar to controls. Whilst the overall volume density of syncytial knots did not increase, the proportion of them containing apoptotic nuclei significantly increased (42%) in structural villi, with a propensity to be larger (average volume) than controls.

In contrast, late-onset pre-eclampsia was associated with a 31% increase in the density and total volume of syncytial nuclei in peripheral villi, which failed to reach significance due to large variation. Conversely, the numerical density of syncytial nuclei remained unchanged, indirectly indicating an increase in the average size of individual syncytial nuclei in peripheral villi. Structural villi on the other hand displayed a 40% reduction in numerical density of syncytiotrophoblast. This resulted in a trend towards a decrease in total numbers of syncytiotrophoblast nuclei (27% reduction). Peripheral villi displayed a trend towards an increase in the volume density of syncytial knots, a significant proportion of which were apoptotic in comparison to age-matched controls but of similar size (52% increase).

In comparison to early-onset pre-eclampsia co-existing with IUGR displaying a dominant role of IUGR in reducing syncytiotrophoblast volumes and number, pre-eclampsia played a dominant role in increasing syncytiotrophoblast volumes in the combined disease in late gestation; 30% increase in the volume density of syncytial nuclei in peripheral villi, which just failed to reach significance ($P=0.068$). The numerical density of syncytial nuclei remained unchanged, whereas total numbers declined by 35% in peripheral villi. Similar to the ‘pure’ pathologies, the volume density of syncytial knots remained unchanged but a significant proportion of them were apoptotic and larger in comparison to controls (32% increase). Furthermore, the severity of the above changes was lessened by the presence of pre-eclampsia in late gestation, whereby ‘pure’ IUGR displayed the most severe phenotype.

5.7.2 Accelerated Syncytialisation in Late-onset Pre-eclampsia

Results from this study reveal that accelerated syncytialisation and villous trophoblast turnover is a shared feature of both early- and late-onset pre-eclampsia. To avoid repetition, data for late-onset pre-eclampsia will be briefly described; for a full explanation of these observations refer to section 5.6.4

Similar to early-onset cases, the epithelial steady state is dysregulated in late-onset pre-eclampsia, shown by a global loss (24%) of (Ki-67 negative) cytotrophoblast cells alongside preserved numbers of syncytiotrophoblast. Such a loss of cytotrophoblast indicates an increased rate of differentiation and fusion into the 'normal' syncytium (numbers of nuclei). There is also indirect evidence for an increase in the size of syncytial nuclei in late-onset pre-eclampsia, since the increase in volume density of syncytiotrophoblast (peripheral villi only) was not accompanied by an increase in number, which remained similar to controls. This may result from the failure of the 'freshly incorporated' syncytiotrophoblast nuclei to undergo terminal differentiation (and hence reduction in size) prior to extrusion, supporting the notion of aponecrotic release of syncytial nuclei in pre-eclampsia (3). Because numbers of syncytial nuclei are maintained, the increased rate of recruitment (i.e. fusion) must therefore be matched by extrusion, since a thicker syncytial membrane is not a feature of these placentas. Whilst the number of proliferating villous cytotrophoblast cells remain similar to controls, the rate of proliferation must be increased, otherwise villous membrane thickness would gradually decline due to the lack of trophoblast input. An increased *rate* would preclude detection of the hypothesised increase in number of proliferating cytotrophoblast cells due to accelerated syncytiotrophoblast differentiation. As such, the increase in the percentage of proliferating cytotrophoblast cells observed for structural villi was due to a decline in cytotrophoblast numbers rather than an increase in the density of Ki-67 positive cells *per se*. Together, these results demonstrate that pre-eclampsia is associated with an increase in the rate of the entire turnover of villous trophoblast, independent of gestational age.

Although there was no significant increase in the volume density of syncytial knots in late-onset pre-eclampsia, peripheral villi displayed a significant increase in percentage of apoptotic syncytial knots. This is unlikely to reflect defective mechanical shedding which would be expected to increase the volume density of syncytial knots. A plausible

explanation is the increased extrusion of syncytial knots via accelerated trophoblast turnover.

5.7.3 Normal Syncytialisation in Late-onset IUGR

A combination of the low number of cases (n=4) and the large intra-group variation (two 33 week cases with abnormal umbilical artery Doppler, and two cases at 37 weeks with normal Dopplers) in the late-onset IUGR groups means that conclusions regarding syncytiotrophoblast cannot be determined with any degree of accuracy. Therefore, only the stereological data is described.

The placental phenotype of late-onset IUGR resembles that of early-onset disease such that the 'small' placenta contains 50% less proliferating cytotrophoblast cells, 50% less villous cytotrophoblast cells and consequently 50% less syncytiotrophoblast nuclei in comparison to term controls. However, in contrast to early-onset pathology, the density of syncytial nuclei remained similar to controls indicating normal syncytialisation, and thus normal villous cytotrophoblast differentiation. Furthermore, proliferating villous cytotrophoblast cells are not depleted, which may account for normal growth of the peripheral villous tree seen in late-onset IUGR. Similar to late-onset pre-eclampsia, the volume density of syncytial knots remained unchanged but the proportion of apoptotic syncytial knots significantly increased. This may reflect failed or retarded extrusion resulting in an ageing syncytium in late-onset IUGR.

Contrary to expectations, the epithelial steady state in late-onset pre-eclampsia with IUGR resembled that of isolated pre-eclampsia and not IUGR as was acknowledged for early-onset disease. Villous cytotrophoblast differentiation was dysregulated in an almost identical manner to that described above for late-onset pre-eclampsia. This includes (i) a trend towards a decrease in the density of (non-proliferating) villous cytotrophoblast cells (P=0.067) and normal numbers of syncytial nuclei indicating accelerated syncytialisation (ii) an increase in volume density of syncytiotrophoblast with no change in number indicating their increased size, (iii) a significant increase (26%) in the percentage of proliferating cytotrophoblast cells for peripheral villi.

This is a paradoxical finding since the 'small' placental phenotype of late-onset pre-eclampsia with IUGR was similar to isolated IUGR, with reductions (albeit less severe)

in total placental and villous volumes, and total numbers of trophoblast. This discrepancy may be explained by the fact that, whilst rates of differentiation and loss seem to be accelerated in pre-eclampsia, rates of proliferation are higher in pre-eclampsia than IUGR, thereby maintaining appropriate 'growth pattern' of the villous trees, but which may have began with less developmental potential (i.e. progenitor cells).

5.7.3.1 Increased Volumes of SCT and Apoptotic Syncytial Knots in SIDS

Data from this study shows that SIDS is associated with a thickened syncytiotrophoblast layer in comparison to term controls, the severity of which is increased in SIDS-LBW. SIDS-NBW placentas displayed a significant increase in the volume density of syncytiotrophoblast nuclei (specifically for stem and mature intermediate villi; 37%, 29%), which was exemplified in the presence of a low birthweight infant (42%, 45%), indicating the effect of LBW on syncytiotrophoblast volume. Although SIDS had no overall effect on the total volume or density of syncytial knots, the percentage of apoptotic syncytial knots increased in the presence of both normal (23%) and low birthweight infants (25%), which tended to be smaller in size (30% smaller but not significantly). This indicates that SIDS placentas are associated with increased numbers of 'smaller' apoptotic syncytial knots in comparison to term controls, independent of fetal birthweight.

Pre-placental fetal hypoxia and the syncytium in SIDS placentas

There is a growing concept that SIDS represents a developmental disorder which originates during fetal development in utero. It is generally believed that biochemical and microscopic developmental abnormalities evidenced in 'hypoxic' SIDS infants (64), especially in the brainstem (80; 80; 343) and central nervous system (70), are the result of protracted or recurrent exposure to 'intrauterine hypoxia', culminating in the sudden death of an infant during a vulnerable postnatal period (i.e. the triple risk hypothesis (71)). Cigarette exposure, either passively or directly during pregnancy is considered the principle cause of intrauterine hypoxia (of the pre-placental type) and SIDS; hematocrit levels suggestive of hypoxia are elevated in both mothers and fetuses of smokers compared to non-smokers.

Maternal smoking during pregnancy is associated with a thicker villous membrane, evidenced to result from the direct effect of tobacco constituents on reducing cytotrophoblast proliferation, differentiation and syncytiotrophoblast apoptosis *in vitro,* in a dose-dependent manner (247; 344). The increased thickness, and hence increased volumes of cytotrophoblast and syncytiotrophoblast, may be expected to compromise diffusional exchange to the fetus from an early stage in pregnancy resulting in a LBW infant. Concordantly, 83% of SIDS-LBW infants were born to heavy smokers (average of 20 cigarettes per day) whilst only 42% of SIDS-NBW infants were born to mild smokers (average of 10 cigarettes per day). This supports previous observations that heavy smoking reduces infant birthweight (246). However, by separating smokers from non-smokers in SIDS-NBW infants, there still remains a significant increase in the volume of syncytiotrophoblast in non-smoking SIDS-NBW placentas compared to non-smoking controls. Furthermore, these alterations were more severe in non-smokers than smokers. Together, these results indicate that SIDS-specific factors and not those relating to maternal smoking, account for the increase in syncytiotrophoblast volume.

The increase in relative syncytiotrophoblast volume is inconsistent with a recent stereological study demonstrating no relative syncytial changes in placentas from pregnancies at high altitude. Mothers at high altitude experience hypobaric hypoxia, representing a natural model for studying 'pre-placental' fetal hypoxia. Experimentally-induced hypoxia (2% O_2) has been shown to stimulate cytotrophoblast proliferation (MIB-1 index) and inhibit syncytial fusion thus reducing syncytiotrophoblast formation *in vitro* (210; 345). Relative volumes of cytotrophoblast are also increased in placentas from high altitude pregnancies alongside a normal syncytium (346). The increase in cytotrophoblast volumes in both SIDS-NBW and SIDS-LBW is therefore consistent with pre-placental hypoxia. However, analysis of cytotrophoblast proliferation and numerical data is needed to confirm whether the increase in volume is due to increased cytotrophoblast proliferation or hypertrophy.

The increase in the number of apoptotic knots indicates that SIDS placentas are associated with an ageing syncytium. Syncytial ageing may result from defective cytotrophoblast differentiation, or alternatively failure to mechanically shed aged nuclei into the intervillous space. The latter explanation is supported by the compact histological appearance of increased volumes of mature intermediate and terminal villi

in SIDS-NBW placentas (Figure 5-6). The 'clusters' of mature and terminal villi (likely due to adaptive angiogenesis secondary to an early hypoxic insult (103)) will be physically unable to shed their nuclei, thus increasing syncytiotrophoblast volume. Furthermore, focal restrictions in maternal blood supply will undoubtedly lead to a relatively hypoxic environment surrounding the villi, shown *in vitro* to increase the incidence of apoptotic syncytial knots (322).

The association of increased syncytiotrophoblast volume in both SIDS-LBW *and* SIDS-NBW seems confusing, since based on the considerations above this would be expected to compromise diffusional exchange to the fetus resulting in a low birthweight infant. In similar situations of pre-placental hypoxia, infant birthweights are reduced despite physiological compensatory adjustments aimed at increasing diffusional exchange such as increased intervillous space, reduced trophoblast thickness (346), and increased capillary volume fraction of terminal villi (154). Thus, increased relative volumes of syncytiotrophoblast and cytotrophoblast are unlikely to represent compensatory mechanisms, and importantly, these structural alterations are not necessarily detrimental to placental function i.e. leading to a low birthweight infant. Other mechanisms must therefore be initiated by SIDS-NBW placentas thus maintaining adequate fetal growth in utero.

One plausible explanation is that SIDS-NBW have compensated for increased trophoblast volume by increasing the volume of terminal villi (45% increase), and hence enlarging the total surface area available for diffusional exchange to the fetus. However, this raises the "chicken-and-egg" question as to whether these infants have a normal birthweight because of increased volumes of terminal villi, or alternatively why would the normal birthweight infant require increased volumes of terminal villi. Although SIDS-LBW placentas displayed an increase in the proportion of terminal villi compared to term controls, it was insufficient to compensate for the small placental phenotype perhaps by failure to elicit mechanistic and functional modifications which SIDS-NBW subsequently display. This gives some credence to the interpretation that SIDS-NBW have initiated a compensatory reserve which SIDS-LBW lack.

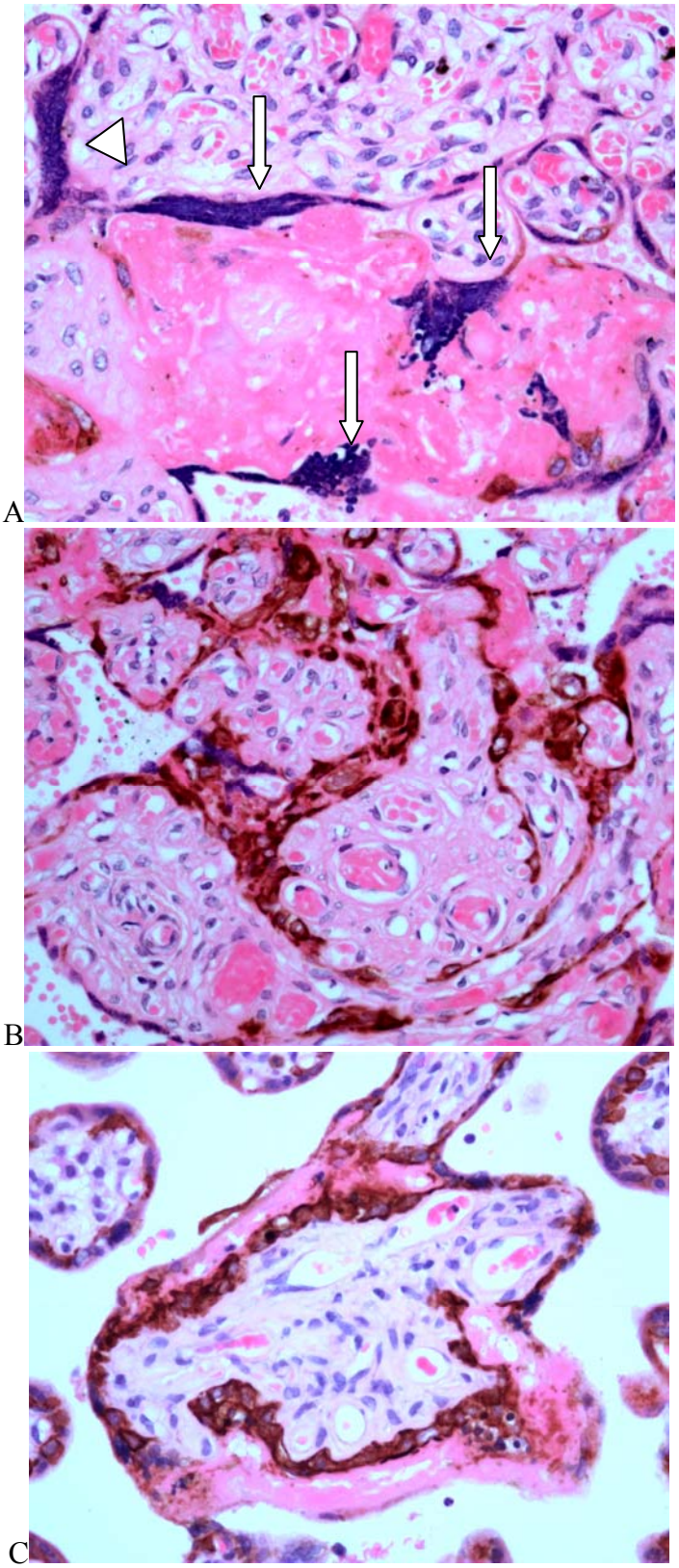

Figure 5-6 Syncytial morphology in SIDS-NBW
(A) Histologically villi are compact with large amounts of fibrin deposition (pink eosin staining) (long white arrows = apoptotic knots, arrowhead =non-apoptotic knot) (x200) (B, C). Multi-layered cytotrophoblast cells (cytokeratin 7, brown chromagen) overlying a thin or absent syncytium (x200).

6 General Discussion

Results presented in this thesis comprise the first stereological report integrating accurate immunohistochemical identification to study the morphological basis of villous cytotrophoblast turnover in placentas from pregnancies complicated by early- and late-onset pre-eclampsia and IUGR, and uniquely, in sudden infant death syndrome.

The significant findings from this study are that:

Severe pre-eclampsia presenting before 32 weeks gestation maintains total placental and villous volume, and the total volume and number of the villous trophoblast compartment. However, the relative volume of cytotrophoblast cells and syncytiotrophoblast nuclei is significantly reduced in structural villi, whereas the relative volume of syncytial knots and those displaying apoptotic nuclei is significantly increased in peripheral villi.

Pre-eclampsia presenting in late gestation is associated with a significant reduction in the total number of cytotrophoblast cells, the percentage of which undergoing proliferation is significantly increased for structural villi. There are an increased number of apoptotic syncytial knots in peripheral villi.

Severe early-onset IUGR with and without pre-eclampsia is associated with significant reductions in total placental and villous volume, and total trophoblast volume and number. The percentage of villous cytotrophoblast cells undergoing proliferation is significantly reduced, accompanied by a significant increase in the number of syncytial knots (PET-IUGR) and in those displaying apoptotic nuclei (IUGR, PET-IUGR).
Late-onset IUGR with and without pre-eclampsia is associated with significant reductions in total placental and villous volume, total trophoblast volume and number, and in the total number of proliferating cytotrophoblast cells. Significant increases were observed in the volume of placental villi (IUGR), in the percentage of proliferating cytotrophoblast cells in peripheral villi (PET-IUGR), along with the number of apoptotic syncytial knots (IUGR, PET-IUGR).

SIDS-NBW is associated with a significant increase in the volume density and total volume of terminal villi, the cytotrophoblast, syncytiotrophoblast, and in the total number and volume of syncytial knots (both non-apoptotic and apoptotic).

SIDS-LBW is associated with a significant decrease in total placental and intermediate villous volume, whereas the percentage of terminal villi was significantly increased. These are associated with a significant increase in the total volume of cytotrophoblast cells, the relative and total volume of syncytiotrophoblast, and in the total volume of apoptotic syncytial knots.

6.1 IUGR and the Villous Trophoblast

In humans, the major determinant of intrauterine fetal growth is the supply of oxygen and nutrients to the developing fetus. This in turn is dependent upon 1) the maternal and fetal nutritional status 2) the delivery of maternal and fetal blood to the placenta by adequate uteroplacental and fetoplacental circulations respectively 3) the size and morphology of the placenta, and 4) the morphology and integrity of the villous trophoblast compartment lining the chorionic villi (83). Fetal growth has the potential to be directly affected by abnormalities in any of these pathways.

The small placentas from severe early-onset IUGR pregnancies in this study display reduced fetoplacental blood flow as shown by abnormal umbilical artery Doppler, signifying increased resistance to blood flow due to defective formation of the fetal capillaries in the gas-exchanging villi (290). These fetuses are at high risk of intrauterine death or stillbirth due to chronic fetal hypoxia and acidosis, secondary to defective transplacental gas-exchange conferred by these malformed capillaries; four stillbirths and one intrauterine death were noted in IUGR pregnancies. Villi also displayed fetal thrombotic lesions, intervillous thrombosis, perivillous fibrin deposition and villous infarction, all of which can compromise maternal-fetal exchange, and are thought to be secondary to poor maternal perfusion of the placenta demonstrated by abnormal uterine artery Doppler, of which there is a strong correlation (140). The net result of reductions in uteroplacental and fetoplacental circulations (along with gross pathological changes) will severely compromise maternal-fetal exchange.

In addition to the dominant vascular pathology, the gas-exchanging villi in severe early-onset IUGR placentas display arrested villous trophoblast turnover, showing reduced villous cytotrophoblast proliferation, decreases in syncytial nuclei, as a consequence of impaired syncytial fusion, and increased numbers of apoptotic syncytial knots. Furthermore, in relation to its altered villous anatomy, these placentas demonstrate increased protein expression of the trophoblast transcription factor, GCM1.

The imbalance in the epithelial steady state between formation (decreased proliferation) and loss of trophoblast material (increased numbers of apoptotic knots) provides a plausible and sufficient explanation for reduced linear growth of the gas-exchanging

villi in severe early-onset IUGR pregnancies with and without pre-eclampsia, with AREDV in the umbilical arteries. Poor villous growth as a consequence of arrested trophoblast turnover, in conjunction with failed non-branching angiogenesis (113), is hypothesized to lead to increased intraplacental oxygen levels relative to the fetus, so-called post-placental fetal hypoxia (153) further perpetuating arrested trophoblast turnover. Furthermore, a focal impairment in syncytial fusion will lead to insufficient numbers of syncytial nuclei (which are the active carrier system in the placenta), likely contributing to the observed reduction in both placental and fetal levels of amino acids and ion transporters in IUGR pregnancies (51; 317; 347; 348), which may be one of the primary factors for growth restriction in utero independent of the reduced surface area for diffusional exchange.

Because the net loss of trophoblastic material was specific for mature intermediate and terminal villi only, this suggests arrest of mitosis at the onset of development of the gas-exchanging villi. A logical explanation follows that in IUGR placentas, there is a failure in differentiation from immature intermediate villi into their mature counterparts, likely involving defective signals from both the villous trophoblast and allantoic mesoderm. This is because in mice, differentiation of trophoblast chorionic cells and chorion morphogenesis (GCM1-mediated (181; 182)) is critically dependent upon signals from the allantois, implying that bi-directional interactions are needed for proper morphogenesis of the chorion involving both fetal endothelial cells and trophoblast; morphogenesis ceases to occur if the allantois fails to attach (182).

In humans, given that fetal vascular proliferation predominates over that of the villous trophoblast suggesting that angiogenesis drives growth of the peripheral villous tree (115), reduced endothelial proliferation of the fetal vasculature in IUGR can be speculated to impact on reduced villous cytotrophoblast proliferation. Interestingly, GCM1 has recently been shown *in vitro* to be involved in the positive regulation of PGF, which mediates non-branching angiogenesis in the third trimester. Since over-expression of GCM1 in trophoblast cell lines significantly increased PGF mRNA levels (349), increased GCM1 protein expression therefore correlates well with increased placental expression of PGF (stimulated by oxygen) over VEGF (113), which is thought to account for the poorly branched villous tree leading to intraplacental hyperoxia in severe early-onset IUGR with AREDV in the umbilical arteries (153).

Given that early placental growth and differentiation determines functional maturation of the placenta in late gestation, why it is that arrested villous trophoblast turnover is effective only in the third trimester, given that some cases display defective extravillous trophoblast differentiation (95; 123) in the first trimester? Premature differentiation of the villous cytotrophoblast provides a plausible explanation:

By definition, an IUGR fetus is one that has been subjected to a pathological failure to reach its predetermined growth potential in utero. Because placental insufficiency is often cited as the major cause in early gestation, one might expect this to be reflected in fetal: placental growth curves. Placental size (weight or volume) has been used as an indicator of placental development and a determinant of fetal growth; the fetal: placental weight ratio is therefore used as a gross measure of placental efficiency.

In normal pregnancy, placental weights correlate with fetal weights throughout gestation, signifying that growth, in terms of mass, is matched throughout gestation, despite the fact that their individual growth trajectories differ whereby placental growth follows an S-curve regression whilst fetal growth follows an exponential pattern with maximal fetal growth in the third trimester (350). In IUGR, placental and fetal weights would be expected to follow the same growth pattern during the first and second trimester of normal pregnancy, but due to arrested trophoblast turnover and failed non-branching angiogenesis, placental supply can no longer match fetal demand in the third trimester, and hence the fetus deviates from its normal growth pattern leading to IUGR.

One explanation is premature differentiation of the villous cytotrophoblast population. Here, if it assumed that the defect(s) in severe early-onset IUGR is intrinsic to the villous trophoblast during the first trimester, then premature differentiation of proliferating villous cytotrophoblast cells into syncytiotrophoblast during the first and second trimester (hypoxia-induced up-regulation of GCM1? (351)) would therefore prematurely deplete the pool of villous progenitor cells, such that sustained trophoblast turnover is impaired and subsequently the regenerative capacity of the villous cytotrophoblast essentially “burns out”, resulting in reduced linear growth of the gas-exchanging villi, and hence surface area for exchange, in the third trimester.

In this situation, the development of the placenta and fetus will not be compromised by impaired development of the uteroplacental circulation in the first and early second trimester (secondary to defective trophoblast invasion), because the nutritional demands of the fetus, in absolute terms, are small. Hence, if the villous trophoblast cannot sustain turnover in the third trimester due to premature differentiation when fetal demands for energy are highest, this may cause a severe derailment from its predetermined growth trajectory, even though this may have been lower to begin with i.e. an SGA versus AGA fetus that has fallen from its growth trajectory in the third trimester.

The concept of premature differentiation is reflected in the relationship between fetal weight and placental weight in IUGR pregnancies between 26 and 37 weeks gestation (Figure 6.1) (352). Cetin *et al* demonstrated that although overall placental and fetal weights are reduced in IUGR pregnancies compared to controls, there is a steeper relationship between lower placental weights and decreases in fetal weight, particularly in the most severe IUGR cases associated with abnormal umbilical artery Doppler (352). This implies that for the same decrease in placental weight, there is a greater decrease in fetal weight compared to controls, signifying that in fact placental growth, in terms of mass, is inefficient to match that of the fetal demand.

In this situation, the *steepness* of this relationship may also denote an accelerated rate of growth. For example, if the slope of the line in normal pregnancy represents a normal villous tree that is appropriate for gestational age e.g. 26 weeks of gestation (Figure 6.1), then for the IUGR placenta to have achieved the same villous maturity but on a steeper growth trajectory (Figure 6.1), then the rate of villous growth must be increased (i.e. premature differentiation), the degree of which is determined by the difference between the two slopes. Conversely, this then begs the question (assuming an intrinsic first trimester defect) as to whether villous growth has been accelerated in an attempt to maintain fetal growth.

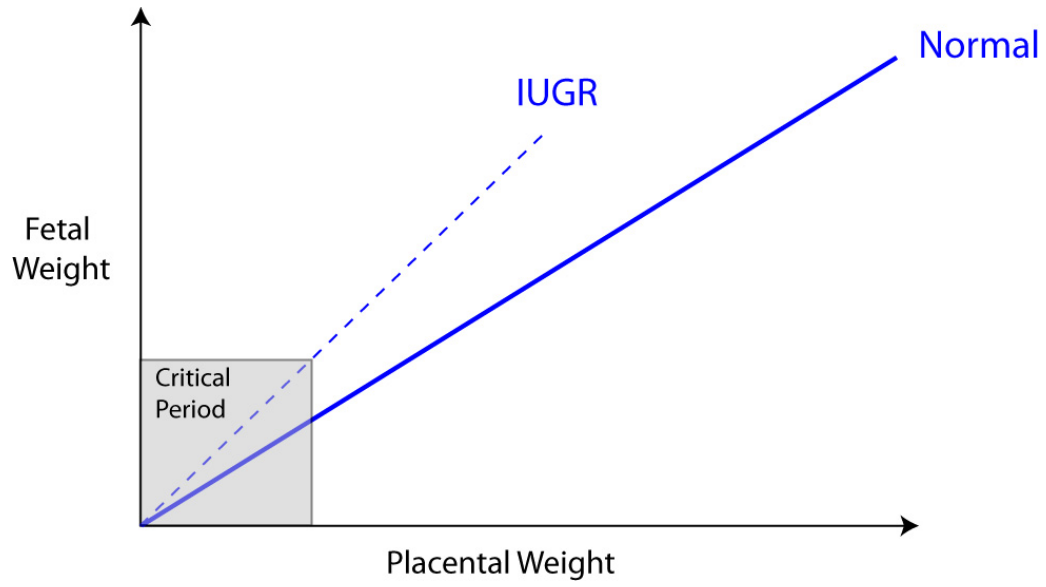

Figure 6-1 Premature trophoblast differentiation in IUGR

Schematic representation of fetal and placental weight growth curves between the first and third trimester of pregnancy. In normal pregnancy (thick blue line) fetal mass is matched to placental mass, indicating that supply and demand between the fetus and the placenta are met. In IUGR, (dashed blue line), fetal mass is matched to placental mass but the slope of the curve is higher. This indicates that for the same decrease in placental weight, there is a greater decrease in fetal weight compared to normal pregnancy, signifying that in fact placental growth, in terms of mass, is inefficient to match fetal demand.

However, overall there were no such changes in fetal: placental weight ratios in both early- and late-onset IUGR when compared to appropriate age-matched controls in this study (4.4 ± 0.3 versus 4.3 ± 0.7; 6.0 ± 0.3 versus 6.3 ± 0.6). Based on these criteria, this demonstrates that although placental and fetal weights are significantly reduced compared to controls, placental supply and fetal demand are met, in terms of mass, regardless of gestational age.

Premature differentiation is partly supported by placental pathologic findings showing that 3 out of the 5 severe early-onset IUGR cases display advanced villous maturity for gestational age (85), such that by 28 weeks of gestation these placentas display an increased presence of mature and terminal villi than is expected for gestational age. However, it cannot be excluded that this may simply be a consequence (or exacerbation) of their prematurity since fully mature villous trees are also observed in a vast number of placentas from spontaneous preterm deliveries (85).

A more accurate way to assess placental efficiency is through its ability to transfer oxygen to the fetus, which can be physiologically expressed as its diffusing capacity, known as the oxygen diffusive conductance (Dp) (353). This morphometric model represents a measure of the volume of gas transferred per minute per gas partial pressure (cm^3 min^{-1} $mmHg^{-1}$), which is estimated by measuring the resistance across the five basic compartments of the maternal-fetal interface (maternal erythrocytes, maternal plasma membrane, the villous trophoblast, fetal plasma and fetal erythrocytes), the reciprocal of which is conductance. This model estimates local structural changes in the villous membrane and how they may impact on overall placental function at the whole organ level.

The greatest resistance to the diffusion of oxygen is the villous trophoblast (353), which depends on surface area and thickness. Trophoblast thickness declines between 10 weeks and term in normal pregnancy due to the expansion in villous surface area and formation of vasculo-syncytial membranes in terminal villi (249). These structural changes are brought about so that placental supply and fetal demand are met in the third trimester when fetal demands for energy are highest, hence, total placental conductance increases commensurately with fetal mass between 10 weeks and term (354). However, when corrected for fetal weight gain, little change in specific Dp is observed over the same period (354), suggesting that there is a constancy between placental supply and fetal demand throughout gestation.

In turn, trophoblast thickness is determined by the spatiotemporal changes in the epithelial steady state, such that a greater recruitment of trophoblast over loss would increase thickness, and vice versa; by decreasing the thickness of the villous membrane however, conductance may be maintained (159). Therefore, it may be hypothesized that the harmonic mean thickness (morphometric measure of membrane thickness accounting for local thickness variation (354)) in severe early-onset IUGR and PET-IUGR placentas may be increased thereby reducing the diffusive capacity of the villous membrane, ultimately leading to IUGR. From another perspective, as soon as the maternal blood supply is unable to meet the demands of the fetus in the third trimester, the placenta may increase vascularisation and/or thin the villous membrane to maintain diffusive capacity, and where this fails, severe early-onset IUGR may result.

To date, there are no published studies investigating oxygen diffusive conductance in placentas from severe early-onset pregnancy pathologies. However, in-house data shows that severe early-onset IUGR placentas are not associated with alterations in villous membrane thickness; however they do display significant reductions in all partial conductances across the villous membrane leading to a reduction in total oxygen diffusive conductance. Accordingly, Macara *et al* noted an increased thickness of the basal lamina in severe early-onset IUGR placentas with abnormal umbilical artery Doppler, although this was not determined using stereological analysis (1).

It may be possible in future studies to determine whether the villous membrane is uniformly affected by estimating the thickness uniformity index (mean arithmetic thickness divided by mean harmonic thickness) (314); a value of 1.0 representing uniformity. Hence, this would be hypothesized to be reduced in severe early-onset IUGR (with and without pre-eclampsia) with AREDV in the umbilical arteries.

In comparison to early-onset disease, IUGR presenting in late gestation is typically associated with fetal growth asymmetry (brain sparing due to redistribution of cerebral blood flow (355)), and normal uterine and umbilical artery Dopplers. Increased capillary volume fraction (356) is thought to be a morphological adaptive response secondary to uteroplacental hypoxia due to failed spiral artery invasion in the first trimester, which in turn may account for the normal umbilical artery Doppler, provided there is no secondary pathology damaging the chorionic villi (i.e. villous infarcts, fetal thrombotic vasculopathy).

In the present study, a group of late-gestation IUGR cases were analyzed with a wide range in their gestational age at delivery, including 33 and 34 week placentas displaying AREDV in the umbilical arteries and two delivered at 37 weeks with normal umbilical artery Doppler. Despite this clinical variation, a significant increase in the relative volume of placental villi was observed, and in contrast to early-onset disease, they did not display morphological alterations in villous trophoblast turnover.

These placentas, similar to their early-onset phenotype, are compromised in terms of overall growth and surface area for exchange, yet in comparison, they continue to sustain fetal growth until late gestation. If it is accepted that late-onset IUGR also has its

origins in the first trimester due to uteroplacental insufficiency, then these placentas are in basic terms more 'efficient' in comparison to early-onset phenotypes, suggesting that the placenta can adapt its nutrient and gas exchange capacity to help meet fetal demands for growth, even when its own growth is compromised.

Animal studies show that when placental growth is compromised experimentally in late gestation (e.g. glucocorticoid administration, under- or over-nutrition, and restriction of maternal uterine blood flow), often more fetus is produced per gram of placenta, signifying an increase in placental efficiency to meet fetal demands (357). Coan *et al* elegantly highlighted the placentas ability to maintain a functional reserve capacity whereby the smallest placenta within a mice litter displayed significant morphological and functional adaptations to increase the active transport of amino acids per gram of placenta to maintain maximal fetal growth in late gestation despite the overall reduction in placental mass (357). The increase in relative volume of villous tissue in late-onset IUGR may therefore represent such an adaptive response in order to maintain overall surface area for transplacental exchange. In these cases, it is very likely that placental supply and fetal demand for diffusional exchange are met.

In an original study, Mayhew *et al* demonstrated an increase in arithmetic mean trophoblast thickness (overall membrane thickness) in IUGR at term which would likely impact on Dp (161), however in a more recent study the same author showed that in fact no such changes are present in IUGR pregnancies (presumably at term although gestational age was not stated) where both arithmetic and harmonic distances of the trophoblast remained similar to controls (163). Overall conductance was reduced by 33% compared to controls (although non-significantly owing to large intra-group variation), however when fetal weight was accounted for no significant changes in mass-specific conductance was observed for IUGR (163).

In a similar study, a shorter harmonic mean distance across the villous trophoblast was observed in SGA infants (thought to represent placental hypoxia due to maternal smoking) at term, which can be interpreted as an adaptive response so as to maintain conductance. However, in this instance, such an adaptive response was inefficient to maintain overall conductance which was significantly reduced, despite the fact that mass-specific conductance was maintained (159).

In this situation, it is therefore difficult to determine whether the slowing of the fetal growth trajectory is a positive adaptation to placental insufficiency or whether early fetal growth defines placental physiology by demand (i.e. undergone changes in their fetal programming). The latter is supported by the suggestion that in IUGR pregnancies, the placenta may register a lack of an appropriate increase in maternal blood flow (i.e. failed spiral artery conversion) and/or nutrition, and as a consequence, may down-regulate essential placental transporter systems in order to decrease growth in late gestation (348).

Although they differ in trophoblast morphology, the question remains however as to whether the divergence between the early- and late-onset pathologies is the result of different developmental pathways or mechanisms.

The turnover of villous trophoblast in the combined disease (PET-IUGR) in early-gestation resembles that of pure early-onset IUGR showing reduced villous cytotrophoblast proliferation, impaired syncytial fusion and increased apoptotic syncytial knotting, which are plausible explanations for reduced linear growth of the peripheral villous tree as previously described. An interesting observation to arise from this study is that the combined disease did not display the most severe alterations in trophoblast morphology, which may be a consequence of the fact that pre-eclampsia in early gestation had no significant effects on trophoblast morphology. Hence, the changes seen in the combined group may relate more to IUGR than pre-eclampsia.

6.2 Pre-eclampsia and the Villous Trophoblast

Several studies have demonstrated that pre-eclampsia presenting in early gestation typically resembles IUGR in terms of villous and trophoblast morphology and that these changes are more severe when the two diseases co-exist (152). The variable clinical disease classifications in these studies has, however, made it difficult to identify individual contributions (152; 156). By carefully selecting a subgroup of early-onset pre-eclamptic pregnancies displaying normal fetal birthweights and normal umbilical artery Dopplers, the present study shows that early-onset pre-eclampsia without any clinical signs of fetal growth restriction has no significant effect on villous or trophoblast morphology. However, where there are trends towards changes in these parameters (i.e. increased rate of turnover), they oppose those for IUGR indicating divergent trophoblast pathologies.

Similar to IUGR, uteroplacental insufficiency is thought to be the 'root cause' of pre-eclampsia regardless of gestational age, and that early- and late-onset disease may represent divergent end points of different developmental pathways reflected in the different fetal phenotypes. Either way, increased villous cytotrophoblast proliferation and syncytial fusion is hypothesized to lead to dysregulated syncytial shedding of aponecrotic syncytial nuclei and the excess release of anti-angiogenic factors into IVS constituting the maternal syndrome of pre-eclampsia (3).

In the present study, whilst there are trends towards such changes (signifying an imbalance between proliferation and differentiation), losses are matched by recruitment because the overall surfaces and volumes of villi are maintained, and hence in comparison to IUGR, they maintain overall diffusing capacity.

Both severe early-onset and late-onset pre-eclamptic placentas display normal placental and fetal weights (between 10-50th centile for gestational age) in comparison to gestational aged-matched controls, indicating that placental supply and fetal demand are met throughout gestation. Because the placental villi are normally grown in terms of overall volume, one would not expect to see any detrimental effects on the villous trophoblast (i.e. thickening of villous membrane) which would perturb the diffusional exchange of oxygen to the fetus with the potential to cause growth restriction in utero.

Given the previous analyses, early-onset pre-eclamptic placentas would be expected to maintain overall conductance, since fetal birthweights are with the normal range for gestational age. Interestingly however, in-house data shows that early-onset pre-eclamptic placentas maintain villous membrane thickness, but not diffusive capacity. This is reflected by the fact that total Dp was significantly reduced from a total Dp of 4.14 cm^3 min^{-1} $mmHg^{-1}$ in gestational-age-matched controls to 2.35 cm^3 min^{-1} $mmHg^{-1}$ in early-onset PET, what's more, this reduction persisted even when corrected for fetal birthweight in which specific Dp declined from 2.39 cm^3 min^{-1} $mmHg^{-1}$ in gestational-age-matched controls to 1.85 cm^3 min^{-1} $mmHg^{-1}$ in early-onset PET. However, fetal birthweights in this cohort were significantly reduced (i.e. SGA), in comparison to controls and severe early-onset IUGR pregnancies, making the contribution of pre-eclampsia alone difficult to interpret. This suggests that in this particular group of early-onset pre-eclamptic placentas, the dominant pathology is vascular in nature. However, that is not to say that the placenta cannot respond to stress in utero by increasing its diffusion capacity, but that its capability to do so is limited.

The latter is also reflected by a significant reduction in the fetal: placental weight ratio, in severe early-onset pre-eclamptic placentas, signifying that for every gram of placenta, there is less gram of fetus. Hence, the placenta is unable to match fetal demand for oxygen in the third trimester of pregnancy, but must display some functional reserve capacity since these infants were not 'clinically' growth restricted. Conversely, SGA infants have been shown to have a reduced placental to fetal weight ratio compared to normal infants of the same birthweight (350), which based on the above considerations, signifies that the placenta in terms of mass is inefficient at meeting fetal demands. This seems confounding since these fetuses are, by definition, constitutionally small in comparison to their growth restricted counterparts.

A novel finding from this study is that placentas from late-onset pre-eclampsia display significant reductions in the total number of villous cytotrophoblast cells. These placentas are typically regarded as normal in terms of villous and vascular morphology (102; 152; 156; 161; 163). In contrast, this study shows that whilst overall villous growth is maintained, the turnover of villous trophoblast may be altered in pre-eclampsia in late gestation.

A reduction in the total complement of villous cytotrophoblast cells indicates an altered balance in villous trophoblast turnover. This may represent a loss of progenitor cells, similar to that which is hypothesized to IUGR, or alternatively, increased syncytial fusion. Because the total number of syncytiotrophoblast was maintained, fusion must therefore be increased. Significantly, the percentage of proliferating cytotrophoblast cells was increased for stem and immature intermediate villi. Such changes may therefore contribute to the maternal syndrome of pre-eclampsia.

Pre-eclampsia at term represents a form of uteroplacental hypoxia. In similar situations such as pregnancies at high altitude and pre-existing maternal diabetes, placentas display increased capillary volume fraction (314) and branching(154), increased endothelial proliferation and both the number and proliferation of villous cytotrophoblast is increased (340). Kingdom and Kaufmann (1997) propose that the net result of these structural changes serve to thin the villous membrane thereby maintaining oxygen transfer (153; 358). Although endothelial proliferation may account for the formation of vasculo-syncytial membranes, increased numbers of villous cytotrophoblast cells may increase local membrane thickness.

The reduction in the total number of cytotrophoblast cells may therefore represent placental adaptation to the maternal environment in order to maintain diffusional exchange. This is supported by in-house data showing that late-onset pre-eclamptic placentas display a significant reduction in the harmonic mean thickness of the villous membrane and therefore maintained total and mass-specific oxygen diffusive conductance. Similarly, Mayhew *et al* demonstrated that pre-eclampsia in late gestation has no detrimental effects on villous membrane thickness or its variability; subsequently these placentas maintained their total and mass-specific oxygen diffusive conductance (163).

Furthermore, whilst the placental phenotype of late-onset pre-eclampsia with IUGR was similar to isolated IUGR, the trophoblast phenotype resembled that of pre-eclampsia with an increase in the percentage of proliferating cytotrophoblast cells. Hence, whilst rates of differentiation and loss seem to be higher in pre-eclampsia, rates of proliferation are higher in pre-eclampsia than IUGR, thereby maintaining appropriate ‘growth

pattern' of the villous trees, but which may have started with less developmental potential (i.e. less progenitor cells).

This shows that placentas from early- and late-onset pre-eclamptic pregnancies differ in their trophoblast morphology and in their ability to maintain overall diffusing capacity, whereby late-onset placentas displays functional reserve capacity in the face of uteroplacental insufficiency.

Is it possible that such a divergence reflects differences in the severity and duration of the initial insult in the first trimester?

The suggestion that the response of the villous tree in the second and third trimester is linked to malinvasion of the spiral arteries in the first trimester is supported by the observation that abnormal uterine artery Doppler (UTAD) (representing a failure in the physiological conversion of the maternal spiral arteries) is significantly correlated with altered cytotrophoblast turnover in severe early-onset IUGR pregnancies with co-existing pre-eclampsia (combined disease) (no correlation with the syncytium).

This showed that in those cases with abnormal UTAD the numerical density of villous cytotrophoblast cells was significantly reduced in comparison to those cases displaying normal UTAD, and that this was primarily attributed to a 30% decline for stem and intermediate villi; consequently the percentage of proliferating cytotrophoblast cells increased, although not significantly. Interestingly these changes resembled pure early-onset pre-eclampsia, and not IUGR. This shows that alterations in villous trophoblast occur early in gestation before they are clinically evident in late gestation supporting the association between abnormal UTAD and placental pathologic condition (140).

Whilst this is not a primary causal factor for developing pre-eclampsia in the combined disease since those women with normal UTAD also developed pre-eclampsia, it shows that the severity of the abnormal uteroplacental blood flow is directly related to the severity of alterations in cytotrophoblast morphology, but not determined by it.

Interestingly, women displaying abnormal UTAD had significantly lower blood pressures than those with normal UTAD (159 ± 4 /102 ± 1.5 versus 177 ± 4 / 107 ± 1.5;

systolic p=0.020, diastolic p=0.035) which may be a maternal consequence of rheological changes in the uteroplacental circulation, i.e. high pressure/velocity/rate of maternal blood flow entering the spiral arteries, which as shown by Burton *et al* is primarily determined by their terminal dilation (128). Despite there being a good correlation between abnormal UTAD and malinvasion of the maternal spiral arteries, women with normal UTAD have been shown to exhibit failed physiological conversion on biopsy (145).

Whether such correlations exist for isolated IUGR or pre-eclampsia could not be determined due to the lack of clinical information and small study groups. Nonetheless, these data suggest that extrinsic as well as intrinsic defects in the villous trophoblast are critical for pregnancy outcome.

6.3 SIDS and the Villous Trophoblast

SIDS placentas are thought to represent a form of pre-placental hypoxia (due to cigarette exposure), similar to pregnancy at high altitude (hypobaric hypoxia) which display increased capillary volume fraction and increased capillary branching (154; 358), (although whether or not the capillaries become dilated is still debated), representing typical cases of placental adaptation to pre-placental hypoxia so as to maintain diffusional exchange to the fetus (153). However, the latter group of placentas and those associated with maternal smoking also display increased volumes and density of villous cytotrophoblast cells and syncytial knotting likely increasing villous trophoblast thickness, which would be expected to impact on diffusional exchange.

The association of increased trophoblast volumes in both SIDS-LBW and SIDS-NBW seems confusing, since based on the considerations above, would be expected to compromise diffusional exchange to the fetus resulting in a low birthweight infant. In similar situations of pre-placental hypoxia, infant birthweights are reduced despite physiological compensatory adjustments aimed at increasing diffusional exchange such as increased intervillous space, reduced trophoblast thickness (346), and increased capillary volume fraction of terminal villi (154). Thus, increased relative volumes of syncytiotrophoblast and cytotrophoblast are unlikely to represent compensatory mechanisms, and importantly, these structural alterations are not necessarily detrimental to placental function i.e. leading to a low birthweight infant. The structural alterations in

the villous trophoblast however were not associated with changes in either the total or specific oxygen diffusive conductance in both SIDS-NBW and SIDS-LBW placentas (82), indicating that in both situations, placental supply and fetal demand for oxygen are maintained at term. Other mechanisms must therefore be initiated by SIDS-NBW placentas thus maintaining adequate fetal growth in utero.

One plausible explanation is that SIDS-NBW have compensated for increased trophoblast volume by increasing the volume of terminal villi (45% increase), and hence enlarging the total surface area available for diffusional exchange to the fetus. However, this raises the "chicken-and-egg" question as to whether these infants have a normal birthweight because of increased volumes of terminal villi, or alternatively why would the normal birthweight infant require increased volumes of terminal villi. Although SIDS-LBW placentas displayed an increase in the proportion of terminal villi compared to term controls, it was insufficient to compensate for the small placental phenotype perhaps by failure to elicit mechanistic and functional modifications which SIDS-NBW subsequently display. This gives some credence to the interpretation that SIDS-NBW have initiated a compensatory reserve which SIDS-LBW lack.

In the context of the triple risk hypothesis, SIDS occurs when a vulnerable infant is exposed to external risk factors during a critical period of physiological postnatal development (70; 71). However, there is now a growing concept that SIDS represents a developmental disorder which originates during fetal development in utero placing the vulnerable infant at risk postnatally.

Fetal development is an active process, and hence normal fetal development requires continuing normal activity. During fetal development, there are critical periods of vulnerability to suboptimal conditions and these vulnerable periods occur at different developmental epochs for different tissues i.e. cells dividing rapidly are at greatest risk (hyperplastic cell growth during the second trimester), and each phase of development provides the required conditions for subsequent development. Because SIDS infants display specific abnormalities in organs critical for survival *ex utero* which can only have occurred in the second trimester during fetal organogenesis in utero, it suggests that the placental adaptations observed in SIDS-NBW (increased terminal villi) compensate for detrimental insult(s) occurring in maternal-placental unit in early

gestation. Hence, whilst overall diffusional exchange is maintained, these changes are insufficient to compensate for compromised organ development in utero, since these vulnerable infants have subsequently succumbed to SIDS.

The above explanation is a classic example of fetal programming in utero, such that programming has permanent effects that alter responses in adult life. If it is assumed, as the data suggests above, that SIDS infants develop in an unfavourable intrauterine environment, then the developing fetus may also attempt to compensate for deficiencies, (i.e. insults in the maternal-placental unit). Following compensation, birthweight may be normal or only slightly decreased. However, postnatally the compensatory effort carries a price such that the infant attempts made after birth to severe the consequences of programming may have their own unwanted consequences. When postnatal conditions prove to be other than those for which the fetus is prepared (i.e. external stressors), problems may arise.

7 Conclusions

The principal conclusions from the present study are that:

- Severe early-onset IUGR with AREDV in the umbilical arteries is associated with arrested trophoblast turnover due to a reduced regenerative capacity of the villous cytotrophoblast population likely contributing to maldevelopment of the peripheral villous in the third trimester of pregnancy.

- In contrast, placentas from severe early-onset pre-eclampsia without any clinical signs of IUGR do not share any similarities in the villous trophoblast with severe early-onset IUGR and shows preliminary morphological evidence for a divergent trophoblast pathway showing an increased rate of villous trophoblast turnover, which may contribute to the maternal endothelial syndrome.

- Late-onset pre-eclamptic placentas display structural alterations which likely represent placental adaptation to the maternal environment which early-onset placentas lack

- The data suggests that the severe early-onset pathologies are associated with defective villous trophoblast differentiation, whereby the relative proportions of proliferating and differentiating cytotrophoblast cells is altered, indicating intrinsic defects in the villous cytotrophoblast lineage which likely originate during early placental development.

- Because early- and late-onset IUGR do not share any similarities in trophoblast morphology, this suggests different disease etiologies for early- and late-onset IUGR, whereas this is likely to be the same for pre-eclampsia since morphological alterations are very similar.

- SIDS infants may represent postnatal consequences of IUGR, or any detrimental hypoxic insult, since they display evidence of placental adaptation by increasing their volumes of gas-exchanging villi.

7.1 Future Goals

With regard to the newly developed stereological-immunohistochemistry methods presented in this thesis, it should now be possible to quantify other areas of villous cytotrophoblast biology in order to understand the morphological basis of these and other placentally-mediated diseases.

These include:

- Determine the accurate localisation and quantification of GCM1 protein and mRNA and in the villous cytotrophoblast and syncytiotrophoblast population.

- Identification of villous cytotrophoblast progenitor cell phenotypes using murine genes that are thought to be expressed in an analogous manner in humans (e.g. Cdx2, Fgfr2).

- Investigate further the role of villous cytotrophoblast apoptosis in both pre-eclampsia and IUGR.

- Find potential immunohistochemical markers of syncytial shedding to link alterations in villous cytotrophoblast biology with pathophysiology of PET.

- Revisit the role of oxygen (HIF proteins) and placental development in PET, IUGR and SIDS.

8 References

1. Macara, L., Kingdom, J. C., Kaufmann, P., Kohnen, G., Hair, J., More, I. A., Lyall, F., & Greer, I. A. 1996, "Structural analysis of placental terminal villi from growth-restricted pregnancies with abnormal umbilical artery Doppler waveforms", *Placenta.17(1):37-48*.

2. Krebs, C., Macara, L. M., Leiser, R., Bowman, A. W., Greer, I. A., & Kingdom, J. C. 1996, "Intrauterine growth restriction with absent end-diastolic flow velocity in the umbilical artery is associated with maldevelopment of the placental terminal villous tree", *American Journal of Obstetrics & Gynecology.175(6):1534-42*.

3. Huppertz B 2006, "Placental Villous Trophoblast: the Altered Balance between Proliferation and Apoptosis Triggers Pre-eclampsia", *J Reprod Endo*, vol. 3 (2), pp. 103-8.

4. Myers J & Brockelsby J. *The epidemiology of Pre-eclampsia*. Baker PN and Kingdom JCP. Pre-eclampsia. 25-42. 2004. USA, The Parthenon Publishing Group.

5. Baker PN & Kingdom JCP 2004, *Pre-eclampsia. Current Perspectives on Managment* The Parthenon Publishing Group, USA.

6. Duley, L. 2009, "The global impact of pre-eclampsia and eclampsia", *Semin.Perinatol.*, vol. 33, no. 3, pp. 130-137.

7. Chun D, Braga C, Chow C, & Lok L 1964, "Clincal observations on some aspects of hydatidiform moles", *J Obstet Gynaecol Br Commonw*, vol. 71, pp. 180-184.

8. Piering, W. F. 1993, "Preeclampsia related to a functioning extrauterine placenta: report of a case and 25-year follow-up", *American journal of kidney diseases*, vol. 21, no. 3, pp. 310-313.

9. American College of Obstetricians and Gynecologists. Diagnosis and management of preeclampsia and eclampsia. Practice Bulletin no.33. Obstetrics Gynecology 99, 159-67. 2002.

10. Hayman R and Myers J 2004, "Definition and Classification," in *Preeclampsia Current Perspectives on Management*, Baker PN & Kingdom JCP, eds., pp. 11-13.

11. von Dadelszen, P., Magee, L. A., & Roberts, J. M. 2003, "Subclassification of preeclampsia.", *Hypertension in Pregnancy.22(2):143-8*.

12. Odegard, R. A., Vatten, L. J., Nilsen, S. T., Salvesen, K. A., & Austgulen, R. 2000, "Preeclampsia and fetal growth", *Obstet.Gynecol.*, vol. 96, no. 6, pp. 950-955.

13. Xiong, X., Demianczuk, N. N., Buekens, P., & Saunders, L. D. 2000, "Association of preeclampsia with high birth weight for age", *Am.J.Obstet.Gynecol.*, vol. 183, no. 1, pp. 148-155.

14. von Dadelszen, P., Magee, L. A., Lee, S. K., Stewart, S. D., Simone, C., Koren, G., Walley, K. R., & Russell, J. A. 2002, "Activated protein C in normal human pregnancy and pregnancies complicated by severe preeclampsia: a therapeutic opportunity?", *Critical Care Medicine.30(8):1883-92*.

15. Huppertz, B. 2008, "Placental origins of preeclampsia: challenging the current hypothesis.", *Hypertension.51(4):970-5*.

16. Paruk, F. & Moodley, J. 2000, "Maternal and neonatal outcome in early- and late-onset pre-eclampsia.", *Seminars in Neonatology.5(3):197-207*.

17. Redman CW 1991, "Pre-eclampsia and the placenta", *Placenta*, vol. 12, no. 4, pp. 301-308.

18. Ilekis, J. V., Reddy, U. M., & Roberts, J. M. 2007, "Review Article: Preeclampsia A Pressing Problem: An Executive Summary of a National Institute of Child Health and Human Development Workshop", *Reproductive Sciences*, vol. 14, no. 6, pp. 508-523.

19. Benyo DF 2001, "Expression of inflammatory cytokines in placentas from women with pre-eclampsia", *Journal of Clinical Endocrinology Metabolism*, vol. 86, p. -2505.

20. Redman CW, Sacks GP, & Sargent IL 2000, "Preeclampsia: an excessive maternal inflammatory response to pregnancy.", *Am J Obstet Gynecol*, vol. 180, pp. 499-506.

21. Vince, G. S., Starkey, P. M., Austgulen, R., Kwiatkowski, D., & Redman, C. W. 1995, "Interleukin-6, tumour necrosis factor and soluble tumour necrosis factor receptors in women with pre-eclampsia.", *British Journal of Obstetrics & Gynaecology.102(1):20-5*.

22. Maynard SE, Min JY, Merchan J, Lim KH, Li J, Mondal S, Libermann TA, Morgan JP, Sellke FW, Stillman IE, Epstein FH, Sukhatme VP, & Karumanchi SA 2003, "Excess placental soluble fms-like tyrosine kinase 1 (sFlt1) may contribute to endothelial dysfunction, hypertension and proteinuria in pre-eclampsia", *J Clin Invest*, vol. 111, pp. 649-658.

23. Goswami, D., Tannetta, D. S., Magee, L. A., Fuchisawa, A., Redman, C. W., Sargent, I. L., & von Dadelszen, P. 2006, "Excess syncytiotrophoblast microparticle shedding is a feature of early-onset pre-eclampsia, but not normotensive intrauterine growth restriction", *Placenta.27(1):56-61*.

24. LaMarca, B. D., Gilbert, J., & Granger, J. P. 2008, "Recent Progress Toward the Understanding of the Pathophysiology of Hypertension During Preeclampsia", *Hypertension*, vol. 51, no. 4, pp. 982-988.

25. Redman, C. W. & Sargent, I. L. 2000, "Placental debris, oxidative stress and pre-eclampsia.", *Placenta.21(7):597-602*.

26. Redman, C. W. G. & Sargent, I. L. 2007, "Microparticles and immunomodulation in pregnancy and pre-eclampsia", *Journal of Reproductive Immunology*, vol. 76, no. 1-2, pp. 61-67.

27. Cockell, A. P., Learmont, J. G., Smarason, A. K., Redman, C. W., Sargent, I. L., & Poston, L. 1997, "Human placental syncytiotrophoblast microvillous membranes impair maternal vascular endothelial function", *British Journal of Obstetrics & Gynaecology.104(2):235-40*.

28. Levine, R. J., Maynard, S. E., Qian, C., Lim, K. H., England, L. J., Yu, K. F., Schisterman, E. F., Thadhani, R., Sachs, B. P., Epstein, F. H., Sibai, B. M., Sukhatme, V. P., & Karumanchi, S. A. 2004, "Circulating Angiogenic Factors and the Risk of Preeclampsia", *The New England Journal of Medicine*, vol. 350, no. 7, pp. 672-683.

29. Lam, C., Lim, K. H., & Karumanchi, S. A. 2005, "Circulating Angiogenic Factors in the Pathogenesis and Prediction of Preeclampsia", *Hypertension*, vol. 46, no. 5, pp. 1077-1085.

30. Tidwell, S. C., Ho, H. N., Chiu, W. H., Torry, R. J., & Torry, D. S. 2001, "Low maternal serum levels of placenta growth factor as an antecedent of clinical preeclampsia", *American Journal of Obstetrics and Gynecology*, vol. 184, no. 6, pp. 1267-1272.

31. Thadhani, R., Mutter, W. P., Wolf, M., Levine, R. J., Taylor, R. N., Sukhatme, V. P., Ecker, J., & Karumanchi, S. A. 2004, "First Trimester Placental Growth Factor and Soluble Fms-Like Tyrosine Kinase 1 and Risk for Preeclampsia", *Journal of Clinical Endocrinology Metabolism*, vol. 89, no. 2, pp. 770-775.

32. Gilbert, J. S., Gilbert, S. A. B., Arany, M., & Granger, J. P. 2009, "Hypertension Produced by Placental Ischemia in Pregnant Rats Is Associated With Increased Soluble Endoglin Expression", *Hypertension*, vol. 53, no. 2, pp. 399-403.

33. Levine, R. J., Lam, C., Qian, C., Yu, K. F., Maynard, S. E., Sachs, B. P., Sibai, B. M., Epstein, F. H., Romero, R., Thadhani, R., Karumanchi, S. A., & the CPEP Study Group 2006, "Soluble

Endoglin and Other Circulating Antiangiogenic Factors in Preeclampsia", *The New England Journal of Medicine*, vol. 355, no. 10, pp. 992-1005.

34. Burger, O., Pick, E., Zwickel, J., Klayman, M., Meiri, H., Slotky, R., Mandel, S., Rabinovitch, L., Paltieli, Y., Admon, A., & Gonen, R. 2004, "Placental protein 13 (PP-13): effects on cultured trophoblasts, and its detection in human body fluids in normal and pathological pregnancies", *Placenta*, vol. 25, no. 7, pp. 608-622.

35. Cetin, I., Cozzi, V., Pasqualini, F., Nebuloni, M., Garlanda, C., Vago, L., Pardi, G., & Mantovani, A. 2006, "Elevated maternal levels of the long pentraxin 3 (PTX3) in preeclampsia and intrauterine growth restriction", *American Journal of Obstetrics and Gynecology*, vol. 194, no. 5, pp. 1347-1353.

36. Spencer, K., Cowans, N., Chefetz, I., Meiri, H., & Tal, J. 2005, "Maternal serum PP13 and PAPP-A in first trimester, and doppler in second trimester, as markers of early pre-eclampsia", *American Journal of Obstetrics and Gynecology*, vol. 193, no. 6, Supplement 1, p. S78.

37. Arias, F. 1997, "Placental histology and clinical characteristics of patients with preterm premature rupture of membranes", *Obstetrics and gynecology*, vol. 89, p. 265.

38. Nevo, O., Many, A., Xu, J., Kingdom, J., Piccoli, E., Zamudio, S., Post, M., Bocking, A., Todros, T., & Caniggia, I. 2008, "Placental Expression of Soluble fms-Like Tyrosine Kinase 1 is Increased in Singletons and Twin Pregnancies with Intrauterine Growth Restriction", *Journal of Clinical Endocrinology Metabolism*, vol. 93, no. 1, pp. 285-292.

39. Roberts, J. M. & Hubel, C. A. 2009, "The Two Stage Model of Preeclampsia: Variations on the Theme", *Placenta*, vol. 30, no. Supplement 1, pp. 32-37.

40. Kingdom J & Baker P 2000, *Intrauterine Growth Restriction. Aetiology and Management* Springer-Verlag, UK.

41. Wollman H 1998, "Intrauterine Growth Restriction: Definition and Etiology", *Hormone Research*, vol. 49, no. (suppl 2), pp. 1-6.

42. Thureen, P. J., Anderson, M. S., & Hay, W. W., Jr. 2001, "The Small-for-Gestational Age Infant", *NeoReviews*, vol. 2, no. 6, p. e139-e149.

43. Cetin, I., Foidart, J. M., Miozzo, M., Raun, T., Jansson, T., Tsatsaris, V., Reik, W., Cross, J., Hauguel-de-Mouzon, S., Illsley, N., Kingdom, J., & Huppertz, B. 2004, "Fetal growth restriction: a workshop report", *Placenta.25(8-9):753-7,* p. -Oct.

44. Mandruzzato G, Antsaklis A, Botet F, Chervenak FA, Figueras F, Grunebaum A, Puerto B, Skupski D, & Stanojevic M 2008, "Intrauterine Growth Restriction (IUGR)* Recommendations and guidelines for perinatal practice", *J Perinat Med*, vol. 36, pp. 277-281.

45. Barker DJP. Fetal Growth Restriction: a Workshop Report. 95, 115-128. 1998. Clin Sci.

46. Barker DJP 1994, *Mothers, Babies, and Disease in Later Life*, 1 edn, London.

47. Cetin, I. & Alvino, G. 2009, "Intrauterine Growth Restriction: Implications for Placental Metabolism and Transport. A Review", *Placenta*, vol. 30, no. Supplement 1, pp. 77-82.

48. Gardosi, J., Chang, A., Kalyan, B., Sahota, D., & Symonds, E. M. 1992, "Customised antenatal growth charts", *The Lancet*, vol. 339, no. 8788, pp. 283-287.

49. Pollack P & Divon, M. Y. 1992, "Intrauterine Growth Retardation: Definition, Classification, and Etiology", *Clinical Obstetrics and Gynecology*, vol. 35, no. 1.

50. Hindmarsh, P. C., Geary, M. P., Rodeck, C. H., Kingdom, J. C., & Cole, T. J. 2002, "Intrauterine growth and its relationship to size and shape at birth", *Pediatric Research.52(2):263-8.*

51. Sibley CP, Turner MA, Cetin I, Ayuk P, Richard Boyd CA, & et al. Placental Phenotypes of Intrauterine Growth. Pediatric Research 58[5], 827-832. 2005.

52. Li, D. K. & Wi, S. 1999, "Maternal Placental Abnormality and the Risk of Sudden Infant Death Syndrome", *American Journal of Epidemiology*, vol. 149, no. 7, pp. 608-611.

53. Li, D. K. 2000, "Maternal pre-eclampsia/eclampsia and the risk of sudden infant death syndrome in offspring", *Paediatric and perinatal epidemiology*, vol. 14, no. 2, p. 141.

54. Hunt, C. E. & Hauck, F. R. 2006, "Sudden infant death syndrome", *Canadian Medical Association Journal*, vol. 174, no. 13, pp. 1861-1869.

55. Bass M 1990, "Intrauterine growth restriction and the risk of sudden infant death syndrome (SIDS)", *Am J Epidemiology*, vol. 132, no. (2), pp. 391-392.

56. Dwyer, T. & Ponsonby, A. L. 1996, "The Decline of SIDS: A Success Story for Epidemiology", *Epidemiology*, vol. 7, no. 3, pp. 323-325.

57. Hauck FR 2004, "Changing Epidemiology. In: Byard RW, Krous HF, editors. *Sudden infant death syndrome. Problems, progress and possibilities.*," Arnhold, London (UK): pp. p.31-57.

58. Malloy, M. H. & MacDorman, M. 2005, "Changes in the classification of sudden unexpected infant deaths: United States, 1992-2001.", *Pediatrics.115(5):1247-53*.

59. Mathews, T. J., Menacker, F., MacDorman, M. F., & Centers for Disease Control and Prevention, N. C. f. H. S. 2004, "Infant mortality statistics from the 2002 period: linked birth/infant death data set", *National Vital Statistics Reports.53(10):1-29*.

60. Willinger, M., James, L. S., & Catz, C. 1991, "Defining the Sudden Infant Death Syndrome (Sids): Deliberations of an Expert Panel Convened by the National Institute of Child Health and Human Development", *Fetal and Pediatric Pathology*, vol. 11, no. 5, pp. 677-684.

61. Leach, C. E. A., Blair, P. S., Fleming, P. J., Smith, I. J., Platt, M. W., Berry, P. J., FRCP, B. C. H., Golding, J., & the CESDI SUDI Research Group 1999, "Epidemiology of SIDS and Explained Sudden Infant Deaths", *Pediatrics*, vol. 104, no. 4, p. e43.

62. Poets, C. F. & Southall, D. P. 1993, "Prone Sleeping Position and Sudden Infant Death", *The New England Journal of Medicine*, vol. 329, no. 6, pp. 425-426.

63. Blackwell CC & Weir DM 1999, "The role of infection in sudden infant death syndrome", *FEMS Immunology & Medical Microbiology*, vol. 25, no. (1-2), pp. 1-6.

64. Prandota J 2004, "Possible Pathomechanisms of Sudden Infatn Death Syndrome. Key Role of Chronic Hypoxia, Infection/Inflammation States, Cytokine Irregularities, and Metabolic Trauma n Genetically Predisposed Infants", *American Journal of Therapeutics*, vol. 11, pp. 517-546.

65. Blackwell, C. C., Moscovis, S. M., Gordon, A. E., Al Madani, O. M., Hall, S. T., Gleeson, M., Scott, R. J., Roberts-Thomson, J., Weir, D. M., & Busuttil, A. 2004, "Ethnicity, infection and sudden infant death syndrome", *FEMS Immunology and Medical Microbiology*, vol. 42, no. 1, pp. 53-65.

66. Roberts SC 1987, "Vaccination and cot deaths in perspective", *Arch Dis Child*, vol. 62, pp. 754-759.

67. Summers, A. M., Summers, C. W., Drucker, D. B., Hajeer, A. H., Barson, A., & Hutchinson, I. V. 2000, "Association of IL-10 genotype with sudden infant death syndrome", *Human Immunology*, vol. 61, no. 12, pp. 1270-1273.

68. Blackwell, C. C., Moscovis, S. M., Gordon, A. E., Al Madani, O. M., Hall, S. T., Gleeson, M., Scott, R. J., Roberts-Thomson, J., Weir, D. M., & Busuttil, A. 2005, "Cytokine responses and

sudden infant death syndrome: genetic, developmental, and environmental risk factors", *Journal of Leukocyte Biology*, vol. 78, no. 6, pp. 1242-1254.

69. Moscovis, S. M., Gordon, A. E., Al Madani, O. M., Gleeson, M., Scott, R. J., Roberts-Thomson, J., Hall, S. T., Weir, D. M., Busuttil, A., & Blackwell, C. C. 2006, "IL6 G-174C Associated With Sudden Infant Death Syndrome in a Caucasian Australian Cohort", *Human Immunology*, vol. 67, no. 10, pp. 819-825.

70. Filiano, J. J. & Kinney, H. C. 1994, "A perspective on neuropathologic findings in victims of the sudden infant death syndrome: the triple-risk model", *Biology of the Neonate.65(3-4):194-7*.

71. Guntheroth, W. G. & Spiers, P. S. 2002, "The Triple Risk Hypotheses in Sudden Infant Death Syndrome", *Pediatrics*, vol. 110, no. 5, p. e64.

72. Jones, K. L., Krous, H. F., Nadeau, J., Blackbourne, B., Zielke, H. R., & Gozal, D. 2003, "Vascular Endothelial Growth Factor in the Cerebrospinal Fluid of Infants Who Died of Sudden Infant Death Syndrome: Evidence for Antecedent Hypoxia", *Pediatrics*, vol. 111, no. 2, pp. 358-363.

73. Ansari, T. 2000, "Analysis of cardiovascular and respiratory nuclei in sudden infant death syndrome infants", *Ambulatory child health*, vol. 6, p. 4.

74. Kinney, H. 2005, "Abnormalities of the Brainstem Serotonergic System in the Sudden Infant Death Syndrome: A Review", *Pediatric and Developmental Pathology*, vol. 8, no. 5, pp. 507-524.

75. Filiano, J. J. 1994, "Arcuate nucleus hypoplasia in sudden infant death syndrome: a review. [Review] [14 refs]", *Biology of the Neonate.65(3-4):156-9*.

76. Sawaguchi, T., Ozawa, Y., Patricia, F., Kadhim, H., Groswasser, J., Sottiaux, M., Takashima, S., Nishida, H., & Kahn, A. 2003, "Substance P in the midbrains of SIDS victims and its correlation with sleep apnea", *Early Human Development*, vol. 75, no. Supplement 1, pp. 51-59.

77. Blackwell, C. C., Gordon, A. E., James, V. S., MacKenzie, D. A. C., Mogensen-Buchanan, M., El Ahmer, O. R., Al Madani, O. M., Toro, K., Csukas, Z., Sotonyi, P., Weir, D. M., & Busuttil, A. 2001, "The role of bacterial toxins in Sudden Infant Death Syndrome (SIDS)", *International Journal of Medical Microbiology*, vol. 291, no. 6-7, pp. 561-570.

78. Rambaud, C. 1999, "Microbiology in sudden infant death syndrome (SIDS) and other childhood deaths", *FEMS Immunology and Medical Microbiology*, vol. 25, no. 1-2, p. 59.

79. Ansari, T., Sibbons, P. D., & Howard, C. V. 2001, "Estimation of mean nuclear volume of neocortical neurons in sudden infant death syndrome cases using the nucleator estimator technique", *Biology of the Neonate.80(1):48-52*.

80. Ansari, T., Sibbons, P. D., Parsons, A., & Rossi, M. L. 2002, "Quantitative neuropathological analysis of sudden infant death syndrome", *Child: Care, Health & Development.28 Suppl 1:3-6*.

81. Buck GM, Cookfair DL, Michalek AM, Nasca PC, Standfast SJ, Sever LE, & Kramer AA 1989, "Intrauterine growth retardation and risk of sudden infant death syndrome (SIDS)", *Am J Epidemiology*, vol. 129, no. 5, pp. 874-884.

82. Ansari, T., Gillan, J. E., Condell, D., Green, C. J., & Sibbons, P. D. 2004, "Analyses of the potential oxygen transfer capability in placentae from infants succumbing to sudden infant death syndrome", *Early Hum Dev.*, vol. 76, no. 2, pp. 127-138.

83. Ayuk P, Hughes J, & Sibley C 2000, "Placental transfer and intrauterine growth restriction," in *Intrauterine Growth Restriction: Aetiology and Management*, Kingdom J & Baker P, eds., Springer-Verlag.

84. Castellucci M & Kaufmann P 1995, "Basic Structure of the Villous Trees," in *Pathology of the Human Placenta*, 3rd edn, Benirschke K & Kaufmann P, eds., Springer-Verlag, pp. 57-115.

85. Benirschke K, Kaufmann P, & Baergen R 2005, *Pathology of the Human Placenta*, 5th edn, Springer, New York.

86. Castellucci, M., Schepe, M., Scheffen, I., Celona, A., & Kaufmann, P. 1990, "The development of the human placental villous tree", *Anatomy and Embryology*, vol. 181, no. 2, pp. 117-128.

87. Pijnenborg, R., Vercruysse, L., & Hanssens, M. 2009, "The Uterine Spiral Arteries In Human Pregnancy: Facts and Controversies", *Placenta*, vol. 27, no. 9-10, pp. 939-958.

88. Lyall, F. 2006, "Mechanisms regulating cytotrophoblast invasion in normal pregnancy and pre-eclampsia", *The Australian & New Zealand journal of obstetrics & gynaecology*, vol. 46, no. 4, p. 266.

89. Kaufmann, P., Black, S., & Huppertz, B. 2003, "Endovascular trophoblast invasion: implications for the pathogenesis of intrauterine growth retardation and preeclampsia.", *Biology of Reproduction.69(1):1-7*.

90. Burton, G. J. & Jauniaux, E. 2001, "Maternal vascularisation of the human placenta: does the embryo develop in an hypoxic environment?", *Gynecologie, Obstetrique & Fertilite.*, vol. 29, pp. 503-508.

91. Genbacev, O., Zhou, Y., Ludlow, J. W., & Fisher, S. J. 1997, "Regulation of Human Placental Development by Oxygen Tension", *Science*, vol. 277, no. 5332, pp. 1669-1672.

92. Caniggia, I., Winter, J., Lye, S. J., & Post, M. 2000, "Oxygen and Placental Development During the First Trimester: Implications for the Pathophysiology of Pre-eclampsia", *Placenta*, vol. 21, no. Supplement 1, p. S25-S30.

93. James, J. L., Stone, P. R., & Chamley, L. W. 2006, "The regulation of trophoblast differentiation by oxygen in the first trimester of pregnancy", *Human Reproduction Update*, vol. 12, no. 2, pp. 137-144.

94. Aplin JD, Haigh T, Lacey H, Chen C-P, & Jones CJP 2000, "Tissue interactions in the control of trophoblast invasion", *J Reprod Fertil Suppl*, vol. 55, pp. 57-64.

95. Lyall, F. 2002, "The Human Placental Bed Revisited", *Placenta*, vol. 23, no. 8-9, pp. 555-562.

96. Luckhardt M, Leiser R, & Kingdom J 1996, "Effect of physiological perfusion-fixation on the morphometrically evaluated dimensions of the term placental cotyledon", *J Soc Gynaecol Invest*, vol. 3, no. 166, p. -71.

97. Castellucci, M., Kosanke, G., Verdenelli, F., Huppertz, B., & Kaufmann, P. 2000, "Villous sprouting: fundamental mechanisms of human placental development.", *Human Reproduction Update.6(5):485-94*, p. -Oct.

98. Kaufmann P, Bruns U, Leiser R, Luckhardt M, & Winterhager E 1985, "The fetal vascularisation of term human placental villi. II. Intermediate and terminal villi", *Anatomy & Embryology.*, vol. 173, pp. 203-14.

99. Larsen WJ 1993, "Fetal development and the fetus as a patient," in *Human Embryology*, 1st edn, Churchill Livingstone, New York, pp. 435-451.

100. Kingdom, J., Huppertz, B., Seaward, G., & Kaufmann, P. 2000, "Development of the placental villous tree and its consequences for fetal growth", *European Journal of Obstetrics, Gynecology, & Reproductive Biology.92(1):35-43*.

101. Kaufmann, P., Mayhew, T. M., & Charnock-Jones, D. S. 2004, "Aspects of human fetoplacental vasculogenesis and angiogenesis. II. Changes during normal pregnancy.", *Placenta.25(2-3):114-26.*

102. Mayhew, T. M., Wijesekara, J., Baker, P. N., & Ong, S. S. 2004, "Morphometric evidence that villous development and fetoplacental angiogenesis are compromised by intrauterine growth restriction but not by pre-eclampsia", *Placenta.25(10):829-33.*

103. Mayhew, T. M. 2003, "Changes in fetal capillaries during preplacental hypoxia: growth, shape remodelling and villous capillarization in placentae from high-altitude pregnancies", *Placenta.24(2-3):191-8,* p. -Mar.

104. Cheung CY 1997, "Vascular endothelial growth factor: possibel role in fetal development and placental function", *J Soc Gynaecol Invest*, vol. 4, pp. 169-77.

105. Ahmed, A., Dunk, C., Ahmad, S., & Khaliq, A. 2000, "Regulation of Placental Vascular Endothelial Growth Factor (VEGF) and Placenta Growth Factor (PlGF) and Soluble Flt-1 by Oxygen-A Review", *Placenta*, vol. 21, no. Supplement 1, p. S16-S24.

106. Hanahan D 1997, "Signaling vascular morphogenesis and maintenance", *Science*, vol. 277, p. 48--50.

107. Demir, R., Seval, Y., & Huppertz, B. 2007, "Vasculogenesis and angiogenesis in the early human placenta", *Acta Histochemica.109(4):257-65*.

108. Breier G 2000, "Angiogenesis in Embryonic Development-A Review", *Placenta*, vol. 21 (suppl A), pp. 511-515.

109. Clark DE, Smith SK, Licence D, Evans AL, & Charnock-Jones DS 2008, "Comparison of expression patterns for placenta growth factor, vascular endothelial growth factor (VEGF), VEGF-B and VEGF-C in the human placenta throughout gestation", *J Endocrinol*, vol. 159, pp. 459-67.

110. Pugh CW & Ratcliffe PJ 2003, "Regulation of angiogenesis by hypoxia: role of the HIF system", *Nat Med*, vol. 20, pp. 5197-206.

111. Evans PW, Wheeler T, Anthony FW, & Osmond C 1998, "A longitudinal study of maternal serum vascular endothelial growth factor in early pregnancy", *Hum Reprod*, vol. 13, no. 1057, p. 62.

112. Crescimanno C 2000, "Expression of bFGF, PIGF and their receptors in the human placenta", *Placenta*, vol. 16, p. Abstract.

113. Khaliq, A., Dunk, C., & Jiang J et al 1999, "Hypoxia down regulates placenta growth factor, whereas fetal growth restriction up-regulates placenta growth factor expression: molecular evidence for 'placental hyperoxia' in intrauterine growth restriction", *Laboratory Investigation*, vol. 79, no. 151, p. -70.

114. Kurz H, Wilting J, Sandau K, & Christ B 1998, "Automated evaluation of angiogenic effects mediated by VEGF and PIGF homo- and heterodimers", *Microvasc Res*, vol. 55, no. 92, p. -102.

115. Mayhew, T. M. 2002, "Fetoplacental angiogenesis during gestation is biphasic, longitudinal and occurs by proliferation and remodelling of vascular endothelial cells", *Placenta.23(10):742-50.*

116. Kingdom, J. C. & Kaufmann, P. 1999, "Oxygen and placental vascular development.", *Advances in Experimental Medicine & Biology.474:259-75*.

117. Lyall, F. 2005, "Priming and remodelling of human placental bed spiral arteries during pregnancy--a review.", *Placenta.26 Suppl A:S31-6*.

118. Jauniaux, E., Watson, A. L., Hempstock, J., Bao, Y. P., Skepper, J. N., & Burton, G. J. 2000, "Onset of Maternal Arterial Blood Flow and Placental Oxidative Stress : A Possible Factor in Human Early Pregnancy Failure", *American Journal of Pathology*, vol. 157, no. 6, pp. 2111-2122.

119. Red-Horse, K. 2004, "Trophoblast differentiation during embryo implantation and formation of the maternal-fetal interface", *Journal of Clinical Investigation*, vol. 114, no. 6, p. 744.

120. Khong, T. Y. 1995, "Placental changes in fetal growth retardation," in *Fetal and neonate. Physiology and clinical applications*, vol. 3 Hanson MA, Spencer JAD, & Rodeck CH, eds., Cambridge University Press, Cambridge, pp. 177-200.

121. Olofsson P, Laurini RN, & Marsal K. A high uterine artery pulsatility index reflects a defective development of placental bed spiral arteries in pregnancies complicated by hypertension and fetal growth retardation. Eur J Ostet Gynecol Reprod Biol 49[161], 8. 1993.

122. Reister, F., Frank, H. G., Kingdom, J. C. P., Heyl, W., Kaufmann, P., Rath, W., & Huppertz, B. Macrophage-Induced Apoptosis Limits Endovascular Trophoblast Invasion in the Uterine Wall of Preeclamptic Women. Lab Invest 81[8], 1143-1152. 2003.

123. Gerretsen G, Huisjes HJ, & Elema JD. Morphological changes of the spiral arteries in the placental bed in relation to pre-eclampsia and fetal growth retardation. British Journal of Obstetrics & Gynaecology 88[(9)], 876-81. 1981.

124. Meekins JW, Pijnenborg R, Hanssens M, McFadyen IR, & Van Asshe FA 1994, "A study of placental bed spiral arteries and trophoblast invasion in normal and severe pre-eclamptic pregnancies", *British Journal of Obstetrics and Gynaecology*, vol. 101, pp. 669-674.

125. Konje JC, Howarth ES, Kaufmann P, & Taylor DJ 2003, "Longitudinal quantification of uterine artery blood volume flow changes during gestation in pregnancies complicated by intrauterine growth restriction", *BJOG*, vol. 110, pp. 301-305.

126. Hung, T. H., Skepper, J. N., Charnock-Jones, D. S., & Burton, G. J. 2002, "Hypoxia-reoxygenation: a potent inducer of apoptotic changes in the human placenta and possible etiological factor in preeclampsia", *Circulation Research.90(12):1274-81*.

127. Kuzmina, I. Y., Hubina-Vakulik, G. I., & Burton, G. J. 2005, "Placental morphometry and Doppler flow velocimetry in cases of chronic human fetal hypoxia", *European Journal of Obstetrics, Gynecology, & Reproductive Biology.120(2):139-45*.

128. Burton, G. J., Woods, A. W., Jauniaux, E., & Kingdom, J. C. P. 2009, "Rheological and Physiological Consequences of Conversion of the Maternal Spiral Arteries for Uteroplacental Blood Flow during Human Pregnancy", *Placenta*, vol. 30, no. 6, pp. 473-482.

129. Viero, S., Chaddha, V., Alkazaleh, F., Simchen, M. J., Malik, A., Kelly, E., Windrim, R., & Kingdom, J. C. 2004, "Prognostic value of placental ultrasound in pregnancies complicated by absent end-diastolic flow velocity in the umbilical arteries", *Placenta.25(8-9):735-41,* p. -Oct.

130. Kadyrov, M., Schmitz, C., Black, S., Kaufmann, P., & Huppertz, B. 2003, "Pre-eclampsia and maternal anaemia display reduced apoptosis and opposite invasive phenotypes of extravillous trophoblast", *Placenta.24(5):540-8*.

131. Zhou, Y. 1997, "Preeclampsia is associated with failure of human cytotrophoblasts to mimic a vascular adhesion phenotype", *Interface*, vol. 99, p. 2152.

132. Damsky CH, Librach C, Lim KH, Fitzgerald ML, McMaster MT, Janatpour MJ, Zhou Y, Logan SK, & Fisher SJ 1994, "Integrin switching regulates normal trophoblast invasion", *Development*, vol. 120, pp. 3657-3666.

133. Zhou Y, McMaster SE, Woo K, Janatpour M, Perry J, Karpanen T, Alitalo K, Damsky C, & Fisher SJ 2002, "Circulating angiogenic factors and the risk of preeclampsia", *Am J Pathol*, vol. 160, pp. 1405-1423.

134. Zhou Y, Bellingard V, Feng KT, McMaster M, & Fisher SJ 2003, "Human cytotrophoblasts promote endothelial survival and vascular remodelling through Ang 2, PIGF and VEGF-C", *Developmental Biology*, vol. 263, pp. 114-125.

135. Bonagura TW, Gerald JP, Enders AC, & Albrecht ED 2008, "Suppression of Extravillous Trophoblast Vascular Endothelial Growth Factor Expression and Uterine Spiral Artery Invasion by Estrogen during Early Baboon Pregnancy", *Endocrinology*, vol. 149, no. 10, pp. 5078-5087.

136. Fisher, S. 2004, "The placental problem: Linking abnormal cytotrophoblast differentiation to the maternal symptoms of preeclampsia", *Reproductive Biology and Endocrinology*, vol. 2, no. 1, p. 53.

137. Zhou, Y., McMaster, M., Woo, K., Janatpour, M., Perry, J., Karpanen, T., Alitalo, K., Damsky, C., & Fisher, S. J. 2002, "Vascular Endothelial Growth Factor Ligands and Receptors That Regulate Human Cytotrophoblast Survival Are Dysregulated in Severe Preeclampsia and Hemolysis, Elevated Liver Enzymes, and Low Platelets Syndrome", *American Journal of Pathology*, vol. 160, no. 4, pp. 1405-1423.

138. Lash, G. E., Cartwright, J. E., Whitley, G. S., Trew, A. J., & Baker, P. N. 1999, "The Effects of Angiogenic Growth Factors on Extravillous Trophoblast Invasion and Motility", *Placenta*, vol. 20, no. 8, pp. 661-667.

139. Vatten, L. J., Eskild, A., Nilsen, T. I. L., Jeansson, S., Jenum, P. A., & Staff, A. C. 2007, "Changes in circulating level of angiogenic factors from the first to second trimester as predictors of preeclampsia", *American Journal of Obstetrics and Gynecology*, vol. 196, no. 3, p. 239.

140. Toal, M., Keating, S., Machin, G., Dodd, J., Adamson, S. L., Windrim, R. C., & Kingdom, J. C. 2008, "Determinants of adverse perinatal outcome in high-risk women with abnormal uterine artery Doppler images", *American Journal of Obstetrics & Gynecology.* no. 3, pp. 330-337.

141. Toal, M., Chan, C., Fallah, S., Alkazaleh, F., Chaddha, V., Windrim, R. C., & Kingdom, J. C. 1996, "Usefulness of a placental profile in high-risk pregnancies", *American Journal of Obstetrics & Gynecology.* no. 4, pp. 363-367.

142. Pardi G, Cetin I, Marconi AM, Bozzetti P, Buscaglia M, Makowski EL, & Bataglia FC. Venous drainage of the human uterus: respiratory gas studies in normal and fetal growth-retarded pregnancies. Am J Obstet Gynecol 166, 699-706. 1992.

143. Kochenour, N. K. 1993, "Doppler velocimetry in pregnancy", *Seminars in Ultrasound, CT, and MRI*, vol. 14, no. 4, pp. 249-266.

144. Papageorghiou AT, Yu CK, Bindra R, Pandis G, & Nicolaides KH 2001, "Multicenter screening for pre-eclampsia and fetal growth restriction by transvaginal uterine artery Doppler at 23 weeks of gestation.", *Ultrasound in Obstetrics & Gynecology*, vol. 18, no. 5, pp. 441-9.

145. Aardema, M. W., Oosterhof, H., Timmer, A., van Rooy, I., & Aarnoudse, J. G. 2001, "Uterine Artery Doppler Flow and Uteroplacental Vascular Pathology in Normal Pregnancies and Pregnancies Complicated by Pre-eclampsia and Small for Gestational Age Fetuses", *Placenta*, vol. 22, no. 5, pp. 405-411.

146. Chaddha, V., Viero, S., Huppertz, B., & Kingdom, J. 2004, "Developmental biology of the placenta and the origins of placental insufficiency", *Seminars in Fetal and Neonatal Medicine*, vol. 9, no. 5, pp. 357-369.

147. Schaaps, J. P., Tsatsaris, V., Goffin, F., Brichant, J. F., Delbecque, K., Tebache, M., Collignon, L., Retz, M. C., & Foidart, J. M. 2005, "Shunting the intervillous space: New concepts in human

uteroplacental vascularization", *American Journal of Obstetrics and Gynecology*, vol. 192, no. 1, pp. 323-332.

148. Ferrazzi, E., Bulfamante, G., Mezzopane, R., Barbera, A., Ghidini, A., & Pardi, G. 1999, "Uterine Doppler Velocimetry and Placental Hypoxic-ischemic Lesion in Pregnancies with Fetal Intrauterine Growth Restriction", *Placenta*, vol. 20, no. 5-6, pp. 389-394.

149. Madazli, R., Somunkiran, A., Calay, Z., Ilvan, S., & Aksu, M. F. 2003, "Histomorphology of the Placenta and the Placental Bed of Growth Restricted Foetuses and Correlation with the Doppler Velocimetries of the Uterine and Umbilical Arteries", *Placenta*, vol. 24, no. 5, pp. 510-516.

150. Todros T, Sciarrone A, Piccoli E, Guiot C, Kaufmann P, & Kingdom J 1999, "Doppler waveforms and placental villous angiogenesis in pregnancies complicated by fetal growth restriction", *Obstetrics Gynecology*, vol. 93, no. 499, p. -503.

151. Jauniaux, E., Hempstock, J., Greenwold, N., & Burton, G. J. 2003, "Trophoblastic Oxidative Stress in Relation to Temporal and Regional Differences in Maternal Placental Blood Flow in Normal and Abnormal Early Pregnancies", *American Journal of Pathology*, vol. 162, no. 1, pp. 115-125.

152. Egbor, M., Ansari, T., Morris, N., Green, C., & Sibbons, P. 2006, "Morphometric placental villous and vascular abnormalities in early- and late-onset pre-eclampsia with and without fetal growth restriction", *British Journal of Obstetrics and Gynaecology*, vol. 113: 1-10.

153. Kingdom, J. C. & Kaufmann, P. 1997, "Oxygen and placental villous development: origins of fetal hypoxia.", *Placenta.18(8):613-21; discussion 623-6*.

154. Burton GJ, Reshetnikova OS, Milovanov AP, & Teleshova OV 1996, "Stereological evaluation of Vascular Adaptations in Human Placental Villi to Differing Forms of Hypoxic Stress", *Placenta*, vol. 17, pp. 49-55.

155. Mayhew TM, Charnock-Jones DS, & Kaufmann P 2004, "Aspects of Human Fetoplacental Vasculogenesis and Angiogenesi. III. Changes in Complicated Pregnancies", *Placenta*, vol. 25, pp. 127-139.

156. Egbor, M., Ansari, T., Morris, N., Green, C., & Sibbons, P. 2006, "Pre-eclampsia and Fetal Growth Restriction: How Morphometrically Different is the Placenta?", *British Journal of Obstetrics and Gynaecology*.

157. Teasdale, F. 1984, "Idiopathic intrauterine growth retardation: histomorphometry of the human placenta", *Placenta*, vol. 5, pp. 83-92.

158. Jackson, M. R., Walsh, A. J., Morrow, R. J., Mullen, J. B., Lye, S. J., & Ritchie, J. W. 1995, "Reduced placental villous tree elaboration in small-for-gestational-age pregnancies: relationship with umbilical artery Doppler waveforms", *American Journal of Obstetrics & Gynecology.172(2 Pt 1):518-25*.

159. Ansari, T., Fenlon, S., Pasha, S., O'Neill, B., Gillan, J. E., Green, C. J., & Sibbons, P. D. 2003, "Morphometric assessment of the oxygen diffusion conductance in placentae from pregnancies complicated by intra-uterine growth restriction", *Placenta.24(6):618-26*.

160. Sagol S, Sagol O, & Ozdemir N 2002, "Stereological quantification of placental villus vascularisation and its relation to umbilical artery Doppler flow in intrauterine growth restriction", *Prenat Diagn*, vol. 22, pp. 398-403.

161. Mayhew, T. M., Ohadike, C., Baker, P. N., Crocker, I. P., Mitchell, C., & Ong, S. S. 2003, "Stereological investigation of placental morphology in pregnancies complicated by pre-eclampsia with and without intrauterine growth restriction", *Placenta.24(2-3):219-26,* p. -Mar.

162. Ansari T, Gillan, J. E., O'Neill, B., & Sibbons, P. D. Morphological Developmental abnormalitities in the placenta and possible fetal growth restriction. Sibbons, P. D., Foster L, and Wade JF. Series No.8, 41-43. 2003. UK, R&W Publications.

163. Mayhew, T. M., Manwani R, Ohadike C, Wijesekara J, & Baker PN 2006, "The Placenta in Pre-eclampsia and Intrauterine Growth Restriction: Studies on Exchange Surface Areas, Diffusion Distances and Villous Membrane Diffusive Conductances", *Placenta*, vol. 28, pp. 233-238.

164. Mai X, Zhuang Y, & Lu H 2000, "Vascular endothelial growth factor expression in placentas from intrauterine growth retardation fetus with abnormal artery flow velocity waveforms", *Zhonghua Fu Chan Ke Za Zhi*, vol. 35, pp. 606-9.

165. Teasdale, F. 1985, "Histomorphometry of the human placenta in maternal preeclampsia", *Am J Obstet Gynecol*, vol. 152, pp. 49-55.

166. Butlery MG, Greenland S, & Kraus JF 1990, "Chronic fetal hypoxia and SIDS: interaction between maternal smoking and low haematocrit during pregnancy", *Pediatrics*, vol. 4, pp. 535-40.

167. Hemberger M & Zechner U 2004, "Genetic and genomic approaches to study placental development", *Cytogenet Genome Res*, vol. 105, p. 257--269.

168. Cross JC, Baczyk D, & Dobric N et al 2003, "Genes, development and evolution of the placenta", *Placenta*, vol. 24, pp. 123-30.

169. Rossant J & Cross JC 2001, "Placental development: lessons from mouse mutants", *Nat Rev Genet*, vol. 2, pp. 538-548.

170. Simmons, D. G. & Cross, J. C. 2005, "Determinants of trophoblast lineage and cell subtype specification in the mouse placenta", *Developmental Biology*, vol. 284, no. 1, pp. 12-24.

171. Uy, G. D., Downs, K. M., & Gardner, R. L. 2002, "Inhibition of trophoblast stem cell potential in chorionic ectoderm coincides with occlusion of the ectoplacental cavity in the mouse", *Development*, vol. 129, no. 16, pp. 3913-3924.

172. Hughes, M., Dobric, N., Scott, I. C., Su, L., Starovic, M., St-Pierre, B., Egan, S. E., Kingdom, J. C., & Cross, J. C. 2004, "The Hand1, Stra13 and GCM1 transcription factors override FGF signaling to promote terminal differentiation of trophoblast stem cells", *Developmental Biology.271(1):26-37*.

173. Tanaka S, Kunath T, Hadjantonakis, AK, Nagy, & Rossant J 1998, "Promotion of trophoblast stem cell population by FGF4", *Science*, vol. 282, pp. 2072-75.

174. Haffner-Krausz, R., Gorivodsky, M., Chen, Y., & Lonai, P. 1999, "Expression of Fgfr2 in the early mouse embryo indicates its involvement in preimplantation development", *Mechanisms of Development*, vol. 85, no. 1-2, pp. 167-172.

175. Chawengsaksophak K, James R, Hammond VE, Kontgen F, & Beck F 1997, "Homeosis and intestinal tumours in Cdx2 mutant mice", *Nature*, vol. 386, pp. 84-87.

176. Russ, A. P., Wattler, S., Colledge, W. H., Aparicio, S. A. J. R., Carlton, M. B. L., Pearce, J. J., Barton, S. C., Surani, M. A., Ryan, K., Nehls, M. C., Wilson, V., & Evans, M. J. 2000, "Eomesodermin is required for mouse trophoblast development and mesoderm formation", *Nature*, vol. 404, no. 6773, pp. 95-99.

177. Roberts RM, Ezashi T, & Das P 2004, "Trophoblast gene expression: Transcription factors in the specification of early trophoblast", *Endocrinology*, vol. 2, pp. 1-9.

178. Kaufman MH & Bard JBL 1999, *The Anatomical Basis of Mouse Development* Academic Press, San Diego.

179. Wu, L., de Bruin, A., Saavedra, H. I., Starovic, M., Trimboli, A., Yang, Y., Opavska, J., Wilson, P., Thompson, J. C., Ostrowski, M. C., Rosol, T. J., Woollett, L. A., Weinstein, M., Cross, J. C., Robinson, M. L., & Leone, G. 2003, "Extra-embryonic function of Rb is essential for embryonic development and viability", *Nature*, vol. 421, no. 6926, pp. 942-947.

180. Jackson M, Baird JW, Nichols J, Wilkie R, Ansell JD, Graham G, & Forrester LM 2003, "Expression of novel homeobox gene Ehox in trophoblast stem cells and pharyngeal pouch endoderm", *Dev Dyn*, vol. 228, pp. 740-744.

181. Anson-Cartwright L, Dawson K, Holmyard D, Fisher SJ, Lazzarini RA, & Cross JC 2000, "The glial cells missing-1 protein is essential for branching morphogenesis in the chorioallantoic placenta", *Nature*, vol. 25, pp. 311-314.

182. Cross JC, Nakano H, Natale DR, Simmons DG, & Watson ED 2006, "Branching morphogenesis during development of placental villi", *Differentiation*, vol. 74, pp. 393-401.

183. Basyuk E et al 1999, "The murine Gcm1 gene is expressed in a subset of placental trophoblast cells", *Dev Dyn*, vol. 214, pp. 303-311.

184. Coan, P. M., Ferguson-Smith, A. C., & Burton, G. J. 2004, "Developmental Dynamics of the Definitive Mouse Placenta Assessed by Stereology", *Biology of Reproduction*, vol. 70, no. 6, pp. 1806-1813.

185. Baczyk, D., Dunk, C., Huppertz, B., Maxwell, C., Reister, F., Giannoulias, D., & Kingdom, J. C. 2006, "Bi-potential behaviour of cytotrophoblasts in first trimester chorionic villi", *Placenta.27(4-5):367-74,* p. -May.

186. McMaster MT, Librach C, Zhou Y, Lim KH, Janatpour MJ, DeMars R, Kovats S, Damsky CH, & Fisher SJ 1995, "Human placental HLA-G expression is restricted to differentiated cytotrophoblasts", *J Immunol*, vol. 154, pp. 3771-3778.

187. James JL, Stone PR, & Chamley LW 2005, "Cytotrophoblast differentiation in the first trimester of pregnancy: evidence for separate progenitors of extravillous trophoblasts and syncytiotrophoblast", *Reprod*, vol. 130, pp. 96-103.

188. Alders M et al 1997, "The human Achaete-Scute homologue 2 (ASCL2, HASH2) maps to chromosome 11p15.5, close to IGF2 and is expressed in extravillus trophoblasts", *Hum Mol Genet*, vol. 6, pp. 859-867.

189. Janatpour MJ, Utset MF, Cross JC, Rossant J, Dong J, Israel MA, & Fisher SJ 1999, "A repertoire of differentially expressed transcription factors that offer insight into mechanisms of human trophoblast differentiation", *Dev Genet*, vol. 25, pp. 146-157.

190. Knofler M, Meinhardt G, Vasicek R, Husslein P, & Egarter C 1998, "Molecular cloning of the human Hand1 gene/cDNA and its tissue-restricted expression in cytotrophoblastic cells and hearts", *Gene*, vol. 224, pp. 77-86.

191. Baczyk, D., Satkunaratnam, A., Nait-Oumesmar, B., Huppertz, B., Cross, J. C., & Kingdom, J. C. 2004, "Complex patterns of GCM1 mRNA and protein in villous and extravillous trophoblast cells of the human placenta", *Placenta.25(6):553-9.*

192. Mi S, Lee X, Li X, Veldman GM, Finnerty H, & Racie L et al 2000, "Syncytin is a captive retroviral envelope protein involved in human placental morphogenesis", *Nature*, vol. 403, pp. 785-9.

193. Yu C, Shen K, Lin M, Chen P, Lin C, Chang GD, & Chen H 2002, "GCMa regulates the syncytin-mediated trophoblast fusion", *J Biol Chem*, vol. 277, pp. 50062-50068.

194. Ellery, P. M., Cindrova-Davies, T., Jauniaux, E., Ferguson-Smith, A. C., & Burton, G. J. 2009, "Evidence for Transcriptional Activity in the Syncytiotrophoblast of the Human Placenta", *Placenta*, vol. 30, no. 4, pp. 329-334.

195. Huppertz B, Frank HG, Kingdom JC, Reister F, & Kaufmann P 1998, "Villous cytotrophoblast regulation of the syncytial apoptotic cascade in the human placenta", *Histochemistry & Cell Biology.114(6):469-75,* vol. 110, pp. 495-508.

196. Lee W, Ginsburg KA, Cotton DB, & Kaufman RH 1986, "Squamous and trophoblstic cells in the maternal circulation identified by invasive hemodynamic monitoring during the peripartum period", *Placenta*, vol. 155, pp. 999-1001.

197. Leung, D. N., Smith, S. C., To, K. F., Sahota, D. S., & Baker, P. N. 2001, "Increased placental apoptosis in pregnancies complicated by preeclampsia", *American Journal of Obstetrics & Gynecology.184(6):1249-50*.

198. Smith, S. C., Baker, P. N., & Symonds, E. M. 1997, "Increased placental apoptosis in intrauterine growth restriction", *American Journal of Obstetrics & Gynecology.177(6):1395-401*.

199. Smith SC, Price E, Hewitt MJ, Symonds ME, & Baker PN 1998, "Cellular Proliferation in the Placenta in Normal Human pregnancy and pregnancy complicated by Intrauterine Growth Restriction", *J Soc Gynaecol Invest*, vol. 5, pp. 317-323.

200. Mayhew, T. M., Wadrop, E., & Simpson, R. A. 1994, "Proliferative versus hypertrophic growth in tissue subcompartments of human placental villi during gestation", *Journal of Anatomy.184 (Pt 3):535-43*.

201. Arnholdt, H., Meisel, F., Fandrey, K., & Lohrs, U. 1991, "Proliferation of villous trophoblast of the human placenta in normal and abnormal pregnancies", *Virchows Archiv.B.Cell Pathology.60(6):365-72*.

202. Smith, S. C., Price, E., Hewitt, M. J., Symonds, E. M., & Baker, P. N. 1998, "Cellular proliferation in the placenta in normal human pregnancy and pregnancy complicated by intrauterine growth restriction", *Journal of the Society for Gynecologic Investigation.5(6):317-23,* p. -Dec.

203. Kaufmann P, Kosanke, G., Neff A, Schweikhart G, & Castellucci M 1991, "Features of growth of placental villous trees", *Placenta*, vol. 12, p. 406.

204. Kosanke, G., Kadyrov, M., Korr, H., & Kaufmann, P. 1998, "Maternal anemia results in increased proliferation in human placental villi", *Placenta*, vol. 19, no. Supplement 1, pp. 339-357.

205. Blankenship TN & King BF 1994, "Developmental expression of Ki-67 antigen and proliferating cell nuclear antigen in the macaque placenta", *Devel Dynamics*, vol. 201, pp. 324-333.

206. Price E, Smith SC, Symonds ME, & Baker P 1997, "An investigation into the role played by variations in the mitotic index within placentae of pregnancies complcated by intrauterine growth restriction", *Placenta*, vol. 18, p. A.46.

207. Genbacev, O., McMaster, M. T., & Fisher, S. J. 2000, "A Repertoire of Cell Cycle Regulators Whose Expression Is Coordinated with Human Cytotrophoblast Differentiation", *American Journal of Pathology*, vol. 157, no. 4, pp. 1337-1351.

208. Li, R. H. & Zhuang, L. Z. 1997, "The effects of growth factors on human normal placental cytotrophoblast cell proliferation", *Human Reproduction*, vol. 12, no. 4, pp. 830-834.

209. Forbes, K., Westwood, M., Baker, P. N., & Aplin, J. D. 2008, "Insulin-like growth factor I and II regulate the life cycle of trophoblast in the developing human placenta", *AJP - Cell Physiology*, vol. 294, no. 6, p. C1313-C1322.

210. Huppertz, B., Kingdom, J., Caniggia, I., Desoye, G., Black, S., Korr, H., & Kaufmann, P. 2003, "Hypoxia favours necrotic versus apoptotic shedding of placental syncytiotrophoblast into the maternal circulation", *Placenta.24(2-3):181-90,* p. -Mar.

211. Huppertz, B., Bartz, C., & Kokozidou, M. 2006, "Trophoblast fusion: fusogenic proteins, syncytins and ADAMs, and other prerequisites for syncytial fusion.", *Micron.37(6):509-17*.

212. Mayhew, T. M. 2001, "Villous trophoblast of human placenta: a coherent view of its turnover, repair and contributions to villous development and maturation.", *Histology & Histopathology.16(4):1213-24*.

213. Huppertz, B., Kadyrov, M., & Kingdom, J. C. 2006, "Apoptosis and its role in the trophoblast.", *American Journal of Obstetrics & Gynecology.* no. 1, pp. 29-39.

214. Baczyk D, Drewlo S, Proctor L, Dunk C, Lye S, & Kingdom J 2009, "Glial cell missing-1 transcription factor is required for the differentiation of the human trophoblast", *Cell Death and Differentiation*.

215. Blond JL, Lavillette, Cheynet V, Bouton O, Oriol G, Chapel-Fernandes S, Mandrand B, Mallet F, & Cosset FL 2000, "An envelope glycoprotein of the human endogenous retrovirus HERV-W is expressed in the human placenta and fuses cells expressing the type D mammalian retrovirus receptor", *J Virol*, vol. 74, pp. 3321-3329.

216. Keryer G, Alsat E, Tasken K, & Evain-Brion D 1998, "Cyclic AMP-dependent protein kinases and human trophoblast cell differentiation in vitro", *Journal of Cell Science*, vol. 111, pp. 995-1004.

217. Lyden TW, Ng AK, & Rote NS 1993, "Modulation of phosphatidylserine epitope expression by BeWo cells during forskolin treatment", *Placenta*, vol. 14, pp. 177-186.

218. Frendo JL, Olivier D, Cheynet V, Blond JL, Bouton O, Vidaud M, Rabreau M, Evain-Brion D, & Mallet F 2003, "Direct involvement of HERV-W Env glycoprotein in human trophoblast cell fusion and differentiation", *Mol Cell Biol*, vol. 23, pp. 3566-3574.

219. Potgens AJG, Drewlo S, Kokozidou M, & Kaufmann P 2004, "Syncytin:the major regulator of trophoblast fusion? Recent developments and hypotheses on its action", *Human Reproduction Update*, vol. 10, no. 6, pp. 487-496.

220. Marin M, Lavillette D, Kelly SM, & Kabat D 2003, "N-linked glycosylation and sequence changes in a critical negative control region of the ASCT1 and ASCT2 neutral amino acid transporters determine their retroviral receptor functions", *J Virol*, vol. 77, pp. 2936-2945.

221. Ito N, Nomur S, Iwase A, Ito T, Kikkawa F, Tsujimoto M, Ishiura S, & Mizutani S 2004, "ADAMs, a disintegrin and metalloproteinases, mediate shedding of oxyocinase", *Biochem Biophys Res Commun*, vol. 314, pp. 1008-1113.

222. Kudo Y, Boyd CAR, Kimura H, Cook PR, Sargent IL, & Redman CRW 2003, "Quantifying the syncytialisation of human placental trophoblast cell line (BeWo) grwon in vitro and effects thereon of manipulation of CD98 expression", *Placenta*, vol. 24, p. A58.

223. Frendo JL, Cronier L, Bertin G, Guibourdenche, J., Vidaud M, Evain-Brion D, & Malassine, A. 2003, "Involvement of connexin 43 in human trophoblast cell fusion and differentiation", *Journal of Cell Science*, vol. 116, pp. 3413-3421.

224. Getsios S & MacCalman CD 2003, "Cadherin-11 modulates the terminal differentiation and fusion of human trophoblastic cells in vitro", *Dev Biol*, vol. 257, pp. 41-54.

225. Black, S., Kadyrov, M., Kaufmann, P., Ugele, B., Emans, N., & Huppertz, B. 2003, "Syncytial fusion of human trophoblast depends on caspase 8", *Cell Death Differ*, vol. 11, no. 1, pp. 90-98.

226. Huppertz, B., Frank, H. G., & Kaufmann, P. 2000, "The apoptosis cascade-morphological and immunohistochemical methods for its visualization.", *Anatomy & Embryology.* no. 1, pp. 1-18.

227. Sakuragi N, Matsuo H, Coukos G, Furth EE, Bronner MP, & van Arsdale et al 1994, "Differentiation-dependent expressio of the Bcl-2 proto-oncogene in the human placenta", *Gynecol Invest*, vol. 1, pp. 164-172.

228. Huppertz, B., Kaufmann, P., & Kingdom JCP. Trophoblast turnover in health and disease. Fetal Maternal Med Rev 13, 103-118. 2002.

229. Steinborn A, von Gall C, Hildenbrand R, Stutte HJ, & Kaufmann M 1998, "Identification of placental cytokine-producing cells in term and preterm labor", *Obstetrics Gynecology*, vol. 91, pp. 329-335.

230. Lea RG, Tulppala M, & Critchley HO 1997, "Deficient syncytiotrophoblast tumpr necrosis factor-aplha characterises failing first trimester pregnancies in a subgroup of recurrent miscarriag patients", *Hum.Reprod*, vol. 12, pp. 1313-1320.

231. Alder RR, Ng AK, & Rote NS 1995, "Monoclonal antiphosphatidylserine antibody inhibits intercellular fusion of choriocarcinoma line, JAR", *Biology of Reproduction*, vol. 53, pp. 905-910.

232. Ratts, V. S., Tao, X. J., Webster, C. B., Swanson, P. E., Smith, S. D., Brownbill, P., Krajewski, S., Reed, J. C., Tilly, J. L., & Nelson, D. M. 2000, "Expression of BCL-2, BAX and BAK in the trophoblast layer of the term human placenta: a unique model of apoptosis within a syncytium", *Placenta.21(4):361-6*.

233. Irmler M, Thome M, Hahne M, Schneider P, Hofmann K, & Steiner V 1997, "Inhibition of the death receptor signals by cellular FLIP", *Nature* no. 388, pp. 190-195.

234. Ka H & Hunt JS 2003, "Temporal and spatial patterns of expression of inhibitors of apoptosis in human placentas", *American Journal of Pathology*, vol. 163, pp. 413-422.

235. Shiozaki EN, Chai J, & Rigotti DJ 2003, "Mechanism of XIAP-mediated inhibition of caspase-9", *Mol Cell*, vol. 11, pp. 519-527.

236. LeBlanc AC 2003, "Natural cellular inhibitors of caspases", *Prog Neuropsychopharmacol Biol Psychiatry*, vol. 27, pp. 215-229.

237. Leers, M. P., Kolgen, W., Bjorklund, V., Bergman, T., Tribbick, G., Persson, B., Bjorklund, P., Ramaekers, F. C., Bjorklund, B., Nap, M., Jornvall, H., & Schutte, B. 1999, "Immunocytochemical detection and mapping of a cytokeratin 18 neo-epitope exposed during early apoptosis", *Journal of Pathology.187(5):567-72*.

238. Staribratova D, Zaprianov Z, & Milchev N 2005, "Proliferation of villous trophoblast and stroma in normal and pathologic pregnancies", *Akush Ginekol (Sofiia)*, vol. 44, no. 2, pp. 20-2.

239. Jeschke, U. P., Schiessl, B. M. D., Mylonas, I. M. D., Kunze, S., Kuhn, C., Schulze, S., Friese, K. M. D., & Mayr, D. M. D. 2006, "Expression of the Proliferation Marker Ki-67 and of p53 Tumor Protein in Trophoblastic Tissue of Preeclamptic, HELLP, and Intrauterine Growth-Restricted Pregnancies.", *International Journal of Gynecological Pathology*, vol. 25, no. 4, pp. 354-360.

240. Ishihara, N., Matsuo, H., Murakoshi, H., Laoag-Fernandez, J. B., Samoto, T., & Maruo, T. 2002, "Increased apoptosis in the syncytiotrophoblast in human term placentas complicated by either preeclampsia or intrauterine growth retardation", *American Journal of Obstetrics & Gynecology.186(1):158-66*.

241. Allaire, A. D., Ballenger, K. A., Wells, S. R., McMahon, M. J., & Lessey, B. A. 2000, "Placental apoptosis in preeclampsia", *Obstetrics & Gynecology.96(2):271-6*.

242. Levy, R., Smith, S. D., Yusuf, K., Huettner, P. C., Kraus, F. T., Sadovsky, Y., & Nelson, D. M. 2002, "Trophoblast apoptosis from pregnancies complicated by fetal growth restriction is associated with enhanced p53 expression", *American Journal of Obstetrics and Gynecology*, vol. 186, no. 5, pp. 1056-1061.

243. Von Dadelszen P, Wilkins T, & Redman CW. Maternal peripheral blood leukocytes in normal and pre-eclamptic pregnancies. British Journal of Obstetrics & Gynaecology 106, 576-81. 1999.

244. Chen CP, Bajoria R, & Aplin JD 2002, "Decreased vascularisation and cell proliferation in placentas of intrauterine growth-restricted fetuses with abnormal umbilical artery flow velocity waveforms", *Am J Obstet Gynecol*, vol. 187, no. 3, pp. 764-769.

245. Izutsu T, Kudo T, Sato T, Hishiya I, Ohyashiki K, & Nakagawara K 1999, "Telomerase and Proliferative Activity in Placenta From Women With and Without Fetal Growth Restriction", *Obstetrics Gynecology*, vol. 93, pp. 124-9.

246. Ashfaq M, Janjua M, & Nawaz M 2000, "Effects of maternal smoking on placental morphology", *J Ayub Med Coll Abbottabad*, vol. 15, no. 3, pp. 12-5.

247. Zdravkovic, T., Genbacev, O., McMaster, M. T., & Fisher, S. J. 2005, "The adverse effects of maternal smoking on the human placenta: A review", *Placenta*, vol. 26, no. Supplement 1, p. S81-S86.

248. Mayhew, T. M. 1997, "Recent applications of the new stereology have thrown fresh light on how the human placenta grows and develops its form", *Journal of Microscopy.186 (Pt 2):153-63.*

249. Mayhew TM 2006, "Allometric studies on growth and development of the human placenta: growth of tissue compartments and diffusive conductances in relation to placental volume and fetal mass", *J Anat*, vol. 208, pp. 785-794.

250. Rasmussen, S. & Irgens, L. M. 2003, "Fetal growth and body proportion in preeclampsia", *Obstetrics & Gynecology.101(3):575-83.*

251. Odenhaal HJ, Pattinson RC, & du Toit R 1987, "Fetal and neonatal outcome in patients with severe pre-eclampsia before 34 weeks", *S Afr Med*, vol. 71, pp. 555-558.

252. Moldenhauer JS, Stanek J, Warshak C, Khoury J, & Sibai B 2003, "The frequency and severity of placental findings in women with pre-eclampsia are gestational age dependent", *Am J Obstet Gynecol*, vol. 189, pp. 1173-7.

253. Sebire NJ, Goldin RD, & Regan L 2005, "Term pre-eclampsia is associated with minimal histopathological placental features regardless of clinical severity", *J Obstet Gynecol*, vol. 25, pp. 117-118.

254. Kramer MS, Platt RW, Wen SW, Joseph KS, Allen A, Abrahamowicz M, Blondel B, & Bréat G 2001, "A New and Improved Population-Based Canadian Reference for Birth Weight for Gestational Age", *Pediatrics*, vol. 108, pp. 1-7.

255. Rognum TO 2001, "Definition and Pathological features," in *Sudden Infant Death Syndrome. Problems, Progress and Possibilities*, 1st Ed edn, Byard RW & Krous HF, eds., Arnhold, pp. 4-30.

256. Mayhew, T. M. 2005, "Stereology and the placenta - Where's the point?", *Placenta*, vol. 26, no. 8-9, p. A2.

257. Mayhew TM 2009, "A stereological perspective on placental morphology in normal and complicated pregnancies", *J Anat*, vol. 215, pp. 77-90.

258. Gundersen HJG 1977, "Notes on the estimation of the numerical density of arbitrary profiles: the edge effect", *Journal of Microscopy*, vol. 111, pp. 219-223.

259. Mayhew TM & Gundersen HJG 1996, "'If you assume, you can make an ass of u and me': a decade of the disector for stereological counting of particles in 3D space", *J Anat*, vol. 188, pp. 1-15.

260. Mayhew, T. M. 1991, "The new stereological methods for interpreting functional morphology from slices of cells and organs.", *Experimental Physiology.76(5):639-65*.

261. Gundersen HJG & Jensen EB 1987, "The efficiency of systematic sampling in stereology and its prediction", *J Microsc*, vol. 147, pp. 229-263.

262. Gundersen, H. J., Bendtsen, T. F., Korbo, L., Marcussen, N., Moller, A., Nielsen, K., Nyengaard, J. R., Pakkenberg, B., Sorensen, F. B., & Vesterby, A. 1988, "Some new, simple and efficient stereological methods and their use in pathological research and diagnosis. [Review] [30 refs]", *APMIS.96(5):379-94*.

263. Mayhew, T. M. 2008, "Taking tissue samples from the placenta: an illustration of principles and strategies. [Review] [46 refs]", *Placenta.29(1):1-14*.

264. Mouton P 2002, *Principles and Practices of Unbiased Stereology, An Introduction for Bioscientists*, 1st edn, The John Hopkins University Press, USA.

265. Howard CV & Reed MG. Unbiased Stereology: Three dimensional measurements in Microscopy. 1998. United States, Springer-Verlag.

266. Stuart A 1976, *Basic Ideas of Scientific Sampling* Charles Griffin, London.

267. Gundersen HJG. Streology of arbitrary particles. A review of unbiased number and size estimators and the presentation of some new ones, in memory of William R. Thompson. Journal of Microscopy 117, 333-345. 1986.

268. Cavalieri B. *Geometria Indivisibilibus Continuorum*. Typis Clemetis Feronij, Bononi [Reprinted (1966) as Geometria degli Indivisibili]. 1635. Torino, Unione Tipografico-Editrice Torinese.

269. Howard CV & Reed MG 1998, "Estimation of component volume and volume fraction," in *Unbiased Stereology. Three-Dimensional Measurement in Microscopy*, Springer-Verlag, New York, pp. 55-65.

270. Cruz-Orive, L. M. & Myking, A. O. 1981, "Stereological estimation of volume ratios by systematic sections", *Journal of Microscopy.122(Pt 2):143-57*.

271. Cruz-Orive LM 1982, "The use of quadrats and test systems in stereology, including magnification corrections", *J.Microsc*, vol. 125, pp. 89-102.

272. Cochran WG 1977, *Sampling Techniques*, 3rd edn, Wiley, New York.

273. Gundersen HJG & Jensen EB. Stereological estimation of the volume-weighted mean volume of arbitrary particles observed on random sections. Journal of Microscopy 138[2], 127-142. 1985.

274. Sterio, D. C. 1984, "The unbiased estimation of number and sizes of arbitrary particles using the disector", *Journal of Microscopy.134(Pt 2):127-36*.

275. Dorph-Petersen KA, Nyengaard JR, & Gundersen HJG 2001, "Tissue shrinkage and unbiased stereological estimation of particel number and size", *Journal of Microscopy*, vol. 204, pp. 232-246.

276. Kaufmann P & Huppertz B 2007, "Tenney-Parker changes and apoptotic versus necrotic shedding of trophoblast in normal pregnancy and pre-eclampsia," in *Pre-eclampsia: etiology and clinical practice*, Lyall F & Belfort M, eds., Cambridge University Press, pp. 152-163.

277. Gundersen, H. J., Bagger, P., Bendtsen, T. F., Evans, S. M., Korbo, L., Marcussen, N., Moller, A., Nielsen, K., Nyengaard, J. R., & Pakkenberg, B. 1988, "The new stereological tools:

disector, fractionator, nucleator and point sampled intercepts and their use in pathological research and diagnosis.", *APMIS.96(10):857-81*.

278. Widdows K, Kingdom JCP, & Ansari T. Double Immuno-labelling of Proliferating Villous Cytotrophoblasts in Thick Paraffin Sections: Integrating Immuno-histochemistry and Stereology in the Human Placenta. Placenta . 2009.

279. Howard CV, Reid S, Baddeley AJ, & Boyde A 1985, "Unbiased estimation of particle density in the tandem scanning reflected light microscope", *Journal of Microscopy*, vol. 138, pp. 203-212.

280. Bradford MM 1976, "A Rapid and Sensitive Method for the Quantitation of Microgram Quantities of Protein Utilizing the Principle of Protein-Dye Binding", *Anal Biochem*, vol. 72, pp. 248-254.

281. Mayhew TM, Huppertz B, Kaufmann P, & Kingdom JCP 2003, "The 'Reference Trap' Revisited: Examples of the Dangers in Using Ratios to Describe Fetoplacental Angiogenesis and Trophoblast Turnover", *Placenta*, vol. 24, pp. 1-7.

282. Reshetnikova OS, Burton, G. J., & Milovanov AP 1994, "Effects of hypobaric hypoxia on the fetoplacental unit: the morphometric diffuing capacity of the villous membrnae at high altitude", *Am J Obstet Gynecol*, vol. 171, pp. 1560-5.

283. Reshetnikova OS, Burton, G. J., & Teleshova OV 1995, "Placental histomorphometry and morphometric diffusing capacity of the villous membrane in pregnancies complicated by maternal iron deficiency", *Am J Obstet Gynecol*, vol. 173, pp. 724-7.

284. Mayhew, T. M. & Burton, G. J. 1988, "Methodological problems in placental morphometry: apologia for the use of stereology based on sound sampling practice.", *Placenta.9(6):565-81,* p. - Dec.

285. Schweikhart G, Kaufmann P, & Beck Th 1986, "Morphology of Placental Villi After Premature Delivery and Its Clinical Relevance", *Arch Gynecol*, vol. 239, pp. 101-114.

286. Mitra SC, Seshan SV, & Riachi LE 2000, "Placental vessel morphometry in growth retardation and increased resistance of the umbilical artery Doppler flow", *J Matern Fetal Med*, vol. 9, pp. 282-6.

287. Jauniaux, E. & Burton, G. J. 1996, "Correlation of umbilical Doppler features and placental morphometry: the need for uniform methodology", *Ultrasound in Obstetrics & Gynecology*, vol. 3, pp. 233-235.

288. Macara, L., Kingdom, J. C., Kohnen, G., Bowman, A. W., Greer, I. A., & Kaufmann, P. 1995, "Elaboration of stem villous vessels in growth restricted pregnancies with abnormal umbilical artery Doppler waveforms.", *British Journal of Obstetrics & Gynaecology.102(10):807-12*.

289. Fox H 2000, "Placental Pathology," in *Intrauterine Growth Restriction. Aetiology and Managment*, Kingdom JCP & Baker PN, eds., Springer Verlag, London, pp. 187-201.

290. Kingdom, J. C., Burrell, S. J., & Kaufmann, P. 1997, "Pathology and clinical implications of abnormal umbilical artery Doppler waveforms", *Ultrasound in Obstetrics & Gynecology.9(4):271-86*.

291. Pfarrer C, Macara, L., & Kingdom JCP 1999, "Adaptive angiogenesis in placentas of heavy smokers", *Lancet*, vol. 354, no. 303.

292. Mayhew, T. M. 1996, "Patterns of villous and intervillous space growth in human placentas from normal and abnormal pregnancies", *European Journal of Obstetrics & Gynecology and Reproductive Biology*, vol. 68, pp. 75-82.

293. Larsen, L. G., Clausen, H. V., & J°nsson, L. 2002, "Stereologic examination of placentas from mothers who smoke during pregnancy", *American Journal of Obstetrics and Gynecology*, vol. 186, no. 3, pp. 531-537.

294. Wang X, Zuckerman B, Pearson C, Kaufman G, Chen C, & Wang G 2002, "Maternal cigarette smoking, metabolic gene polymorphism, and infant birth weight", *JAMA*, vol. 287, pp. 195-202.

295. Mayhew, T. M. & Barker, B. L. 2001, "Villous trophoblast: morphometric perspectives on growth, differentiation, turnover and deposition of fibrin-type fibrinoid during gestation", *Placenta.22(7):628-38*.

296. Simpson, R. A., Mayhew, T. M., & Barnes, P. R. 1992, "From 13 weeks to term, the trophoblast of human placenta grows by the continuous recruitment of new proliferative units: a study of nuclear number using the disector", *Placenta.13(5):501-12,* p. -Oct.

297. Gurel D, Ozer E, Altunyurt S, Guclu S, & Demir N 2003, "Expression of IGR-IR and VEGF and trophoblastic proliferative activity in placentals from pregnancies complicated by IUGR", *Pathol Res Pract*, vol. 199, no. 12, pp. 803-9.

298. Potgens AJG, Kataoka H, Ferstl S, Frank HG, & Kaufmann P. A Positive Immunoselection Method to Isolate Vilous Cytotrophoblast Cells from First Trimester and term Placenta to High Purity. Placenta 24, 412-423. 2003.

299. Hallikas, O. K., Aaltonen, J. M., von, K. H., Lindberg, L. A., Valmu, L., Kalkkinen, N., Wahlstrom, T., Kataoka, H., Andersson, L., Lindholm, D., & Schroder, J. 2006, "Identification of antibodies against HAI-1 and integrin alpha6beta4 as immunohistochemical markers of human villous cytotrophoblast", *Journal of Histochemistry & Cytochemistry.54(7):745-52*.

300. Tanaka, H., Nagaike, K., Takeda, N., Itoh, H., Kohama, K., Fukushima, T., Miyata, S., Uchiyama, S., Uchinokura, S., Shimomura, T., Miyazawa, K., Kitamura, N., Yamada, G., & Kataoka, H. 2005, "Hepatocyte growth factor activator inhibitor type 1 (HAI-1) is required for branching morphogenesis in the chorioallantoic placenta", *Molecular & Cellular Biology.25(13):5687-98*.

301. Muhlhauser, J., Crescimanno, C., Kasper, M., Zaccheo, D., & Castellucci, M. 1995, "Differentiation of human trophoblast populations involves alterations in cytokeratin patterns", *Journal of Histochemistry & Cytochemistry.43(6):579-89*.

302. Owens, D. W. & Lane, E. B. 2003, "The quest for the function of simple epithelial keratins.", *Bioessays.25(8):748-58*.

303. Kadyrov, M., Kaufmann, P., & Huppertz, B. 2001, "Expression of a cytokeratin 18 neo-epitope is a specific marker for trophoblast apoptosis in human placenta", *Placenta.22(1):44-8*.

304. Gerdes, J., Schwab U, Lemke H, & Stein H 1983, "Production of a mouse monoclonal antibody reactive with a human nuclear antigen associated with cell proliferation", *Int J Cancer*, vol. 31, pp. 13-20.

305. Gerdes J, Lemke H, Baisch H, Wacker H-H, Schwab U, & Stein H 1984, "Cell cycle analysis of a cell proliferation-associated human nuclear antigen defined by the monoclonal antibody Ki-67", *J Immunol*, vol. 133, pp. 1710-15.

306. Scholzen T & Gerdes J 2000, "The Ki-67 Protein: From the Known and the Unknown", *Journal of Cellular Pathology*, vol. 182, no. 311, p. 322.

307. Mayhew, T. M., Leach, L., McGee, R., Ismail, W. W., Myklebust, R., & Lammiman, M. J. 1999, "Proliferation, differentiation and apoptosis in villous trophoblast at 13-41 weeks of gestation (including observations on annulate lamellae and nuclear pore complexes)", *Placenta.* no. 5-6, pp. 407-422.

308. Burton, G. J., Skepper, J. N., Hempstock, J., Cindrova T, Jones, C. J., & Jauniaux, E. 2003, "A Reappraisal of the Contrasting Morphological Appearances of Villous Cytotrophoblast Cells During Early Human pregnancy; Evidence for both Apoptosis and Primary Necrosis", *Placenta*, vol. 24, pp. 297-305.

309. Langbein M, Strick R, Stirssel PL, Vogt N, Parsch H, Beckmann MW, & Schild RL 2008, "Impaired cytotrophoblast Cell-Cell Fusion is Assoicated with Reduced Syncytin and Increased Apoptosis in Patients with Placental Dysfunction", *Mol Reprod Dev*, vol. 75, pp. 175-183.

310. Chen CP, Chen CY, Yang YC, Su TH, & Chen H 2004, "Decreased placental GCM1 (glial cell missing) gene expression in pre-eclampsia", *Placenta*, vol. 25, pp. 413-421.

311. Fox, C. 1964, "The villous cytotrophoblast as an index of placental ischaemia", *Journal of Obstet and Gynaecol of Brit Common*, vol. 71, pp. 885-893.

312. Ali, K. Z. M. 1997, "Stereological study of the effect of altitude on the trophoblast cell populations of human term placental villi", *Placenta*, vol. 18, no. 5-6, pp. 447-450.

313. Mayhew, T. M., Jackson, M. R., & Haas, J. D. 1990, "Oxygen diffusive conductances of human placentae from term pregnancies at low and high altitudes", *Placenta.11(6):493-503,* p. -Dec.

314. Jackson, M. R., Joy, C. F., Mayhew, T. M., & Haas, J. D. 1985, "Stereological studies on the true thickness of the villous membrane in human term placentae: a study of placentae from high-altitude pregnancies", *Placenta.6(3):249-58,* p. -Jun.

315. MacAuley, A., Cross, J. C., & Werb, Z. 1998, "Reprogramming the Cell Cycle for Endoreduplication in Rodent Trophoblast Cells", *Molecular Biology of the Cell*, vol. 9, no. 4, pp. 795-807.

316. Fox H 1968, "Fibrinoid necrosis of placental villi", *Obstet Gynaecol Br.Commonw*, vol. 75, pp. 448-452.

317. Jones HN, Powell TL, & Jansson T 2007, "Regulation of Placental Nutrient Transport- A Review", *Placenta*, vol. 28, pp. 763-774.

318. Mayhew, T. M. & Simpson, R. A. 1994, "Quantitative evidence for the spatial dispersal of trophoblast nuclei in human placental villi during gestation", *Placenta.15(8):837-44*.

319. Mayhew TM, Bowles C, & Yücel F 2002, "Villous trophoblast growth in pregnancy at high altitude", *J Anat*, vol. 200, pp. 523-534.

320. Tenney B & Parker F 1940, "The placenta in toxemia of pregnancy", *Am J Obstet Gynecol*, vol. 39, pp. 1000-5.

321. Jones CJP & Fox H 1977, "Syncytial knots and intervillous bridges in the human placenta: an ultrastructural study", *J Anat*, vol. 124, pp. 275-286.

322. Heazell, A. E. P., Moll, S. J., Jones, C. J. P., Baker, P. N., & Crocker, I. P. 2007, "Formation of Syncytial Knots is Increased by Hyperoxia, Hypoxia and Reactive Oxygen Species", *Placenta*, vol. 28, no. Supplement 1, p. S33-S40.

323. Fox H 1965, "The significance of villous syncytial knots in the human placenta", *J Obstet Gynaecol Br Commonw*, vol. 72, pp. 347-355.

324. Frendo, J. L., Vidaud, M., Guibourdenche, J., Luton, D., Muller, F., Bellet, D., Giovagrandi, Y., Tarrade, A., Porquet, D., Blot, P., & Evain-Brion, D. 2000, "Defect of Villous Cytotrophoblast Differentiation into Syncytiotrophoblast in Down's Syndrome", *Journal of Clinical Endocrinology Metabolism*, vol. 85, no. 10, pp. 3700-3707.

325. Keith JC, Pijnenborg R, & van Assche FA 2002, "Placental syncytin expression in normal and pre-eclamptic pregnancies", *Am J Obstet Gynecol*, vol. 187, pp. 1122-3.

326. Endo H, Okamoto A, Yamada K, Nikaido T, & Tanaka T 2005, "Frequent apoptosis in placental villi from pregnancies complicated with intrauterine growth restriction and without maternal symptoms", *Int J Mol Med*, vol. 16, no. 1, pp. 79-84.

327. Aban, M., Cinel, L., Arslan, M., Dilek, U., Kaplanoglu, M., Arpaci, R., & Dilek, S. 2004, "Expression of Nuclear Factor-Kappa B and Placental Apoptosis in Pregnancies Complicated with Intrauterine Growth Restriction and Preeclampsia: An Immunohistochemical Study", *The Tohoku Journal of Experimental Medicine*, vol. 204, no. 3, pp. 195-202.

328. Heazell, A. E. P. & Crocker, I. P. 2008, "Live and Let Die - Regulation of Villous Trophoblast Apoptosis in Normal and Abnormal Pregnancies", *Placenta*, vol. 29, no. 9, pp. 772-783.

329. Crocker, I. P., Cooper, S., Ong, S. C., & Baker, P. N. 2003, "Differences in apoptotic susceptibility of cytotrophoblasts and syncytiotrophoblasts in normal pregnancy to those complicated with preeclampsia and intrauterine growth restriction", *American Journal of Pathology.162(2):637-43*.

330. Knerr I, Schare M, Hermann K, Kausler S, Lehner M, Vogler T, Rascher W, & Meißner U 2007, "Fusiogenic endogenous-retroviral syncytin-1 exerts anti-apoptotic functions in straurosporine-challenged CHO cells", *Apoptosis*, vol. 12, pp. 37-43.

331. Makris, A., Thornton, C., Thompson, J., Thomson, S., Martin, R., Ogle, R., Waugh, R., McKenzie, P., Kirwan, P., & Hennessy, A. 2007, "Uteroplacental ischemia results in proteinuric hypertension and elevated sFLT-1", *Kidney Int*, vol. 71, no. 10, pp. 977-984.

332. Walsh SW et al 2000, "Placental isoprotane is significantly increased in pre-eclampsia", *Faseb*, vol. 14, pp. 1289-1296.

333. Myatt L & Cui X 2004, "Oxidative stress in the placenta", *Histochemistry & Cell Biology*, vol. 122, pp. 369-382.

334. Luft, F. C. 2006, "Soluble endoglin (sEng) joins the soluble fms-like tyrosine kinase (sFlt) receptor as a pre-eclampsia molecule", *Nephrology Dialysis Transplantation*, vol. 21, no. 11, pp. 3052-3054.

335. Knight M, Redman CWG, Linton EA, & Sargent IL 1998, "Shedding of syncytiotrophblast microvilli into the maternal circulation in pre-eclamptic pregnancies", *British Journal of Obstetrics & Gynaecology*, vol. 105, pp. 632-640.

336. Chen CP, Wang KG, Chen CY, Yu C, Chuang HC, & Chen H 2006, "Altered placental syncytin and its receptor ASCT2 expression in placental development and pre-eclampsia", *BJOG*, vol. 113, no. 2, pp. 152-158.

337. Knerr I, Beinder E, & Rascher W 2002, "Syncytin, a novel human endogenous retroviral gene in human placenta: Evidence for its dysregulation in pre-eclampsia and HELLP syndrome", *Am J Obstet Gynecol*, vol. 186, pp. 210-213.

338. Lee X, Keith JC Jr, Strumm N, Moutsatsos I, McCoy JM, Crum CP, Genest D, Chin D, Ehrenfels C, Pijnenborg R, van Assche FA, & Mi S 2001, "Downregulation of placental syncytin expression and abnormal protein localisation in pre-eclampsia", *Placenta*, vol. 22, pp. 808-812.

339. Wich C, Kausler S, Dotsch J, Rascher W, & Knerr I 2009, "Syncytin-1 and Glial Cells Missing a: Hypoxia-induced Deregulated Gene Expression along with Disordered Cell Fusion in Primary Term Human Trophoblasts", *Gynecol Obstet Invest*, vol. 68, pp. 9-18.

340. Jones CJ & Fox H 1980, "An ultrastructural and ultrahistochemical study of the human placenta in maternal pre-eclampsia", *Placenta*, vol. 1, pp. 61-76.

341. Aupeix K, Hugel B, Martin T, Bischoff P, Lill H, Pasquali JL, & Freyssinet JM 1997, "The significance of shed membrane particles during programmed cell death in vitro, and in vivo, in HIV-1 infection", *J Clin Invest*, vol. 99, pp. 1546-1554.

342. Drewlo S, Baczyk D, & Kingdom J. GCM1 Regulation of sflt-1 Expression in First Trimester Placental Villi: The Missing Link between Disordered Trophoblast Differentiation and the Development of Severe Early-Onset Preeclampsia. Meeting for the Society for Gynecological Investigation, Glasgow . 2009.

343. Filiano, J. J. 1994, "Arcuate nucleus hypoplasia in sudden infant death syndrome: a review.", *Biology of the Neonate.65(3-4):156-9*.

344. Jauniaux, E. & Burton, G. J. 2007, "Morphological and biological effects of maternal exposure to tobacco smoke on the feto-placental unit. [Review] [83 refs]", *Early Human Development.83(11):699-706*.

345. Alsat W, Wyplosz P, Malassine A, Guibourdenche J, Porquet D, Nessmann C, & Evain-Brion D 1996, "Hypoxia impairs cell fusion and differentiation process in human cytotrophoblast, in vitro", *J Cell Physiol*, vol. 168, pp. 346-353.

346. Mayhew TM, Bowles C, & Yücel F 2002, "Hypobaric Hypoxia and Villous rophoblast: Evidence that Human Pregnancy at High Altitude Perturbs Epithelial Turnover and Coagulation-Fibrinolysis in the Intervillous Space", *Placenta*, vol. 23, pp. 154-162.

347. Myatt, L. 2006, "Placental adaptive responses and fetal programming", *The Journal of Physiology*, vol. 572, no. 1, pp. 25-30.

348. Jansson, T. & Powell, T. L. 2006, "Human Placental Transport in Altered Fetal Growth: Does the Placenta Function as a Nutrient Sensor? - A Review", *Placenta*, vol. 27, no. Supplement 1, pp. 91-97.

349. Chang, M., Mukherjea, D., Gobble, R. M., Groesch, K. A., Torry, R. J., & Torry, D. S. 2008, "Glial Cell Missing 1 Regulates Placental Growth Factor (PGF) Gene Transcription in Human Trophoblast", *Biology of Reproduction*, vol. 78, no. 5, pp. 841-851.

350. Heinonen, S., Taipale, P., & Saarikoski, S. 2001, "Weights of Placentae From Small-for-Gestational Age Infants Revisited", *Placenta*, vol. 22, no. 5, pp. 399-404.

351. McCaig, D. & Lyall, F. 2009, "Hypoxia Upregulates GCM1 in Human Placenta Explants", *Hypertension in Pregnancy*.

352. Pardi, G., Marconi, A. M., & Cetin, I. 2002, "Placental-fetal Interrelationship in IUGR Fetuses-A Review", *Placenta*, vol. 23, no. Supplement 1, p. S136-S141.

353. Mayhew, T. M., Jackson, M. R., & Haas, J. D. 1986, "Microscopical morphology of the human placenta and its effects on oxygen diffusion: a morphometric model", *Placenta.7(2):121-31,* p. -Apr.

354. Mayhew, T. M., Jackson, M. R., & Boyd, P. A. 1993, "Changes in oxygen diffusive conductances of human placentae during gestation (10-41 weeks) are commensurate with the gain in fetal weight", *Placenta.14(1):51-61,* p. -Feb.

355. Hershkovitz R, Kingdom JC, Geary M, & Rodeck CH. Fetal cerebral blood flow redistribution in late gestation: identification of compromise in small fetuses with normal umbilical artery Doppler. Ultrasound in Obstetrics & Gynecology 15[3], 209-212. 2000.

356. Burton GJ & Jauniaux E. Sonographic, stereological and Doppler flow velocimetric assessments of placental maturity. Br J Obstet Gynaecol 102, 818-25. 1995.

357. Coan, P. M., Angiolini E, Sandovici I, Burton G.J, Constância M, & Fowden A.L 2008, "Adaptations in placental nutrient transfer capacity to meet fetal growth demands depend on placental size in mice", *The Journal of Physiology Online*, vol. 586, no. 18, pp. 4567-4576.

358. Jackson, M. R., Mayhew, T. M., & Haas, J. D. 1988, "On the factors which contribute to thinning of the villous membrane in human placentae at high altitude. I. Thinning and regional variation in thickness of trophoblast", *Placenta.9(1):1-8,* p. -Feb.

9 Appendix

Appendix 1: Clinical Data

1. Toronto Cohort

Case	Diagnosis	PM No.	ID	GA	BW	BW Centile	MA	Parity	Sex	Highest BP	Uterine Doppler	Umbilical art PI	Umbilical EDF	Obstetric Hist	Medical Hist.	MOD
1	PT control	P4677	3828	26	970	50-90	17	0	M	NA	ND	ND	ND	No	No	vag
2	PT control	P4320	CD7	27.4	990	10-50	27	G3P2	M	NA	ND	ND	ND			vag
3	PT control	P4661	3414	28	1150	10-50		0	M	NA	0	ND	ND	No	No	vag
4	PT control	P4675	3685	28	1510	90-95	29	0	M	NA	ND	ND	ND	No	No	c/s
5	PT control	P4322	CD11	29	1400	50-90	29		M	NA	ND	ND	ND			vag
6	PT control	P4893	4183	30	1615	10-50	34	0	M	NA	ND	ND	ND			vag
7	PT control	P4323	CD1	30	1600	50-90	33	G1P0	M	NA	ND	ND	ND			vag
8	PT control	P4321	1159	30	1810	90-95		2	F	NA	ND	ND	ND	PT	IDDM	c/s
9	PT control	P4319	1226	31	1780	50-90	38	G5P0	F	NA	ND	ND	ND			c/s
10	PT control	P4665	3428	31	1800	50-90	34	0	F	NA	0	ND	ND	No	No	vag
11	PT control	P4663	3416	32	1500	10-50	23	2	F	NA	ND	ND	ND	No	ITP	c/s
12	PT control	P3853	756	32	1630	10-50	19	G2P0	M	NA	ND	ND	ND			c/s
13	Term control	P4672	3698	33	2300	50-90	30	0	F	NA	ND	0.8	0	No	No	c/s
14	Term control	P4899	4736	33	2020	10-50	32	1	M	NA	ND	ND	ND	No	No	vag
15	Term control	P4324	1183	35	2700	50-90	34	G4P3	M	NA	ND	ND	ND			c/s
16	Term control	P4666	3412	37	2640	10-50	42	0	F	NA	ND	ND	ND	No	DVT	c/s
17	Term control	P4676	3867	38	3090	10-50	30	1	F	NA	ND	ND	ND	No	No	c/s
18	Term control	P4892	4006	38	3910	90-95	36	1	F	NA	ND	ND	ND	No	No	c/s
19	Term control	P5182	5076	38	3020	10-50	35	0	M	NA	ND	ND	ND	No	No	c/s
20	Term control	P5178	4827	39	2960	10-50	33	0	M	NA	ND	ND	ND	No	No	c/s
21	Term control	P5179	4835	40	3260	10-50	26	0	M	NA	ND	ND	ND	No	No	vag
22	Term control	P5183	5077	40	4110	10-50	26	2	M	NA	ND	ND	ND	No	No	vag
23	Term control	P3903	N/A	41	3520	50-90	37	1	M	120/80	normal	ND	ND	No	No	c/s
24	Term control	P4895	4333	41	4690	95-97	33	0	M	NA	ND	ND	ND	No	No	c/s
25	Term control	P4901	4791	41	4070	50-90	37	1	M	120/80	ND	ND	ND	No	No	vag

Case	Diagnosis	ACOG	GA	BW	BW Centile	MA	Parity	Sex	Highest BP	Protein-uria	Uterine Doppler	Umbilical art PI	Umbilical EDF	Obstetric Hist	Medical Hist.	MOD	PD
1	PET + HELLP	severe	26	710	10-50	23	0	M	180/100	3	ND	normal	normal	No	No	c/s	
2	PET	severe	27	790	10-50	28	0	M	180/123	4	normal	normal	normal	No	No	c/s	
3	PET	severe	33	940	10-50	33	1	F	180/118	4	normal	PI 1.7	1 (0)	PET, PT	Chr.HTN	c/s	
4	PET	severe	29	1210	10-50	35	0	F	150/110	4	1	normal	normal	No	No	c/s	
5	PET + HELLP	severe	29	1130	10-50	43	0	F	160/90	540mg/24hr	normal		1 (0)	ND	ND	c/s	
6	PET + HELLP	severe	29	1200	10-50	35	ND	M	160/110	4	ND	normal	normal	No	IDDM	c/s	
7	PET	severe	30	1280	10-50	17	0	M	170/120	2	normal	normal	normal	ND	ND	c/s	
8	PET	severe	30	1280	10-50	22			160/110	2	normal	normal	normal				
9	PET + HELLP	severe	31	1400	10-50	37	G1P0	M	170/110	3	normal	normal	normal			c/s	
10	PET	severe	31	1300	10-50	26	G3P2	F	180/120	3	ND		1	ND	ND	c/s	
11	PET	severe	32	1550	10-50	ND			140/92	3	ND	normal	normal				
12	PET	mild	33	1970	10-50	28	0	M	150/105	2	normal	normal	normal	ND	ND	c/s	
13	PET	severe	35	2250	10-50	27	1	M	164/107	3	0	normal	normal	No	No	vag	
14	PET + HELLP	severe	36	2640	10-50	30	0	M	164/94	3	ND	normal	normal	No	No	c/s	
15	PET	mild	36.5	3360	10-50				146/98	trace	utero.insuf						
16	PET	severe	38	4020	10-50	38	ND	ND	160/95		normal	normal	normal	ND	ND	ND	
17	PET	mild	40	3400	10-50	28	ND	ND	155/100		normal	normal	normal	ND	ND	ND	
1	IUGR	severe	26	475	<3	24	0	F		nil	2		ND	No	No	vag	IUD
2	IUGR	severe	28	680	<3	33	0	F	140/95	nil						c/s	
3	IUGR	severe	30	900	3'-5	28	0	M		nil	0		2	No	No	c/s	No
4	IUGR	severe	31	700	<3			M	128/74	nil		20	1				
5	IUGR	severe	31.4	1260	5-10th			F	127/98	nil			1				
6	IUGR	severe	33	1160	<3	27	1	M		nil	0		1	No	No	c/s	No
7	IUGR	severe	34.3	1304	<3	38	G2P1	M		nil			1*2			c/s	No
8	IUGR		37	2040	<3	34	G2P1	F	115/67	1+	0		ND			c/s	
9	IUGR		37	2400	5-10	30	0	M		nil	0		0	No	No	vag	No

Case	Diagnosis	ACOG	GA	BW	BW Centile	MA	Parity	Sex	Highest BP	PU	Uterine Doppler	Umbilical art. PI	Umbilical EDF	Obs. Hist	Medical Hist.	MOD	PD
1	IUGR + PET	severe	24	420	< 5	38	G1P0		180/100	2	ND	normal	normal			vag	SB
2	IUGR + PET + HELLP	severe	25	500	<3	31	1	M	150/100	3	normal	normal	normal	PET,PT	No	c/s	No
3	IUGR + PET		26	560	<3	30	G10P0	M			normal	PI 1.7	1 (0)			vag	SB
4	IUGR + PET	severe	26	680	5-10	40	G1P0	M	190/110	4	1	normal	normal			c/s	
5	IUGR + PET	severe	26	790	5-10th	36	3	M	160/100	3	normal		1 (0)	PET, PT	Chr.HTN	c/s	
6	IUGR + PET	severe	26	740	5-10th	28		M	150/100	3	ND	normal	normal	No	Chr.HTN	c/s	No
7	IUGR + PET	severe	26	480	5	30	1	F	170/106	3	normal	normal	normal	No	Chr.HTN	vag	IUD
8	IUGR + PET	severe	29	820	5-10	33	G2P1	F	160/100	3	normal	normal	normal			c/s	SB
9	IUGR + PET	severe	28	750	3-5	35	0	F	180/110	4	normal	normal	normal	No	No	vag	No
10	IUGR + PET + HELLP	severe	28	750	3-5	39	G2P1	M	180/110	4	ND		1		Chr.HTN	c/s	
11	IUGR + PET + HELLP	severe	28	720	<3	20	G1P0	M	150/100	3	ND	normal	normal			vag	
12	IUGR + PET + HELLP	severe	29	960	5-10	29	G1P0	M	160/110	3	normal	normal	normal			c/s	No
13	IUGR + PET	severe	29	860	5-10	41	G3P0	F	175/105	2	0	normal	normal			c/s	No
14	IUGR + PET	severe	29	820	<3	24	G1P0	M	180/110	3	ND	normal	normal			c/s	No
15	IUGR + PET		29	770	<5	39	0	F	200/110	nil	utero.insuf					c/s	
16	IUGR + PET	severe	30	860	3-5	19	0	F	144/96	2	normal	normal	normal	No	No	c/s	No
17	IUGR + PET		31	1160	5-10	30	0	F	190/100	nil	normal	normal	normal			c/s	
18	IUGR + PET	severe	31	1080	5-10	22	0	F	160/110	2	2		ND	No	No	c/s	No
19	IUGR + PET	severe	32	1370	5'-10	36	1	M	160/100	3				No	DDM	c/s	No
20	IUGR + PET	severe	34	570	<3	43	1	F	150/80	2	0		2	No	Ess.HTN	c/s	No
21	IUGR + PET	severe	35	1560	<3				160/90	3		20	1				
22	IUGR + PET	severe	37	2160	<3	34	0	M	160/110	4			1	No	No	vag	No
23	IUGR + PET	severe	34.5	1640	<3	32	G2P0	M	150/100	4	0		1			c/s	No
24	IUGR + PET	severe	37	1440	<3				150/110				1*2				No
25	IUGR + PET	severe	38	2325	<3	28	0	M	140/100	2	0		ND	No	No	vag	No

2. SIDS Cohort

Case	Diagnosis	GA	BW	MA	Parity	Sex	Highest BP	Smoker	MOD	PM
1	Term Control	40	3080		0+2	F	ND	0	svd	2
2	Term Control	40	4026		3+0	M	ND	0	svd	0
3	Term Control	41	3360	27	3+1	F		5-12	svd	1
4	Term Control	41	4070	37	1	M	120/80	0	svd	0
5	Term Control	41	4690	33	0	M	ND	0	c/s	0
6	Term Control	41	3520	37	1	M	120/80	0	c/s	0
7	Term Control	41	3260			M		10	svd	0
8	Term Control	38	2730	36	1	M	ND	0	c/s	0
9	Term Control	40	3260	26	0	M	ND	0	svd	0
10	Term Control	40	4110	26	2	M	ND	0	svd	0
11	Term Control	39	2960	33	0	M	ND	0	c/s	0
12	Term Control	38	3020	35	0	M	ND	0	c/s	0
1	SIDS NBW	38	3110	24	1	M		10-20	svd	3
2	SIDS NBW	40	3210	19	1+0	F		20	svd	0
3	SIDS NBW	40	3910	19	1	F		20	svd epi	1
4	SIDS NBW	40	3595	15	0	M		30	lscs	0
5	SIDS NBW	40	3585	27	2	F		20	svd	0
6	SIDS NBW	41	3360	18	2	M		0	lscs	0
7	SIDS NBW	40	3620	20	1+0	F		10	bfd	0
8	SIDS NBW	40	3130	31	2	F		0	svd	0
9	SIDS NBW	39	3600	25	2+0	F	120/60	5	svd	0
10	SIDS NBW	37	3540	39	5	M	130/80	20	LSCS	1
11	SIDS NBW	39	3220	22	G2P1	F	120/74	10	SVD	0
12	SIDS NBW	38	3220	33	0+1	M	120/85	20	lscs	0
13	SIDS LBW	39	2320	25	3+0	F		0	lscs	0
14	SIDS LBW	39	3420	30	1	F		25	svd	0
15	SIDS LBW	39	2375	26	1+1	M		5	lscs em	0
16	SIDS LBW	40	2800	32	1	M		0	svd	0
17	SIDS LBW	40	2570	21	1	F		5-10	svd	0
18	SIDS LBW	41	2655	31	0	F		7	svd	0
19	SIDS LBW	41	3070	19	0	M		0-10	svd	0
20	SIDS LBW	41	3115	33	0	M		10	svd	0
21	SIDS LBW	41	3000	22	1	M		0	lscs	2
22	SIDS LBW	41	1740	41	0+1	M		0	lscs em	0
23	SIDS LBW	41	2320	24	1+0	F	120/70	10	vacuum	1
24	SIDS LBW	39	1920	46	1+0	F		ND	svd	1

Appendix 2: Villous Volumes

1. Toronto Cohort

			TOTAL VOLUME (cm^3)				VOLUME DENSITY		
CASE	DIAGNOSIS	PLACENTAL WT. (g)	PLACENTAL VOL	ALL VILLI	SV & IMV	MV & TV	ALL VILLI	SV & IMV	MV & TV
1	PT control	350	320	144	129	15	0.45	0.40	0.05
2	PT control	220	220	107	35	72	0.49	0.16	0.33
3	PT control	280	300	115	83	32	0.38	0.28	0.11
4	PT control	230	220	107	74	32	0.48	0.34	0.15
5	PT control	300	280	144	89	55	0.51	0.32	0.20
6	PT control	387	480	215	167	48	0.45	0.35	0.10
7	PT control	450	345	150	81	69	0.43	0.23	0.20
8	PT control	500	425	219	132	86	0.51	0.31	0.20
9	PT control	360	350	175	77	98	0.50	0.22	0.28
10	PT control	350	360	147	56	90	0.41	0.16	0.25
11	PT control	360	350	120	30	89	0.34	0.09	0.26
12	PT control	330	230	118	34	83	0.51	0.15	0.36
13	Term control	500	501	287	135	152	0.57	0.27	0.30
14	Term control	360	360	153	65	88	0.43	0.18	0.24
15	Term control	477	702	264	64	200	0.38	0.09	0.29
16	Term control	550	540	209	112	97	0.39	0.21	0.18
17	Term control	640	630	312	196	115	0.49	0.31	0.18
18	Term control	640	620	304	87	216	0.49	0.14	0.35
19	Term control	650	620	281	183	98	0.45	0.29	0.16
20	Term control	450	450	187	90	97	0.42	0.20	0.22
21	Term control	480	490	226	95	132	0.46	0.19	0.27
22	Term control	600	620	279	210	69	0.45	0.34	0.11
23	Term control	398.4	340	182	127	55	0.54	0.37	0.16
24	Term control	660	640	271	144	126	0.42	0.23	0.20
25	Term control	700	700	265	165	100	0.38	0.24	0.14

			TOTAL VOLUME (cm^3)				VOLUME DENSITY		
CASE	**DIAGNOSIS**	**PLACENTAL WT. (g)**	**PLACENTAL VOL**	**ALL VILLI**	**SV & IMV**	**MV & TV**	**ALL VILLI**	**SV & IMV**	**MV & TV**
1	PET + HELLP	150	130	58	26	32	0.45	0.20	0.25
2	PET	410	420	262	233	30	0.62	0.55	0.07
3	PET	300	250	107	72	35	0.43	0.29	0.14
4	PET	300	290	148	73	75	0.51	0.25	0.26
5	PET + HELLP	410	260	111	49	62	0.43	0.19	0.24
6	PET + HELLP	310	350	184	120	64	0.53	0.34	0.18
7	PET	300	320	109	46	63	0.34	0.15	0.20
8	PET	300	320	120	52	68	0.37	0.16	0.21
9	PET + HELLP	400	400	205	126	79	0.51	0.32	0.20
10	PET	350	425	204	103	101	0.48	0.24	0.24
11	PET	400	380	170	89	81	0.45	0.23	0.21
12	PET	352	300	146	80	66	0.49	0.27	0.22
13	PET	400	600	249	85	164	0.42	0.14	0.27
14	PET + HELLP	580	380	142	76	66	0.37	0.20	0.17
15	PET	505	550	254	125	129	0.46	0.23	0.23
16	PET	603	575	362	97	265	0.63	0.17	0.46
17	PET	534	515	327	73	254	0.64	0.14	0.49
1	IUGR	260	220	106	85	21	0.48	0.39	0.09
2	IUGR	200	126.5	65	50	15	0.52	0.39	0.12
3	IUGR	150	180	81	52	30	0.45	0.29	0.16
4	IUGR	185	100	34	15	19	0.34	0.15	0.19
5	IUGR	195	165	75	43	31	0.45	0.26	0.19
6	IUGR	180	150	72	46	26	0.48	0.30	0.17
7	IUGR	270	300	162	113	49	0.54	0.38	0.16
8	IUGR	338	338	162	79	82	0.48	0.24	0.24
9	IUGR	302	312	193	83	110	0.62	0.27	0.35

			TOTAL VOLUME (cm^3)				VOLUME DENSITY		
CASE	DIAGNOSIS	PLACENTAL WT. (g)	PLACENTAL VOL	ALL VILLI	SV & IMV	MV & TV	ALL VILLI	SV & IMV	MV & TV
1	IUGR + PET	100	127.5	59	35	24	0.46	0.28	0.19
2	IUGR + PET + HELLP	150	150	74	50	24	0.49	0.33	0.16
3	IUGR + PET	270	160	59	20	39	0.37	0.13	0.24
4	IUGR + PET	160	130	73	62	11	0.56	0.48	0.09
5	IUGR + PET	240	220	117	86	30	0.53	0.39	0.14
6	IUGR + PET	220	99	42	28	15	0.43	0.28	0.15
7	IUGR + PET	109	150	74	52	22	0.49	0.35	0.15
8	IUGR + PET	220	150	84	62	22	0.56	0.42	0.14
9	IUGR + PET	170	130	51	18	32	0.39	0.14	0.25
10	IUGR + PET + HELLP	170	145	74	49	25	0.51	0.34	0.17
11	IUGR + PET + HELLP	163	150	56	21	35	0.37	0.14	0.23
12	IUGR + PET + HELLP	264	325	141	103	39	0.43	0.32	0.12
13	IUGR + PET	170	130	72	58	14	0.55	0.44	0.11
14	IUGR + PET	300	200	110	73	37	0.55	0.37	0.18
15	IUGR + PET	200	220	96	61	35	0.44	0.28	0.16
16	IUGR + PET	190	160	73	42	31	0.45	0.26	0.19
17	IUGR + PET	180	200	104	60	44	0.52	0.30	0.22
18	IUGR + PET	290	89	47	34	14	0.53	0.38	0.15
19	IUGR + PET	314	276	152	63	89	0.55	0.23	0.32
20	IUGR + PET	420	250	127	87	41	0.51	0.35	0.16
21	IUGR + PET	475	410	149	21	128	0.36	0.05	0.31
22	IUGR + PET	400	455	207	89	118	0.45	0.20	0.26
23	IUGR + PET	260	400	182	104	79	0.46	0.26	0.20
24	IUGR + PET	256	240	135	89	47	0.56	0.37	0.19
25	IUGR + PET	500	460	199	130	69	0.43	0.28	0.15

2. SIDS Cohort

CASE	DIAGNOSIS	PLACENTAL WT. (g)	PLACENTAL VOL	ALL VILLI	SV	INT	TV
1	Term Control	458	540	224	62	141	20
2	Term Control	598	450	178	90	58	39
3	Term Control	480	488	295	37	130	129
4	Term Control	700	510	360	18	197	145
5	Term Control	660	490	226	92	99	36
6	Term Control	398	620	279	52	214	12
7	Term Control	462	413	281	55	188	38
8	Term Control	656	496	324	42	87	194
9	Term Control	480	464	288	45	90	154
10	Term Control	600	340	182	67	109	6
11	Term Control	450	700	265	74	164	27
12	Term Control	650	640	270	55	168	47
1	SIDS NBW	280	596	444	59	126	258
2	SIDS NBW	462	434	322	42	103	176
3	SIDS NBW	608	556	394	83	132	178
4	SIDS NBW	444	535	350	52	96	196
5	SIDS NBW	466	454	365	39	130	196
6	SIDS NBW	580	399	216	23	47	145
7	SIDS NBW	570	432	333	29	144	190
8	SIDS NBW	560	502	325	65	90	184
9	SIDS NBW	458	573	353	109	71	173
10	SIDS NBW	524	373	251	42	80	129
11	SIDS NBW	700	460	359	40	131	188
12	SIDS NBW	480	607	449	211	161	77
13	SIDS LBW	434	391	271	37	98	135
14	SIDS LBW	376	645	362	81	74	208
15	SIDS LBW	443	445	275	52	65	157
16	SIDS LBW	406	365	210	38	44	128
17	SIDS LBW	412	248	178	80	62	35
18	SIDS LBW	360	392	315	30	105	181
19	SIDS LBW	676	449	318	64	106	148
20	SIDS LBW	456	405	280	53	98	129
21	SIDS LBW	408	420	345	44	128	174
22	SIDS LBW	176	361	290	34	120	136
23	SIDS LBW	254	159	98	44	42	12
24	SIDS LBW	290	297	196	107	68	21

Appendix 3: Cytotrophoblast Volume and Number

1. Toronto Cohort

		TOTALS									DENSITIES (μm^{-3})								
CASE	**DIAGNOSIS**	**VOL. CT (cm^3)**	SV & IMV (cm^3)	MV & TV (cm^3)	**NO.CT**	SV & IMV	MV & TV	**NO. Ki-67 +VE CT**	MV & TV	SV & IMV	**VOL. CT**	SV & IMV	MV & TV	**NO. CT**	SV & IMV	MV & TV	**NO. Ki-67 +VE CT**	SV & IMV	MV & TV
1	PT control	1.87	1.72	0.15	9.2E+10	4.5E+10	4.7E+10	4.0E+10	1.6E+10	2.4E+10	0.023	0.013	0.010	2.9E-04	1.4E-04	1.5E-04	1.2E-04	4.9E-05	7.5E-05
2	PT control	1.00	0.28	0.72	5.2E+10	5.3E+09	4.7E+10	1.1E+10	1.1E+09	1.0E+10	0.018	0.008	0.010	2.4E-04	2.4E-05	2.1E-04	5.2E-05	4.9E-06	4.7E-05
3	PT control	1.08	0.86	0.22	7.0E+10	2.8E+10	4.2E+10	1.7E+10	7.2E+09	9.6E+09	0.017	0.010	0.007	2.3E-04	9.4E-05	1.4E-04	5.6E-05	2.4E-05	3.2E-05
4	PT control	0.56	0.36	0.19	5.1E+10	1.1E+10	4.0E+10	1.8E+10	3.5E+09	1.5E+10	0.011	0.005	0.006	2.3E-04	5.1E-05	1.8E-04	8.3E-05	1.6E-05	6.7E-05
5	PT control	1.25	0.52	0.72	7.8E+10	1.3E+10	6.6E+10	1.3E+10	9.6E+08	1.2E+10	0.019	0.006	0.013	2.8E-04	4.5E-05	2.3E-04	4.5E-05	3.4E-06	4.1E-05
6	PT control	1.40	0.75	0.65	8.5E+10	3.6E+10	4.9E+10	2.9E+10	1.4E+10	1.5E+10	0.018	0.005	0.014	1.8E-04	7.5E-05	1.0E-04	6.1E-05	2.9E-05	3.2E-05
7	PT control	1.02	0.40	0.61	6.3E+10	7.0E+09	5.5E+10	1.8E+10	3.3E+09	1.4E+10	0.014	0.005	0.009	1.8E-04	2.0E-05	1.6E-04	5.2E-05	9.7E-06	4.2E-05
8	PT control	1.59	0.89	0.71	7.8E+10	1.9E+10	6.0E+10	1.3E+10	2.9E+09	1.0E+10	0.015	0.007	0.008	1.8E-04	4.5E-05	1.4E-04	3.1E-05	6.9E-06	2.4E-05
9	PT control	1.39	0.46	0.94	7.3E+10	1.5E+10	5.8E+10	2.5E+10	3.2E+09	2.2E+10	0.016	0.006	0.010	2.1E-04	4.4E-05	1.6E-04	7.1E-05	9.1E-06	6.2E-05
10	PT control	0.94	0.20	0.74	6.5E+10	1.1E+10	5.6E+10	3.2E+10	2.7E+09	2.9E+10	0.012	0.004	0.008	1.8E-04	3.0E-05	1.6E-04	8.8E-05	7.5E-06	8.0E-05
11	PT control	0.69	0.06	0.63	5.7E+10	1.2E+10	4.5E+10	1.2E+10	2.5E+09	9.8E+09	0.009	0.002	0.007	1.6E-04	3.5E-05	1.3E-04	3.5E-05	7.0E-06	2.8E-05
12	PT control	1.33	0.13	1.21	4.6E+10	9.7E+09	3.6E+10	1.1E+10	2.0E+09	8.9E+09	0.018	0.004	0.015	2.0E-04	4.2E-05	1.6E-04	4.7E-05	8.8E-06	3.9E-05
13	Term control	2.87	0.64	2.23	1.1E+11	1.5E+10	9.4E+10	2.0E+10	8.6E+08	1.9E+10	0.019	0.005	0.015	2.2E-04	3.1E-05	1.9E-04	4.0E-05	1.7E-06	3.8E-05
14	Term control	1.33	0.37	0.96	8.6E+10	3.1E+10	5.5E+10	2.3E+10	5.8E+09	1.7E+10	0.017	0.006	0.011	2.4E-04	8.6E-05	1.5E-04	6.4E-05	1.6E-05	4.8E-05
15	Term control	1.65	0.07	1.58	1.2E+11	1.6E+10	1.0E+11	3.1E+10	5.5E+09	2.5E+10	0.009	0.001	0.008	1.7E-04	2.3E-05	1.4E-04	4.4E-05	7.8E-06	3.6E-05
16	Term control	1.37	0.49	0.87	1.1E+11	1.7E+10	9.1E+10	3.0E+10	5.3E+09	2.5E+10	0.013	0.004	0.009	2.0E-04	3.2E-05	1.7E-04	5.6E-05	9.7E-06	4.6E-05
17	Term control	1.10	0.55	0.55	1.1E+11	1.6E+10	1.0E+11	2.5E+10	2.4E+09	2.3E+10	0.008	0.003	0.005	1.8E-04	2.6E-05	1.6E-04	4.0E-05	3.8E-06	3.6E-05
18	Term control	2.07	0.10	1.97	9.0E+10	1.4E+10	7.4E+10	3.4E+10	4.2E+09	3.0E+10	0.010	0.001	0.009	1.5E-04	2.3E-05	1.2E-04	5.4E-05	6.8E-06	4.8E-05
19	Term control	5.37	4.20	1.17	1.1E+11	3.6E+10	7.0E+10	3.7E+10	9.5E+09	2.7E+10	0.035	0.023	0.012	1.7E-04	5.8E-05	1.1E-04	5.9E-05	1.5E-05	4.4E-05
20	Term control	1.86	0.26	1.60	5.6E+10	8.8E+09	4.7E+10	1.4E+10	2.9E+09	1.1E+10	0.019	0.003	0.017	1.3E-04	2.0E-05	1.1E-04	3.1E-05	6.5E-06	2.4E-05
21	Term control	3.80	1.06	2.74	6.7E+10	2.6E+10	4.1E+10	1.6E+10	4.5E+09	1.1E+10	0.032	0.011	0.021	1.4E-04	5.4E-05	8.3E-05	3.2E-05	9.2E-06	2.3E-05
22	Term control	5.94	5.19	0.75	1.1E+11	2.1E+10	8.8E+10	2.3E+10	4.0E+09	1.9E+10	0.036	0.025	0.011	1.8E-04	3.4E-05	1.4E-04	3.6E-05	6.4E-06	3.0E-05
23	Term control	0.92	0.44	0.47	5.8E+10	2.3E+10	3.5E+10	2.1E+10	6.6E+09	1.4E+10	0.012	0.004	0.009	1.7E-04	6.8E-05	1.0E-04	6.1E-05	1.9E-05	4.2E-05
24	Term control	2.01	0.52	1.49	1.1E+11	3.0E+10	8.2E+10	2.4E+10	5.0E+09	1.9E+10	0.015	0.004	0.012	1.8E-04	4.7E-05	1.3E-04	3.7E-05	7.8E-06	2.9E-05
25	Term control	1.18	0.56	0.62	1.4E+11	6.0E+10	7.6E+10	4.1E+10	2.0E+10	2.1E+10	0.010	0.003	0.006	2.0E-04	8.6E-05	1.1E-04	5.8E-05	2.8E-05	3.0E-05

		TOTALS									DENSITIES (µm^{-3})								
CASE	**DIAGNOSIS**	**VOL. CT (cm^3)**	SV & IMV (cm^3)	MV & TV (cm^3)	**NO.CT**	SV & IMV	MV & TV	**NO. Ki-67 +VE CT**	MV & TV	SV & IMV	**VOL. CT**	SV & IMV	MV & TV	**NO. CT**	SV & IMV	MV & TV	**NO. Ki-67 +VE CT**	SV & IMV	MV & TV
1	PET + HELLP	0.41	0.10	0.31	2.4E+10	3.7E+09	2.0E+10	7.0E+09	1.2E+09	5.8E+09	0.014	0.004	0.010	2.4E+10	3.7E+09	2.0E+10	7.0E+09	1.2E+09	5.8E+09
2	PET	1.21	1.02	0.18	1.2E+11	6.8E+10	4.5E+10	2.3E+10	1.5E+10	8.5E+09	0.011	0.004	0.006	1.2E+11	6.8E+10	4.5E+10	2.3E+10	1.5E+10	8.5E+09
3	PET	0.84	0.36	0.48	4.4E+10	1.6E+10	2.9E+10	1.7E+10	5.0E+09	1.2E+10	0.019	0.005	0.014	4.4E+10	1.6E+10	2.9E+10	1.7E+10	5.0E+09	1.2E+10
4	PET	1.24	0.20	1.04	5.7E+10	5.2E+09	5.2E+10	2.9E+10	3.3E+09	2.6E+10	0.017	0.003	0.014	5.7E+10	5.2E+09	5.2E+10	2.9E+10	3.3E+09	2.6E+10
5	PET + HELLP	0.35	0.04	0.30	3.9E+10	8.4E+08	3.8E+10	1.7E+10	8.0E+08	1.6E+10	0.006	0.001	0.005	3.9E+10	8.4E+08	3.8E+10	1.7E+10	8.0E+08	1.6E+10
6	PET + HELLP	1.42	0.65	0.77	7.8E+10	3.6E+10	4.1E+10	2.7E+10	1.2E+10	1.5E+10	0.018	0.005	0.012	7.8E+10	3.6E+10	4.1E+10	2.7E+10	1.2E+10	1.5E+10
7	PET	0.89	0.16	0.73	5.7E+10	8.6E+09	4.8E+10	1.3E+10	1.7E+09	1.1E+10	0.015	0.003	0.012	5.7E+10	8.6E+09	4.8E+10	1.3E+10	1.7E+09	1.1E+10
8	PET	0.60	0.14	0.46	4.6E+10	1.5E+10	3.1E+10	1.3E+10	3.2E+09	1.0E+10	0.010	0.003	0.007	4.6E+10	1.5E+10	3.1E+10	1.3E+10	3.2E+09	1.0E+10
9	PET + HELLP	1.97	0.55	1.42	7.8E+10	1.6E+10	6.1E+10	2.9E+10	4.5E+09	2.4E+10	0.022	0.004	0.018	7.8E+10	1.6E+10	6.1E+10	2.9E+10	4.5E+09	2.4E+10
10	PET	1.74	0.32	1.42	9.0E+10	2.6E+10	6.5E+10	1.6E+10	8.8E+09	6.9E+09	0.017	0.003	0.014	9.0E+10	2.6E+10	6.5E+10	1.6E+10	8.8E+09	6.9E+09
11	PET	2.11	1.19	0.93	7.3E+10	3.5E+10	3.8E+10	2.2E+10	1.1E+10	1.1E+10	0.025	0.013	0.011	7.3E+10	3.5E+10	3.8E+10	2.2E+10	1.1E+10	1.1E+10
12	PET	0.77	0.21	0.56	5.3E+10	7.0E+09	4.6E+10	9.4E+09	1.0E+09	8.4E+09	0.011	0.003	0.009	1.8E-04	2.3E-05	1.5E-04	3.1E-05	3.5E-06	2.8E-05
13	PET	0.90	0.25	0.66	8.0E+10	9.3E+09	7.1E+10	2.7E+10	6.2E+09	2.1E+10	0.007	0.003	0.004	2.1E-04	2.4E-05	1.9E-04	7.1E-05	1.6E-05	5.5E-05
14	PET + HELLP	0.48	0.22	0.26	8.1E+10	2.3E+10	5.8E+10	3.2E+10	5.3E+09	2.6E+10	0.007	0.003	0.004	1.3E-04	3.8E-05	9.7E-05	5.3E-05	8.8E-06	4.4E-05
15	PET	3.20	1.08	2.13	1.0E+11	3.4E+10	6.9E+10	2.6E+10	1.1E+10	1.5E+10	0.025	0.009	0.017	1.9E-04	6.2E-05	1.3E-04	4.8E-05	2.0E-05	2.7E-05
16	PET	7.33	0.32	7.01	7.3E+10	8.0E+09	6.5E+10	2.7E+10	4.0E+09	2.3E+10	0.030	0.003	0.027	1.3E-04	1.4E-05	1.1E-04	4.6E-05	6.9E-06	3.9E-05
17	PET	6.14	0.29	5.85	5.6E+10	1.1E+10	4.5E+10	1.3E+10	4.2E+09	8.4E+09	0.027	0.004	0.023	1.1E-04	2.0E-05	8.8E-05	2.4E-05	8.2E-06	1.6E-05
1	IUGR	0.85	0.72	0.13	5.8E+10	2.3E+10	3.5E+10	7.9E+09	4.0E+09	4.0E+09	0.015	0.008	0.006	2.7E-04	1.1E-04	1.6E-04	3.6E-05	1.8E-05	1.8E-05
2	IUGR	0.31	0.19	0.12	2.5E+10	4.4E+09	2.1E+10	3.0E+09	9.9E+08	2.0E+09	0.012	0.004	0.008	2.0E-04	3.5E-05	1.6E-04	2.4E-05	7.8E-06	1.6E-05
3	IUGR	0.61	0.39	0.22	3.4E+10	1.1E+10	2.3E+10	8.5E+09	4.4E+09	4.0E+09	0.015	0.008	0.007	1.9E-04	6.3E-05	1.3E-04	4.7E-05	2.5E-05	2.2E-05
4	IUGR	0.30	0.08	0.21	2.0E+10	3.6E+09	1.6E+10	3.6E+09	3.6E+08	3.2E+09	0.017	0.006	0.011	2.0E-04	3.6E-05	1.6E-04	3.6E-05	3.6E-06	3.2E-05
5	IUGR	0.42	0.20	0.21	2.9E+10	1.2E+10	1.7E+10	6.1E+09	3.3E+09	2.9E+09	0.011	0.005	0.007	1.7E-04	7.2E-05	1.0E-04	3.7E-05	2.0E-05	1.7E-05
6	IUGR	0.20	0.09	0.10	3.1E+10	9.6E+09	2.1E+10	6.8E+09	2.4E+09	4.5E+09	0.006	0.002	0.004	2.0E-04	6.4E-05	1.4E-04	4.6E-05	1.6E-05	3.0E-05
7	IUGR	0.79	0.54	0.24	5.2E+10	1.2E+10	4.1E+10	1.3E+10	2.3E+09	1.1E+10	0.010	0.005	0.005	1.7E-04	4.0E-05	1.4E-04	4.3E-05	7.5E-06	3.5E-05
8	IUGR	0.81	0.24	0.58	6.8E+10	1.1E+10	5.7E+10	1.8E+10	2.0E+09	1.6E+10	0.010	0.003	0.007	2.0E-04	3.1E-05	1.7E-04	5.5E-05	5.9E-06	4.9E-05
9	IUGR	2.83	0.83	2.00	4.7E+10	8.1E+09	3.8E+10	1.5E+10	2.6E+09	1.3E+10	0.028	0.010	0.018	1.5E-04	2.6E-05	1.2E-04	4.9E-05	8.2E-06	4.1E-05

		TOTALS									DENSITIES (μm^{-3})								
CASE	**DIAGNOSIS**	**VOL. CT (cm^3)**	SV & IMV (cm^3)	MV & TV (cm^3)	**NO.CT**	SV & IMV	MV & TV	**NO. Ki-67 +VE CT**	MV & TV	SV & IMV	**VOL. CT**	SV & IMV	MV & TV	**NO. CT**	SV & IMV	MV & TV	**NO. Ki-67 +VE CT**	SV & IMV	MV & TV
1	IUGR + PET	0.32	0.17	0.15	2.6E+10	6.2E+09	2.0E+10	3.9E+09	2.6E+08	3.6E+09	0.011	0.005	0.006	2.0E-04	4.9E-05	1.5E-04	3.1E-05	2.0E-06	2.9E-05
2	IUGR + PET + HELLI	0.46	0.22	0.24	2.8E+10	4.2E+09	2.4E+10	7.0E+09	1.1E+09	5.9E+09	0.014	0.004	0.010	1.9E-04	2.8E-05	1.6E-04	4.7E-05	7.4E-06	3.9E-05
3	IUGR + PET	0.40	0.07	0.33	2.4E+10	5.9E+09	1.8E+10	8.6E+09	1.9E+09	6.7E+09	0.012	0.004	0.008	1.5E-04	3.7E-05	1.1E-04	5.3E-05	1.2E-05	4.2E-05
4	IUGR + PET	0.26	0.20	0.06	2.3E+10	8.4E+09	1.4E+10	3.9E+09	1.8E+09	2.1E+09	0.008	0.003	0.005	1.8E-04	6.5E-05	1.1E-04	3.0E-05	1.4E-05	1.6E-05
5	IUGR + PET	0.96	0.75	0.21	4.7E+10	7.4E+09	3.9E+10	1.0E+10	1.6E+09	8.9E+09	0.016	0.009	0.007	2.1E-04	3.3E-05	1.8E-04	4.8E-05	7.3E-06	4.0E-05
6	IUGR + PET	0.12	0.06	0.06	2.2E+10	3.8E+09	1.8E+10	4.8E+09	6.4E+08	4.1E+09	0.007	0.002	0.004	2.3E-04	3.8E-05	1.9E-04	4.8E-05	6.4E-06	4.2E-05
7	IUGR + PET	0.48	0.28	0.20	3.8E+10	1.1E+10	2.8E+10	6.2E+09	2.9E+09	3.3E+09	0.015	0.005	0.009	2.5E-04	7.1E-05	1.8E-04	4.2E-05	2.0E-05	2.2E-05
8	IUGR + PET	0.58	0.30	0.28	3.4E+10	7.6E+09	2.6E+10	6.0E+09	2.6E+08	5.8E+09	0.018	0.005	0.013	2.3E-04	5.1E-05	1.7E-04	4.0E-05	1.8E-06	3.9E-05
9	IUGR + PET	0.17	0.04	0.13	2.3E+10	5.1E+09	1.8E+10	4.6E+09	8.1E+08	3.8E+09	0.006	0.002	0.004	1.8E-04	3.9E-05	1.4E-04	3.5E-05	6.2E-06	2.9E-05
10	IUGR + PET + HELLI	0.38	0.09	0.30	2.6E+10	1.3E+09	2.4E+10	5.7E+09	2.6E+08	5.4E+09	0.014	0.002	0.012	1.8E-04	9.0E-06	1.7E-04	3.9E-05	1.8E-06	3.7E-05
11	IUGR + PET + HELLI	0.38	0.11	0.27	3.7E+10	1.7E+10	2.0E+10	7.2E+09	4.6E+09	2.6E+09	0.013	0.005	0.008	2.5E-04	1.1E-04	1.3E-04	4.8E-05	3.1E-05	1.8E-05
12	IUGR + PET + HELLI	0.60	0.30	0.30	7.2E+10	1.6E+10	5.6E+10	2.0E+10	5.6E+09	1.5E+10	0.011	0.003	0.008	2.2E-04	5.0E-05	1.7E-04	6.3E-05	1.7E-05	4.6E-05
13	IUGR + PET	0.35	0.23	0.12	2.4E+10	5.1E+09	1.9E+10	2.8E+09	5.1E+08	2.3E+09	0.013	0.004	0.009	1.8E-04	3.9E-05	1.4E-04	2.1E-05	3.9E-06	1.8E-05
14	IUGR + PET	0.46	0.20	0.26	4.4E+10	1.6E+10	2.9E+10	8.6E+09	3.0E+09	5.6E+09	0.010	0.003	0.007	2.2E-04	7.8E-05	1.4E-04	4.3E-05	1.5E-05	2.8E-05
15	IUGR + PET	0.47	0.15	0.33	2.8E+10	3.3E+09	2.4E+10	1.2E+10	2.9E+09	9.5E+09	0.012	0.002	0.009	1.8E-04	2.1E-05	1.5E-04	7.7E-05	1.8E-05	5.9E-05
16	IUGR + PET	0.38	0.09	0.29	3.7E+10	6.6E+09	3.1E+10	1.0E+10	2.2E+09	8.0E+09	0.012	0.002	0.010	1.9E-04	3.3E-05	1.6E-04	5.1E-05	1.1E-05	4.0E-05
17	IUGR + PET	0.41	0.14	0.26	1.8E+10	4.0E+09	1.4E+10	4.0E+09	1.2E+09	2.8E+09	0.008	0.002	0.006	2.0E-04	4.5E-05	1.6E-04	4.5E-05	1.3E-05	3.1E-05
18	IUGR + PET	0.43	0.27	0.16	4.0E+10	1.6E+09	3.8E+10	1.0E+10	0.0E+00	1.0E+10	0.020	0.008	0.012	1.8E-04	7.2E-06	1.7E-04	4.7E-05	0.0E+00	4.7E-05
19	IUGR + PET	3.24	0.28	2.97	4.2E+10	1.1E+10	3.0E+10	1.1E+10	1.2E+09	9.6E+09	0.038	0.004	0.034	1.5E-04	4.0E-05	1.1E-04	3.9E-05	4.4E-06	3.5E-05
20	IUGR + PET	0.77	0.57	0.20	4.1E+10	8.0E+09	3.3E+10	1.7E+10	3.0E+09	1.4E+10	0.012	0.007	0.005	1.6E-04	3.2E-05	1.3E-04	6.8E-05	1.2E-05	5.6E-05
21	IUGR + PET	3.11	0.10	3.01	5.6E+10	2.0E+10	3.7E+10	8.5E+09	3.2E+09	5.4E+09	0.028	0.005	0.024	1.4E-04	4.9E-05	9.0E-05	2.1E-05	7.7E-06	1.3E-05
22	IUGR + PET	2.71	0.76	1.94	9.5E+10	4.3E+10	5.0E+10	3.3E+10	9.9E+09	2.3E+10	0.025	0.009	0.017	2.1E-04	9.5E-05	1.1E-04	7.2E-05	2.2E-05	5.0E-05
23	IUGR + PET	0.99	0.33	0.66	6.4E+10	1.4E+10	5.0E+10	2.1E+10	3.1E+09	1.8E+10	0.012	0.003	0.008	1.6E-04	3.4E-05	1.2E-04	5.3E-05	7.6E-06	4.6E-05
24	IUGR + PET	0.91	0.37	0.54	3.0E+10	5.0E+09	2.5E+10	1.1E+10	1.7E+09	9.4E+09	0.016	0.004	0.012	1.2E-04	2.1E-05	1.0E-04	4.6E-05	6.9E-06	3.9E-05
25	IUGR + PET	1.01	0.42	0.59	6.4E+10	1.8E+10	4.6E+10	3.1E+10	7.1E+09	2.4E+10	0.012	0.003	0.009	1.4E-04	3.9E-05	1.0E-04	6.7E-05	1.5E-05	5.2E-05

2. SIDS Cohort

		TOTAL VOL (cm^3)				VOL. DENSITIES			
CASE	DIAGNOSIS	VOL. CT	SV	INT	TV	VOL. CT	SV	INT	TV
1	Term Control	2.98	0.52	1.59	0.90	0.013	0.0023	0.0071	0.0040
2	Term Control	3.38	0.52	1.37	1.57	0.019	0.0029	0.0077	0.0088
3	Term Control	3.54	0.92	1.51	1.12	0.012	0.0031	0.0051	0.0038
4	Term Control	3.60	0.83	1.33	1.33	0.010	0.0023	0.0037	0.0037
5	Term Control	7.23	0.79	5.45	0.99	0.032	0.0035	0.0241	0.0044
6	Term Control	10.04	0.17	9.60	0.17	0.036	0.0006	0.0344	0.0006
7	Term Control	9.84	0.34	8.21	1.26	0.035	0.0012	0.0292	0.0045
8	Term Control	8.74	0.42	3.82	4.63	0.027	0.0013	0.0118	0.0143
9	Term Control	5.48	1.12	2.33	1.90	0.019	0.0039	0.0081	0.0066
10	Term Control	2.20	0.56	0.80	0.84	0.012	0.0031	0.0044	0.0046
11	Term Control	2.52	0.24	1.51	0.80	0.010	0.0009	0.0057	0.0030
12	Term Control	4.16	0.84	2.38	0.95	0.015	0.0031	0.0088	0.0035
1	SIDS NBW	12.42	2.17	4.97	5.28	0.028	0.0049	0.0112	0.0119
2	SIDS NBW	8.04	1.35	4.99	1.71	0.025	0.0042	0.0155	0.0053
3	SIDS NBW	6.30	2.09	2.99	1.38	0.016	0.0053	0.0076	0.0035
4	SIDS NBW	8.40	1.02	5.50	1.86	0.024	0.0029	0.0157	0.0053
5	SIDS NBW	6.21	0.77	3.47	1.93	0.017	0.0021	0.0095	0.0053
6	SIDS NBW	5.40	0.63	2.48	2.24	0.025	0.0029	0.0115	0.0104
7	SIDS NBW	11.32	1.80	5.60	3.80	0.034	0.0054	0.0168	0.0114
8	SIDS NBW	11.37	2.31	5.62	3.44	0.035	0.0071	0.0173	0.0106
9	SIDS NBW	10.60	1.17	4.63	4.88	0.030	0.0033	0.0131	0.0138
10	SIDS NBW	5.26	0.98	3.28	1.03	0.021	0.0039	0.0131	0.0041
11	SIDS NBW	11.84	4.70	5.20	1.97	0.033	0.0131	0.0145	0.0055
12	SIDS NBW	15.26	2.47	6.33	6.33	0.034	0.0055	0.0141	0.0141
13	SIDS LBW	13.82	3.82	6.77	3.20	0.051	0.0141	0.0250	0.0118
14	SIDS LBW	5.44	1.41	2.21	1.85	0.015	0.0039	0.0061	0.0051
15	SIDS LBW	5.22	1.95	2.12	1.13	0.019	0.0071	0.0077	0.0041
16	SIDS LBW	5.46	1.18	3.11	1.20	0.026	0.0056	0.0148	0.0057
17	SIDS LBW	4.09	0.87	1.76	1.53	0.023	0.0049	0.0099	0.0086
18	SIDS LBW	7.86	0.63	4.59	2.77	0.025	0.0020	0.0146	0.0088
19	SIDS LBW	8.59	0.64	5.38	2.67	0.027	0.0020	0.0169	0.0084
20	SIDS LBW	11.20	1.34	8.34	1.46	0.040	0.0048	0.0298	0.0052
21	SIDS LBW	7.94	0.97	3.94	3.07	0.023	0.0028	0.0114	0.0089
22	SIDS LBW	9.27	1.39	4.37	3.42	0.032	0.0048	0.0151	0.0118
23	SIDS LBW	2.64	0.69	1.87	0.06	0.027	0.0070	0.0191	0.0006
24	SIDS LBW	7.46	0.75	4.62	2.02	0.038	0.0038	0.0235	0.0103

Appendix 4: Syncytiotrophoblast Volume and Number

1. Toronto Cohort

		TOTALS						DENSITIES (μm^{-3})					
CASE	**DIAGNOSIS**	**VOL. SCT (cm^3)**	SV & IMV (cm^3)	MV & TV (cm^3)	**NO.SCT**	SV & IMV	MV & TV	**VOL. SCT**	SV & IMV	MV & TV	**NO. SCT (μm^{-3})**	SV & IMV (μm^{-3})	MV & TV (μm^{-3})
1	PT control	3.05	2.78	0.27	3.9E+11	2.0E+11	1.9E+11	0.039	0.022	0.018	1.21E-03	6.30E-04	5.82E-04
2	PT control	3.13	0.57	2.55	2.9E+11	1.0E+11	1.8E+11	0.052	0.016	0.036	1.32E-03	4.74E-04	8.21E-04
3	PT control	2.65	2.13	0.52	3.3E+11	1.5E+11	1.8E+11	0.042	0.026	0.016	1.10E-03	4.88E-04	6.14E-04
4	PT control	1.78	1.15	0.64	2.4E+11	6.6E+10	1.8E+11	0.035	0.015	0.020	1.10E-03	3.02E-04	8.00E-04
5	PT control	3.94	1.78	2.16	3.4E+11	1.0E+11	2.3E+11	0.059	0.020	0.039	1.21E-03	3.74E-04	8.13E-04
6	PT control	4.56	2.77	1.79	3.7E+11	2.0E+11	1.7E+11	0.054	0.017	0.038	7.79E-04	4.17E-04	3.62E-04
7	PT control	3.24	1.26	1.98	3.2E+11	1.1E+11	2.1E+11	0.044	0.016	0.029	9.27E-04	3.12E-04	6.14E-04
8	PT control	4.98	2.35	2.62	4.0E+11	1.8E+11	2.3E+11	0.048	0.018	0.030	9.47E-04	4.17E-04	5.30E-04
9	PT control	5.81	1.48	4.33	4.2E+11	5.8E+10	3.7E+11	0.063	0.019	0.044	1.21E-03	1.66E-04	1.04E-03
10	PT control	3.32	0.60	2.72	4.4E+11	9.4E+10	3.3E+11	0.041	0.011	0.030	1.21E-03	2.62E-04	9.18E-04
11	PT control	3.55	0.33	3.22	2.8E+11	2.4E+10	2.5E+11	0.047	0.011	0.036	7.87E-04	6.83E-05	7.19E-04
12	PT control	3.42	0.23	3.19	2.2E+11	5.0E+10	1.7E+11	0.045	0.007	0.038	9.75E-04	2.15E-04	7.30E-04
13	Term control	5.75	1.43	4.31	6.1E+11	2.4E+11	3.7E+11	0.039	0.011	0.028	1.21E-03	4.76E-04	7.37E-04
14	Term control	4.13	0.69	3.44	3.3E+11	8.8E+10	2.4E+11	0.050	0.011	0.039	9.20E-04	2.44E-04	6.76E-04
15	Term control	7.39	0.20	7.19	5.5E+11	5.5E+10	5.0E+11	0.039	0.003	0.036	7.90E-04	7.90E-05	7.10E-04
16	Term control	3.68	1.19	2.49	6.0E+11	2.2E+11	3.7E+11	0.036	0.011	0.026	1.10E-03	4.14E-04	6.88E-04
17	Term control	4.84	1.30	3.54	5.4E+11	2.3E+11	3.1E+11	0.037	0.007	0.031	8.51E-04	3.60E-04	4.91E-04
18	Term control	10.72	0.62	10.10	5.7E+11	1.2E+11	4.5E+11	0.054	0.007	0.047	9.18E-04	1.91E-04	7.27E-04
19	Term control	9.78	7.36	2.42	4.5E+11	1.8E+11	2.7E+11	0.065	0.040	0.025	7.25E-04	2.90E-04	4.34E-04
20	Term control	0.85	0.43	0.42	2.6E+11	4.1E+10	2.2E+11	0.009	0.005	0.004	5.79E-04	9.04E-05	4.85E-04
21	Term control	6.03	1.74	4.29	2.5E+11	4.7E+10	2.1E+11	0.051	0.018	0.033	5.18E-04	9.59E-05	4.19E-04
22	Term control	6.46	6.01	0.45	3.9E+11	8.9E+10	3.0E+11	0.035	0.029	0.007	6.23E-04	1.43E-04	4.85E-04
23	Term control	3.19	1.38	1.80	3.1E+11	1.1E+11	2.0E+11	0.044	0.011	0.033	9.18E-04	3.25E-04	5.84E-04
24	Term control	6.21	0.95	5.25	6.0E+11	2.8E+11	3.1E+11	0.048	0.007	0.042	9.34E-04	4.43E-04	4.91E-04
25	Term control	5.24	2.17	3.07	8.5E+11	3.1E+11	5.3E+11	0.044	0.013	0.031	1.21E-03	4.44E-04	7.58E-04

		TOTALS						DENSITIES (μm^{-3})					
CASE	**DIAGNOSIS**	**VOL. SCT (cm^3)**	SV & IMV (cm^3)	MV & TV (cm^3)	**NO.SCT**	SV & IMV	MV & TV	**VOL. SCT**	SV & IMV	MV & TV	**NO. SCT (μm^{-3})**	SV & IMV (μm^{-3})	MV & TV (μm^{-3})
1	PET + HELLP	1.3	0.2	0.27	1.1E+11	1.1E+10	1.0E+11	0.041	0.007	0.033	8.67E-04	8.21E-05	7.85E-04
2	PET	5.4	4.5	2.55	5.6E+11	4.1E+11	1.4E+11	0.049	0.019	0.030	1.32E-03	9.84E-04	3.38E-04
3	PET	2.4	0.9	0.52	2.6E+11	8.4E+10	1.8E+11	0.055	0.013	0.042	1.04E-03	3.37E-04	7.07E-04
4	PET	3.8	0.5	0.64	3.2E+11	4.5E+10	2.7E+11	0.051	0.007	0.043	1.10E-03	1.55E-04	9.46E-04
5	PET + HELLP	2.6	0.3	2.16	2.4E+11	3.5E+10	2.1E+11	0.043	0.006	0.037	9.31E-04	1.34E-04	7.98E-04
6	PET + HELLP	2.7	0.9	1.79	2.4E+11	1.3E+11	1.1E+11	0.037	0.007	0.030	6.99E-04	3.76E-04	3.23E-04
7	PET	2.8	0.5	1.98	3.0E+11	6.4E+10	2.3E+11	0.047	0.010	0.037	9.23E-04	2.00E-04	7.23E-04
8	PET	3.2	0.6	2.62	2.4E+11	7.6E+10	1.6E+11	0.050	0.012	0.038	7.43E-04	2.37E-04	5.06E-04
9	PET + HELLP	4.9	1.3	4.33	6.6E+11	2.5E+11	4.2E+11	0.057	0.011	0.046	1.65E-03	6.14E-04	1.04E-03
10	PET	5.1	0.8	2.72	2.6E+11	7.6E+10	1.8E+11	0.050	0.008	0.042	6.10E-04	1.79E-04	4.31E-04
11	PET	4.0	1.6	3.22	2.6E+11	1.2E+11	1.4E+11	0.048	0.018	0.030	6.82E-04	3.09E-04	3.75E-04
12	PET	2.4	0.6	1.8	2.8E+11	8.2E+10	1.9E+11	0.034	0.008	0.026	9.21E-04	2.75E-04	6.47E-04
13	PET	4.4	0.8	3.6	3.4E+11	3.5E+10	3.1E+11	0.031	0.009	0.022	8.98E-04	9.24E-05	8.05E-04
14	PET + HELLP	2.2	0.7	1.5	4.5E+11	1.6E+11	3.0E+11	0.031	0.009	0.022	7.55E-04	2.62E-04	4.93E-04
15	PET	6.4	1.6	4.8	3.5E+11	8.5E+10	2.7E+11	0.050	0.013	0.037	6.41E-04	1.54E-04	4.85E-04
16	PET	20.0	1.1	18.9	3.7E+11	4.0E+10	3.3E+11	0.083	0.012	0.071	6.50E-04	7.01E-05	5.80E-04
17	PET	19.2	0.5	18.7	3.4E+11	6.9E+10	2.7E+11	0.080	0.007	0.074	6.52E-04	1.35E-04	5.18E-04
1	IUGR	1.8	1.4	0.4	2.7E+11	1.4E+11	1.2E+11	0.036	0.016	0.020	1.21E-03	6.40E-04	5.61E-04
2	IUGR	0.8	0.5	0.4	9.7E+10	2.2E+10	7.5E+10	0.033	0.009	0.024	7.66E-04	1.77E-04	5.90E-04
3	IUGR	2.4	1.6	0.8	2.6E+11	1.4E+11	1.1E+11	0.057	0.031	0.026	1.43E-03	8.02E-04	6.31E-04
4	IUGR	0.9	0.3	0.7	9.2E+10	4.3E+10	4.9E+10	0.052	0.018	0.034	9.16E-04	4.29E-04	4.89E-04
5	IUGR	2.2	1.0	1.1	1.5E+11	5.8E+10	8.8E+10	0.060	0.024	0.036	8.84E-04	3.49E-04	5.35E-04
6	IUGR	1.1	0.5	0.6	1.4E+11	6.0E+10	8.2E+10	0.035	0.012	0.023	9.51E-04	4.02E-04	5.49E-04
7	IUGR	2.5	1.4	1.2	2.0E+11	4.4E+10	1.5E+11	0.036	0.012	0.024	6.59E-04	1.48E-04	5.11E-04
8	IUGR	3.5	0.7	2.7	2.8E+11	5.0E+10	2.3E+11	0.042	0.009	0.033	8.39E-04	1.47E-04	6.91E-04
9	IUGR	7.2	1.8	5.4	2.6E+11	4.9E+10	2.1E+11	0.071	0.022	0.049	8.43E-04	1.57E-04	6.86E-04

		TOTALS						DENSITIES (μm^{-3})					
CASE	**DIAGNOSIS**	**VOL. SCT (cm^3)**	SV & IMV (cm^3)	MV & TV (cm^3)	**NO.SCT**	SV & IMV	MV & TV	**VOL. SCT**	SV & IMV	MV & TV	**NO. SCT (μm^{-3})**	SV & IMV (μm^{-3})	MV & TV (μm^{-3})
1	IUGR + PET	1.3	0.6	0.7	1.2E+11	3.8E+10	7.9E+10	0.048	0.018	0.029	9.20E-04	2.96E-04	6.23E-04
2	IUGR + PET + HELLP	1.9	0.9	1.0	1.8E+11	4.7E+10	1.3E+11	0.060	0.018	0.041	1.21E-03	3.15E-04	8.97E-04
3	IUGR + PET	1.7	0.2	1.4	1.1E+11	4.3E+10	6.5E+10	0.049	0.011	0.037	6.72E-04	2.66E-04	4.06E-04
4	IUGR + PET	1.5	1.2	0.3	1.2E+11	6.4E+10	5.8E+10	0.047	0.020	0.027	9.39E-04	4.95E-04	4.44E-04
5	IUGR + PET	1.9	1.2	0.7	1.9E+11	5.9E+10	1.4E+11	0.036	0.014	0.022	8.86E-04	2.69E-04	6.17E-04
6	IUGR + PET	0.6	0.3	0.3	7.4E+10	2.3E+10	5.1E+10	0.033	0.012	0.021	7.52E-04	2.33E-04	5.19E-04
7	IUGR + PET	1.5	0.8	0.8	1.4E+11	1.9E+10	1.2E+11	0.049	0.015	0.034	9.12E-04	1.24E-04	7.87E-04
8	IUGR + PET	1.4	0.6	0.8	1.2E+11	4.0E+10	7.9E+10	0.046	0.010	0.036	7.91E-04	2.65E-04	5.26E-04
9	IUGR + PET	0.8	0.1	0.6	1.2E+11	3.3E+10	8.6E+10	0.027	0.008	0.019	9.12E-04	2.52E-04	6.60E-04
10	IUGR + PET + HELLP	1.9	0.7	1.2	1.5E+11	2.6E+10	1.2E+11	0.062	0.014	0.048	1.04E-03	1.81E-04	8.59E-04
11	IUGR + PET + HELLP	1.7	0.4	1.4	1.4E+11	5.5E+10	8.9E+10	0.056	0.017	0.039	9.65E-04	3.69E-04	5.96E-04
12	IUGR + PET + HELLP	2.1	1.0	1.0	1.9E+11	3.9E+10	1.5E+11	0.037	0.010	0.027	5.88E-04	1.20E-04	4.69E-04
13	IUGR + PET	1.3	1.0	0.4	1.6E+11	4.6E+10	1.1E+11	0.044	0.017	0.028	1.21E-03	3.55E-04	8.57E-04
14	IUGR + PET	1.8	0.7	1.1	2.1E+11	8.9E+10	1.2E+11	0.039	0.010	0.030	1.04E-03	4.46E-04	5.97E-04
15	IUGR + PET	2.1	0.6	1.5	1.8E+11	6.1E+10	1.2E+11	0.054	0.010	0.044	1.10E-03	3.83E-04	7.19E-04
16	IUGR + PET	1.4	0.4	1.0	1.8E+11	5.1E+10	1.3E+11	0.042	0.010	0.032	8.98E-04	2.54E-04	6.44E-04
17	IUGR + PET	1.2	0.4	0.8	9.8E+10	3.8E+10	6.0E+10	0.025	0.007	0.018	1.10E-03	4.26E-04	6.76E-04
18	IUGR + PET	1.1	0.7	0.4	2.4E+11	5.4E+10	1.9E+11	0.050	0.020	0.030	1.10E-03	2.46E-04	8.56E-04
19	IUGR + PET	5.2	0.3	4.9	1.8E+11	4.9E+10	1.3E+11	0.060	0.004	0.056	6.62E-04	1.76E-04	4.85E-04
1	IUGR + PET	2.2	1.2	1.0	2.8E+11	1.5E+11	1.2E+11	0.039	0.013	0.025	1.10E-03	6.07E-04	4.95E-04
2	IUGR + PET	6.3	0.1	6.1	2.3E+11	7.8E+10	1.5E+11	0.054	0.007	0.048	5.68E-04	1.90E-04	3.78E-04
3	IUGR + PET	5.5	1.2	4.4	4.0E+11	1.6E+11	2.5E+11	0.050	0.013	0.037	8.79E-04	3.42E-04	5.40E-04
4	IUGR + PET	3.6	0.7	2.9	3.2E+11	1.2E+11	1.9E+11	0.043	0.007	0.037	7.96E-04	3.11E-04	4.85E-04
5	IUGR + PET	3.7	1.0	2.7	1.8E+11	2.6E+10	1.6E+11	0.069	0.012	0.057	7.70E-04	1.10E-04	6.60E-04
6	IUGR + PET	4.4	1.6	2.8	5.6E+11	1.5E+11	4.1E+11	0.053	0.012	0.041	1.21E-03	3.30E-04	8.82E-04

2. SIDS Cohort

		TOTAL VOL (cm^3)				VOL. DENSITIES			
CASE	DIAGNOSIS	VOL. SCT	SV	INT	TV	VOL. SCT	SV	INT	TV
1	Term Control	8.06	1.12	3.65	3.36	0.036	0.0050	0.0163	0.0150
2	Term Control	10.15	0.85	4.38	4.95	0.057	0.0048	0.0246	0.0278
3	Term Control	18.32	3.49	9.42	5.32	0.062	0.0118	0.0319	0.0180
4	Term Control	21.97	2.02	9.83	10.16	0.061	0.0056	0.0273	0.0282
5	Term Control	11.53	1.72	7.71	2.10	0.051	0.0076	0.0341	0.0093
6	Term Control	9.77	0.53	9.26	0.00	0.035	0.0019	0.0332	0.0000
7	Term Control	18.27	0.45	15.29	2.53	0.065	0.0016	0.0544	0.0090
8	Term Control	19.42	0.97	8.19	10.26	0.060	0.0030	0.0253	0.0317
9	Term Control	17.29	2.33	7.20	7.69	0.060	0.0081	0.0250	0.0267
10	Term Control	8.01	1.80	2.88	3.26	0.044	0.0099	0.0158	0.0179
11	Term Control	11.66	1.03	6.86	3.74	0.044	0.0039	0.0259	0.0141
12	Term Control	13.01	1.22	8.07	3.73	0.048	0.0045	0.0299	0.0138
1	SIDS NBW	27.05	1.95	9.67	15.48	0.061	0.0044	0.0218	0.0349
2	SIDS NBW	19.95	3.93	10.72	5.31	0.062	0.0122	0.0333	0.0165
3	SIDS NBW	15.35	3.15	8.70	3.42	0.039	0.0080	0.0221	0.0087
4	SIDS NBW	21.35	1.44	13.93	6.02	0.061	0.0041	0.0398	0.0172
5	SIDS NBW	26.28	5.73	12.63	7.96	0.072	0.0157	0.0346	0.0218
6	SIDS NBW	12.09	1.81	4.47	5.70	0.056	0.0084	0.0207	0.0264
7	SIDS NBW	15.99	2.90	5.60	7.46	0.048	0.0087	0.0168	0.0224
8	SIDS NBW	16.24	2.14	8.38	5.78	0.050	0.0066	0.0258	0.0178
9	SIDS NBW	18.02	3.15	6.86	8.13	0.051	0.0089	0.0194	0.0230
10	SIDS NBW	17.30	2.11	11.98	3.28	0.069	0.0084	0.0478	0.0131
11	SIDS NBW	13.99	4.09	7.00	2.91	0.039	0.0114	0.0195	0.0081
12	SIDS NBW	44.00	5.30	20.56	18.18	0.098	0.0118	0.0458	0.0405
13	SIDS LBW	20.86	4.06	12.73	4.06	0.077	0.0150	0.0470	0.0150
14	SIDS LBW	21.02	3.26	10.51	7.61	0.058	0.0090	0.0290	0.0210
15	SIDS LBW	14.29	3.30	8.52	2.47	0.052	0.0120	0.0310	0.0090
16	SIDS LBW	10.91	1.26	5.88	3.57	0.052	0.0060	0.0280	0.0170
17	SIDS LBW	16.73	2.14	9.08	5.52	0.094	0.0120	0.0510	0.0310
18	SIDS LBW	17.93	1.73	8.24	7.96	0.057	0.0055	0.0262	0.0253
19	SIDS LBW	22.27	1.11	14.45	6.59	0.070	0.0035	0.0454	0.0207
20	SIDS LBW	18.48	3.86	12.82	1.68	0.066	0.0138	0.0458	0.0060
21	SIDS LBW	27.97	3.83	13.16	10.84	0.081	0.0111	0.0381	0.0314
22	SIDS LBW	20.86	2.98	11.50	6.32	0.072	0.0103	0.0397	0.0218
23	SIDS LBW	6.95	1.59	4.84	0.51	0.071	0.0162	0.0494	0.0052
24	SIDS LBW	11.59	0.79	6.56	4.22	0.059	0.0040	0.0334	0.0215

Appendix 5: Syncytial Knots

1. Toronto Cohort

		TOTALS (cm^3)									VOL. DENSITIES									PSI (μm^3)						
CASE	DIAGNOSIS	VOL. SK	SV & IMV	MV & TV	VOL APOP. SK	SV & IMV	MV & TV	VOL NON-APOP. SK	SV & IMV	MV & TV	VOL. SK	SV & IMV	MV & TV	VOL. APOP.SK	SV & IMV	MV & TV	VOL NON-APOP. SK	SV & IMV	MV & TV	TOTAL PSI	TOTAL APOP. PSI	SV & IMV	MV & TV	TOTAL NON APOP. PSI	SV & IMV	MV & TV
1	PT control	6.72	4.26	2.40	3.42	2.88	0.54	3.23	1.38	1.86	0.021	0.013	0.008	0.011	0.009	0.002	0.010	0.004	0.006	1.9E+04	5.9E+03	5.3E+03	5.9E+02	1.3E+04	1.1E+04	1.5E+03
2	PT control	4.80	3.41	1.39	1.72	0.99	0.73	3.08	2.42	0.66	0.022	0.016	0.006	0.008	0.005	0.003	0.014	0.011	0.003	1.6E+04	5.0E+03	2.9E+03	2.1E+03	1.1E+04	5.2E+03	5.7E+03
3	PT control	7.11	6.39	0.72	2.37	2.19	0.18	4.74	4.20	0.54	0.024	0.021	0.002	0.008	0.007	0.001	0.016	0.014	0.002	2.7E+04	1.0E+04	9.1E+03	1.3E+03	1.6E+04	1.1E+04	5.8E+03
4	PT control	4.00	3.65	0.35	2.05	2.02	0.02	1.96	1.63	0.33	0.018	0.017	0.002	0.009	0.009	0.000	0.009	0.007	0.002	1.4E+04	3.9E+03	3.3E+03	6.4E+02	9.6E+03	6.5E+03	3.1E+03
5	PT control	8.82	5.29	3.53	6.38	4.20	2.18	2.44	1.09	1.34	0.032	0.019	0.013	0.023	0.015	0.008	0.009	0.004	0.005	3.2E+04	8.6E+03	2.7E+03	5.9E+03	2.3E+04	1.7E+04	6.2E+03
6	PT control	12.34	7.73	4.61	7.06	4.61	2.45	5.28	3.12	2.16	0.026	0.016	0.010	0.015	0.010	0.005	0.011	0.007	0.005	2.6E+04	1.1E+04	5.8E+03	5.0E+03	1.6E+04	8.9E+03	6.6E+03
7	PT control	7.56	5.04	2.52	3.90	3.11	0.79	3.66	1.93	1.73	0.022	0.015	0.007	0.011	0.009	0.002	0.011	0.006	0.005	6.6E+04	1.1E+04	7.4E+03	3.5E+03	5.6E+04	4.8E+04	7.4E+03
8	PT control	9.35	5.31	4.17	4.00	2.76	1.23	5.53	2.55	2.93	0.022	0.013	0.010	0.009	0.007	0.003	0.013	0.006	0.007	2.1E+04	7.8E+03	4.9E+03	2.9E+03	1.3E+04	9.6E+03	3.3E+03
9	PT control	10.29	6.58	3.71	6.23	3.78	2.45	4.06	2.80	1.26	0.029	0.019	0.011	0.018	0.011	0.007	0.012	0.008	0.004	2.7E+04	7.1E+03	4.0E+03	9.7E+03	2.0E+04	1.4E+04	6.3E+03
10	PT control	6.98	2.74	4.25	2.09	1.44	0.65	4.90	1.30	3.60	0.019	0.008	0.012	0.006	0.004	0.002	0.014	0.004	0.010	1.9E+04	4.5E+03	3.5E+03	1.0E+03	1.4E+04	6.8E+03	7.5E+03
11	PT control	12.64	7.00	5.64	4.94	3.26	1.68	7.70	3.75	3.96	0.036	0.020	0.016	0.014	0.009	0.005	0.022	0.011	0.011	1.8E+04	1.0E+04	7.2E+03	2.8E+03	8.0E+03	2.7E+03	5.3E+03
12	PT control	5.18	2.60	2.58	3.57	2.39	1.17	1.61	0.21	1.40	0.023	0.011	0.011	0.016	0.010	0.005	0.007	0.001	0.006	6.6E+04	2.2E+04	7.1E+03	1.5E+04	4.4E+04	5.9E+03	3.8E+04
13	Term control	14.03	4.01	9.97	3.51	1.55	1.90	10.52	2.45	8.07	0.028	0.008	0.0199	0.007	0.003	0.004	0.021	0.005	0.016	4.8E+04	2.7E+04	1.6E+04	1.1E+04	2.7E+04	1.1E+04	1.0E+04
14	Term control	8.75	4.28	4.46	3.85	2.23	1.62	4.90	2.05	2.84	0.024	0.012	0.0124	0.011	0.006	0.005	0.014	0.006	0.008	2.5E+04	1.4E+04	4.4E+03	9.1E+03	1.1E+04	4.1E+03	6.9E+03
15	Term control	12.00	4.77	7.23	3.93	2.60	1.33	8.07	2.18	5.90	0.017	0.007	0.0103	0.006	0.004	0.002	0.012	0.003	0.008	2.5E+04	7.3E+03	3.9E+03	3.4E+03	1.8E+04	1.2E+04	6.0E+03
16	Term control	12.80	6.70	6.10	6.37	3.78	2.59	6.43	2.92	3.51	0.024	0.012	0.0113	0.012	0.007	0.005	0.012	0.005	0.007	2.9E+04	1.5E+04	1.1E+04	3.8E+03	1.4E+04	3.4E+03	1.1E+04
17	Term control	15.75	9.70	5.67	6.30	4.03	2.27	9.07	5.67	3.40	0.025	0.015	0.0090	0.010	0.006	0.004	0.014	0.009	0.005	3.7E+04	1.6E+04	6.2E+03	1.0E+04	2.0E+04	1.3E+04	7.0E+03
18	Term control	16.99	6.82	10.17	9.42	4.34	5.08	7.56	2.48	5.08	0.027	0.011	0.0164	0.015	0.007	0.008	0.012	0.004	0.008	3.1E+04	1.3E+04	9.5E+03	3.7E+03	1.8E+04	7.1E+03	1.1E+04
19	Term control	23.31	10.97	12.34	4.03	2.29	1.74	19.28	8.68	10.60	0.038	0.018	0.0199	0.007	0.004	0.003	0.031	0.014	0.017	4.9E+04	6.9E+03	3.5E+03	3.4E+03	4.2E+04	2.9E+04	1.3E+04
20	Term control	13.64	2.30	11.34	4.19	1.94	2.25	9.45	0.36	9.09	0.030	0.005	0.0252	0.009	0.004	0.005	0.021	0.001	0.020	2.4E+04	8.9E+03	4.2E+03	4.8E+03	1.5E+04	1.6E+03	1.4E+04
21	Term control	8.72	3.19	5.54	3.92	2.35	1.57	4.80	0.83	3.97	0.018	0.007	0.0113	0.008	0.005	0.003	0.010	0.002	0.008	2.6E+04	6.3E+03	4.1E+03	2.2E+03	2.0E+04	1.4E+04	6.1E+03
22	Term control	11.47	5.70	5.77	5.08	3.22	1.86	6.39	2.48	3.91	0.019	0.009	0.0093	0.008	0.005	0.003	0.010	0.004	0.006	6.7E+04	4.7E+03	2.5E+03	2.2E+03	6.2E+04	2.7E+04	3.5E+04
23	Term control	8.50	4.62	3.84	4.05	2.79	1.26	4.42	1.84	2.58	0.025	0.014	0.0113	0.012	0.008	0.004	0.013	0.005	0.008	3.3E+04	1.4E+04	9.6E+03	4.8E+03	1.8E+04	8.0E+03	1.0E+04
24	Term control	21.12	14.27	6.66	11.07	8.38	2.69	9.60	5.89	3.97	0.033	0.022	0.0104	0.017	0.013	0.004	0.015	0.009	0.006	4.3E+04	2.2E+04	8.6E+03	1.3E+04	1.8E+04	4.4E+03	1.6E+04
25	Term control	21.70	14.70	6.79	13.16	10.01	3.15	8.33	4.69	3.64	0.031	0.021	0.0097	0.019	0.014	0.005	0.012	0.007	0.005	3.5E+04	1.7E+04	1.4E+04	3.6E+03	1.8E+04	1.0E+04	8.1E+03

		TOTALS (cm^3)									VOL. DENSITIES									PSI (μm^3)						
CASE	DIAGNOSIS	VOL. SK	SV & IMV	MV & TV	VOL APOP. SK	SV & IMV	MV & TV	VOL NON-APOP. SK	SV & IMV	MV & TV	VOL. SK	SV & IMV	MV & TV	VOL. APOP.SK	SV & IMV	MV & TV	VOL NON-APOP. SK	SV & IMV	MV & TV	TOTAL PSI	TOTAL APOP. PSI	SV & IMV	MV & TV	TOTAL NON-APOP. PSI	SV & IMV	MV & TV
1	PET + HELLP	3.80	1.37	2.43	2.80	1.09	1.70	1.00	0.27	0.73	0.029	0.011	0.019	0.022	0.008	0.013	0.008	0.002	0.006	1.9E+04	9.6E+03	6.0E+03	3.6E+03	9.8E+03	6.0E+03	3.8E+03
2	PET	14.70	9.16	5.54	6.85	5.29	1.55	7.85	3.86	3.99	0.035	0.022	0.013	0.016	0.013	0.004	0.019	0.009	0.010	3.4E+04	1.0E+04	8.2E+03	1.9E+03	2.4E+04	1.5E+04	8.4E+03
3	PET	5.75	3.65	2.00	1.50	0.90	0.65	4.10	2.75	1.35	0.023	0.015	0.008	0.006	0.004	0.003	0.016	0.011	0.005	1.9E+04	4.7E+03	2.0E+03	2.7E+03	1.4E+04	1.3E+04	1.9E+03
4	PET	9.28	3.34	5.80	3.51	1.22	2.29	5.51	2.12	3.51	0.032	0.012	0.020	0.012	0.004	0.008	0.019	0.007	0.012	2.5E+04	8.1E+03	4.7E+03	3.5E+03	1.7E+04	3.4E+03	1.3E+04
5	PET + HELLP	6.19	2.37	3.95	4.68	2.00	2.81	1.51	0.36	1.14	0.024	0.009	0.015	0.018	0.008	0.011	0.006	0.001	0.004	2.9E+04	1.2E+04	3.6E+03	7.9E+03	1.7E+04	1.3E+04	3.9E+03
6	PET + HELLP	14.70	4.97	9.66	10.15	3.99	6.23	4.55	0.98	3.43	0.042	0.014	0.028	0.029	0.011	0.018	0.013	0.003	0.010	2.8E+04	1.3E+04	3.3E+03	9.9E+03	1.4E+04	5.8E+03	8.5E+03
7	PET	8.26	3.55	4.70	4.19	1.98	2.21	4.06	1.57	2.50	0.026	0.011	0.015	0.013	0.006	0.007	0.013	0.005	0.008	2.9E+04	1.2E+04	6.5E+03	5.7E+03	1.7E+04	9.0E+03	7.6E+03
8	PET	7.94	1.73	6.21	5.34	1.12	4.22	2.59	0.61	1.98	0.025	0.005	0.019	0.017	0.004	0.013	0.008	0.002	0.006	2.6E+04	1.0E+04	2.6E+03	7.7E+03	1.6E+04	3.1E+03	1.3E+04
9	PET + HELLP	12.24	5.76	6.48	6.28	3.44	2.84	5.96	2.32	3.64	0.031	0.014	0.016	0.016	0.009	0.007	0.015	0.006	0.009	2.1E+04	7.3E+03	4.6E+03	2.7E+03	1.3E+04	6.5E+03	6.8E+03
10	PET	12.33	4.34	8.03	6.38	2.85	3.61	5.95	1.49	4.42	0.029	0.010	0.019	0.015	0.007	0.009	0.014	0.004	0.010	4.8E+04	2.7E+04	1.8E+04	9.1E+03	2.1E+04	1.4E+04	6.7E+03
11	PET	6.19	1.67	4.29	2.28	0.57	1.47	3.91	1.10	2.81	0.016	0.004	0.011	0.006	0.002	0.004	0.010	0.003	0.007	2.8E+04	6.2E+03	3.6E+03	2.6E+03	2.1E+04	3.1E+03	1.8E+04
12	PET	4.89	1.29	3.60	1.38	0.39	0.99	3.51	0.90	2.61	0.016	0.004	0.0120	0.005	0.001	0.003	0.012	0.003	0.009	1.5E+04	4.4E+03	9.6E+03	3.0E+03	1.0E+04	7.0E+03	3.4E+03
13	PET	15.60	8.28	7.68	6.60	4.50	2.46	9.00	3.78	5.22	0.026	0.014	0.0128	0.011	0.008	0.004	0.015	0.006	0.009	4.8E+04	1.3E+04	8.0E+03	4.9E+03	3.5E+04	2.5E+04	1.0E+04
14	PET + HELLP	9.88	5.36	4.37	4.22	2.01	2.20	5.70	3.34	2.17	0.026	0.014	0.0115	0.011	0.005	0.006	0.015	0.009	0.006	5.1E+04	1.1E+04	7.2E+03	3.7E+03	4.0E+04	2.0E+04	2.0E+04
15	PET	14.30	4.51	9.74	8.25	1.76	6.49	6.05	2.75	3.25	0.026	0.008	0.0177	0.015	0.003	0.012	0.011	0.005	0.006	2.5E+04	1.6E+04	8.3E+03	7.6E+03	9.4E+03	2.7E+03	6.7E+03
16	PET	18.98	3.45	15.53	9.32	1.38	7.94	9.66	2.07	7.59	0.033	0.006	0.0270	0.016	0.002	0.014	0.017	0.004	0.013	3.7E+04	1.4E+04	4.6E+03	9.5E+03	2.2E+04	1.1E+04	1.1E+04
17	PET	15.71	5.51	10.20	8.50	2.11	6.39	7.21	3.40	3.81	0.031	0.011	0.0198	0.017	0.004	0.012	0.014	0.007	0.007	5.7E+04	2.2E+04	1.4E+04	7.5E+03	3.5E+04	2.0E+04	1.5E+04
1	IUGR	5.32	2.64	2.68	2.42	1.10	1.32	2.90	1.54	1.36	0.024	0.012	0.012	0.011	0.005	0.006	0.013	0.007	0.006	2.7E+04	5.6E+03	3.6E+03	2.0E+03	2.2E+04	1.8E+04	3.1E+03
2	IUGR	3.71	2.19	1.52	2.88	1.68	1.20	0.82	0.51	0.32	0.029	0.017	0.012	0.023	0.013	0.010	0.007	0.004	0.003	1.7E+04	6.3E+03	3.5E+03	2.9E+03	1.1E+04	8.1E+03	2.7E+03
3	IUGR	4.36	2.70	1.66	1.91	1.42	0.49	2.45	1.28	1.17	0.024	0.015	0.009	0.011	0.008	0.003	0.014	0.007	0.007	2.0E+04	7.8E+03	4.5E+03	3.2E+03	1.2E+04	7.1E+03	5.0E+03
4	IUGR	3.00	1.32	1.69	2.00	1.05	0.98	1.00	0.27	0.71	0.030	0.013	0.017	0.020	0.011	0.010	0.010	0.003	0.007	3.6E+04	1.6E+04	9.6E+03	6.8E+03	2.0E+04	6.7E+03	1.3E+04
5	IUGR	6.93	4.19	2.79	5.12	2.49	2.62	1.82	1.70	0.17	0.042	0.025	0.017	0.031	0.015	0.016	0.011	0.010	0.001	2.7E+04	1.5E+04	9.5E+03	5.2E+03	1.3E+04	6.8E+03	5.8E+03
6	IUGR	5.09	3.78	1.31	4.22	3.63	0.59	0.87	0.15	0.72	0.034	0.025	0.0087	0.028	0.024	0.004	0.006	0.001	0.005	3.5E+04	1.4E+04	5.2E+03	9.1E+03	2.1E+04	7.0E+03	1.4E+04
7	IUGR	6.87	4.14	2.73	3.81	2.16	1.65	3.06	1.98	1.08	0.023	0.014	0.0091	0.013	0.007	0.006	0.010	0.007	0.004	1.3E+04	3.0E+03	1.5E+03	1.5E+03	1.0E+04	4.8E+03	5.6E+03
8	IUGR	8.82	5.61	3.21	6.56	4.63	1.93	2.26	0.98	1.28	0.026	0.017	0.0095	0.019	0.014	0.006	0.007	0.003	0.004	5.2E+04	3.5E+04	7.5E+03	2.7E+04	1.7E+04	1.6E+04	1.6E+03
9	IUGR	9.42	4.56	4.87	4.49	2.34	2.15	4.93	2.22	2.71	0.030	0.015	0.0156	0.014	0.008	0.007	0.016	0.007	0.009	6.7E+04	1.1E+04	5.5E+03	5.2E+03	5.6E+04	3.5E+04	2.1E+04

		TOTALS (cm^3)									VOL. DENSITIES									PSI (μm^3)						
CASE	DIAGNOSIS	VOL. SK	SV & IMV	MV & TV	VOL APOP. SK	SV & IMV	MV & TV	VOL NON-APOP. SK	SV & IMV	MV & TV	VOL. SK	SV & IMV	MV & TV	VOL. APOP.SK	SV & IMV	MV & TV	VOL NON-APOP. SK	SV & IMV	MV & TV	TOTAL PSI	TOTAL APOP. PSI	SV & IMV	MV & TV	TOTAL NON-APOP. PSI	SV & IMV	MV & TV
1	IUGR + PET	3.65	2.61	1.10	1.48	1.11	0.37	2.17	1.50	0.73	0.029	0.021	0.009	0.012	0.009	0.003	0.017	0.012	0.006	3.0E+04	2.0E+04	1.8E+04	1.4E+03	7.9E+03	7.3E+03	3.5E+03
2	IUGR + PET + HELLP	5.96	3.17	2.79	3.14	1.77	1.37	2.82	1.40	1.43	0.040	0.021	0.019	0.021	0.012	0.009	0.019	0.009	0.010	5.7E+04	1.2E+04	6.2E+03	5.5E+03	4.5E+04	2.9E+04	1.6E+04
3	IUGR + PET	4.78	1.17	3.62	3.50	1.17	2.34	1.28	0.00	1.28	0.030	0.007	0.023	0.022	0.007	0.015	0.008	0.000	0.008	2.2E+04	1.5E+04	9.8E+03	5.2E+03	7.4E+03	0.0E+00	7.4E+03
4	IUGR + PET	4.02	3.32	0.70	1.92	1.92	0.00	2.09	1.39	0.70	0.031	0.026	0.005	0.015	0.015	0.000	0.016	0.011	0.005	1.5E+04	3.1E+03	2.4E+03	6.6E+02	1.2E+04	6.1E+03	6.1E+03
5	IUGR + PET	6.18	4.44	1.74	2.53	1.94	0.59	3.65	2.51	1.14	0.028	0.020	0.008	0.012	0.009	0.003	0.017	0.011	0.005	3.2E+04	1.0E+04	5.3E+03	5.0E+03	2.2E+04	8.4E+03	1.3E+04
6	IUGR + PET	2.77	0.95	1.95	2.08	0.80	1.41	0.69	0.15	0.54	0.028	0.010	0.020	0.021	0.008	0.014	0.007	0.002	0.006	2.8E+04	1.1E+04	3.0E+03	7.6E+03	1.7E+04	7.4E+03	9.8E+03
7	IUGR + PET	4.13	1.02	3.11	2.61	0.69	1.92	1.52	0.33	1.19	0.028	0.007	0.021	0.017	0.005	0.013	0.010	0.002	0.008	2.4E+04	1.7E+04	1.3E+04	3.5E+03	6.7E+03	2.9E+03	3.8E+03
8	IUGR + PET	3.75	2.78	1.01	2.06	1.50	0.56	1.73	1.28	0.45	0.025	0.019	0.007	0.014	0.010	0.004	0.012	0.009	0.003	2.2E+04	8.7E+03	3.0E+03	5.7E+03	1.3E+04	9.0E+03	3.8E+03
9	IUGR + PET	3.13	1.13	2.00	1.89	0.79	1.09	1.25	0.34	0.91	0.024	0.009	0.015	0.015	0.006	0.008	0.010	0.003	0.007	3.7E+04	6.0E+03	2.8E+03	3.2E+03	3.1E+04	2.2E+04	9.4E+03
10	IUGR + PET + HELLP	5.84	3.09	2.76	2.41	0.97	1.44	3.44	2.12	1.32	0.040	0.021	0.019	0.017	0.007	0.010	0.024	0.015	0.009	2.7E+04	6.1E+03	4.4E+03	1.7E+03	2.1E+04	1.9E+04	1.7E+03
11	IUGR + PET + HELLP	4.67	2.00	2.67	3.72	1.65	2.07	0.95	0.35	0.60	0.031	0.013	0.018	0.025	0.011	0.014	0.006	0.002	0.004	1.8E+04	8.4E+03	3.8E+03	4.6E+03	9.5E+03	5.8E+03	3.8E+03
12	IUGR + PET + HELLP	8.91	5.30	3.61	4.42	2.05	2.37	4.49	3.25	1.24	0.027	0.016	0.011	0.014	0.006	0.007	0.014	0.010	0.004	2.7E+04	1.2E+04	5.3E+03	6.3E+03	1.5E+04	9.7E+03	5.6E+03
13	IUGR + PET	3.15	1.92	1.22	1.13	0.74	0.39	2.02	1.18	0.83	0.024	0.015	0.009	0.009	0.006	0.003	0.016	0.009	0.006	4.1E+04	8.3E+03	7.0E+03	1.3E+03	3.3E+04	1.0E+04	2.3E+04
14	IUGR + PET	5.32	1.58	3.74	1.16	0.74	0.42	4.16	0.84	3.32	0.027	0.008	0.019	0.006	0.004	0.002	0.021	0.004	0.017	8.8E+04	8.1E+03	5.6E+03	2.6E+03	8.0E+04	7.2E+04	7.9E+03
15	IUGR + PET	6.07	3.08	2.99	2.55	1.83	0.73	3.52	1.25	2.27	0.028	0.014	0.014	0.012	0.008	0.003	0.016	0.006	0.010	3.6E+04	9.0E+03	5.4E+03	3.6E+03	2.7E+04	1.2E+04	1.5E+04
16	IUGR + PET	5.30	2.11	3.18	2.94	1.23	1.71	2.35	0.88	1.47	0.033	0.013	0.020	0.018	0.008	0.011	0.015	0.006	0.009	1.1E+05	1.1E+05	1.0E+05	6.5E+03	5.1E+03	2.6E+03	2.6E+03
17	IUGR + PET	4.88	2.74	2.14	3.06	1.92	1.14	1.82	0.82	1.00	0.024	0.014	0.011	0.015	0.010	0.006	0.009	0.004	0.005	3.3E+04	1.2E+04	5.1E+03	7.0E+03	2.1E+04	1.4E+04	6.7E+03
18	IUGR + PET	2.67	1.49	1.17	2.23	1.23	0.98	0.45	0.26	0.19	0.030	0.017	0.013	0.025	0.014	0.011	0.005	0.003	0.002	6.3E+04	1.7E+04	1.2E+04	4.6E+03	4.6E+04	2.1E+04	2.5E+04
19	IUGR + PET	7.45	1.27	6.29	3.59	0.66	2.79	4.14	0.61	3.51	0.027	0.005	0.023	0.013	0.002	0.010	0.015	0.002	0.013	3.6E+04	1.0E+04	1.4E+03	8.9E+03	2.6E+04	1.7E+04	8.5E+03
1	IUGR + PET	7.98	2.55	5.43	4.68	1.45	3.23	3.30	1.10	2.20	0.032	0.010	0.022	0.019	0.006	0.013	0.013	0.004	0.009	3.2E+04	1.2E+04	4.5E+03	7.4E+03	2.0E+04	1.6E+04	3.7E+03
2	IUGR + PET	9.84	2.34	7.34	3.73	1.39	2.34	6.15	0.94	5.00	0.024	0.006	0.018	0.009	0.003	0.006	0.015	0.002	0.012	1.7E+04	8.2E+03	2.4E+03	5.8E+03	8.8E+03	3.6E+03	5.1E+03
3	IUGR + PET	10.01	5.87	4.10	6.37	4.73	1.50	3.64	1.14	2.59	0.022	0.013	0.009	0.014	0.010	0.003	0.008	0.003	0.006	4.2E+04	2.0E+04	8.2E+03	1.2E+04	2.2E+04	8.1E+03	1.4E+04
4	IUGR + PET	6.26	1.94	4.32	5.74	1.70	4.03	0.53	0.24	0.29	0.026	0.008	0.018	0.024	0.007	0.017	0.002	0.001	0.001	3.7E+04	2.3E+04	1.2E+04	1.1E+04	1.3E+04	6.9E+03	6.5E+03
5	IUGR + PET	8.56	4.08	4.48	4.48	2.36	2.12	4.08	1.72	2.36	0.021	0.010	0.011	0.011	0.006	0.005	0.010	0.004	0.006	1.2E+04	7.5E+03	3.5E+03	4.0E+03	4.2E+03	2.6E+03	1.6E+03
6	IUGR + PET	13.34	7.36	5.98	8.46	4.74	3.73	4.88	2.62	2.25	0.029	0.016	0.013	0.018	0.010	0.008	0.011	0.006	0.005	3.2E+04	2.1E+04	1.6E+04	4.8E+03	1.1E+04	7.9E+03	2.6E+03

2. SIDS Cohort

		TOTALS (cm^3)												VOL. DENSITIES												PSI (μm^3)							
CASE	DIAGNOSIS	VOL. SK	SV	INT	TV	VOL APOP. SK	SV	INT	TV	VOL NON-APOP. SK	SV	INT	TV	VOL. SK	SV	INT	TV	VOL. APOP. SK	SV	INT	TV	VOL NON-APOP. SK	SV	INT	TV	TOTAL PSI	TOTAL APOP. PSI	SV	INT	TV	TOTAL NON-APOP. PSI	SV	INT	TV
1	Term Control	6.2	1.77	2.45	2.01	3.81	1.36	1.30	1.15	2.42	0.41	1.15	0.86	0.021	0.006	0.0083	0.007	0.013	0.005	0.004	0.004	0.008	0.001	0.004	0.003	1.3E+04	3.9E+03	1.8E+04	1.3E+03	1.4E+03	9.4E+03	5.3E+03	2.0E+03	2.1E+03
2	Term Control	6.1	1.62	2.45	2.05	4.14	1.48	1.62	1.04	1.98	0.14	0.83	1.01	0.017	0.005	0.0068	0.006	0.011	0.004	0.005	0.003	0.006	0.000	0.002	0.003	1.7E+04	4.3E+03	6.2E+03	1.3E+03	1.3E+03	1.3E+04	7.3E+03	2.2E+03	3.3E+03
3	Term Control	7.5	1.82	3.89	1.67	2.51	0.43	1.53	0.55	4.87	1.38	2.36	1.12	0.026	0.006	0.0135	0.006	0.009	0.002	0.005	0.002	0.017	0.005	0.008	0.004	2.9E+04	1.5E+04	9.8E+03	6.1E+03	1.9E+03	1.5E+04	6.8E+03	5.6E+03	2.3E+03
4	Term Control	8.2	2.86	4.85	0.42	4.98	2.60	2.01	0.37	3.15	0.27	2.84	0.05	0.031	0.011	0.0183	0.002	0.019	0.010	0.008	0.001	0.012	0.001	0.011	0.000	3.5E+04	1.7E+04	2.4E+03	5.0E+03	1.0E+03	1.8E+04	4.5E+03	1.2E+04	2.1E+03
5	Term Control	8.9	2.21	4.97	1.65	4.67	1.76	2.24	0.68	4.16	0.46	2.73	0.97	0.033	0.008	0.0184	0.006	0.017	0.007	0.008	0.003	0.015	0.002	0.010	0.004	4.3E+04	2.2E+04	5.3E+03	4.1E+03	1.1E+04	2.1E+04	2.4E+03	8.4E+03	9.8E+03
6	Term Control	4.6	1.35	2.73	0.25	2.17	1.35	0.56	0.25	2.17	0.00	2.17	0.00	0.025	0.007	0.0150	0.001	0.012	0.007	0.003	0.001	0.013	0.000	0.012	0.000	3.3E+04	1.4E+04	3.0E+03	8.8E+03	2.2E+03	1.8E+04	8.3E+02	9.9E+03	7.7E+03
7	Term Control	9.7	1.68	5.34	2.65	4.24	1.52	1.81	0.91	5.44	0.16	3.53	1.75	0.030	0.005	0.0165	0.008	0.013	0.005	0.006	0.003	0.017	0.001	0.011	0.005	4.5E+04	2.0E+04	1.3E+04	3.5E+03	4.5E+03	2.5E+04	1.5E+04	4.3E+03	6.2E+03
8	Term Control	7.2	1.16	5.20	0.76	4.55	0.65	3.29	0.60	2.58	0.52	1.90	0.16	0.032	0.005	0.0232	0.003	0.020	0.003	0.015	0.003	0.011	0.002	0.009	0.001	4.2E+04	1.2E+04	3.0E+03	5.0E+03	5.9E+03	3.0E+04	2.2E+04	3.2E+03	4.5E+03
9	Term Control	4.1	0.84	2.24	0.95	1.81	0.68	0.95	0.18	2.21	0.16	1.29	0.77	0.018	0.004	0.0099	0.004	0.008	0.003	0.004	0.001	0.010	0.001	0.006	0.003	2.6E+04	6.3E+03	2.8E+03	4.3E+03	3.7E+02	2.0E+04	6.0E+03	1.1E+04	2.7E+03
10	Term Control	5.3	0.42	4.63	0.11	2.29	0.42	1.87	0.00	2.87	0.00	2.76	0.11	0.019	0.002	0.0166	0.000	0.008	0.002	0.007	0.000	0.010	0.000	0.010	0.000	6.7E+04	4.7E+03	4.4E+03	4.2E+03	0.0E+00	6.2E+04	0.0E+00	3.2E+04	3.0E+04
11	Term Control	5.3	0.91	3.56	0.93	1.66	0.77	0.59	0.30	3.74	0.14	2.97	0.62	0.030	0.005	0.0200	0.005	0.009	0.004	0.003	0.002	0.021	0.001	0.017	0.004	2.4E+04	8.9E+03	3.8E+03	2.2E+03	2.6E+03	1.5E+04	1.6E+03	7.0E+03	6.5E+03
12	Term Control	10.7	2.14	7.56	0.87	1.83	0.76	0.87	0.20	8.74	1.38	6.69	0.67	0.038	0.008	0.0269	0.003	0.006	0.003	0.003	0.001	0.031	0.005	0.024	0.002	4.9E+04	6.9E+03	5.3E+03	4.2E+03	1.4E+03	4.2E+04	2.2E+04	1.8E+04	2.7E+03
1	SIDS NBW	9.3	2.84	4.88	1.37	6.34	2.31	3.19	0.84	2.75	0.53	1.69	0.53	0.021	0.006	0.0110	0.003	0.014	0.005	0.007	0.002	0.006	0.001	0.004	0.001	1.5E+04	7.2E+03	1.7E+03	2.5E+03	3.0E+03	7.3E+03	3.4E+03	2.1E+03	1.9E+03
2	SIDS NBW	7.7	2.70	3.67	1.45	3.67	1.67	1.77	0.23	4.15	1.03	1.90	1.22	0.024	0.008	0.0114	0.005	0.011	0.005	0.006	0.001	0.013	0.003	0.006	0.004	2.2E+04	6.3E+03	1.9E+03	3.2E+03	1.2E+03	1.6E+04	1.8E+03	7.3E+03	6.9E+03
3	SIDS NBW	10.2	2.99	4.84	2.20	3.98	1.42	1.73	0.83	6.06	1.57	3.11	1.38	0.026	0.008	0.0123	0.006	0.010	0.004	0.004	0.002	0.015	0.004	0.008	0.004	1.8E+04	8.3E+03	3.4E+03	2.7E+03	2.3E+03	9.5E+03	4.2E+03	2.8E+03	2.4E+03
4	SIDS NBW	7.4	2.10	4.38	0.74	5.25	1.75	2.98	0.53	1.96	0.35	1.40	0.21	0.021	0.006	0.0125	0.002	0.015	0.005	0.009	0.002	0.006	0.001	0.004	0.001	3.3E+04	6.9E+03	2.7E+03	1.5E+03	2.6E+03	2.6E+04	3.1E+03	2.7E+03	2.1E+04
5	SIDS NBW	8.8	2.19	4.71	1.93	6.06	2.19	2.66	1.20	2.77	0.00	2.04	0.73	0.024	0.006	0.0129	0.005	0.017	0.006	0.007	0.003	0.008	0.000	0.006	0.002	3.4E+04	9.8E+03	4.2E+03	1.1E+03	4.4E+03	2.4E+04	0.0E+00	9.1E+03	1.5E+04
6	SIDS NBW	5.8	1.23	3.28	1.38	4.38	1.10	2.27	1.01	1.51	0.13	1.01	0.37	0.027	0.006	0.0152	0.006	0.020	0.005	0.011	0.005	0.007	0.001	0.005	0.002	2.7E+04	1.1E+04	6.0E+03	3.1E+03	1.7E+03	1.6E+04	7.7E+03	2.1E+03	5.9E+03
7	SIDS NBW	7.3	1.60	2.70	2.96	4.73	1.20	2.07	1.47	2.53	0.40	0.63	1.50	0.022	0.005	0.0081	0.009	0.014	0.004	0.006	0.004	0.008	0.001	0.002	0.005	2.7E+04	9.7E+03	3.5E+03	2.2E+03	4.0E+03	1.7E+04	6.3E+03	6.4E+03	4.4E+03
8	SIDS NBW	8.4	2.21	4.55	1.72	7.66	2.21	4.06	1.40	0.81	0.00	0.49	0.32	0.026	0.007	0.0140	0.005	0.024	0.007	0.013	0.004	0.002	0.000	0.002	0.001	1.7E+04	8.2E+03	3.9E+03	2.7E+03	1.5E+03	8.4E+03	0.0E+00	4.3E+03	4.1E+03
9	SIDS NBW	8.5	2.37	3.78	2.16	6.75	2.19	2.51	2.05	1.56	0.18	1.27	0.11	0.024	0.007	0.0107	0.006	0.019	0.006	0.007	0.006	0.004	0.001	0.004	0.000	5.0E+04	6.3E+03	2.6E+03	1.4E+03	2.3E+03	4.4E+04	7.6E+03	1.4E+03	3.5E+04
10	SIDS NBW	8.0	1.63	4.79	1.58	4.64	1.38	2.41	0.85	3.36	0.25	2.38	0.73	0.032	0.007	0.0191	0.006	0.018	0.006	0.010	0.003	0.013	0.001	0.010	0.003	1.9E+04	9.7E+03	1.9E+03	7.0E+03	7.9E+02	9.6E+03	2.8E+03	2.5E+03	4.3E+03
11	SIDS NBW	6.8	2.83	2.76	1.36	2.22	1.04	1.04	0.14	4.74	1.79	1.72	1.22	0.019	0.008	0.0077	0.004	0.006	0.003	0.003	0.000	0.013	0.005	0.005	0.003	1.6E+04	8.6E+03	1.8E+03	4.2E+03	2.6E+03	7.3E+03	3.4E+03	2.4E+03	1.5E+03
12	SIDS NBW	10.8	3.73	4.22	2.83	5.93	2.38	2.60	0.94	4.85	1.35	1.62	1.89	0.024	0.008	0.0094	0.006	0.013	0.005	0.006	0.002	0.011	0.003	0.004	0.004	2.5E+04	1.4E+04	6.4E+03	4.0E+03	3.6E+03	1.1E+04	5.0E+03	2.5E+03	3.6E+03
13	SIDS LBW	8.7	3.33	5.20	0.22	6.37	2.98	3.39	0.00	2.38	0.35	1.81	0.22	0.032	0.012	0.0192	0.001	0.023	0.011	0.013	0.000	0.009	0.001	0.007	0.001	2.5E+04	4.9E+03	8.0E+02	4.1E+03	0.0E+00	2.0E+04	6.8E+03	3.6E+03	9.9E+03
14	SIDS LBW	7.2	2.43	3.91	1.01	5.07	2.43	2.43	0.22	2.28	0.00	1.49	0.80	0.020	0.007	0.0108	0.003	0.014	0.007	0.007	0.001	0.006	0.000	0.004	0.002	2.0E+04	8.8E+03	6.1E+03	1.6E+03	1.1E+03	1.1E+04	0.0E+00	7.7E+03	3.6E+03
15	SIDS LBW	6.3	1.98	3.60	0.88	2.01	1.29	0.71	0.00	4.45	0.69	2.89	0.88	0.023	0.007	0.0131	0.003	0.007	0.005	0.003	0.000	0.016	0.003	0.011	0.003	3.9E+04	1.2E+04	5.3E+03	6.8E+03	0.0E+00	2.7E+04	4.3E+03	2.0E+04	2.0E+03
16	SIDS LBW	4.4	0.90	2.04	1.34	3.78	0.90	1.80	1.07	0.50	0.00	0.23	0.27	0.021	0.004	0.0097	0.006	0.018	0.004	0.009	0.005	0.002	0.000	0.001	0.001	1.0E+04	7.9E+03	7.9E+03	6.0E+03	1.9E+03	2.2E+03	0.0E+00	1.0E+03	1.1E+03
17	SIDS LBW	6.6	1.44	4.18	0.93	5.87	1.44	3.70	0.73	0.68	0.00	0.48	0.20	0.037	0.008	0.0235	0.005	0.033	0.008	0.021	0.004	0.004	0.000	0.003	0.001	1.7E+04	7.7E+03	3.7E+03	2.5E+03	1.8E+03	9.6E+03	0.0E+00	3.4E+03	6.2E+03
18	SIDS LBW	8.2	1.10	1.95	4.44	3.08	0.57	1.23	1.29	4.40	0.53	0.72	3.15	0.026	0.004	0.0062	0.014	0.012	0.002	0.004	0.004	0.014	0.002	0.002	0.010	2.8E+04	1.4E+04	6.0E+03	4.7E+03	3.2E+03	1.4E+04	1.9E+03	8.9E+03	3.4E+03
19	SIDS LBW	6.4	2.29	2.39	1.75	5.60	2.29	1.88	1.43	0.83	0.00	0.51	0.32	0.020	0.007	0.0075	0.006	0.018	0.007	0.006	0.005	0.003	0.000	0.002	0.001	3.1E+04	1.6E+04	1.9E+03	9.5E+03	4.8E+03	1.5E+04	9.0E+03	4.0E+03	1.5E+03
20	SIDS LBW	7.3	1.51	4.96	0.70	4.87	1.34	3.22	0.31	2.30	0.17	1.74	0.39	0.026	0.005	0.0177	0.003	0.017	0.005	0.012	0.001	0.008	0.001	0.006	0.001	3.2E+04	1.2E+04	5.6E+04	4.9E+03	1.6E+03	2.0E+04	4.7E+03	1.3E+04	3.0E+03
21	SIDS LBW	10.4	2.42	5.73	2.31	4.70	1.76	2.18	0.76	5.77	0.66	3.56	1.55	0.030	0.007	0.0166	0.007	0.014	0.005	0.006	0.002	0.017	0.002	0.010	0.005	4.2E+04	1.8E+04	1.1E+04	2.3E+03	4.5E+03	2.5E+04	1.4E+04	5.2E+03	5.1E+03
22	SIDS LBW	9.0	1.91	4.98	2.00	5.36	1.59	2.78	0.99	3.53	0.32	2.20	1.01	0.031	0.007	0.0172	0.007	0.019	0.006	0.010	0.003	0.012	0.001	0.008	0.004	4.2E+04	7.1E+03	2.3E+03	2.5E+03	2.3E+03	3.5E+04	1.4E+03	3.1E+04	2.7E+03
23	SIDS LBW	4.1	1.16	2.70	0.22	3.00	1.02	1.88	0.10	1.08	0.14	0.82	0.12	0.042	0.012	0.0276	0.002	0.031	0.010	0.019	0.001	0.011	0.001	0.008	0.001	4.0E+04	1.9E+04	4.5E+03	1.3E+04	1.8E+03	2.1E+04	8.8E+03	9.6E+03	2.5E+03
24	SIDS LBW	6.1	1.18	3.61	1.22	3.65	0.98	2.10	0.57	2.36	0.20	1.51	0.65	0.031	0.006	0.0184	0.006	0.019	0.005	0.011	0.003	0.012	0.001	0.008	0.003	2.7E+04	1.5E+04	8.0E+03	3.4E+03	3.3E+03	1.3E+04	2.6E+03	3.3E+03	6.7E+03

Appendix 6

Placenta 30 (2009) 735–738

Contents lists available at ScienceDirect

Placenta

journal homepage: www.elsevier.com/locate/placenta

Technical Note

Double Immuno-labelling of Proliferating Villous Cytotrophoblasts in Thick Paraffin Sections: Integrating Immuno-histochemistry and Stereology in the Human Placenta

K. Widdows [a], J.C.P. Kingdom [b], T. Ansari [a,*]

[a] Department of Surgical Research, NPIMR, Harrow, UK
[b] Maternal-Fetal Medicine Division, Department of Obstetrics & Gynaecology, Mount Sinai Hospital, University of Toronto, Toronto, Canada

ARTICLE INFO

Article history:
Accepted 14 May 2009

Keywords:
Villous cytotrophoblast
Double-labelling
Proliferation marker Ki-67
Cytokeratin 7
Thick paraffin sections
Stereology

ABSTRACT

In order to understand the pathological basis of abnormal villous trophoblast development in diseased placentas, the organ must be sampled by non-biased methods and subject to analysis by stereological tools. This approach permits quantification of cytotrophoblast density and syncytiotrophoblast structure including evidence of apoptotic shedding via syncytial knots. The stereological quantification of cells (or their) nuclei requires that each should be unambiguously identified and counted within a defined volume of tissue. A major limitation of such studies at present is the inability to accurately identify and phenotype subsets of villous cytotrophoblasts that either proliferate or are destined to fuse into the overlying syncytiotrophoblast.

We describe the development of a novel double immuno-labelling protocol to selectively identify proliferating villous cytotrophoblast cells in human placental villi using thick (25 μm) paraffin sections suitable for stereological quantification. Cytotrophoblast cells were selectively stained using a monoclonal anti-cytokeratin 7 (CK 7) antibody without antigen retrieval, followed by nuclear Ki-67 co-localisation. Both antibodies displayed full depth penetration with sharp, clearly defined staining precipitates and no cross-reactivity. This double immuno-labelling protocol is reproducible, cost effective and time efficient (8 h). Use of a variety of antibodies following antigen retrieval will be a significant advancement in the ability to accurately quantify sub-populations of villous cytotrophoblast in normal and pathological placentas.

1. Introduction

The regulation of villous trophoblast turnover in human pregnancy is of increasing importance especially in pathological pregnancies [1–3]. Considerable molecular knowledge in normal trophoblast development and pathologically mediated dysregulation is available [4]. Yet to date few studies have been able to integrate specific changes occurring at a molecular level with predicted structural changes in the syncytiotrophoblast layer responsible for fetal growth and maternal well-being. This dual approach of integrating molecular techniques with stereological quantification within a single placenta therefore provides a physiologically integrated model to study trophoblast development and dysregulation. The numerical correlation between proliferation, fusion and apoptotic shedding within the trophoblast compartment is paramount and can be achieved using stereological methods.

In order to investigate trophoblast kinetics using stereological techniques two factors need to be met 1) each cell or nucleus to be counted must be unambiguously identified and 2) cells or nuclei must be counted within a defined volume of tissue (i.e. the area of the counting frame multiplied by the disector height, see equation (1)) within which they reside. Counting within a defined volume of tissue at this level provides a numerical density estimate (N_v), which then multiplied by total placental volume, provides an estimate for the total number of cells within the entire placenta (N_{tot}).

The ability to accurately identify and phenotype the villous cytotrophoblast population from the overlying syncytiotrophoblast histologically has been attempted using morphological features or various antibody markers. Reliable identification based on

* Corresponding author. Dept of Surgical Research, NPIMR, Block Y, Level 3, Harrow HA1 3UJ, UK. Tel.: +44 (0) 20 8869 2099; fax: +44 (0) 20 8869 3270.
E-mail address: t.i.ansari@ic.ac.uk (T. Ansari).

0143-4004/$ – see front matter
doi:10.1016/j.placenta.2009.05.007

morphology alone is difficult, especially as villous cytotrophoblast changes from a cuboidal-like continuous layer of cells to a discontinuous layer at term. Identification based on antibody markers, for example, E-cadherin [5], hepatocyte growth factor inhibitor (HAI-1) [6] and cytokeratin 7 [7] have all been used in a variety of applications. Despite their specificity for cytotrophoblasts, these markers are not exclusive displaying some cross-reactivity with the syncytium and stromal cells. Since no generic marker with the ability to consistently and accurately label cytotrophoblasts exists, attempts were made to modify the staining procedure using a monoclonal cytokeratin 7 antibody [8].

Stereological techniques have previously been employed to quantify the number of cytotrophoblast cells and syncytiotrophoblast nuclei based on their morphology and topography. Mayhew and colleagues used a Gomori trichrome tinctorial stain to identify different trophoblast populations using thin histological sections [9]. By using the physical disector technique [10,11], which employs two thin sections a known distance apart, these authors were able to quantify the different population of nuclei within a defined volume of tissue. Although unbiased, this method is time consuming since each pair of sections requires registration (see Sterio 1984 [11] for a detailed explanation). A more efficient method for generating a defined volume is the optical brick/disector technique [12,13], which employs a single thick (25 μm) section. This can be achieved using resin sections; however, full depth antibody penetration in thick resin sections is not possible.

To overcome these limitations, a method for the reliable and consistent identification of double immuno-histochemically labelled proliferating cytotrophoblast cells in a thick (25 μm) paraffin section, which fulfilled the criteria for stereological quantification was conceived. The ability to accurately and consistently identify subsets of trophoblast cells in a defined volume of placental villous tissue is an important technical advance for future quantitative analysis and will provide invaluable insight into villous trophoblast kinetics in pathological pregnancies.

2. Materials and methods

2.1. Tissue collection and preparation

Placental tissues from normal third trimester pregnancies were obtained from Mount Sinai Hospital, Toronto, Canada, following local ethical approval and informed patient consent. Uniform/systematic random placental samples were taken as previously described [1,14], fixed in 10% neutral buffered formalin for 48 h processed and embedded into wax blocks. Paraffin sections were cut at 5 μm and 25 μm thickness and mounted onto 3-aminopropyltriethoxysilane (APTS) coated slides (Sigma, UK) and dried at 60 °C overnight.

2.2. Antibodies

Cytotrophoblast cells were immuno-localised using an anti-human mouse monoclonal cytokeratin 7 [1:300] (clone OV-TL) antibody. Proliferating cytotrophoblast cells were visualised using a mouse monoclonal antibody to Ki-67 [1:50] (clone MIB-1). Both antibodies were obtained from Dako, Cambridge, UK.

2.3. Double-labelling of cytokeratin 7 and Ki-67

All incubations were carried out at room temperature (RT) and all reagents were obtained from Vector labs, Peterborough, UK unless otherwise stated. A high salt TBS-T wash buffer (100 mM Tris, 300 mM NaCl, 0.05% Tween, pH 7.6) was used for all washes during the double-labelling procedure to ensure minimal background staining.

Localisation of cytokeratin 7 *exclusively* to the cytotrophoblast required *omission* of antigen retrieval, necessitating it as the first antibody in the double-labelling procedure. Sections were dewaxed in xylene for 15 min and rehydrated through descending alcohol concentrations following routine procedure. Endogenous peroxide activity was quenched by incubation with 10% hydrogen peroxide (H_2O_2) in methanol for 30 min, followed by washing with TBS-T (Sigma, UK) for 3 × 3 min. Non-specific protein binding sites were blocked using 2.5% ready-to-use normal horse serum for 20 min, immediately followed by a 20 min incubation with mAb CK 7. Sections were then incubated with Vector ImmPRESS anti-mouse polymer detection reagent for 20 min, followed by extensive washing in TBS for 3 × 5 min. Cytokeratin 7 was visualised using ImmPACT DAB (diaminobenzidine) incubated for 2 min, producing a brown end product; sections were then washed in deionised water for 5 min.

Immediately after staining with CK 7, antigen retrieval was carried out on the same sections to allow for labelling of the second antibody Ki-67. Slides were placed in a coplin jar containing 20 mM citrate buffer, 2 mM EDTA, 0.05% Tween (Sigma, UK), pH 6.2, heated to 90 °C for 15 min, followed by cooling at RT, for a further 20 min. After washing in TBS-T for 3 × 3 min, non-specific proteins were blocked using 2.5% ready-to-use normal horse serum for 30 min, followed by incubation with mAb Ki-67 diluted in TBS for 2 h, and subsequently a 30 min incubation with Vector ImmPRESS anti-mouse Ig polymer reagent. Sections were thoroughly washed with TBS-T for 3 × 5 min to remove unwanted polymer. Ki-67 was visualised using a contrasting purple chromagen, Vector VIP, incubated for 2 min, followed by immersion in deionised water for 10 min. Sections were then counterstained using methyl green for 2 min at RT, differentiated in 0.05% acetic acid/acetone for 10 s, rinsed in deionised water for 10 s, dehydrated in 95% and 100% ethanol (2 min each), and finally cleared in xylene and mounted in DPX; excess DPX was used to avoid sections 'drying out' due to their increased thickness.

2.4. Estimating numerical density using the optical brick technique

The double-labelled sections were used to obtain the numerical density of CK 7 and Ki-67 positive cytotrophoblast cells. Numerical density estimation was performed with the aid of a BH2 Olympus light microscope (magnification ×100 NA 1.25), a Heidenhain microcator (ND 281A) attached to the z-axis of the microscope stage, and Kinetic Digital Stereology 5.0 software. An unbiased counting frame (UCF) was applied under software control to each uniformly–randomly selected image (field of view) and the microcator set to zero. Each section was focused through in the z-axis in a continuous motion; cells in the first (0–5 μm) and last (20–25 μm) 5 μm of the 25 μm sections were not counted to avoid the lost cap effect [13], generating a disector height of 15 μm within which cells were counted (verified by the microcator). Cells positive for CK 7 (non-proliferating), and CK 7 with Ki-67 (proliferating), were counted provided they obeyed the rules of the UCF and were within maximum focus within the 15 μm disector height (see Fig. 2). Approximately 10 fields of view per slide were sampled using a uniform random sampling approach resulting in an average 50 fields of view per placenta.

Numerical density estimates were calculated using the following formula (equation (1)):

$$N_v = \frac{\sum Q}{\sum P\left(A_f h\right)} \tag{1}$$

where (N_v) is numerical density, $\sum Q$ is the total number of cells counted divided by the total number of disectors $\sum P$ multiplied by the volume of each disector i.e. area of the unbiased counting (A_f) and the disector height (h).

The total number of cells (N_{tot}) was estimated by multiplying numerical density with total placenta volume (equation (2)):

$$N_{tot} = N_v \times V_{ref} \tag{2}$$

where (V_{ref}) is the volume of the placenta estimated by fluid displacement.

3. Results and discussion

Cytokeratin 7 is an intermediate filament protein expressed in epithelial cells. Although this monoclonal antibody stains both villous cytotrophoblast cells and the overlying syncytiotrophoblast in antigen-retrieved sections [15] we demonstrate the specific localisation of CK 7 exclusively to the cytotrophoblast cytoplasm when the antigen retrieval step is omitted (Fig. 1). Ki-67 was co-localised to the nucleus of labelled villous cytotrophoblast cells following antigen retrieval in this double-labelling protocol in 25 μm thick paraffin sections (Fig. 1). Both antibodies displayed full depth penetration of the tissue sections permitting accurate identification and future quantification of proliferating cytotrophoblast cells from other proliferating cell populations in the stromal compartment of chorionic villi.

Each antibody in the double-labelling protocol was first optimised as a single stain on thin 5 μm paraffin sections and then tested for full penetration and cytotrophoblast specificity in 25 μm thick sections; once individually optimized, they were combined in a sequential double-labelling protocol. This approach ensured complete penetration of each antibody, minimal background

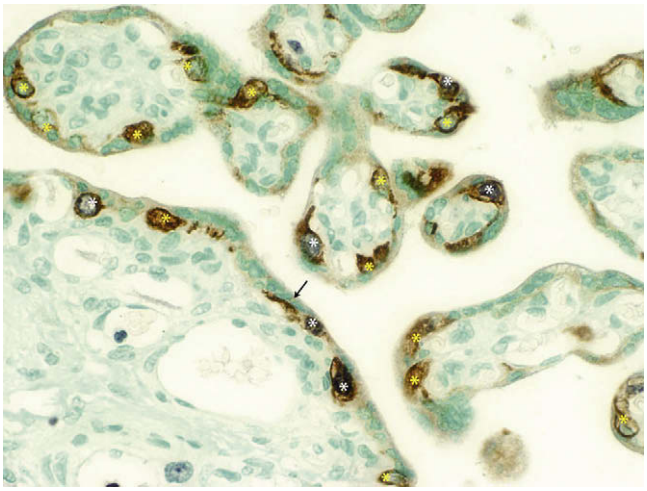

Fig. 1. Specific immuno-localisation of anti-cytokeratin 7 to the cytoplasm of cytotrophoblast cells (brown chromagen) displaying no cross-reactivity with overlying syncytiotrophoblast nuclei (counterstained with methyl green) in term placenta. White asterisk denotes proliferating cytotrophoblast cells (purple chromagen); yellow asterisk denotes non-proliferating cytotrophoblast cells (5 μm sections, ×400). Cross-reactivity with the syncytium was not observed (arrow shows the clear delineation between the labelled cytotrophoblast cell and syncytiotrophoblast nuclei).

staining and efficiency of time; the protocol can be carried out in one day taking approximately 8 h for completion.

The most striking observation of this protocol was the reduction in the CK 7 primary antibody concentration and decreased incubation time required to achieve full depth selective staining of villous cytotrophoblast in a 25 μm section when compared with a 5 μm histological section. Conversely, staining for Ki-67 in a thick section required increased incubation time to ensure full depth antibody penetration following antigen retrieval. The Ki-67 antigen retrieval solution concentration was also increased along with the addition of detergents EDTA and Tween (Sigma, UK). These observations illustrate the influence of antigen location, whether nuclear or cytoplasmic, in determining the optimal protocol when staining thick paraffin sections of human placental villi.

The order of the antibodies in the sequential double-labelling protocol was influenced by antigen retrieval requirements. Since cytokeratin 7 localised selectively to villous cytotrophoblasts only with the omission of antigen retrieval, this protocol had to be performed prior to the required antigen retrieval step for nuclear localisation of Ki-67, necessitating CK 7 as the first labelling protocol. Significantly, this indicates that antigen-retrieved antibodies can be used in conjunction with antibodies that do not require this step in a sequential double-labelling procedure (not applicable to simultaneous double-labelling procedures), provided the chromagen used to visualise the first antigen can withstand the physical parameters of antigen retrieval in the second protocol. Additionally, the colours of the first and second chromagen and any counterstain must all contrast sufficiently with each other to ensure accurate identification. This was achieved using a brown chromagen, ImmPACT DAB, to visualise cytokeratin 7, a purple chromagen Vector VIP for Ki-67 and a methyl green nuclear counterstain (Vector Labs, UK). Sections were initially over-stained with ImmPACT DAB to ensure crisp and localised staining of cytotrophoblasts following immersion in antigen retrieval solution; conditions were optimized to those comparable to single stains in 5 μm sections. Since most of the purple chromagen, Vector VIP, was lost due to its instability at high temperatures, it was used to visualise Ki-67. Importantly, the high sensitivity of the ImmPRESS polymer reporter enzyme kit gave superior staining to the routinely

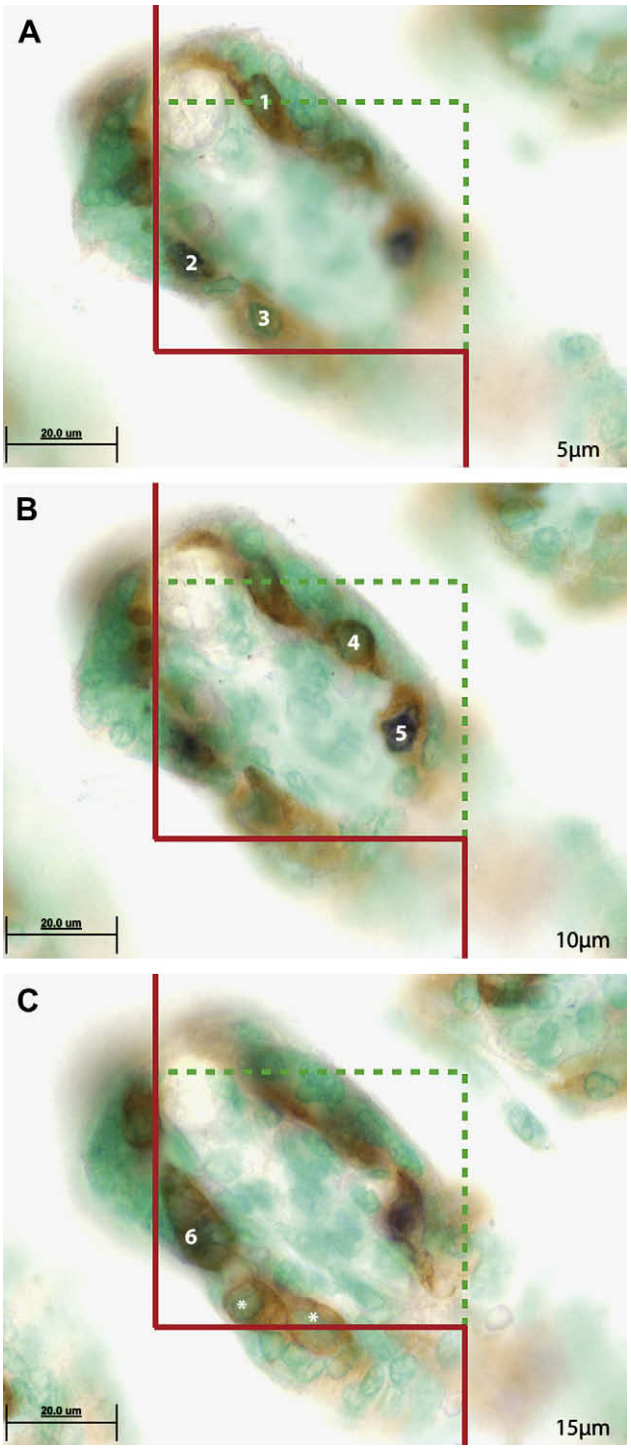

Fig. 2. Counting the number of proliferating cytotrophoblast cells in 25 μm sections double immuno-labelled with CK 7 and Ki-67 using the optical brick technique (A–C, ×1000). An unbiased counting frame (UCF) (red and green lines) is randomly superimposed onto each uniform-randomly sampled field of view. As the section is scanned through the z-axis within the disector height (i.e. 15 μm), each labelled cytotrophoblast cell (brown chromagen) that comes into sharp focus and does not intercept the red forbidden line of the UCF (cells marked with an asterisk) is counted as a '*new event*' (A, no.1, 2, and 3) (B, no. 4 and 5) (C, no.6). The number of cytotrophoblast cells co-localised with Ki-67 (purple *and* brown chromagen) is also counted (A, no. 2, C no. 5). Hence, for this field of view, 6 cytotrophoblast cells are counted, 2 of which are positive for Ki-67. The sum of the counts (per placenta) is then multiplied by the disector height (i.e. 15 μm × area of the UCF) generating a numerical density.

Table 1
Stereological estimates of the total number of Ki-67 positive cytotrophoblast nuclei in the term placenta.

Parameter	($n = 5$)
Numerical density of CT cells (μm^{-3})	$1.5 \times 10^{-4} \pm 1.0 \times 10^{-5}$
Numerical density of Ki-67 positive CT nuclei (μm^{-3})	$4.3 \times 10^{-5} \pm 5.7 \times 10^{-6}$
Total placental volume (cm^3)	562 ± 38
Total no. CT cells	$8.6 \times 10^{10} \pm 1.1 \times 10^{10}$
Total no. Ki-67 positive CT nuclei	$2.5 \times 10^{10} \pm 4.6 \times 10^{9}$
% of Ki-67 positive CT nuclei	28.4 ± 3.1

Data presented as the mean $\pm$ SEM. CT, cytotrophoblast.

used avidin–biotin system which was unable to withstand the high temperature antigen retrieval required for Ki-67 (staining not shown), and consequently staining was lost for both ImmPACT DAB and Vector VIP. Whilst the increased sensitivity of the polymer kit reduced antibody concentration and hence cost, it increased non-specific background staining which was minimised using a high salt wash buffer displaying no deleterious effect on the stability of the antibodies or their chromagens.

Although the optical brick technique is far more efficient in terms of time and cost compared to the physical disector, bias (inaccuracy) may be introduced into the final stereological estimate through tissue deformation of thick sections (shrinkage or expansion for example by high temperature antigen retrieval), especially when paraffin embedded. Correcting for tissue deformation (Dolph-Petersen et al. [16] provide a detailed review on estimating tissue deformation) however, is not always necessary providing deformation is homogenous, (and comparable within and between groups of placentas), since the cardinality of nuclei will be preserved. Since the present aim was to assess the applicability of the double-labelling technique for use in cytotrophoblast number estimation using stereological analysis, the comparative data shown in Table 1 was not corrected for tissue deformation.

The ability to quantify both the total number of proliferating (Ki-67 positive) and non-proliferating villous cytotrophoblast in the human placenta has significant potential for advancing future stereological studies of trophoblast turnover and kinetics, since alterations of which are hypothesised to underpin placental insufficiency syndromes of severe pre-eclampsia and IUGR [17]. However, it is acknowledged that Ki-67 identifies all cycling cells withholding the potential to divide [18], and that additional phase labelling indices (e.g. BrdU for S phase and mitotic counts for M phase) should be considered (in combination with CK 7) to quantify the actual growth fraction of villous cytotrophoblast cells. In future studies it will therefore be possible to address whether a steady state exists between proliferation and fusion of villous cytotrophoblasts into the overlying syncytium; the dual immuno-stereological approach will potentially allow the quantification of different villous cytotrophoblast phenotypes.

In summary, the development of this novel double-labelling protocol provides a technical advance in the field of stereological analysis permitting the unbiased quantification of the total number of proliferating villous cytotrophoblast cells in the human placenta using the optical brick technique, thereby facilitating future morphometric studies of the pathological placenta.

Acknowledgment

The authors would like to acknowledge the financial support provided by both the Henry Smith and Scottish Cot Death Trust. Special thanks to Gez Boxall and Carinna Hockham for technical advice and assistance with the staining. Funded in Canada by CIHR (64302) to JK.

References

[1] Ansari T, Gillan JE, Condell D, Green CJ, Sibbons PD. Analyses of the potential oxygen transfer capability in placentae from infants succumbing to sudden infant death syndrome. Early Hum Dev Feb 2004;76(2):127–38.
[2] Egbor M, Ansari T, Morris N, Green CJ, Sibbons PD. Morphometric placental villous and vascular abnormalities in early- and late-onset pre-eclampsia with and without fetal growth restriction. BJOG May 2006;113(5):580–9.
[3] Mayhew TM, Manwani R, Ohadike C, Wijesekara J, Baker PN. The placenta in pre-eclampsia and intrauterine growth restriction: studies on exchange surface areas, diffusion distances and villous membrane diffusive conductances. Placenta Feb 2007;28(2–3):233–8.
[4] Baczyk D, Drewlo S, Proctor L, Dunk C, Lye S, Kingdom J. Glial cell missing-1 transcription factor is required for the differentiation of the human trophoblast. Cell Death Differ May 2009;16(5):719–27.
[5] Brown LM, Lacey HA, Baker PN, Crocker IP. E-cadherin in the assessment of aberrant placental cytotrophoblast turnover in pregnancies complicated by pre-eclampsia. Histochem Cell Biol Dec 2005;124(6):499–506.
[6] Hallikas OK, Aaltonen JM, von KH, Lindberg LA, Valmu L, Kalkkinen N, et al. Identification of antibodies against HAI-1 and integrin alpha6beta4 as immunohistochemical markers of human villous cytotrophoblast. J Histochem Cytochem Jul 2006;54(7):745–52.
[7] Maldonado-Estrada J, Menu E, Roques P, Barre-Sinoussi F, Chaouat G. Evaluation of cytokeratin 7 as an accurate intracellular marker with which to assess the purity of human placental villous trophoblast cells by flow cytometry. J Immunol Methods Mar 2004;286(1–2):21–34.
[8] Mayhew TM, Leach L, McGee R, Ismail WW, Myklebust R, Lammiman MJ. Proliferation, differentiation and apoptosis in villous trophoblast at 13–41 weeks of gestation (including observations on annulate lamellae and nuclear pore complexes). Placenta Jul 1999;20(5–6):407–22.
[9] Mayhew TM, Wadrop E, Simpson RA. Proliferative versus hypertrophic growth in tissue subcompartments of human placental villi during gestation. J Anat 1994;184:535–43. 26-11-1993, Ref type: Generic.
[10] Gundersen HJ. Stereology of arbitrary particles. A review of unbiased number and size estimators and the presentation of some new ones, in memory of William R. Thompson. J Microsc Jul 1986;143(Pt 1):3–45.
[11] Sterio DC. The unbiased estimation of number and sizes of arbitrary particles using the disector. J Microsc 1984;134:127–36.
[12] Braendgaard H, Evans SM, Howard CV, Gundersen HJG. The total number of neurons in the human neocortex unbiasedly estimated using the optical disectors. J Microsc 1990;157:285–304.
[13] Howard V, Reid S, Baddeley AJ, Boyde A. Unbiased estimation of particle density in the tandem scanning reflected light microscope. J Microsc 1985;138:203–12.
[14] Gundersen HJ, Jensen EB. The efficiency of systematic sampling in stereology and its prediction. J Microsc Sep 1987;147(Pt 3):229–63.
[15] Baczyk D, Dunk C, Huppertz B, Maxwell C, Reister F, Giannoulias D, et al. Bi-potential behaviour of cytotrophoblasts in first trimester chorionic villi. Placenta Apr 2006;27(4–5):367–74.
[16] Dorph-Petersen K-A, Nyengaard JR, Gundersen HJG. Tissue shrinkage and unbiased stereological estimation of particle number and size. J Microsc Dec 2001;204:232–46.
[17] Huppertz B, Kaufmann P, Kingdom JCP. Trophoblast turnover in health and disease. Fetal Matern Med Rev 2002;13:103–18. Ref type: Generic.
[18] Duchrow M, Schluter C, Key G, Kubbutat MH, Wohlenberg C, Flad HD, et al. Cell proliferation-associated nuclear antigen defined by antibody Ki-67: a new kind of cell cycle-maintaining proteins [Review] [30 refs]. Archivum Immunologiae et Therapiae Experimentalis 1995;43(2):117–21.